Master Thesis

Optimization of steel plate girders in bending

Using FEM-analyses on S690 and S890 steel plate girders

By

Wouter van Gemeren

Faculty of Civil Engineering and Geosciences
Delft University of Technology

May 21th, 2019

Thesis committee

Prof.dr.ir. M. Veljkovic	Delft University of Technology; Structural and Building Engineering
Dr.ir. R. Abspoel	Delft University of Technology; Structural and Building Engineering
Dr.ir. M.A.N. Hendriks	Delft University of Technology; Structural Mechanics
Ir. M. Feijen	I-Saac

TU Delft Delft University of Technology

Contents

Abstract

Plate girders have been used since the 19th century, to bridge spans. The girders progressed from riveted steel plates to welded steel sections using a variety of dimensions. With hot rolled sections becoming cheaper and labor getting more expensive the plate girders use became more limited to large spanning girders, since this is where a significant reduction in material cost could be beneficial. The lack of technical knowledge of plate girders, in which plate buckling was present did not help in propagating the use of plate girders.

Technological advance and a sharper focus on the ecological footprint of our society could change this equilibrium. Machine welding is more advanced than ever, to the point that plate girders could be built from plate material fully automatically. Since the 1960's researchers have been looking into the behavior and calculation of plate girders, resulting in the availability of using its post buckling strength increases the capacity and ease of design for plate girders and limiting the slenderness of the girder webs to design safe structures.

On the other hand looking at the environmental part of the claim. In general plate girders are much more slender in comparison to the standard hot rolled section, therefor consuming less steel per unit length. The impact of using plate girders leads to a reduction in the use of steel not only limits the negative effects of the amount of steel being forged but also the volume of traffic is reduced from mine to forgery and from forgery to factory and building site.

The positive effect of using plate girders could be optimized by using optimized layouts, to further reduce the needed steel. In general the layout used was a plate girder several transverse stiffeners over the length of the span. Previous TU Delft researchers have tried to find an optimized shape for a plate girder to have the highest bending moment capacity, without using these stiffeners. Abspoel [1] concluded that to optimize a plate girder in bending, the most significant parameter was found to be the distance between the top and bottom flange, using a ratio between web and flange area of 1, as this was shown to be the ideal ratio for very slender girders.

Using parametric studies in which the total area of steel was kept constant Abspoel [2] optimized plate girders on a constant bending moment, using FEM-software, using S235 and S460 steel, making use of a geometry which depended on the height of the plate girder. The analysis resulted in a maximized web slenderness which was much higher than the limits proposed, therefore finding much higher capacities compared to the analytical models used to calculate the plate girders. Also a fixed maximum slenderness was found for these steel grades, independent of the used total area of steel in the cross-section.

After this Cimpoi [3] extended the research using S690 steel as steel grade to optimize the bending moment capacity, using the same geometry as Abspoel. The results also showed much more slender girders, compared to the given limitations. The maximum web slenderness found in this work for S690 steel was not constant for the tested steel areas, which were 6000 mm^2 and 12000mm^2.

A parametric study, using the FEM-software package ABAQUS, validated on experimental results found by Abspoel, was conducted on S690 steel plate girders to address if the results of the previous researches was valid. Using a slightly different analytical model the results show the maximum web slenderness of this steel grade in both 6000 mm^2 and 12000mm^2 was the same. It was shown that the maximum bending moment was found when the top flange was able to yield, shortly followed by sudden collapse.

A new parametric study, to expend the optimizing plate girders using S890 steel was conducted as well to address the usefulness of steels with higher yield strength in plate girders subjected to bending. This study again used the geometry used by Abspoel. The results showed a decrease in maximum web slenderness, but still a significant increase in bending moment capacity compared to the S690 plate girders. It was shown that using an optimized S890 plate girders compared to hot rolled section made also from S890 steel, could reduce the use of steel by more than 80%.

After the parametric studies showed increasing capacity, the geometry used to numerically model the plate girders, was critically addressed, using small scale numerical studies using FEM-software. These tests showed that not only the slenderness of the web was a factor in the bending moment capacity of a plate girder, but also the flange geometry plays a significant role. It was shown that increasing the length of the tested part of the girder, the failure mode could change from flange yielding to an instable mode in which the flange rotated around its longitudinal axis, resulting in a much lower bending moment capacity.

An extra investigation in using a hybrid steel composition resulted in showing the potential of this optimization. Because by adding lower grade steel, more ductility was shown due to these parts yielding prior to yielding of the compressive flange, resulting in possible safer design.

Nomenclature

Symbol	Description	Unit
a	Length of a plate girder between transverse stiffeners	[mm]
b	Height of a plate girder	[mm]
$\bar{b}$	Reference width	[mm]
b_{eff}	Effective width	[mm]
$b_{e1,2}$	Parts of the effective compressed part of the web	[mm]
b_f	Width of the flange	[mm]
f_y	Yield strength	[MPa]
$f_{y.235}$	Yield strength of S235 steel	[MPa]
f_u	Ultimate strength	[MPa]
h_w	Depth of the web, between the flanges	[mm]
k_σ	Plate buckling stiffness	[-]
l	Length	[mm]
l_{buc}	Buckling length	[mm]
l_{max}	Maximum mid-panel length	[mm]
r	Radius of gyration	[mm]
t_f	Flange thickness	[mm]
t_w	Web thickness	[mm]
A_{tot}	Total cross sectional area of steel	[mm^2]
A_{fl}	Flange area of steel	[mm^2]
A_w	Web area of steel	[mm^2]
A_{tot}	Total cross sectional area of steel	[mm^2]
E	Modulus of elasticity	[MPa]
F	Applied force	[kN]
F_{max}	Maximum applied force	[kN]
G	Shear modulus	[MPa]
I	Second moment of area	[mm^4]
I_{eff}	Effective second moment of area	[mm^4]
I_{trans}	Transverse effective second moment of area	[mm^4]
M	Bending moment	[kNm]
M_{eff}	Effective Bending moment resistance	[kNm]
M_{el}	Elastic Bending moment resistance	[kNm]
M_{fl}	Plastic flange moment resistance	[kNm]
M_{pl}	Plastic moment resistance	[kNm]
M_u	Ultimate Bending moment resistance	[kNm]
N	Normal force	[kN]
N_{cr}	Critical Normal force	[kN]
W	First moment of area	[mm^3]
W_{eff}	Effective first moment of area	[mm^3]
W_{pl}	Plastic first moment of area	[mm^3]

Symbol	Description	Unit
α	Web panel aspect ratio	[-]
β	Slenderness	[-]
β_f	Flange slenderness	[-]
β_w	Web slenderness	[-]
$\beta_{w,max}$	Maximum web slenderness	[-]
δ	Deflenction	[mm]
ε	Strain	[-]
ε_y	Yield strain	[-]
ε_{true}	True strain	[-]
ε_{nom}	Nominal strain	[-]
$\bar{\lambda}, \lambda_{rel}$	Relative slenderness	[-]
σ	Stress	[MPa]
σ_{true}	True stress	[-]
σ_{nom}	Nominal stress	[-]
σ_{cr}	Critical stress	[MPa]
ρ	Ratio between web and flange area	[-]
ρ	Reduction factor effective width	[-]
ψ	Stress ratio	[-]

1. Introduction

1.1. Plate girders

Plate girders have been used since the 19th century in bridge building and other projects with large spans. The versatility in shapes and strength and stiffness to weight ratio make plate girders very useful in civil engineering solutions. Because of the availability of cheap, high quality, hot rolled sections, plate girders are not often used in small span applications. The needed welding to construct the girder from plate material made it, although some steel can be saved, mostly too expensive.

Plate girders are often an economic choice in the span ranges where generally castellated beams and trusses are used. A castellated beam is cheaper to make, because it is made out of hot rolled sections and therefor the welding is limited, but with longer spans a plate girder would be cheaper due to the reduction in used steel. A truss is very expensive to make, but is more rigid than plate girders. Plate girders can be a good alternative for relatively small trusses in which the required stiffness is limited.

Plate girders do behave very well in bending and are very stiff in comparison to hot-rolled sections made with the same amount of steel per unit of length. For example, a plate girder used in experimental tests by Abspoel[2], with the dimensions given below has got a total area of 1712.7 mm^2 and its effective moment of inertia is 18710*104 mm^4, calculated using the effective width method from EN1993-1-5 for plated structures.

- Top flange: 80x5.6mm
- Bottom flange: 80x5.6mm
- Web: 800x1.0mm

Comparing this to IPE-profiles makes clear that plate girders can be beneficial. For example, comparing the amount of used steel per unit length, leads to a IPE160-girder, which has a total cross-sectional area of 2009mm2. This is 17% more than the plate girder, but the section only has a moment of inertia of 869*104 mm4, which is more than 20 times smaller compared to the described plate girder.

When a competing IPE-section in bending stiffness is chosen, the IPE360 and 400 compare the best, with 16266 and 23128*10^4 mm^4. These profiles have a total area of 6261 and 7273 mm2, which have a 3.6 and 4.2 times larger amount of steel so the transported weight is much larger, see also Figure 1.

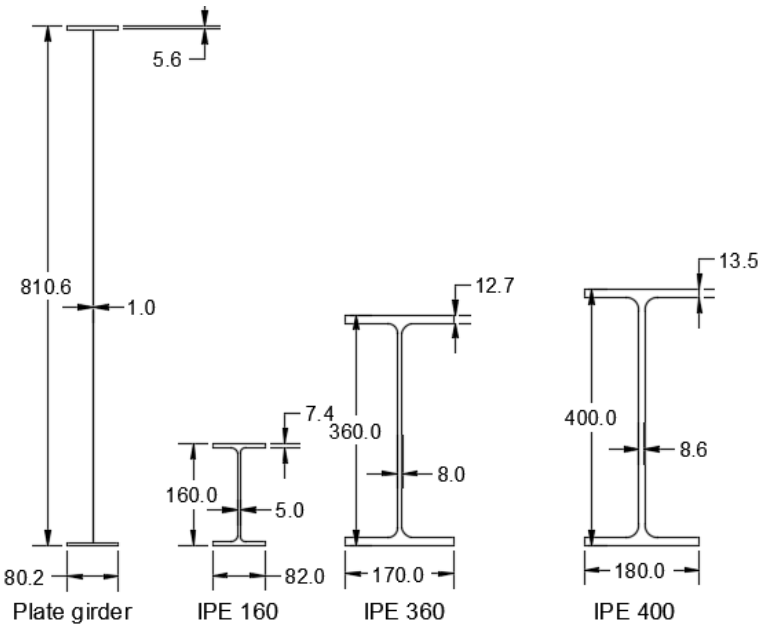

FIGURE 1: COMPARING A SLENDER PLATE GIRDER WITH IPE-PROFILES

This example shows the much higher potential in strength to weight ratio of plate girders, compared to hot-rolled sections. The fabrication on the other hand has been expensive in the past, so only big projects where the steel consumption is a large factor in the cost could benefit enough, to make plate girders a competitive solution. Recent developments could make a change in this equilibrium, because automated welding is said to be possible in very thin plates nowadays, leading to lower production costs for plate girders, which in terms could be a competitor for the cheap hot-rolled sections we mostly use, also in solutions with medium and small spans.

The decrease in used steel would not only be economically preferable. Looking at environmental aspect a plate girder would be a great improvement. Producing and/or recycling steel consumes significant amounts of energy and generates a lot of greenhouse gasses, as well as the transport of the steel, from mine to smelter and from smelter to end user. Reducing the amount of steel used, would thus reduce the environmental impact of a construction in several ways.

Not every aspect of a plate girder is better compared to hot rolled sections. For example, the outer surface is much bigger, leading to larger needed amounts of protective coating against corrosion. This property is also a disadvantage in the case of fire. The thin plates will heat up very fast due to its large contact area, certainly in comparison to total area. This will lead to fast decrease of its bearing capacity in a fire, without using proper fire protection.

The size of the plate girders can also be a disadvantage in transportation and use. Due to the slenderness, not a lot of rigidity is present in the out-of-plane direction, which could lead to deformation during transport and erection of the structure when not handled carefully. Also, the need of a lot of space to incorporate the higher sections in the structure can be a disadvantage, leading for example to higher needed ceilings and possible visual blockage.

1.1.1. Plate girders geometry

A plate girder, made from steel or aluminum, is formed from metal plates welded together to form an effective section for its use, mostly stiffened with transverse and/or longitudinally welded stiffeners to help stabilize and strengthen the girder. The most efficient girders in bending are designed with deep, slender webs and thick flanges. Girders subjected to predominately shear have less slender webs and have less benefits from deep girders. Transverse stiffeners give extra shear resistance.

A general layout for a plate girder is shown on Figure 2, showing a double stiffened end-post and a transvers stiffener. These stiffeners are mostly equilly spaced, with a distance a. The most important parameters are given below in equation (1.1): the aspect ration α, the web slenderness β_w and the ratio between the area of the web and the area of a single flange, denominated as ρ.

$$\alpha = \frac{a}{h_w},\ \beta_w = \frac{h_w}{t_w},\ \rho = \frac{A_f}{A_w},\ \text{with } A_{tot} = 2 * A_f + A_w \tag{1.1}$$

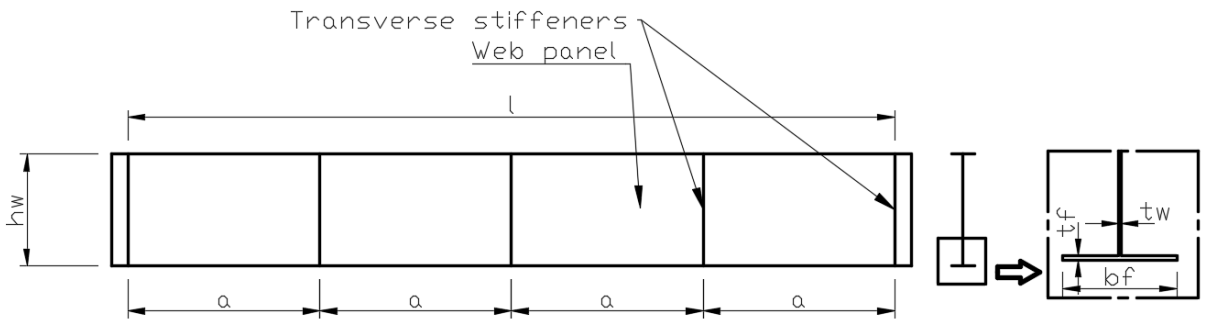

FIGURE 2: GENERAL BUILDUP OF A PLATE GIRDER

Because of the slenderness of plate girders, they are likely to be subjected to instabilities in their use. The slenderness generally leads to buckling of the plates, which limits the elastic capacity of these structures. The plate girders therefor have calculated using this buckling limit, limiting the use, until the 1960's, although there was proof of extra capacity after buckling.

Basler was the first to describe the behavior after buckling, the post-buckling behavior, and developed calculation methods, thereby giving possibilities to use the extra capacity safely in the design of plate girders in shear and bending. After Basler numerous other researchers have studied the behavior of the plated girders and came up with different solutions to describe the behavior and resistance of these structures, expanding the limits for web slenderness and the capacity of the girders in bending and shear.

Together with the development and research on bending and shear, fatigue and patch loading have been studied as well. Other research focused on plate girders with corrugated webs, the resistance of corroded girders and girders with holes in their webs. Also tapering of the web plates has been studied in the past.

1.1.2. Plate girder calculation in bending

Several authors have described bending behavior of plate girders. The first part of the resistance is the elastic resistance, limited by buckling of the plate girder, which has been described by Timoshenko. The post-buckling models use 2 approaches in general. The most common is the use of an effective width method. These methods take the non-uniform bending stress distribution in thin plates into account, using an effective part of the cross section to calculate an ultimate bending moment resistance, using the yield limit of the use steel.

Basler for example used a model in which 30 times the thickness of the web at the compressive part of the girder is effective and the tensile half of the cross section is fully effective, shown in Figure 3[5]. In the case of Basler's model, if the slenderness is high, the ultimate stress is also reduced, depending on the slenderness and steel quality.

The other general direction in calculation methods uses a reduced stress in a full cross section to calculate the maximum bending moment resistance. A more elaborated study in bending models is found in paragraph 2.3.

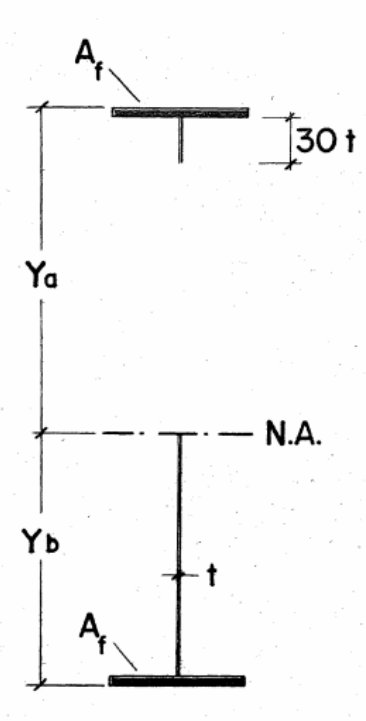

FIGURE 3: EFFECTIVE WIDTH MODEL BY BASLER

1.1.3. Plate girder calculation in shear

As well as the bending models, plate girders in shear have been analyzed by many, leading to several models describing the behavior and resulting in an ultimate shear resistance. As seen in bending, the first part of the resistance comes from elastic shear resistance, until the critical shear stress is achieved in the web. For this calculation there is however a difference in opinion about how to model the flange-web connection to be either simple, fixed or anywhere in between.

The second part of the resistance in all classic models is described by a tension field. After buckling of the web, the compressive stress can't increase and only tensile stress increases to provide shear resistance. The modeling of this tension field differs in the models. For example, Basler[6] describes a tension field which follows the diagonal of the web, where Höglund[7] formulates an optimizable, rotatable tension field.

In some models an extra third portion of resistance is given by the flanges, which can form a mechanism after the web has started yielding, resulting in failure. Models which don't add this contribution assume failure when the tension field yields.

The two most used classical models are the Cardiff tension-field model, by Rockey and Skaloud and the rotating-stress-field model by Höglund[8], using both plastic hinges in the shear resistance calculation.

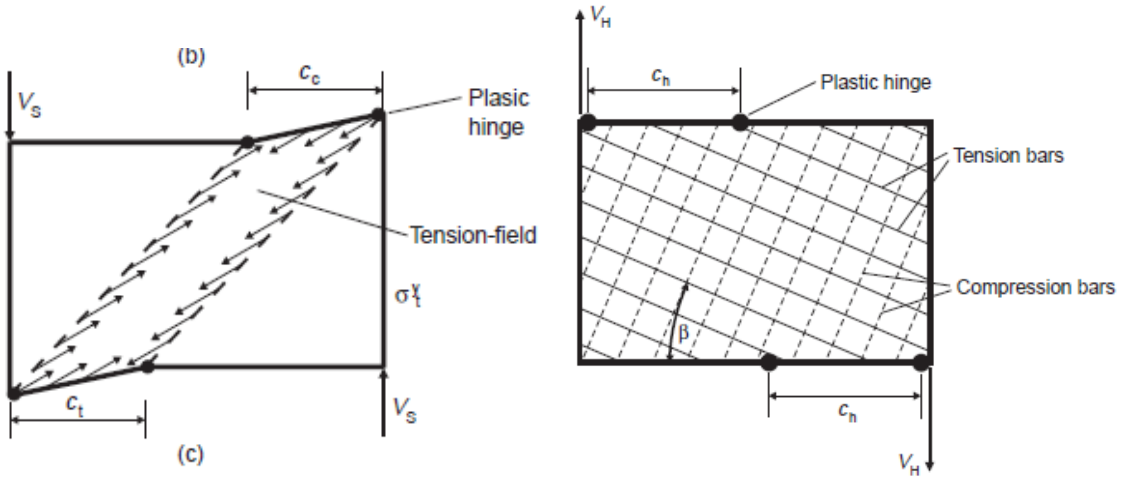

FIGURE 4:(L) CARDIFF TENSION-FIELD THEORY AND (R) ROTATING-STRESS-FIELD THEORY[9]

A recently developed method is the method described in Glassman[10], using a compression model to describe post-buckling behavior. This model uses a tension-field, which reduces the length of the compressive diagonal, thereby reducing the buckling length of this diagonal. The model has been found due to the analogy of the stress distribution in axially compressed, simply supported plates and plate girder webs in shear. This stress field is rotated to resemble shear stress. The failure characteristics of this model are the buckling of the compressive diagonal in shear.

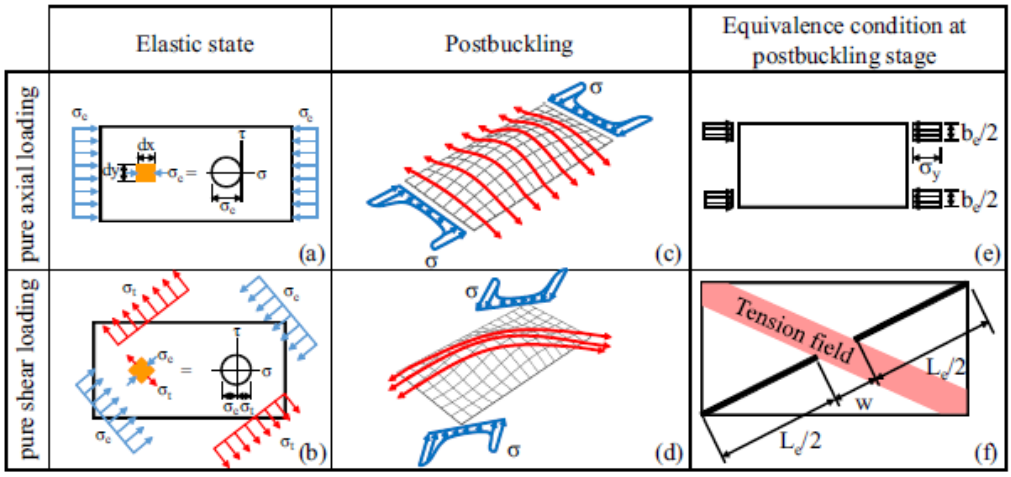

FIGURE 5: BASE OF THE COMPRESSION MODEL DESCRIBING SHEAR RESISTANCE IN THIN PLATES, BY GLASSMAN

Most models prescribe a limitation for it to be used. Most bending models have a limit in the web slenderness, which is linked to the yield stress of the used steel. This limit is there to minimize the possibility for the plate girders to fail due to instabilities, torsional buckling, lateral buckling and vertical buckling have been described as possible ways leading to failure. Shear models have limits for the aspect ratio, in which it can be used. Because this thesis only studies the effect of bending on plate girders, the shear behavior of plate girders will not be discussed in more detail.

1.2. Previous research at TU Delft

The limits for slenderness and the capacity of plate girders have slowly gone up over time due to research, definitely when situations using lateral bracings where analyzed. Abspoel tested plate girders with web slenderness up to 800 experimentally and in a numerical model found a web slenderness of 1450 to be achievable in S235 steel.

A question rose, what the optimum geometries would be for a plate girder in bending, this was the base of 2 previous researches done at TU Delft, by Abspoel and Cimpoi, also for example Stark[11] found optimization equations.

For the optimization of steel plate girder on bending, Abspoel and Cimpoi did research to find the optimum in web slenderness to get the highest possible ultimate bending moment resistance using a described amount of steel per unit of length. In this numerical parametric study, the steel plate girders were laterally supported, unstiffened and thin-webbed. These specific researches and their parametric study are described below.

1.2.1. Research by Abspoel

Abspoel [2] did experimental research on 10 unstiffened, laterally supported, plate girders with webs of 1 mm thick and their height ranging from 400 to 800 mm. The ratio between gross section of a flange and the web ranged from 1 up to 4. All girders had a steel quality of S235. These tests where used to validate a non-linear FEM-model using MSc Marc Mentat 2005r3 software.

The validated model was the base to a parametric study showing the web slenderness was the most influencing factor in the ultimate moment resistance of a plate girder, followed by the flange dimensions. The web thickness was found to be not very influential.

3 approaches where taken after this to find the answers to the research: to achieve the maximum ultimate bending moment resistance for a certain amount of steel on S235 and S460 steel. To do this MSc Marc Mentat 2005r3 software was again used. To model the steel behavior an engineered stress-strain relationship was used. Until yielding the E=210000 MPa after yielding the slope is E/1000000=2.1 MPa. Also, initial geometric imperfections where taken into account, using a half sine shape in transverse direction and a 6-sine shape in length direction.

The parametric study was conducted on girders with, or close to, 6000 mm^2 total sectional area. The absolute maxima from this parametric study where found using an approach where the flange area and the web-thickness where constant and the web height was the changing parameter. This led to a higher total area than 6000mm^2 (9600 and 7200 mm^2 for respectively S235 and S460). All FEM-calculations where plotted to compare results with analytical calculations. The calculation using the simplified effective width method according to Abspoel showed a good fit with the results.

Calculation on the Abspoel method showed that a ratio of area between flange area of one flange and the web area of close to 1 lead to a maximum moment resistance with high web slenderness and for less slender webs this ratio moves up and also that this optimum ratio is independent of cross-sectional area. The difference in ultimate bending resistance was hardly influenced when using a value of 1 in comparison to using the optimum value for this ratio. (Figure 7-23, 24 and 25 on page 302-304).

Further on an assumption is made that the maximum web slenderness giving the highest bending moment resistance is a constant value for a certain steel quality and the iterative process, found in the Eurocode, to determine the effective width is simplified by a function. This function only uses the web slenderness as a variable and calculates the effective bending moment similar to a truss. With this assumption and the inter-/extrapolation of the maximum web slenderness to S690 and S355 steel predictions are made for the maximum bending moment resistance for 4 steel qualities, using A= 6000 and 12000 mm^2

The found maxima are given in Table 1, the dark columns give FEM-results, the white columns are inter- and extrapolations for the web slenderness. The ultimate moment resistances are calculated using the reduced effective width method by Abspoel.

ρ=1, β_f=20	S235		S355		S460		S690	
A	6000	12000	6000	12000	6000	12000	6000	12000
$B_{w,max}$	1450	1450	1076	1076	850	850	509	509
$M_{u,max}$	822,4	2357,4	1068,5	3025,9	1220,3	3495,4	1445,7	4095,4

TABLE 1: RESULTS OF FEM ANALYSIS (GRAY) AND INTER-/EXTRAPOLATION OF THESE RESULTS

1.2.2. Research by Cimpoi

Cimpoi[3] did a research, following up on the research of Abspoel, with 3 goals, which are given below:

1. to check if vertical buckling of the compressive flange is not the phenomenon to determine the maximum web slenderness β, to a certain limit;
2. to find the optimum steel grade – limit until the above conclusion is valid;
3. to verify the optimum ratio of area Aw/At to determine the ultimate bending moment resistance of a plate girder;

To achieve this, a similar parametric study to that of Abspoel was conducted, but using ABAQUS as FEM software. First a validation of the proposed ABAQUS model, using S235 steel was conducted, comparing the model with 2 models from the parametric study of Abspoel (slenderness 700 and 1000, S235 steel, 6000 mm^2 area).

The ABAQUS model used explicit, non-linear calculation and imperfections generated by an eigenmode analysis, magnified to follow the prescribed magnitude by the Eurocode. The first eigenmode was used, being a shape of 6-sine lengthwise and a half-sine shape on the top-half of the girder in transverse direction. Also, an engineered stress-strain diagram was used, using the E=210000 MPa until the yield stress, after yielding an incline of 1 was used (following Eurocode prescription).

The results found during validation where a little different from the FEM-model made by Abspoel, about 2% for strength and stiffness, which was assumed to be useable. The model was used to model a parametric study, using different steel properties to model S460 and S690 steel properties. The S460 parametric study was conducted on plates with a total section area of 12000 mm^2, the S690 on both 6000 and 12000 mm^2, using a ratio between flange area and web area of 1 (both flange and web area are 2000/4000 mm^2). The results for the maximum bending moment resistance and the corresponding web slenderness are shown in Table 2 (the values for the ultimate bending moment were taken from a

graph, they are not exact). All the girders which found the highest bending moment resistance failed on yielding of the top flanges and did have vertical flange buckling after this limit, as post-failure behavior.

ρ=1, β_f=?	S460	Abspoel S460		S690		Abspoel S690	
A	12000	6000	12000	6000	12000	6000	12000
$B_{w,max}$	850	850	850	800	450	509	509
$M_{u,max}$	±3400	1220.3	3495,4	±1700	±3600	1445,7	4095,4

TABLE 2: FEM RESULTS OF CIMPOI AND SPECIFIC ABSPOEL RESULTS

The conclusions on the research objectives are presented below. The first goal was to find out if vertical compressive flange buckling is the phenomenon to limit the web slenderness. For S460 and S690 this is not the case. Goal 2 was to find the maximum web slenderness, this is shown in Table 2. The third goal isn't addressed in the thesis, only ratio 1,0 is used to do the calculations, the flange slenderness is not given in the report, but is presumed to be equal to the flange slenderness used by Abspoel, which was 20.

1.2.3. Remarks on previous research

The results shown in both Table 1 and Table 2 show the increase in ultimate bending moment when using a higher steel grade and using a larger sectional area of steel. The results of the research of Cimpoi, on S460 steel with an area of 12000 mm^2 show almost the same maximum web slenderness as the FEM-results of Abspoel on this type of steel, with the use of 6000 mm^2 area. The predicted failure load by the method proposed by Abspoel is quite good.

Looking at results found by using S690 steel, it can be seen that the FEM-results show very different values compared to the predicted load by Abspoel. The maximum slenderness of the web using 6000 and 12000 mm^2 is not the same, as was predicted. It can be seen that the 12000 mm^2 results for maximum slenderness are similar to those of the Abspoel extrapolation, the results of the 6000 mm^2 ultimate load do show a significantly higher value. The web slenderness is 800 (75% larger) and the failure load of about 1700 kNm (17% more than predicted). See also Figure 6 below.

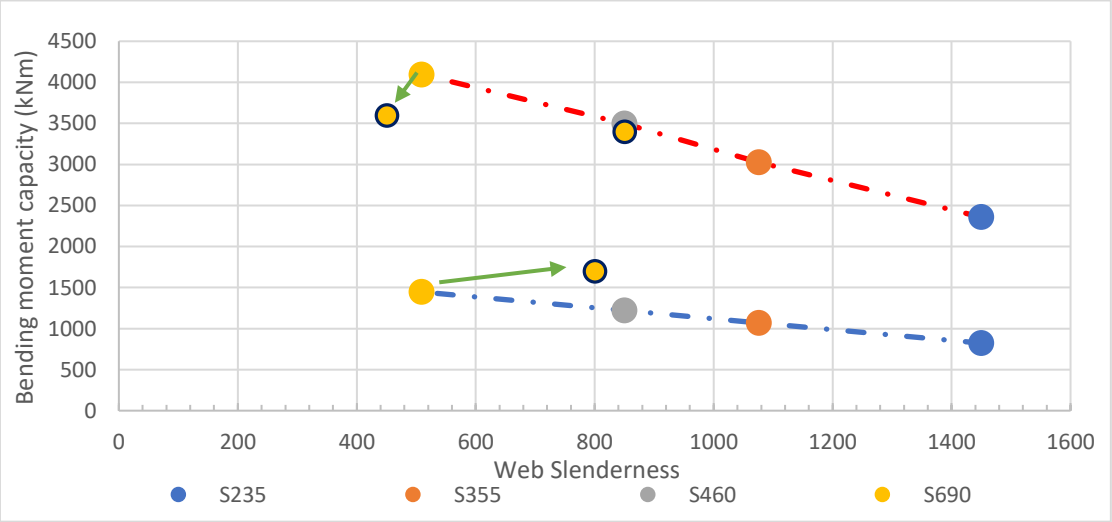

FIGURE 6: GRAPH SHOWING THE MAXIMUM BENDING MOMENT RESISTANCE AT MAXIMUM WEB SLENDERNESS (FIGURE 7-27 AND 7-29 OUT OF ABSPOEL) INCLUDING FEM RESULTS OF CIMPOI.

These results lead to questions about the dependency of the maximum web slenderness, when searching for the maximum bending moment, to the total used sectional area of steel. Abspoel assumed the maximum web slenderness was constant for a steel grade, but the result of Cimpoi seem to contradict this.

The results for 12000 mm^2 could lead to a line, which isn't linear but has a maximum (asymptotic or parabolic). The results for A=6000 mm^2 give a completely different trend. From the view of Figure 6 it could be concluded that the web slenderness is not only related to the steel grade, assumed that both the FEM-analysis results of Cimpoi or of Abspoel can be trusted. It cannot be concluded if there is a certain shape of the curve for all total areas and/or steel grades.

Looking at the FEM-models some differences have been found, which are given below:

1. Stiffener information was not given by Abspoel, Cimpoi used 12 mm steel for all transverse stiffeners.
2. Different modelling
    a. Stress-strain relation at the plastic region: incline is 2,1 vs 1,0
    b. Initial imperfections: Abspoel used a 6-sine shape + half-sine transverse imperfection, Cimpoi used the first buckling eigenmode, a 6,5-sine shape + half-sine transverse on the top part of the web.
    c. FEM-method: Marc Mentat 2005r3 vs ABAQUS
        i. Abaqus model was calculated explicitly, there was no information about Marc Mentat model described, both implicit and explicit, are possible according to website.
    d. Mesh shape and size: Cimpoi use a described mesh size of 35x35mm, Abspoel used a mesh dividing certain parts of the structure in a specific number of elements (see page 238).
    e. Shape of the girder: ending with extra plate length after stiffener vs. ending with stiffener

1.2.4. Unanswered questions

The results of both previous researches do lead to more questions which have not yet been answered. This is why there is a relevant cause for this thesis to study the behavior of steel plate girders in bending in more detail.

The results of both Abspoel and Cimpoi could not conclude if there is a constant maximum web-slenderness of steel plate girders for a specific steel grade. Abspoel concluded that this was the case, but the results of Cimpoi object against this claim. The results found by Cimpoi lead to the possibility that the maximum web slenderness is dependent on the total used area of steel, but this could not be confirmed yet. A question which first has to be answered is if the results of Abspoel and Cimpoi are valid and repeatable?

A different question concerning the behavior of the plate girders in bending is if the use of steels with a higher yield strength, than the steels tested in previous works. Is it possible to increase the maximum bending moment and if the possible increase is significant or very small? Also the web slenderness in which the maximum bending moment is achieved cannot be estimated from the earlier results.

It is also interesting to find out if the mode of failure changes in higher strength steels, because up until the S690 steel tested, the failure mode has been described as yielding of the top flange by Abspoel and Cimpoi, while earlier work by other authors described vertical buckling of the top flange as the critical failure mode.

Both the work of Abspoel and Cimpoi concluded the maximum bending moment using a typical geometry, which will be discussed later. The work of Abspoel also showed different bending capacity when the parametric study was conducted in a different way. Therefor it is of interest to critically look into the modeling of the parametric study to find out the influences of several locked parameters.

1.3. Research questions

Looking at the summation of unanswered questions above, this thesis will look into the subject of bending moment capacity of steel slender plate girders further. During this research, the main goal will be to address the question: does increasing the steel grade beyond S690 increase the capacity of unstiffened steel plate girders in bending, when it is laterally supported.

To answer this question the following sub questions will have to be answered:

First of all, we need to find out if the results found by Cimpoi are realistic and valid for S690 steel plate girders, because the results no not link easily to the results found by Abspoel. It is therefore of interest to confirm the results by numerically remodeling and retesting the girders tested by Abspoel and Cimpoi. For this part the aim is to find an answer to the following questions:

- What is the maximum bending moment capacity for S690, using 6000 mm^2 and 12000 mm^2 as total cross-sectional area?
- At which web slenderness are the above-mentioned maximum bending moments achieved?
- Which failure behavior governs the failure of steel slender plate girders using S690 steel?

After assessing the bending behavior of the S690 steel plate girders the aim is to find out what happens to the bending behavior of an unstiffened plate girder when S890 steel is used in the numerical models. Again it is the aim to find the answers to the above mentioned questions for the S690 steel.

1.4. Research methodology

This chapter gives an overview of the methodology used in this research project. The research will be split up in 4 stages. At first a study of literature, instabilities, the used software and modeling gratings will take place. After this a parametric study on the bended plate girder will be done, started with a validation of the model. After this stage analyzation and simultaneous parametric study of the shear stressed part will be done. Finally, the results will be analyzed and conclusions will be drawn from these.

1.4.1. Study phase

The literature survey will be continued to review the models describing the behavior of the shear stressed part of the plate girder and formulate statements the way to address the parametric study the most efficient. Also, a reference model must be picked to be able to validate the models which will analyze the shear stressed part of the girder. In addition, the elastic plate theory will be studied more to be able to describe the plate buckling better. Lastly, the knowledge in the use, acquiring and processing of the results from the FEM software Abaqus will be studied in this phase.

1.4.2. Validating model phase

To analyze the problem numerical study will be conducted, using the FEM-package Abaqus. The models will need to represent the real behavior of plate girders, to address this validation is needed. To validate the models, used in the analyzation of the part of the girder in bending, the models will be validated using models made by Abspoel and Cimpoi.

1.4.3. Parametric study phase

After there is enough confidence that the models describe real behavior the parametric study will take place. The parametric study on the bending part of the plate girder will be conducted to find the maximum slenderness for higher strength steels in comparison to the numerical tests done by Abspoel and Cimpoi. The steels used will be S890 and S960. The method used will be the method described by Abspoel as approach 1 [2] will be used with total cross-sectional areas of 6000 and 12000 mm^2, varying the web-slenderness of the girder.

1.4.4. Conclusion phase

After the parametric study on the bending part is completed, conclusions will be drawn about the maximum bending moment resistance of steel plate girders, using S890 and S960 steel and which maximum web slenderness is the optimal one for these types of steel. Also, the difference for 6000 and 12000mm^2 cross sectional area will be analyzed to be able to conclude if the maximal web slenderness depends on the area or is a constant for a steel type.

2. Literature study

2.1. Introduction

To describe and understand the behavior Plate girders in a 4-point bending test, a literature study has been subjected. First the elastic plate buckling theory, which is needed to describe the bending and shear-models, is presented. The classic post-buckling strength models, found in the second part of the 20th century are discussed, together with the state-of-the-art in research, predominately done using Finite Element models.

2.2. Slender plate theory

2.2.1. Elastic buckling

The plates of the plate girder web will be subjected to in-plane stresses. These stresses could result in buckling of these thin web plates the following paragraph will address this phenomenon.

The differential equation concerning this behavior is a bidirectional equation, given in (2.1), when no distributed load is applied to the plate in the out-of-plane direction, is given by Timoshenko [12].

$$\frac{\partial^4 w}{\partial x^4} + 2\frac{\partial^4 w}{\partial x^2 \partial y^2} + \frac{\partial^4 w}{\partial y^4} = \frac{1}{D}\left(N_x \frac{\partial^4 w}{\partial x^4} + N_y \frac{\partial^4 w}{\partial y^4} + 2N_{xy} \frac{\partial^4 w}{\partial x^2 \partial y^2} \right) \tag{2.1}$$

This equation governs the elastic deformations (w) of a plate, which can be solved using the boundary conditions, the shape of the plate and the applied stresses. D is the flexural rigidity of the plate, which is given by equation (2.2).

$$D = \frac{E * t^3}{12(1-\nu^2)} \tag{2.2}$$

The theory will be shown on a compressed plate first, simply supported on the 2 compressed edges, see Figure 7

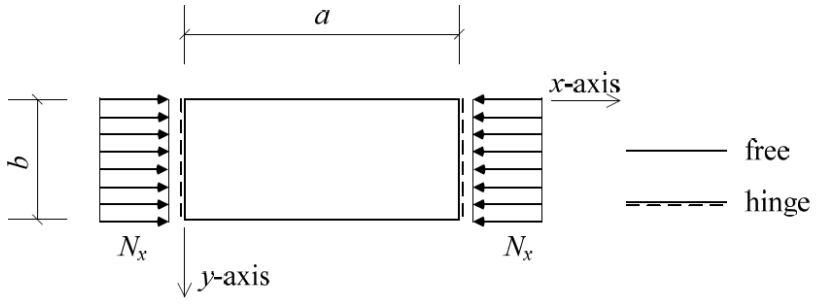

FIGURE 7: SIMPLY SUPPORTED PLATE AT X=0 AND X=A

We assume a deflection shape of a sin along the x-axis, seen in (2.3). Deriving this to the forth power and inserting it into equation (2.1), with the assumption that the horizontal force is the critical buckling force, we find equation (2.4) as general assumption.

$$w = A*\sin\left(\frac{\pi x}{a}\right) \tag{2.3}$$

$$N_x = N_{cr} = \left(\frac{\pi^2}{a^2}\right)D = -k_\sigma * \left(\frac{\pi^2}{b^2}\right)D \tag{2.4}$$

In equation (2.4) we find that k_σ should be given by (2.5).

$$k_\sigma = \left(\frac{b^2}{a^2}\right) \tag{2.5}$$

To be able to calculate the critical buckling stress, the buckling force needs to be divided by the web thickness, also with the assumption that compressive stress has a positive sign. This is shown in equation (2.6).

$$\sigma_{cr} = \frac{N_{cr}}{t_w} = k_\sigma * \left(\frac{\pi^2}{\left(\frac{b^2}{t^2}\right)}\right) * D = k_\sigma \frac{\pi^2 E}{12(1-\nu^2)\left(\frac{b}{t}\right)^2} \tag{2.6}$$

A plate in compression, with simply supported edges on all sides comes closer to the behavior of plate girders, since the plates in plate girders are connected to the flanges on the top and bottom and to the stiffeners and/or end-posts on the sides, the suggested deflections shape will be a double sin now, see equation (2.7), in this equation, we use m as a the amount of buckles formed.

$$w = A*\sin\left(\frac{m\pi x}{a}\right)*\sin\left(\frac{m\pi y}{a}\right) \tag{2.7}$$

In solving equation (2.1) we are able to find the equation (2.8) as a solution.

$$\left(\frac{\pi}{a}\right)^4 + 2*\left(\frac{m\pi}{a}\right)^2 * \left(\frac{m\pi}{b}\right)^2 + \left(\frac{m\pi}{b}\right)^4 = \frac{1}{D} * \left(-N_x * A * \left(\frac{m\pi}{a}\right)^2\right) \tag{2.8}$$

Again the general solution, given in equation (2.4), is used to find k_σ, this should be:

$$k_\sigma = \left(\frac{mb}{a}\right)^2 + 2 + \left(\frac{a}{mb}\right)^2 = \left(\frac{a}{mb} + \frac{mb}{a}\right)^2 \tag{2.9}$$

Now the critical stress can be found using equation (2.6), now with an unknown m . Altering the m will result in different critical buckling values, where the lowest is the governing one, which is different for combinations of a and b.

2.2.1.a. Simply supported plate on bending

For the calculation of the critical buckling stress on a plate loaded in bending, the same method is used. Using the general equations (2.1), (2.4) and a presumed deformation shape given in equation (2.7), with the boundaries given in Figure 8, we find the k_σ to be as given in equation (2.10).

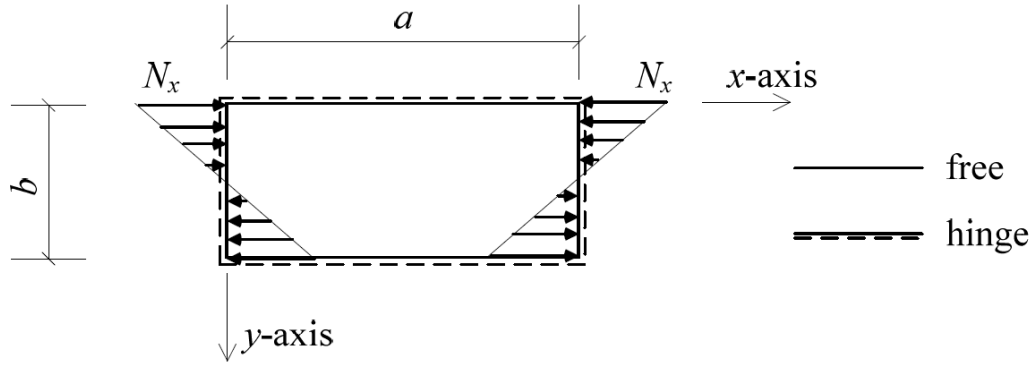

FIGURE 8: SIMPLY SUPPORTED PLATE IN BENDING

$$k_\sigma = \frac{\pi^2}{\left(\frac{a}{b}\right)^2} \frac{\left(m^2+\frac{a^2}{b^2}\right)*\left(m^2+4\frac{a^2}{b^2}\right)*\left(m^2+9\frac{a^2}{b^2}\right)}{\sqrt{\left(m^2+\frac{a^2}{b^2}\right)^2*\left(16m^2\frac{6}{25}\right)^2+\left(m^2+9\frac{a^2}{b^2}\right)*\left(16m^2+\frac{2}{9}\right)^2}} \qquad (2.10)$$

For a plate loaded in bending, it can be seen that the critical buckling stress, filling in the result of equation (2.10) into equation (2.6), is dependent on the shape of the panel (a and b), as well as the thickness of the plate. Finding the minimal k-factor, using the unknown m, leads to the smallest critical stress.

2.2.2. Non-linear plate theory

In the previous paragraph the elastic limits for plate girders were found. Until the critical stress is reached the stresses are linear and uniform over the cross section. The elastic theory also has a limitation in the use of perfect plates. In theory the plates will have to be perfectly flat to be able to achieve this buckling stress. In reality plates, and especially very thin plates, will never be perfectly flat, the impact of the imperfections in thin plates is also great. In addition to this, researchers found post-buckling strength in plate girders, which can't be described by the elastic theory, therefor non-linear theory is needed.

The theory describes the redistribution of stresses after buckling of the plates, changing from a uniform to a non-uniform distribution. This behavior is a complex issue, using membrane stresses, shear stresses, deformations and applied loads in differential equations, described by Von Kármán, to form a solution.

Von Kármán [13] determined an effective width to describe ultimate load of the plates, in 1932, for plates under compression. In this theory failure occurs when the largest edge stress in the plate reaches the yield level. The force needed to achieve this is found using the critical plate buckling stress and with this force the effective width is calculated. The width of this part of the plate is given by equation (2.11).

$$\sigma_{cr} * b * t = f_y * b_{eff} * t \tag{2.11}$$

It can also be written as the Von Kármán effective width-formula, given in equation (2.12).

$$b_{eff} = b\sqrt{\frac{\sigma_{cr}}{f_y}} \tag{2.12}$$

Using the well-known parameter for column buckling, given in (2.13) , the following expression, (2.14) is valid for a plate in uniform compression.

$$\lambda_p = \sqrt{\frac{\sigma_{cr}}{f_y}} = 1.05\frac{b}{t}\sqrt{\frac{f_y}{k_{cr} * E}} \tag{2.13}$$

$$\frac{b_{eff}}{b} = \frac{1}{\lambda_p}, \quad \text{for } \lambda_p \geq 1 \tag{2.14}$$

This equation is only theoretical, but offers an easy design method and the start of other research in effective width. Winter [14], used experimental research to find a change in the equation describing the effective width, given in equation (2.15). The factor 0.22 was first established as 0.25 but changed later.

$$\frac{b_{eff}}{b} = \frac{1}{\lambda_p} * \left(1 - \frac{0.22}{\lambda_p}\right), \quad \text{for } \lambda_p \geq 0.55 \tag{2.15}$$

Other authors modified the von Kármán equation as well, Gerard in 1957 proposed equation (2.16) and Faulkner in 1965 proposed

$$\frac{b_{eff}}{b} = \frac{1.05}{\lambda_p} * \left(1 - \frac{0.26}{\lambda_p}\right), \quad \text{for } \lambda_p \geq 0.55 \tag{2.16}$$

$$\frac{b_{eff}}{b} = \frac{0.82}{\lambda_p^{0.85}} \tag{2.17}$$

2.3. Plate girders subjected to bending

In this paragraph the main focus is to address the models describing maximum bending moment of a given plate girder. An important factor in these models is the range of structures in which it can be used, because the authors presented limitations for their models to be used on. The model limits are given in an applicable range of web-slenderness'. In earlier work Abspoel [2] and Cimpoi [3] described the models thoroughly, this paragraph uses there work.

2.3.1. Maximum web slenderness

In general, the moment capacity of plate girders will increase when the distance, as it is the lever arm for the force-couple made of the axial forces in the flanges, between the flanges increases and when the flange area is increased. The distance between the flanges is the height of the girder, which is one of the two factors in the web slenderness of the girder.

Basler suggested a limitation to this web slenderness, given by equation (2.18). This limitation is based on experimental research done at the Lehigh university, by Basler and Thürlimann [13] and [5] in which one of the girders experienced failure by vertical buckling of the compressive flange into the web.

$$\beta_w = \frac{h_w}{t_w} = 0.55 \frac{E}{f_{yf}} \sqrt{\frac{A_w}{A_f}} \tag{2.18}$$

2.3.1.a. Maximum slenderness according to Basler

The model, which Basler used to describe the vertical buckling of the flange, models the web as compressive columns, pin-jointed to the flanges, seen in Figure 9. The columns are compressed by the curvature of the girder due to a bending force. To prevent the flange from buckling into the web, the applied force will have to be smaller than the critical buckling resistance of the column, given by equation (2.19).

$$\sigma_{cr} = \frac{\pi^2 E}{12\left(1-\nu^2\right)\left(\frac{h_w}{t_w}\right)^2} \tag{2.19}$$

And the applied force is the vertical component of the top flange force, depended on the curvature of the girder, which is the strain of the flange divided by half of the height of the girder, given in equation (2.20).

$$F_{f.v} = F_{f.ax} * \kappa = A_f * f_{yf} * \frac{\varepsilon_f}{0.5 h_w} \tag{2.20}$$

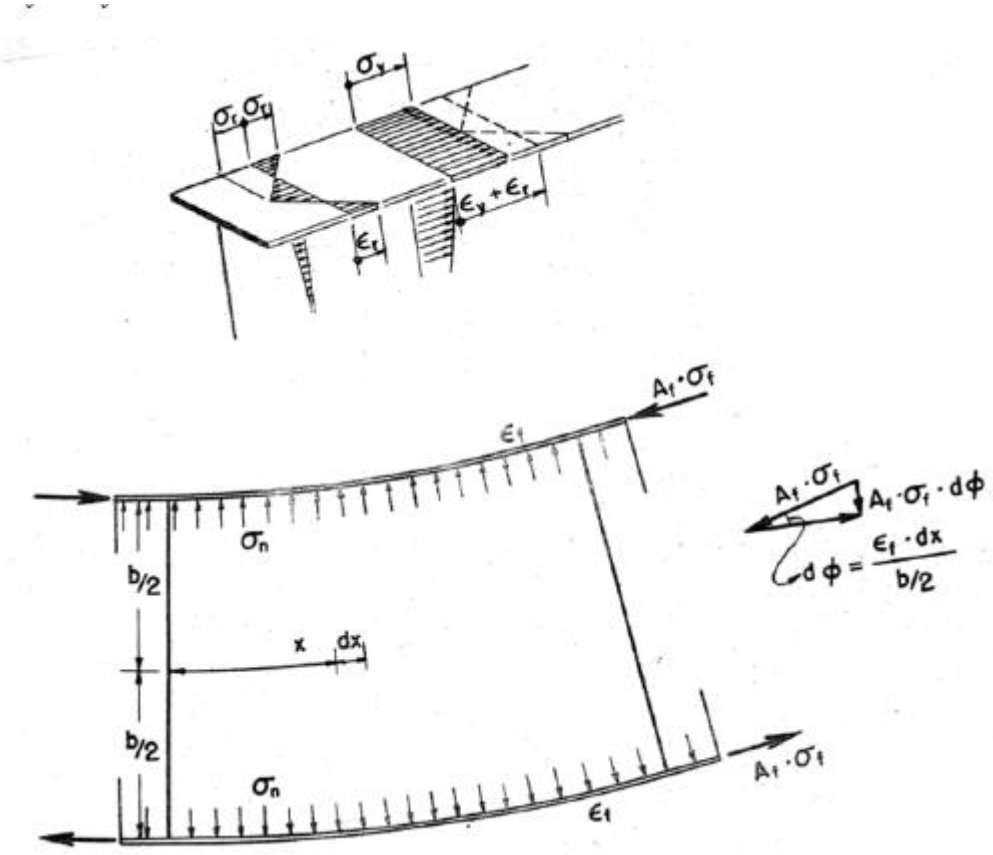

FIGURE 9: BASLER'S MODEL FOR VERTICAL BUCKLING OF THE COMPRESSED FLANGE

When equation (2.20) is now divided by the web thickness, an applied stress is found. Making this equal to the critical column stress, gives a maximum for the web slenderness, this is shown in equation (2.21).

$$\sigma_v = A_f * f_{yf} * \frac{2\varepsilon_f}{h_w * t_w} \approx \frac{A_f}{A_w} * 2\varepsilon_f * f_{yf} = \frac{\pi^2 E}{12\left(1-\nu^2\right)\left(\frac{h_w}{t_w}\right)^2} \qquad (2.21)$$

$$\beta_{w.\max} = \sqrt{\frac{\pi^2 E}{12\left(1-\nu^2\right)} * \frac{A_w}{A_f} * \frac{1}{\varepsilon_f * f_{yf}}}$$

Using Basler's assumptions that the strain is more than the yield strain, due to residual stresses from welding and using his assumption for the residual stress being half the yield stress, we find equation (2.22).

$$\varepsilon_f = \frac{f_{yf} + \sigma_r}{E}, \sigma_r = \frac{f_{yf}}{2}, \beta_{w.\max} = \sqrt{\frac{\pi^2 E}{12\left(1-\nu^2\right)} * \frac{A_w}{A_f} * \frac{1}{\left(\frac{2f_{yf}}{3E}\right) * f_{yf}}} \qquad (2.22)$$

$$\beta_{w.\max} = 0.55 \frac{E}{f_{yf}} \sqrt{\frac{A_w}{A_f}}$$

If S235 is used, using a web to flange ratio of 1, the maximum web slenderness prescribed by Basler is 491, S355 lead to 325 and S460 gives a maximum web slenderness of 251.

The to be tested steel grades S690 and S890 would be limited to a web slenderness of 167 and 129

2.3.1.b. Remarks on maximum web slenderness

Abspoel [1], [2] did experimental and numerical research on plate girders in bending, using the results of Basler to validate the numerical model. It was concluded that vertical buckling of the compressive flange is not the governing failure mode for plate girders in bending and the web slenderness is therefore not limited by this failure mode.

Abspoel tested girders made up from S235 steel, up to a web slenderness of 800 experimentally and up to 1450 using FEM analysis, without observing this vertical buckling behavior before the ultimate moment was applied. The phenomenon occurred, but only after the ultimate load was recorded. The governing failure mode observed was yielding of the flanges.

Unterweger and Kettler [16] also did numerical research on plate girders subjected to bending and concluded that the limit given by (2.22) was very conservative and using normal calculation methods up to a web slenderness of 900 would give safe results.

2.3.2. Bending resistance models

Several authors have described ultimate bending resistance of plate girders. The first part of the resistance is the elastic resistance, limited by buckling of the plate girder, which has been described by Timoshenko, also to be found in paragraph 2.2.1. The post-buckling models use 2 approaches in general. The most common is the use of an effective width method. These methods take the non-uniform bending stress distribution in thin plates into account, using an effective part of the cross section to calculate an ultimate bending moment resistance, using the yield limit of the applied steel. The other general direction in calculation methods uses a reduced stress in a full cross section to calculate the maximum bending moment resistance.

The following paragraph will describe ultimate bending moment models briefly

2.3.2.a. Bending model by Basler

The model proposed by Basler [5], [15] makes use of an effective width. The effective part of the compressive side is purely dependent on the thickness of the web and given in Figure 10. The flanges are fully effective, as well as the tensile part of the web. The compressive part of the web is 30 times the web thickness.

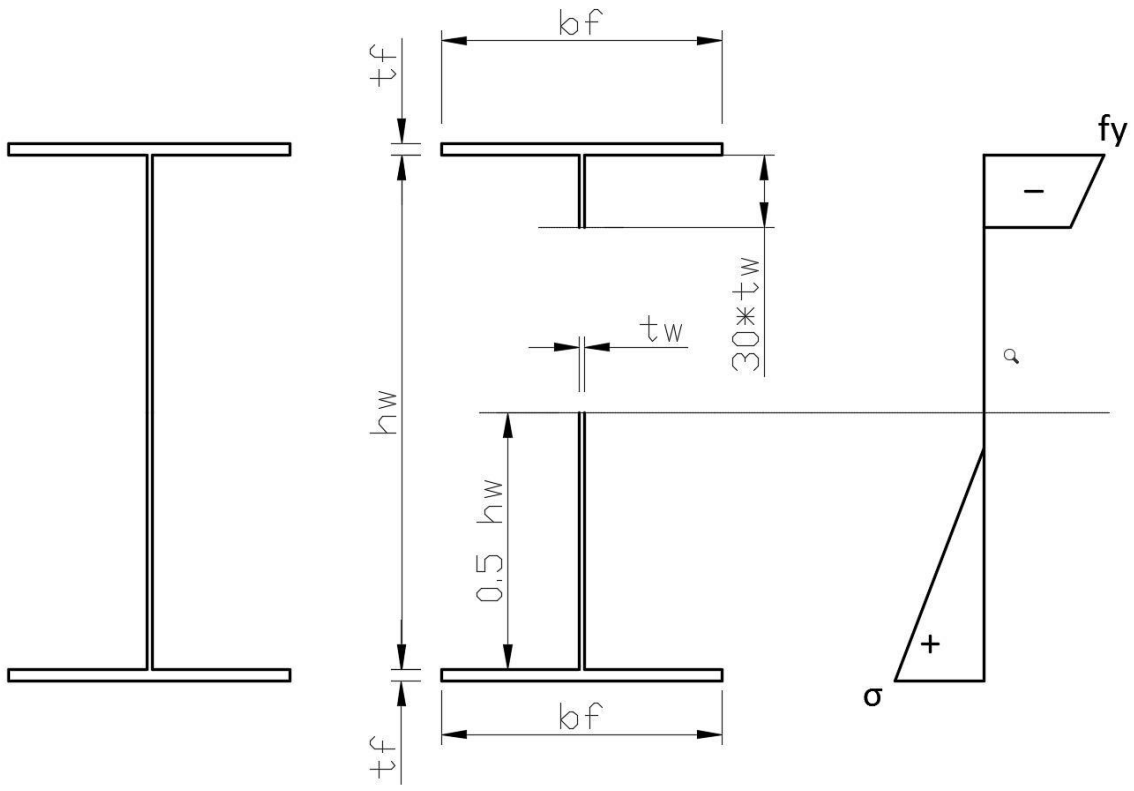

FIGURE 10: EFFECTIVE WIDTH MODEL IN BENDING, BY BASLER

The ultimate bending moment can be found using the picture, but can also be found using following equation (2.23), where the elastic moment of the full cross section is reduced or increased.

$$\xi = \frac{M_u}{M_{el}} = \frac{W_{eff} * f_y}{W_{el} * f_y} = 1 - C * (\beta_w - \beta_0)$$

$$C = \frac{A_w}{2000 A_f}, \qquad \text{for } \frac{A_w}{A_f} < 2 \tag{2.23}$$

$$\beta_0 = 5.7\sqrt{\frac{E}{f_y}}$$

The reduction occurs when the web slenderness is less than β_0, otherwise it is increased due to strain hardening, which would happen in a stocky plate girder.

2.3.2.b. Bending model by Herzog

The model proposed by Herzog is a reduced stress method, in which the maximum stress in the compressive part of the web is reduced to half the yield stress. The neutral axis will therefor at 1/3th of the web height, from the tensile flange. This is based on the assumed stresses found by Herzog, seen in Figure 11.

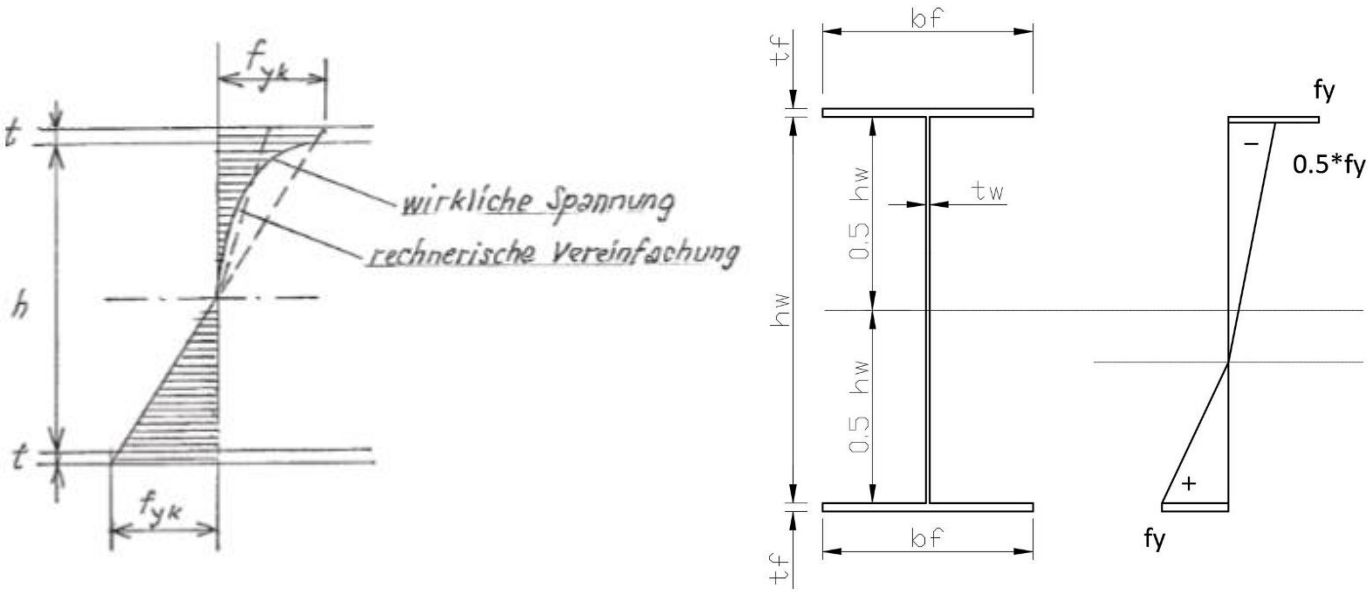

FIGURE 11: ASSUMED STRESS DISTRIBUTION AND ENGINEERING MODEL FOR A PLATE GIRDER IN BENDING, BY HERZOG

The bending moment resistance can then be found using equation (2.24).

$$M_u = K_1 * K_2 * K_3 * A_f * f_{yf} \left(h_w + t_f\right) + \frac{1}{9} A_w * f_{yw} * h_w \tag{2.24}$$

This found moment is reduced using factors which take the influences of 3 types of buckling into account, namely torsional buckling (K_1) of the girder and horizontal (K_2) and vertical buckling of the compressive flange (K_3), which are given below, in equation (2.25).

$$K_1 = \sqrt{\frac{16 * t_f}{b}} < 1.0$$
$$K_2 = \sqrt{1 - \left(\frac{\lambda_y}{70}\right)^2} < 1.0 \qquad (2.25)$$
$$K_3 = 1.17 - \frac{h_w}{2000 * t_w} < 1.0$$

2.3.2.c. Bending model by Veljkovic and Johansson

The model described by Veljkovic and Johansson [17] in 2004 can be used to predict the moment resistance of plate girders with homogeneous and hybrid material use. It gives an equation for cross sections which belong to cross section class 3 and 4, reducing the effective section modulus of the girder, given in the European code EC3-1-5 (2.26). This effective section modulus is given in (2.27).

$$M_{Rk} = f_{yf}\left(W_{eff} - \Delta W\right) \qquad (2.26)$$

$$W_{eff} = W\left[1 - 0.1\frac{A_w}{A_f}\left(1 - 124\varepsilon\frac{t_w}{h_w}\right)\right], \quad \text{for } \frac{h_w}{t_w} > 124\varepsilon, \quad \varepsilon = \sqrt{\frac{235}{f_{yf}}} \qquad (2.27)$$

The reduction is given by equation (2.28), it can be seen that a plate girder made from a homogeneous material will not be reduced.

$$\Delta W = h_w A_w \left(1 - \frac{f_{yw}}{f_{yf}}\right)^2 * \frac{\left(2 + \frac{f_{yw}}{f_{yf}}\right)}{12} \qquad (2.28)$$

2.3.2.d. Bending model by Stark

Stark [11] did research in effective width models used to describe the moment capacity of plate girders and proposed a simplification. This model, based on truss action is shown in Figure 12. It can be seen that the tensile web contribution is significantly lowered in comparison to for example Basler and Herzog. Both the compressive and tensile side are equal in length, both being (2.29).

$$b_{w.eff} = 0.85 * t_w * \sqrt{\frac{E}{f_y}} \qquad (2.29)$$

The moment capacity is given by equation (2.30), and can be found on Figure 12.

$$M_u \approx A_f * \left(h_w + t_f\right) * f_y + b_{w.eff} * t_w \left(h_w - b_{w.eff}\right) * f_y \left(1 - \left(\frac{h_w - 0.5 b_{w.eff}}{2} / \frac{h_w + t_w}{2}\right)\right) \qquad (2.30)$$

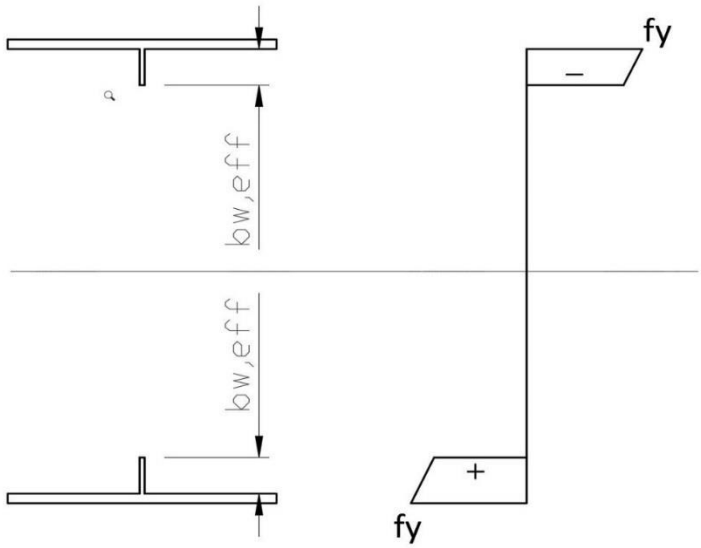

FIGURE 12: EFFECTIVE WIDTH MODEL BY STARK

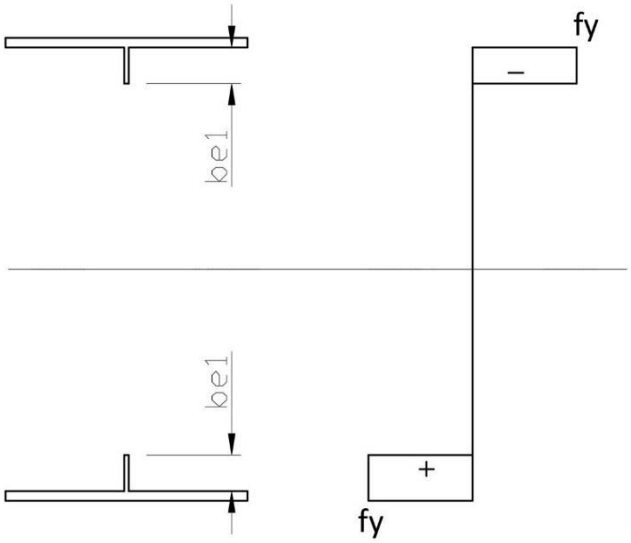

FIGURE 13: EFFECTIVE WIDTH MODEL, PROPOSED BY ABSPOEL

2.3.2.e. Bending model by Abspoel

Abspoel [2] proposed an effective width model, similar to the model of Stark, based on experimental research done. The model also uses the same specific effective width for both the compressive as well as the tensile part of the web. This effective width is the width found using an equation given in EC3-1-5 for plated structures. The stress used in the model is always the yield strength of the material, there for the moment capacity of the plate girder is given by equation (2.31), and is shown on Figure 13.

$$M_{u.Abspoel} = \left[A_f * \left(h_w + t_f \right) + b_{e1} * t_w * \left(h_w - b_{e1} \right) \right] * f_y \qquad (2.31)$$

2.3.3. Eurocode 1993-1-5 for plated structures on bending

The Eurocode has a specific code to address steel plated structural elements [18], also used to design steel plate girders. The code, based on research of different authors, gives information about the way to calculate the structures, using an effective width method and a stress reduction method.

Chapter 4 shows the equations to calculate the effective width of an axially loaded plates, which is the case for webs and flanges of plate girder in bending. The tensile side of the girder is assumed to be fully effective.

The calculation is based on the stress distribution in the cross section and the slenderness of the cross section, given in (2.32).

$$\bar{\lambda}_p = \sqrt{\frac{f_y}{\sigma_{cr}}} = \frac{\bar{b}/t}{28.3\varepsilon\sqrt{k_\sigma}} \qquad (2.32)$$

$$\psi = \sigma_2 / \sigma_1, \text{ with } \sigma_1 = \sigma_c = \text{positive}$$

Using these expressions the effective compressive area can be found, with the use of equation (2.33)

$$A_{c.eff} = \rho * A_c \qquad (2.33)$$

Where the reduction factor can be found using equation (2.34), which is used for internal members, like the web of the plate girder. If the slenderness is less than the value given in the top part, there is no reduction in area of the compressed part. If the situation of pure compression is addressed ($\psi = 1$) than the bottom equation becomes the winter equation, given in (2.15).

$$\rho = \begin{Bmatrix} 1,0 & \text{for } \bar{\lambda}_p \le 0.5 + \sqrt{0.085 - 0.055\psi} \\ \dfrac{\bar{\lambda}_p - 0.055(3+\psi)}{\bar{\lambda}_p{}^2} \le 1 & \text{for } \bar{\lambda}_p > 0.5 + \sqrt{0.085 - 0.055\psi} \end{Bmatrix} \qquad (2.34)$$

For a beam loaded in bending, there will be a compressive stress in one of the flanges and a tensile stress in the other flange, therefor ψ will be smaller than 0. Table 4.1 from [18] gives the effective width (2.35) and the plate buckling factor (2.36) for this case.

$$b_{eff} = \rho * b_c = \frac{\rho * \bar{b}}{1-\psi} = b_{e1} + b_{e2} = 0.4 * b_{eff} + 0.6 * b_{eff} \qquad (2.35)$$

$$k_\sigma = \begin{Bmatrix} 7.81 + 6.29\psi + 9.78\psi^2, & \text{for } 0 > \psi > -1 \\ 23.9, & \text{for } \psi = -1 \\ 5.98(1-\psi)^2, & \text{for } -1 > \psi \ge -3 \end{Bmatrix} \qquad (2.36)$$

In chapter 8 the code specifies a maximum slenderness of the web for the compressive flange to not buckle into the web. The limitation is given by equation (2.37) for elastic bending and is found by Basler, see paragraph 2.3.1.a.

$$\frac{h_w}{t_w} \le k \frac{E}{f_{yf}} \sqrt{\frac{A_w}{A_{fc}}}, \quad k = 0.55 \tag{2.37}$$

The model to find the bending moment capacity is shown in Figure 14, which shows the neutral axis travels downwards to be able to find equilibrium. The stress in the bottom does not have to be equal to the yields stress. With flanges having the same yield stress and area, the bottom flange is likely to not yield in this model.

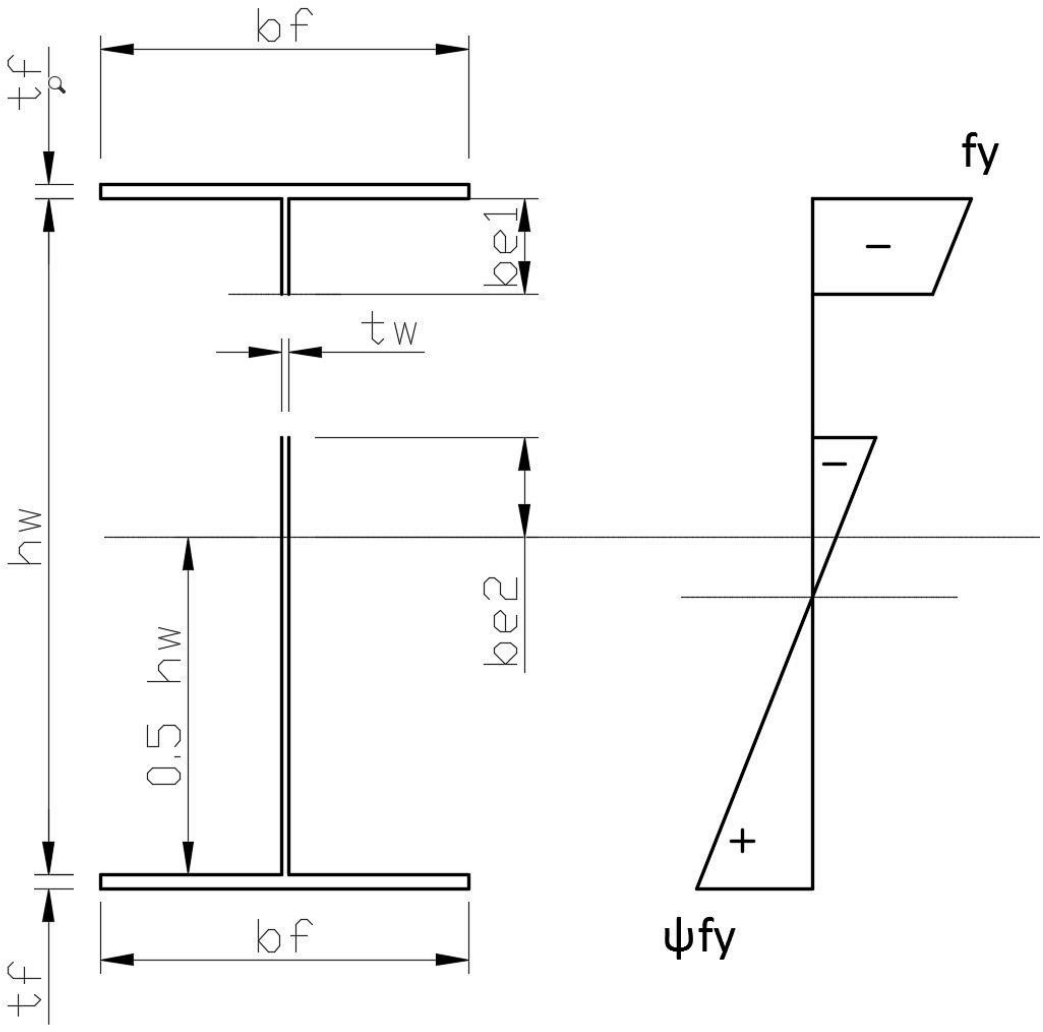

FIGURE 14: EN1993-1-5 EFFECTIVE WIDTH METHOD

2.3.4. Plate girder optimization for bending

In the previous chapter models for the calculation of the ultimate moment capacity of plate girders are described. A major role in this capacity are the flange dimensions and the web height, as well as the limiting maximum slenderness of the web. The height of the plate girder cannot be increased unlimitedly and be infinitely thin for it to work as a combined section.

In this view several authors have tried to find optimum dimensions for plate girders, trying to direct the material to the most efficient places.

2.3.4.a. Optimization by Stark

Stark [11] found optimization equations for plate girders, taking into account the strength, stiffness and stability of the girder, using a iterative process. The applied moment and shear force must be calculated and are used as input for the iteration. Either the height of the girder or the thickness of the web, or both, can be chosen as a starting value to speed up the iteration process.

The optimization equations are given for 2 methods. The first is the classic stress-reduction method. The optimization, for a girder loaded by only a moment, for the web dimensions and the total area are given below in (2.38), with M being the moment in N/mm^2

$$\begin{aligned} t_{opt} &= 0.007632\sqrt[3]{M} \\ h_{opt} &= 0.915 * \sqrt{\frac{235}{f_y}} * \sqrt[3]{M} \\ A_{tot.opt} &= 0.014\sqrt{\frac{235}{f_y}} * \sqrt[3]{M^2} \end{aligned} \tag{2.38}$$

The second method is a section-reduction method, which is more advanced. The optimization is given below, in equation (2.39).

$$\begin{aligned} t_{opt} &= \sqrt[3]{M} * \sqrt[3]{\frac{1}{\lambda\sqrt{f_y} * \left(\lambda\sqrt{f_y} - 513.3\right)}} \\ h_{opt} &= \frac{1}{f_y} * \sqrt[3]{M} * \sqrt[3]{\frac{\left(\lambda\sqrt{f_y}\right)^2}{\left(\lambda\sqrt{f_y} - 513.3\right)}} \\ A_{tot.opt} &= \frac{1}{f_y} * \sqrt[3]{M^2 * \frac{27\left(\lambda\sqrt{f_y} - 513.3\right)}{\left(\lambda\sqrt{f_y}\right)^2}} \end{aligned} \tag{2.39}$$

In this equation the maximum slenderness gives the best dimensions for a plate girder in bending. This slenderness is limited by (2.40), which is based on the vertical buckling of the compressive flange into the web.

$$\lambda_{\max} = 357 * \left(\frac{235}{f_y} \right) \tag{2.40}$$

The flange dimensions are found by using equation (2.41), which is an equation based on warping of the flange.

$$\begin{aligned} b_f &= \sqrt{A_f * 27 * \sqrt{\frac{235}{f_y}}}, A_f = 0.5 * \left(A_{tot} - A_w \right) \\ t_f &= \frac{b_f}{27\sqrt{\frac{235}{f_y}}} \end{aligned} \tag{2.41}$$

With the use of equations above a plate girder can be dimensioned for a specific applied moment.

2.3.4.b. Optimization by Abspoel

Abspoel [2] found several important factors about the optimization of plate girders, during experimental, analytical and numerical research.

During experimental tests on plate girders made from S235 steel, it was noticed that the maximum slenderness of plate girders can be largely increased. As well as the failure mode which the maximum slenderness would govern, which Basler assumed to be vertical buckling of the compressed flange into the web, did not appear. A slenderness of 800 was found to be stable and governed by yielding of the flanges.

Abspoel found that the most influential geometric factor in moment resistance was the height of the girder, followed by the width and thickness of the flange in comparing the extra moment capacity with respect to the extra weight. The relative extra capacity for 10% extra web height was 6.2%, the relative increase due to 10% increase in one of the flange parameters was 2.5% for both the thickness and the width. It was found that increasing the web thickness by 10%, the relative moment capacity decreased by 1.8%

Using the method to calculate the ultimate bending moment by Abspoel (2.31) it was found that the optimum ratio between the areas of the flange and the web was asymptotic and decreasing towards 1.0 with increasing web slenderness and also dependent on the steel quality, see Figure 15.

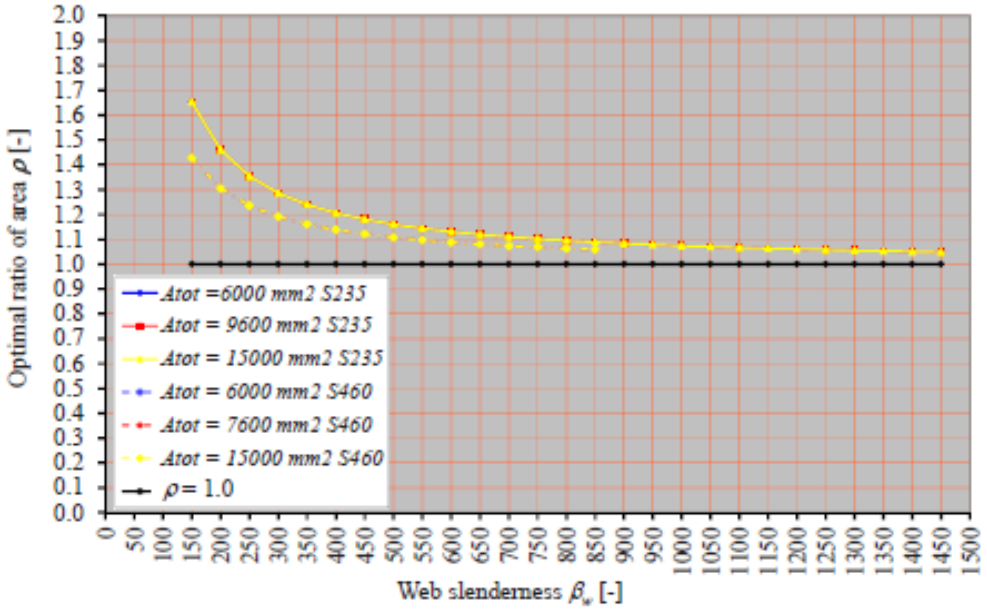

FIGURE 15: OPTIMAL RATIO OF AREA VERSUS THE WEB SLENDERNESS FOR S235 AND S460 [2]

It was also shown that using 1.0 as an approximation in calculating the maximum bending moment would not result in significant loss of moment capacity, especially with increasing web slenderness. This justifies the choice of Abspoel to use of 1 as the ratio between web and flange area in the parametric study to find the optimum web slenderness in plate girders for specific amounts of cross-sectional area.

The results of this parametric study for areas of 6000 and 12000 mm^2 are given below on Figure 16 and Figure 17, with added inter- and extrapolations in S355 and S690. It was found, using FEM analysis, that

the moment resistance of plate girders made from S235 steel increases up to a web slenderness of 1450. And web slenderness's up to 850 for S460 is still increasingly beneficial.

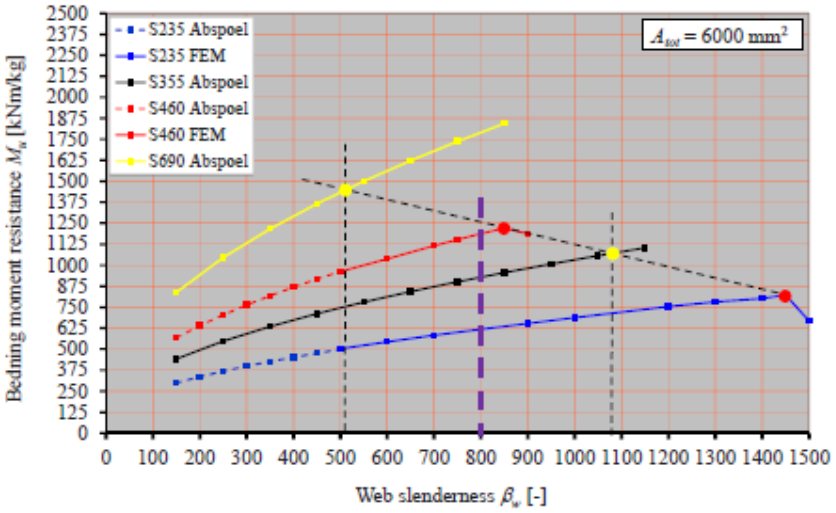

FIGURE 16: BENDING MOMENT RESISTANCE FOR P = 1 AND A= 6000 MM²

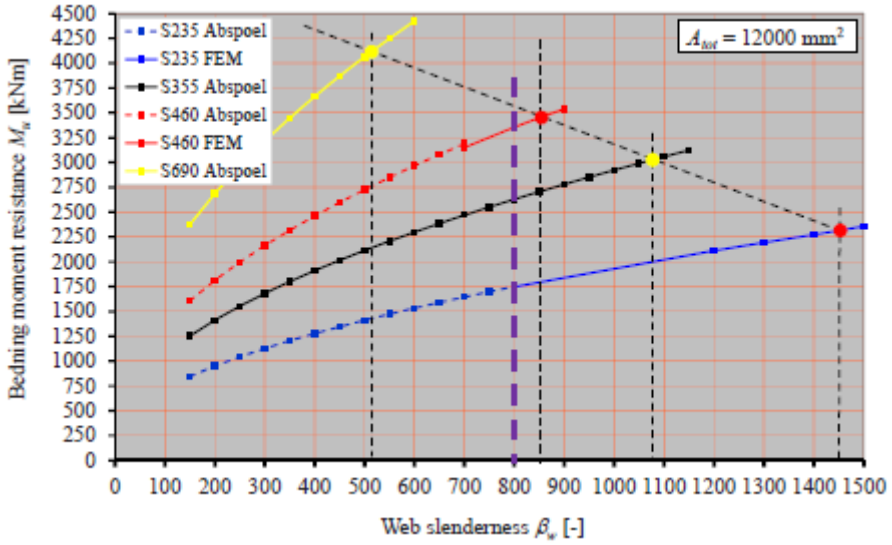

FIGURE 17: BENDING MOMENT RESISTANCE FOR P = 1 AND A= 12000 MM²

Both figures show the same maximum web-slenderness although a rise in moment capacity after the limiting value can be observed in Figure 17. Abspoel concluded that the web slenderness was a constant for a given steel grade, linearly reducing by increasing the steel grade. The found maximum web slenderness's are given in Table 3, in which the dark columns are FEM-results and the light columns are inter- and extrapolated results.

ρ=1, β_f=20	S235		S355		S460		S690	
A	6000	12000	6000	12000	6000	12000	6000	12000
$B_{w,max}$	1450	1450	1076	1076	850	850	509	509
$M_{u,max}$	822,4	2357,4	1068,5	3025,9	1220,3	3495,4	1445,7	4095,4

TABLE 3: RESULTS OF FEM BY ABSPOEL AND INTER-/EXTRAPOLATION OF THESE RESULTS

2.3.4.c. Research Cimpoi to optimize the bending capacity

The goal of the research of Cimpoi [3] was to increase the range of FEM-analysis conducted by Abspoel and to address higher strength steels. The assumptions for maximum web slenderness and maximum moment capacity on S690 girders of 6000 and 12000 mm^2 by Abspoel where checked using FEM-software Abaqus. Also, an extra analysis on S460 girders with 12000 mm^2 area was conducted.

Cimpoi found that the tested girders did not fail on flange induced buckling of the compressive flange into the web and that the maximum web slenderness's where found, which are given in Table 4. A significant difference in maximum slenderness can be observed between the different areas in S690 steel, where the S460 steel test on 12000 mm^2 by Cimpoi resulted in the same maximum slenderness as the test of Abspoel on 6000 mm^2 total area.

ρ=1, β_f=20	S460	S690	
A	12000	6000	12000
$B_{w,max}$	850	800	450
$M_{u,max}$	±3400	±1700	±3600

TABLE 4: RESULTS OF FEM ANALYSIS BY CIMPOI

3. Numerical model validation

3.1. Introduction

To be able to assess the questions given in paragraph 1.3, the models will have to be compared to experimental test data to be able to confirm if the reaction of the model is a realistic representation of the real behavior. The aim of this chapter is to find proof of the effectiveness of the model to represent the real behavior of steel plate girders.

The validation will be done using numerical data found by Abspoel. This numerical data was found by his FEM-analysis validated on experimental data found by 2 authors. The assumption that the validated models based on the experimental data also lead to realistic behavior has to be used. If both datasets are comparable the model will be found suited to describe the behavior of the plate girder and therefor can be used to analyze a wider variety of comparable geometries.

3.2. Model description

The model, in which a 4-point bending test will be used to analyze the structures, will be validated using 2 different results found by Abspoel [2], during his numerical parametric study to address the maximum bending resistance of steel plate girders.

Abspoel did numerical research on a FEM-model, which was validated on experimental research conducted by Basler [15] in the 1960's. This model was then used to model the geometry of the experiments done in Delft by Abspoel and again checked for its accuracy to represent the real behavior, which showed to overestimate the resistance by 0-4 % in maximum bending for 8 out of 10 tests, the other two results overestimated it by 7 and 13%.

The FEM-model, used in Marc-software, was therefor found good enough to use in a parametric study to find the optimum geometry for maximized bending resistance in steel plate girders. The validated model was used for a series of parametric studies to first find the most influential parameters and after this the ultimate bending moment resistance using several different approaches.

The 2 models to validate the current model, were used by Abspoel in the parametric study in which only influence of the web slenderness was analyzed. The models had a total cross-sectional area of 6000 mm^2, using S235 steel and having a with a web slenderness of 700 and 1000. These models were also used by Cimpoi [3] to validate her model.

3.2.1. Overall geometry

For the original numerical and experimental tests, the plate girders were made from only one type of steel, using different thicknesses over the geometry. The overall layout of the girder, is given in Figure 18. The length of the span is dependent on the web height. The plate girder consists of 4 different sections: The flanges, the transverse stiffeners, the web panel in the middle and the web panel in the end-panels. In this model the middle section is tested, using 2 places for the load to be applied in the y-direction.

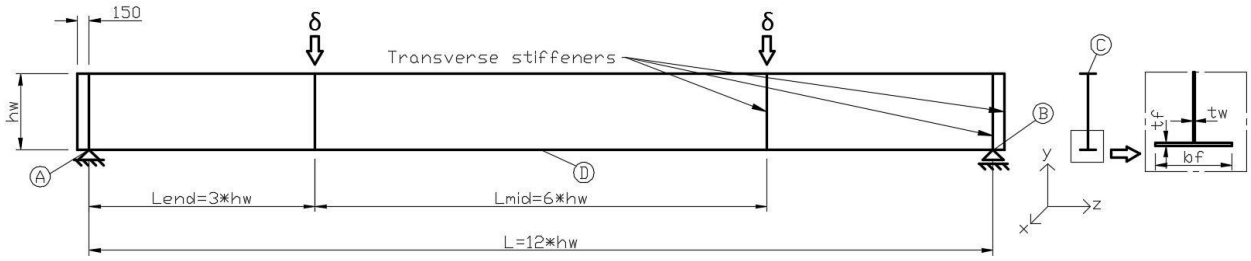

FIGURE 18: OVERALL LAYOUT OF THE PLATE GIRDERS TESTED ON BENDING

The boundary conditions are given in Table 5, in which the points refer to Figure 18. Point D isn't limited in its deflection, but is important because this is the midspan point in which the deflection is recorded. Point A and B are the points in which the flange, the web and the stiffener collide. In this point the movement is limited in the x-direction. The y-direction displacement is fixed over the full width of the bottom flange.

Point C is the point in which the web connects to the top flange. In this point the lateral movement is fixed over the full length of the beam to resemble the effect of the lateral bracing used in the experimental tests.

TABLE 5: BOUNDARY CONDITIONS FOR THE NUMERICALLY MODELLED PLATE GIRDERS.

Point in figure	u_x	u_y	u_z	Rotations
A	Fixed	Fixed (over full width)	Fixed	Free
B	Fixed	Fixed (over full width)	Free	Free
C	Fixed (over full length)	Free	Free	Free
D	Free	Free	Free	Free

TABLE 6: BOUNDARY CONDITIONS FOR THE NUMERICALLY MODELLED PLATE GIRDERS.

3.2.2. Dimensions

The dimensions are chosen to be able to force the mid-section to fail first. To be able to achieve this, the end-panel webs are modeled to be very thick in comparison with the web of the middle part of the girder. Over dimensioning is also done with the thickness of the transverse stiffeners, for the same purpose. In the following paragraphs each part will be addressed in further detail and a summary is given in Table 7. Since Abaqus is a FEM-program which is not based on specific units, it's of key importance to work systematically with respect to the units in use. For this model the base units will be millimeter and Newton were used. The geometry was built up from shell elements which have been given a specific thickness, according to the following paragraphs.

3.2.2.a. Total cross-sectional area

The girders are modelled to be able to compare them in efficiency. This has been described by Abspoel as the bending moment resistance of the cross section divided by the weight of the cross section. To be able to simplify this comparison Abspoel used a constant cross-sectional area in his "approach 2". For this model, the total cross-sectional area is 6000 mm^2.

3.2.2.b. Ratio between web and flange area

In the parametric study done by Abspoel, the girders with a ratio of area between flange and web of 1,0, where shown to have the highest efficiency. Therefore, in this validation model this ratio is also used and the flange area, as well as the web area are taken as 2000 mm^2.

3.2.2.c. Flanges

The top and bottom flanges are modelled with the same dimensions, the dimensions are chosen so that the top flange in compression is just a class 2 cross section, in accordance with EN 1993-1-1, table 5.2. [19], shown below. Taking this into account the following equation (3.1) should be justified:

$$\frac{c}{t} \le 10 * \varepsilon \approx \frac{0.5 * b_f}{t_f} \le 10 * \varepsilon, \ \varepsilon = \sqrt{\frac{235}{f_y}} \tag{3.1}$$

For the total area to be 2000 mm^2, with the use of S235 steel, the flange width will be 200mm and the thickness 10mm.

3.2.2.d. Webs

The web height, in the parametric study done by Abspoel, where shown to influence the moment resistance capacity largely. Therefor the dimensions of this parameter were varied to find the optimal steel distribution in the steel plate girders bounded by the previous boundaries.

The dimensions can be calculated using the equations (3.2) and (3.3) below.

$$t_w = \sqrt{\frac{A_w}{\beta_w}} = \sqrt{\frac{\rho}{\rho + 2}} * \sqrt{\frac{1}{\beta_w}} * \sqrt{A_{tot}} \tag{3.2}$$

$$h_w = \beta_w * t_w = \sqrt{\frac{\rho}{\rho + 2}} * \sqrt{\beta_w} * \sqrt{A_{tot}} \tag{3.3}$$

The web panel in the end-panels is over dimensioned and taken as 12mm.

3.2.2.e. Stiffeners

The stiffeners are used to help introduce both the induced displacement and the reaction forces into the plate girder gradually and without local failure. Because the stiffeners are not subjected to this study and may not fail during testing, the stiffeners are over dimensioned to prevent this. The plates are given a thickness of 12 mm, spanning from flange to flange and they have a width in x-direction equal to that of the flanges.

Global geometry	Bw700	Bw1000	
Total span	14198.591	16970.563	mm
Length mid-section	7099.296	8485.281	mm
Length end panel	3549.648	4242.641	mm
End-post length	150	150	mm
Total area	6000	6000	mm^2
Flange area (per flange)	2000	2000	mm^2
Web area	2000	2000	mm^2
Flanges			
Flange width	200	200	mm
Flange thickness	10	10	mm
Webs			
Web height	1183.216	1414.214	mm
Web thickness	1.690	1.414	mm
Thickness end-panel	12	12	mm
Transverse stiffeners			
Stiffener thickness	12	12	mm
Stiffener width	200	200	mm

TABLE 7: DIMENSIONS FOR BOTH MODELS USED IN THE VALIDATION

3.3. Material properties

3.3.1. Stress-strain relationship

The material properties used in the model will have to be modeled carefully to avoid unrealistic behavior. When a beam, with enough capacity to rotate and enough stability to get to the yield limit of the material, is loaded with increasing deformation, at a certain point the force needed will have a maximum. This maximum is found when the full cross section is yielding. When the beam is now loaded further, the resulting maximum force will stay constant for some time before failure occurs.

To model this, in engineering practices, normally an engineering stress-strain relationship is used to calculate the stresses in the material, without taking the effect of poison's ratio into account. The engineering stress-strain relationship makes use of a non-changing cross section, in which after yielding no increase in strength is found due to the fact that the engineering yield stress is a non-changing value.

In reality if a material is loaded, the cross section will respond to this loading, because the volume of the steel beams will not increase or decrease limitless. The amount of this behavior is described using Poisson's ratio, which is 0.3 for steel. If this ratio is 0.5 the volume will stay constant, for a low value, going to 0, the beam dimensions will not change in the transverse direction.

The numerical model will take Poisson's ratio into account. To be able to model the described constant reaction force, with the changing cross section, there is a need for a changing yield stress as well, because using a constant yield stress would lead to a decreasing force after yielding. To counter this effect a true stress and true strain must be introduced, due to strain hardening.

The following equations (3.4) and (3.5) describe true stress and true strain in relation to the nominal stresses and strains used in the engineering approach.

$$\sigma_{true} = \sigma_{nom}(1+\varepsilon_{nom}) \tag{3.4}$$

$$\varepsilon_{true} = \ln(1+\varepsilon_{nom}) \tag{3.5}$$

Where the nominal stress and strain are governed by the notions in [18]. The appendixes in this code give leads to model the stress strain relationship, where can be chosen to use 4 different methods, see Figure 19.

In the 4 diagrams the first part is always the same, until yield the modus of elasticity governs the relation between stress and strain, with the relationship given in (3.6).

$$\sigma_{nom} = E * \varepsilon_{nom} \tag{3.6}$$

The first two models than have limited to no hardening, where the 3rd and 4th model do model the material hardening. Abspoel [2] introduced a second slope with an angle of E/100000 in the model 2 (Model III). He concluded that the influence on the bending moment resistance in model III, 3 and 4 is very limited and therefor chose his model III to be used. This model will be used in the to-be validated model as well.

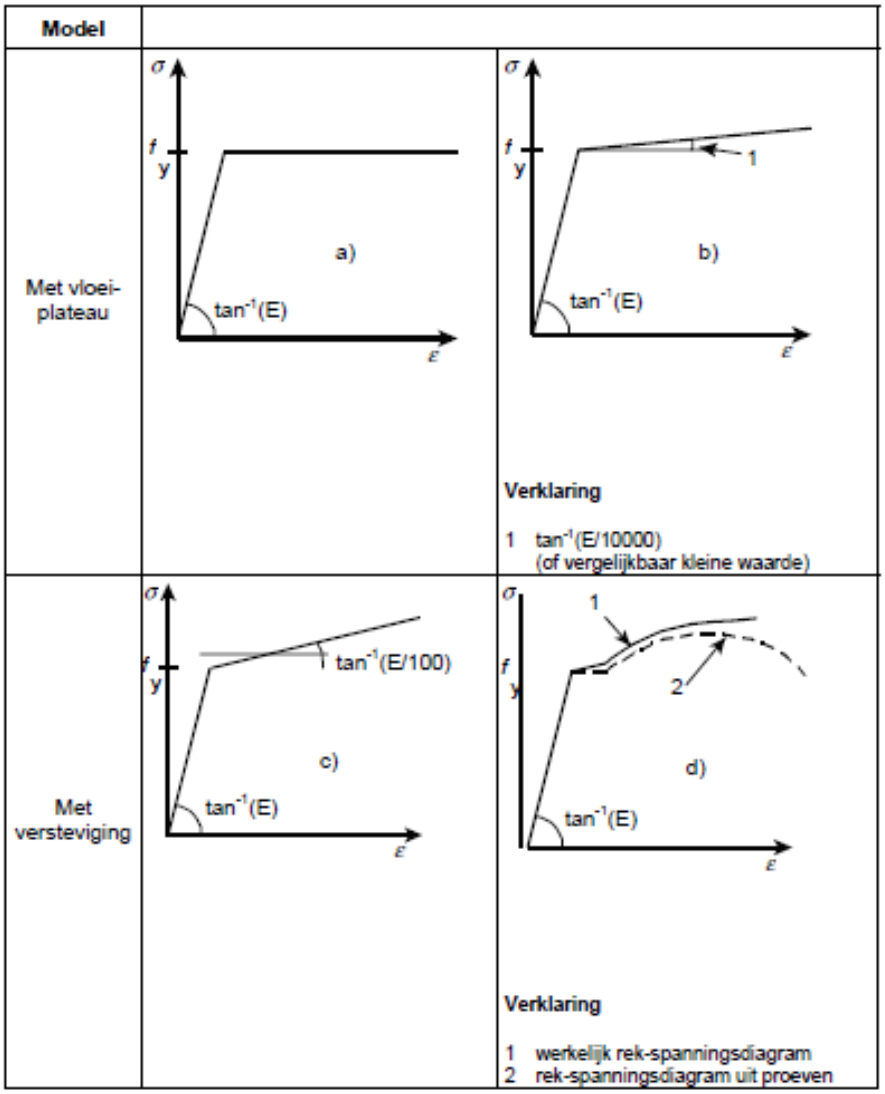

FIGURE 19: 4 METHODS TO MODEL THE STRESS STRAIN RELATIONSHIP ACCORDING TO EN1993-1-1

The relationship between nominal and true stress can be found in Figure 20 and zoom in on Figure 21, as well as the values of the graph.

3.3.2. Material density

The material density used is a 7800 kN/m^3, which is a mean value in between the values given in EN1991-1-1 table A.4 for steel. To introduce this the units will have to be altered to the base units: millimeter and Newton, choosing 10 as the gravitational acceleration. This way the density will be modeled as 7.8*10^{-5} N/mm^3

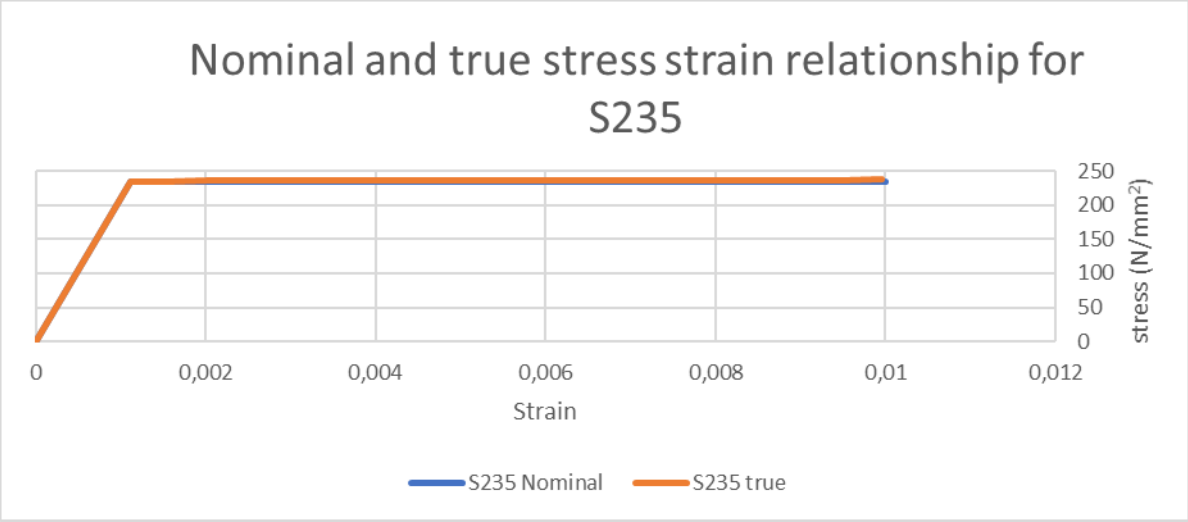

FIGURE 20: NOMINAL AND TRUE VALUES FOR S235 STRESS-STRAIN RELATIONSHIP USED IN THE MODEL

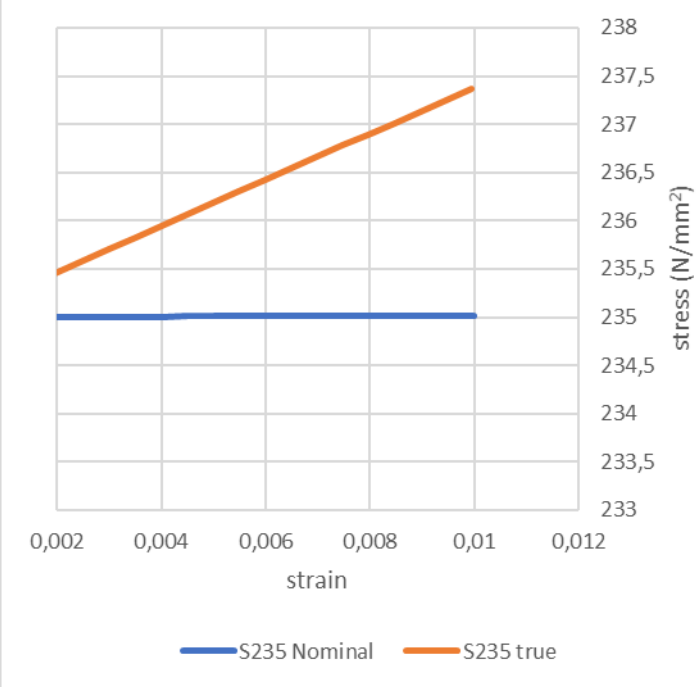

Nominal		TRUE	
σ	ε	σ	ε
0	0	0	0
235	0,001119	235,263	0,001118
235,0008	0,0015	235,3533	0,001499
235,0019	0,002	235,4719	0,001998
235,0029	0,0025	235,5904	0,002497
235,004	0,003	235,709	0,002996
235,005	0,0035	235,8275	0,003494
235,0061	0,004	235,9461	0,003992
235,0071	0,0045	236,0646	0,00449
235,0082	0,005	236,1832	0,004988
235,0092	0,0055	236,3018	0,005485
235,0103	0,006	236,4203	0,005982
235,0113	0,0065	236,5389	0,006479
235,0124	0,007	236,6574	0,006976
235,0134	0,0075	236,776	0,007472
235,0145	0,008	236,8946	0,007968
235,0155	0,0085	237,0131	0,008464
235,0166	0,009	237,1317	0,00896
235,0176	0,0095	237,2503	0,009455
235,0187	0,01	237,3688	0,00995

FIGURE 21: ZOOM IN ON NOMINAL AND TRUE VALUES FOR S235 STRESS-STRAIN RELATIONSHIP USED IN THE MODEL

3.4. Analysis description

3.4.1. Imperfections

In reality a girder will never be perfectly straight, due to tolerances in its production, deformations due to for example welding, etcetera. To be able to model a realistic, non-perfect plate girder an initial imperfection will be used to model these geometric imperfections to the girder.

The imperfections will be modeled using the first eigenmode of the plate girder, found using ABAQUS, multiplied by a factor found in Appendix C of [18], which is given in equation (3.7), which is the magnification factor for applying a buckling shape to a geometry.

$$\min\left(\frac{a}{200},\frac{b}{200}\right), a = h_w, b = l_{mid} \tag{3.7}$$

The process of finding the eigenmode uses the elastic buckling analysis, found in ABAQUS. It can be programmed to give a number of eigenmodes from a given geometry, using the modeled boundary conditions and load conditions. The eigenmode is found as a factorized deformation pattern.

The effect of the imperfections is analyzed by changing the amplification factor, also the effect of not using an imperfection to the model is looked into.

3.4.2. Loading method

The girder will be loaded on 2 points of the top flange of the girder, to model a 4-point bending test. These points are shown on Figure 18, marked with a δ. In the verification process multiple loading methods are used to address their behavior and to find the best possible method for the analysis. The first method examined is a force driven method, using an increasingly larger force to find the reaction of the plate girder. This force is modeled on a single node on the top flange of the plate girder, above the intermediate transverse stiffener.

The second method is done using a displacement driven analysis, to address the reaction of the plate girder. This displacement is modeled as a boundary condition on the top-flange node above the transverse stiffener, with an imposed deformation in the negative y-direction

3.4.3. Meshing

To let the FEM software -Abaqus- do a calculation a geometry needs to be divided in parts, being a finite element model. The coarseness of this mesh influences the results of the analysis, as well as the type of element which is used. Element types differ in their amounts of integration point and their degrees of freedom. The more integration points are present, in general, the more realistic the result will become. On the other hand, a finer mesh leads to a longer computing time, increase in output data and doesn't necessarily leads to better and more useful results.

Abspoel [1] and Cimpoi [3] analyzed the meshing of their analyzed girders both, where Abspoel used a non-uniform mesh and Cimpoi used a uniform, automatically generated mesh with 35x35mm elements. This will be the base of the model also the effect of a smaller mesh (25x25mm) will be analyzed.

Element type which is used is a S4R type element. This element is a standard linear shell element with 4 integration points, which can both be used for thin and thick shells.

3.4.4. Analysis methods

The goal for the analysis is to find a static solution for the maximum bending moment capacity of the steel plate girders. For this problem Abaqus has a lot of options to choose from. Since the geometries of the plate girders are likely to buckle prior to failure, there is a need for non-linear geometric analysis, allowing large deformations.

3.4.4.a. RIKS analysis

The RIKS analysis is a static analysis, used to obtain static non-linear solutions for unstable problems, using a proportional load, increasing the load every step with a certain automatically chosen quantity. The model assumes the result is reasonably smooth and its only task is to predict the failure of an unstable, geometrically non-linear, collapse mode. It will be used with an applied force and an applied imperfection.

3.4.4.b. Explicit non-linear dynamic analysis

A dynamic analysis using explicit central-difference time integration, which is an inexpensive calculation procedure compared to implicit dynamics. This method uses a converted element matrix to add speed in calculation. The analysis gives options to increase the speed of calculation, by artificially increasing the mass of the structure leading to a faster converging result. The analysis is ideal for high-speed dynamic events, but also possible for a slow, quasi-static process, although using the explicit dynamic model in a quasi-static way can make the computer time increase largely.

For the analysis the step size will be 5 seconds, with a smooth step and mass scaling to let a time increment of $1*10^{5}$ seconds be stable.

3.4.4.c. Implicit non-linear dynamic analysis

A dynamic analysis using direct implicit integration, the Hilber-Hughes-Taylor time integration, using the global mass matrix of the structure. This analysis is very suitable for analysis in which considerable energy dissipation is needed to find a stable solution, which is very likely to happen in buckling of the web prior to failure. On the other hand, this analysis is prone to errors, when the mass of the model is not correctly modeled. For the analysis several step choices were used, which can be found in the next paragraph.

3.5. 1st validation on the S235 girder with β_w 1000

3.5.1. Introduction

The models for a web slenderness of 700 and the models with web slenderness of 1000 were created simultaneous. The boundary conditions, material parameters and loading were kept the same, only the geometry, which was given is paragraph 3.2.1, differs.

Because the influence of the mesh is tested in the models with a 700-web slenderness, described in the next paragraph, therefor this is not done in this validation. Because the size of the model is increasing, the amount of element is increasing as well and the results, with the same 35x35mm mesh as in the 700 validation, are assumed to of similar or better precision in comparison.

The different analyses, described in paragraph 3.4.4 were conducted for this validation to address the choice for a good method. Also, the imperfections and their magnitude were analyzed to address the influence of the slenderness in the reaction to imperfections.

3.5.2. Results of the FEM-validation

The graphs of this paragraph show the results of the FEM-validation for the 1000 web slenderness models. The first 2 pictures (Figure 22 and Figure 23) show the force-displacement diagram, in which the displacement is given in the middle of the girder in the middle of the bottom flange, which is point D on Figure 18.

3.5.2.a. Influence on the results due to the analysis method

The figures show 4 methods are used, all with the same amplitude of initial imperfections, using the first eigenmode as shape. In this figure the imperfections are 1%, or 1/100 of the height of the girder. In Figure 23, the zoomed in graph, it can be seen that the three analysis result in very similar, almost identical, maximum reaction forces and therefor also the maximum bending moment is nearly identical. There are 2 RIKS-models, one using a force controlled 4-point bending test and the other one being a displacement controlled 4-point bending test. Both dynamic analyses are displacement controlled.

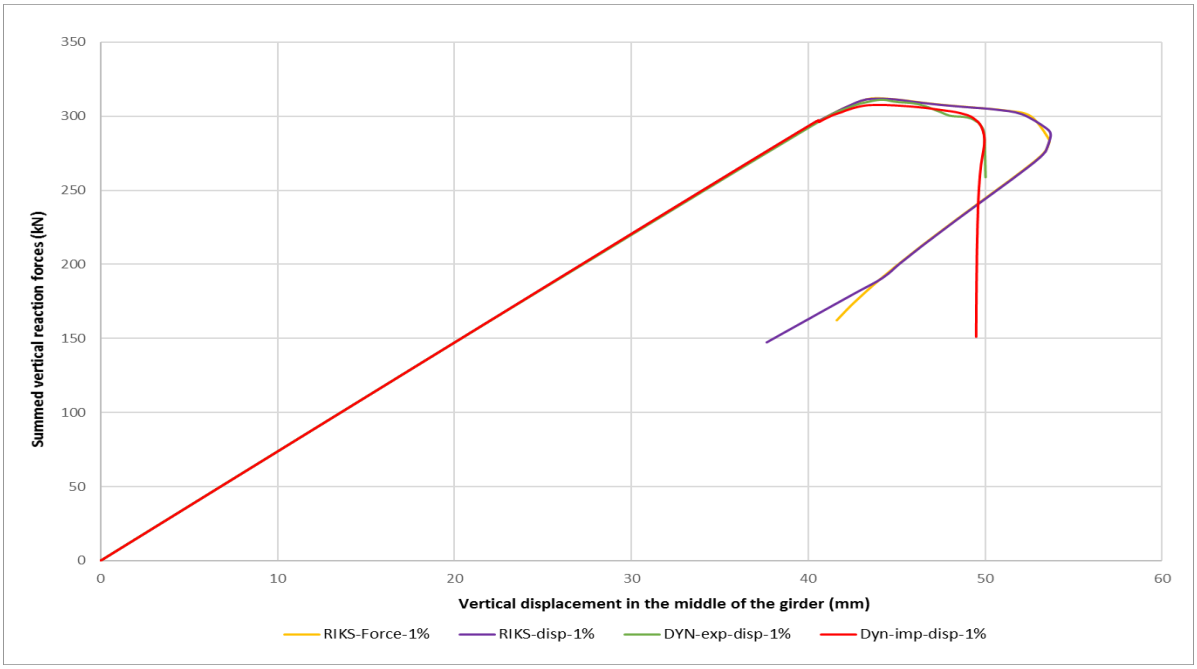

FIGURE 22: THE FU-DIAGRAMS FOR THE 1000 WEB SLENDERNESS MODELS USING DIFFERENT ANALYSIS

The difference in forces and bending moment resistance can be found in the first 4 rows of Table 8. The reaction to the applied displacements is also nearly identical up to the point that the maximum bending moment is achieved. The stiffness of the girders is found to be linear and elastic up until that point. After the reaction force peaks, the girders heave some extra rotational capacity which makes the girder deflect an extra 5 or 6 mm until the girder collapses. Both the RIKS-analysis are behaving almost the same, showing no difference in results, but the calculation time for the force driven analysis was significantly longer.

This collapsing path is found to be realistic for all analysis. The post-collapse behavior is more likely to be as shown by the explicit and implicit dynamic analysis, in comparison to the RIKS-analysis, which is unable to increase the deflection while still finding an equilibrium. The previous results only show that the results for different analysis are comparable when applying a certain initial imperfection. Therefor Table 8 is also gives additional information about the results for 2 analysis with 0.5% imperfection, also showing nearly identical bending moment resistances.

model	*F (N)*	*M (kNm)*
Fu-RIKS-disp-1%	311	660
Fu-RIKS-Force-1%	312	661
Fu-imp-disp-1%	307	652
Fu-exp- disp-1%	311	659
Fu-RIKS-disp-0,5%	319	677
Fu-imp-disp-0,5%	319	677

TABLE 8: REACTION FORCES AND ULTIMATE BENDING MOMENT FOR 6 MODELS USING 3 DIFFERENT ANALYTICAL METHODS.

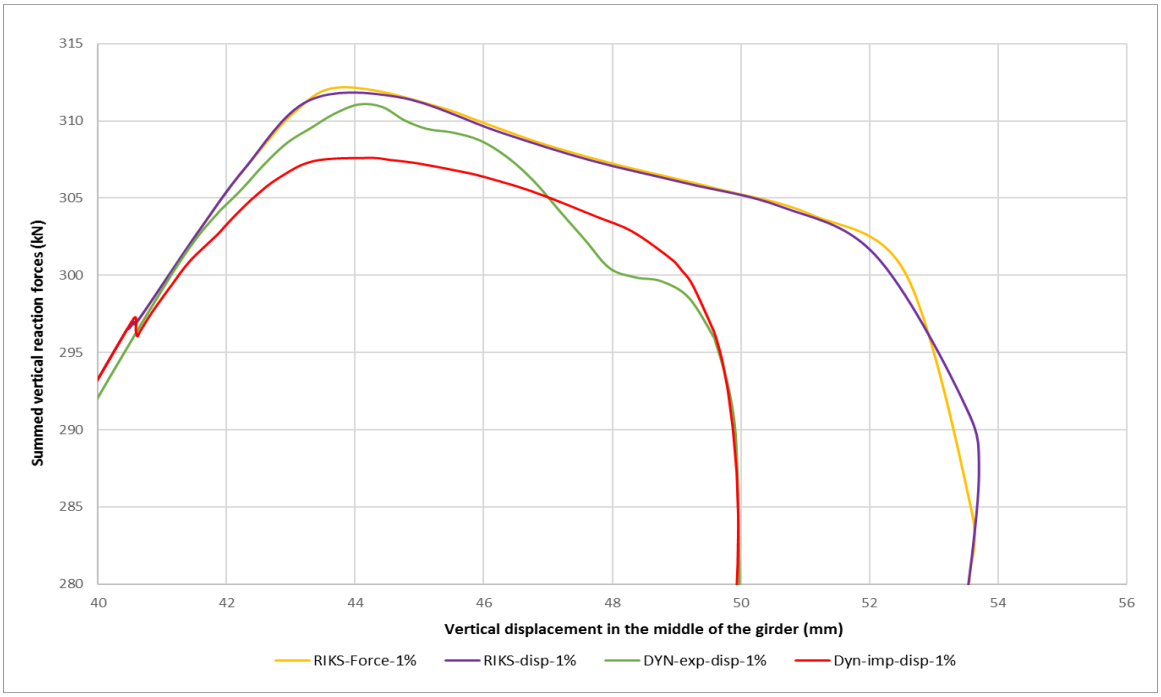

FIGURE 23: THE FU-DIAGRAMS FOR THE 1000 WEB SLENDERNESS MODELS USING DIFFERENT ANALYSIS, ZOOMED IN ON THE PEAKS

3.5.2.b. Influence of initial imperfections

After addressing the influence of the analysis method, a parametric study to analysis the influence of the amplitude of the imperfection was conducted. On Figure 24 the analysis of 7 different dynamic implicit analysis is shown, using different amplitudes for the implied initial imperfections.

The amplitude ranges from no imperfection to 20% imperfection, which is $1/5^{th}$ of the panel length of the girder mid-section. Looking at the graphs it can be seen that the girder with the biggest amplitude of its initial imperfection differs greatly from the other 6 graphs, showing a significantly lower maximum reaction force as well as a different stiffness, which is higher than the others. Due to the fact that this difference exists, the 20% graph will not be discussed in the rest of the qualitative analysis of the results.

It can be seen that the graphs show a linear elastic curve up until approximately 40 mm of deflection. After this point the 1%-graph flattens out at first, leading to the lowest maximum bending moment resistance of the 6 remaining analysis. The analysis with 2 and 4% imperfection behaves elastically somewhat longer, where the 2% fails with a lower reaction force and deflection in comparison to the 4% analysis.

Looking at the 7mm, 0,5% and the analysis without initial imperfections, Figure 24, and in more detail Figure 25, show there is a similar force displacement curve for these 3 analyses. The reactions of the girders with imperfections shows a very small decrease in moment capacity with respect to the girder without imperfection. All of these girders have a lot more rotation capacity after the maximum bending moment have been achieved, compared to the 1, 2 and 4% curves.

The maximum bending moment resistance and summed vertical reaction forces, as well as the maximum imperfection amplitude, are given below in Table 9, with the values from Abspoel and Cimpoi additionally added.

model	*Imperfection amplitude (mm)*	*F (N)*	*M (kNm)*
Fu-imp-no	0	321	681
Fu-imp-7mm	7,1	320	680
Fu-imp-0,5%	21,2	319	677
Fu-imp-1%	42,4	307	652
Fu-imp-2%	84,8	311	661
Fu-imp-4%	169,7	316	670
Fu-imp-20%	848,5	271	575
Cimpoi	7,1	312	668
Abspoel		321	686

TABLE 9: REACTION FORCES AND ULTIMATE BENDING MOMENT FOR 5 IMPLICIT MODELS WITH DIFFERENT IMPERFECTIONS

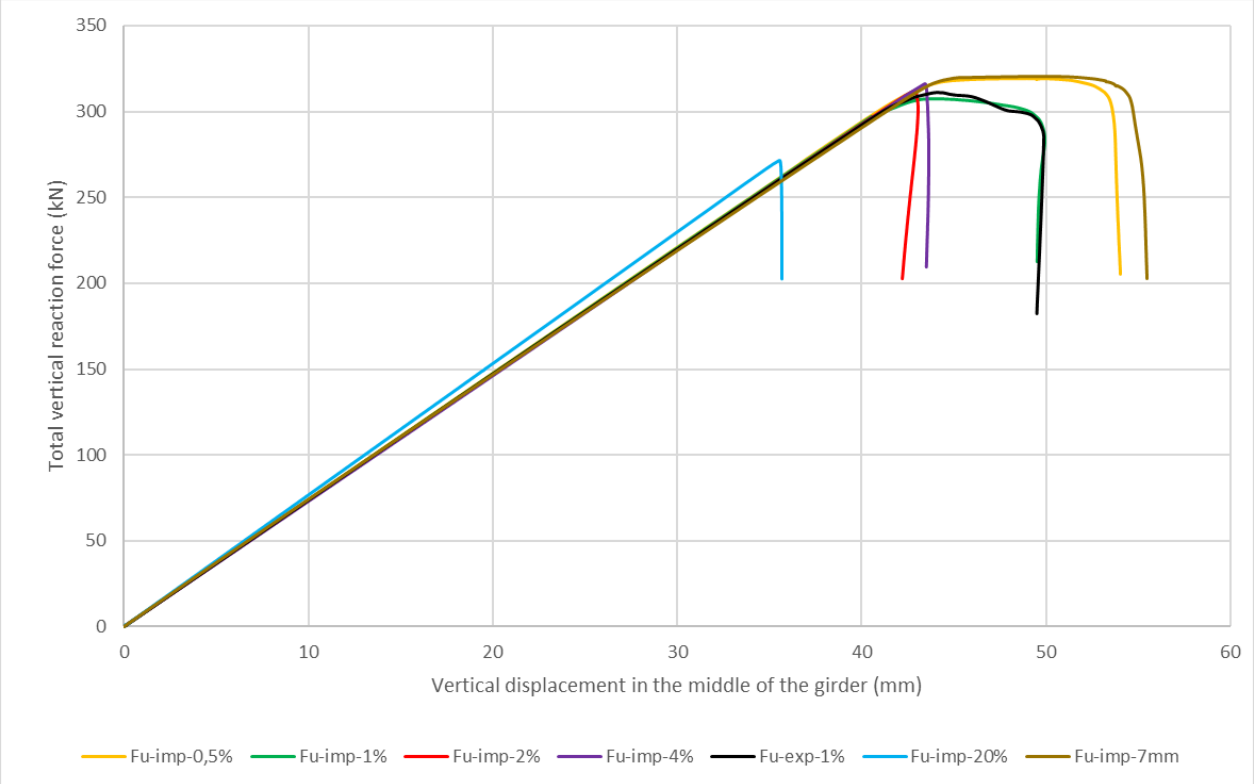

FIGURE 24: FU-DIAGRAMS OF 5 IMPLICIT DYNAMIC ANALYSIS ON A GIRDER WITH A WEB SLENDERNESS OF 1000 MADE USING S235 STEEL

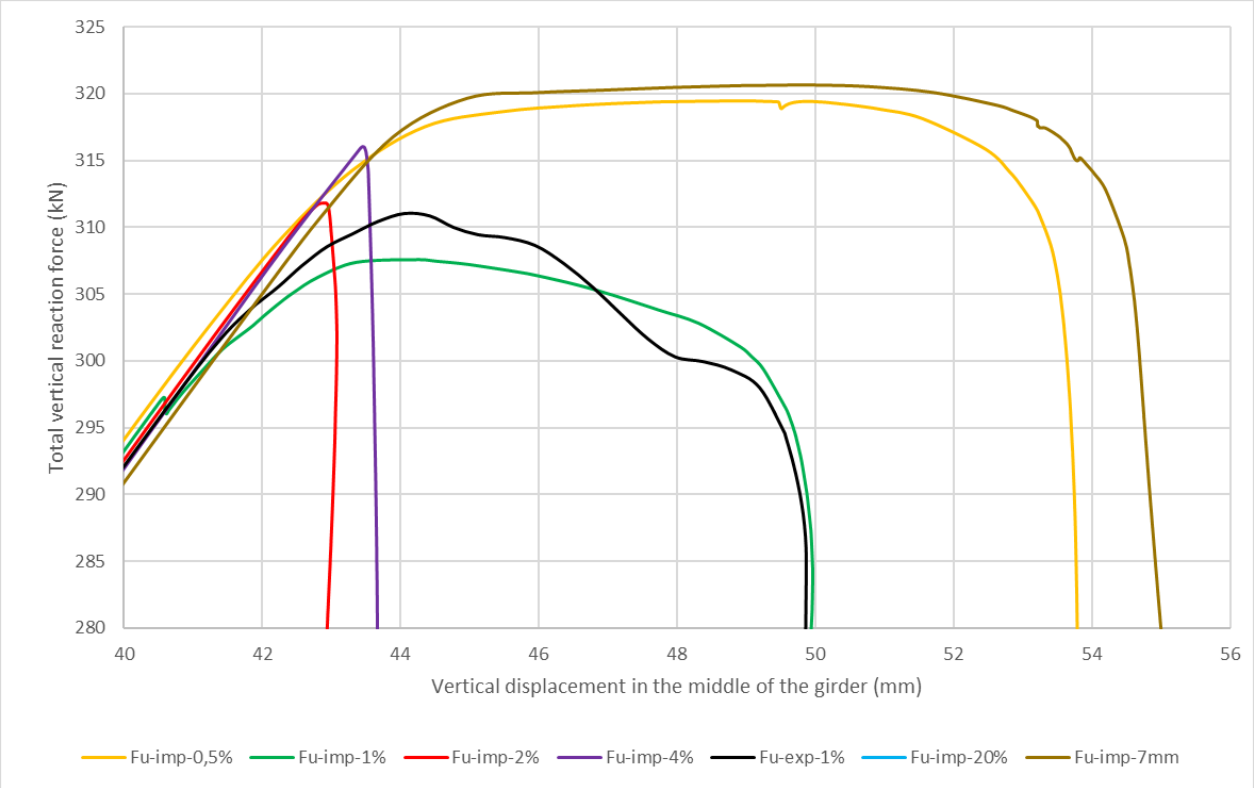

FIGURE 25: ZOOMED FU-DIAGRAMS OF 5 IMPLICIT DYNAMIC ANALYSIS ON A GIRDER WITH A WEB SLENDERNESS OF 1000 MADE USING S235 STEEL

3.5.2.c. Comparison to earlier research

The goal of the parametric study is to address if the model represents real behavior by comparing the output of the model to the found experimental results. In this case Abspoel used experimental data to validate his model, this model is used by Cimpoi to validate her model. This method is also used in this thesis. In the following paragraph the results are presented as load-displacement diagrams, but now using the applied displacement instead of the found displacement in the middle of the girder.

The graph is given on Figure 26, showing a good similarity when looking at the maximum summed vertical reaction forces, which can also be found in Table 9. The summed reaction force totals of the 3 new graphs are between 319,4 and 321,2 and the reaction forces for Abspoel's reference model was 323,8 (or 321,6) kN, which is within 1,5% (or 0.7%).

The difference in the graph is clearly visible in the stiffness, the girder-model made by Abspoel is significantly stiffer in comparison to the other 4 graphs. The reaction of the girder in the Cimpoi-model is very similar to the models made for this thesis, although the maximum force is lower for the Cimpoi model.

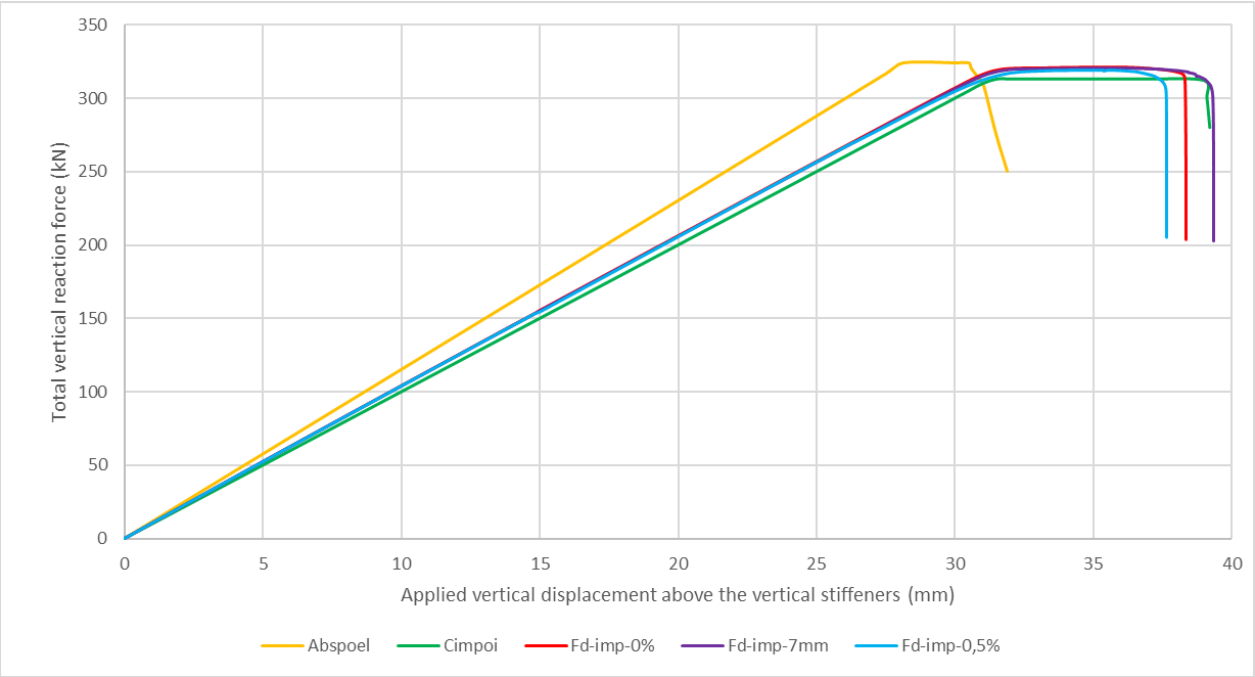

FIGURE 26: FΔ-DIAGRAMS OF 3 IMPLICIT DYNAMIC ANALYSIS COMPARED TO THE RESULTS OF ABSPOEL AND CIMPOI ON A GIRDER WITH A WEB SLENDERNESS OF 1000 MADE USING S235 STEEL

3.5.2.d. Plots of the Bw1000 validation

In the following paragraph the results of the plate girder modeling will be presented in plots generated by the program Abaqus, to address the way in which the girder failed. The pictures are taken from the analysis in which the amplitude of the imperfection was 7mm and the analytical method was the dynamic implicit method.

The pictures will be described and analyzed as well as a comparing description with the other analysis is made, in some cases with an additional plot for clarity. In this paragraph only the models with small imperfections are discussed. Below, on Figure 27, the same graph as in Figure 26 is given only for the 7mm imperfection model. In this model, 4 dots are presented referring to the given plots in the rest of this paragraph.

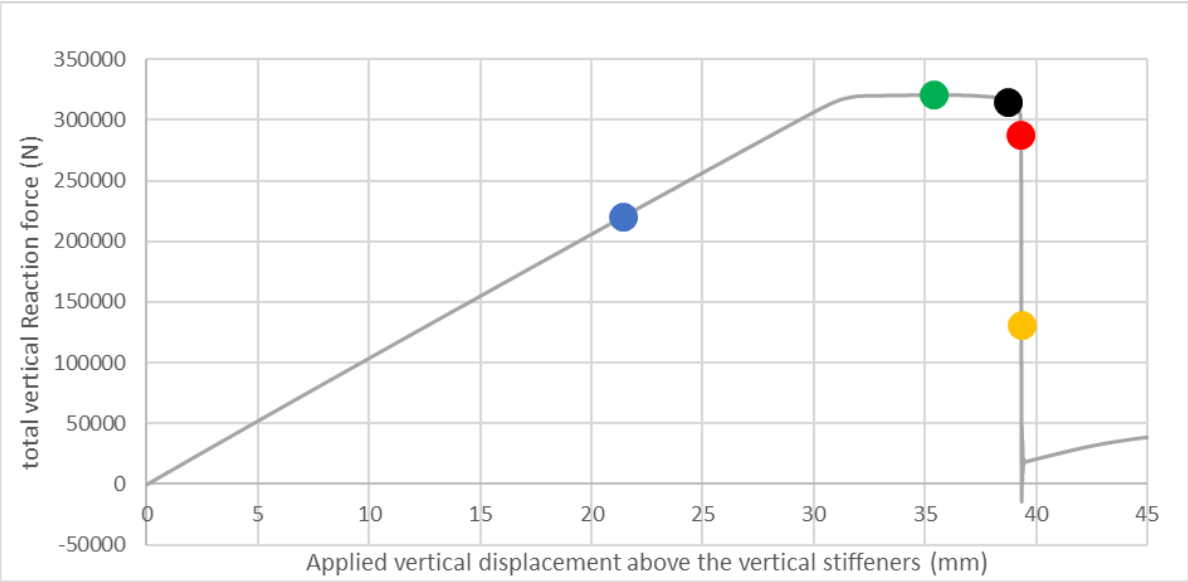

FIGURE 27: FORCE DISPLACEMENT DIAGRAM OF THE 7MM MODEL, WITH MARKINGS TO REFERRING TO PLOTS

Linear elastic behavior

The first part of the graph on Figure 27, is linear elastic. With an increasing applied displacement, the resulting vertical force increases linearly. In Figure 28 the stress distribution is given for the plate girder after the load point have moved 21,44 mm in the negative y-direction. Blue represents a low Von mises stress, where yellow and maximum red are higher stresses. It can be seen that the highest stress is located in the flanges, which is a logical outcome since the mid-section is loaded in bending.

The stress distribution is not uniform, which can be concluded due to the fact that the top flange doesn't experience the same stress over the full length and the part of the web just below the top flange is also noticeably disturbed. If the model would have featured a girder with a thicker web the top flange distribution would be similar to that of the bottom flange.

This observation can be explained by the fact that this very slender web experiences buckling before failure, which leads to redistribution of the stresses. This theory can be confirmed by looking at Figure 29, showing the out-off plane displacement on the same moment.

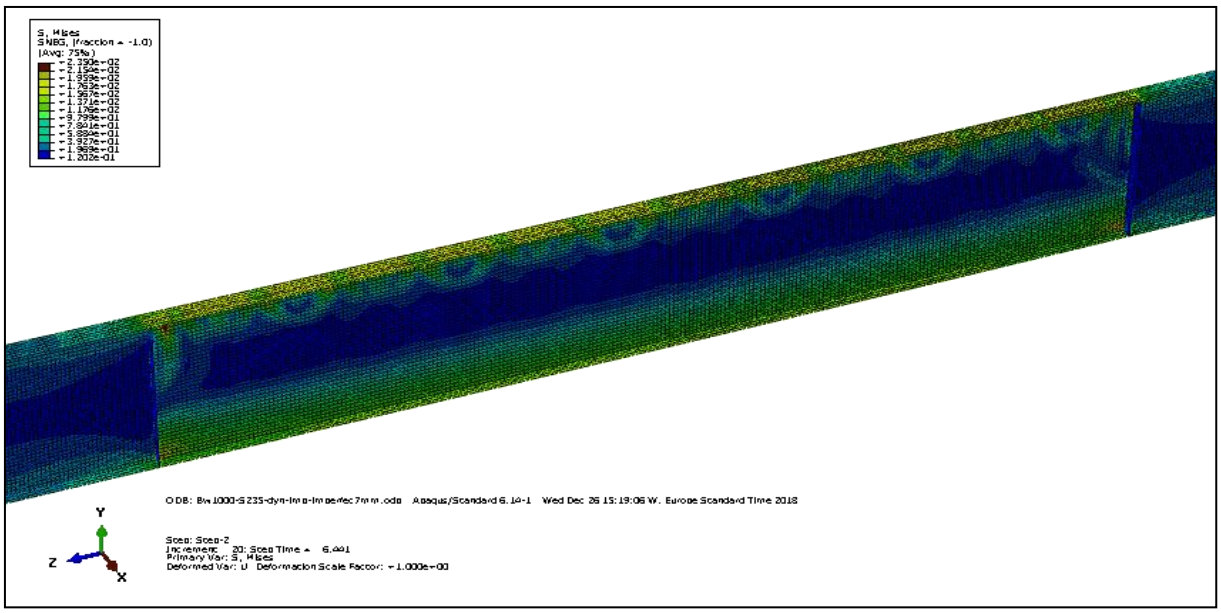

FIGURE 28: VON MISES STRESS, PRIOR OF REACHING YIELDING (BLUE DOT)

For the other analysis, explicit dynamic and RIKS, the linear elastic part behaves the same for the small displacement. The stress distribution is very similar to that on Figure 28 and also the out-of-plane displacement with these analysis looks the same, even for the model which didn't have initial imperfections. In this model the imperfections get into the model by buckling of the web plate.

Looking at the models with a 0.5% and 1% imperfection, the shape of the out-off the plane displacement changes to a shape which is shown on Figure 30. This deformation doesn't lead to less stiffness or a significant change in stress distribution.

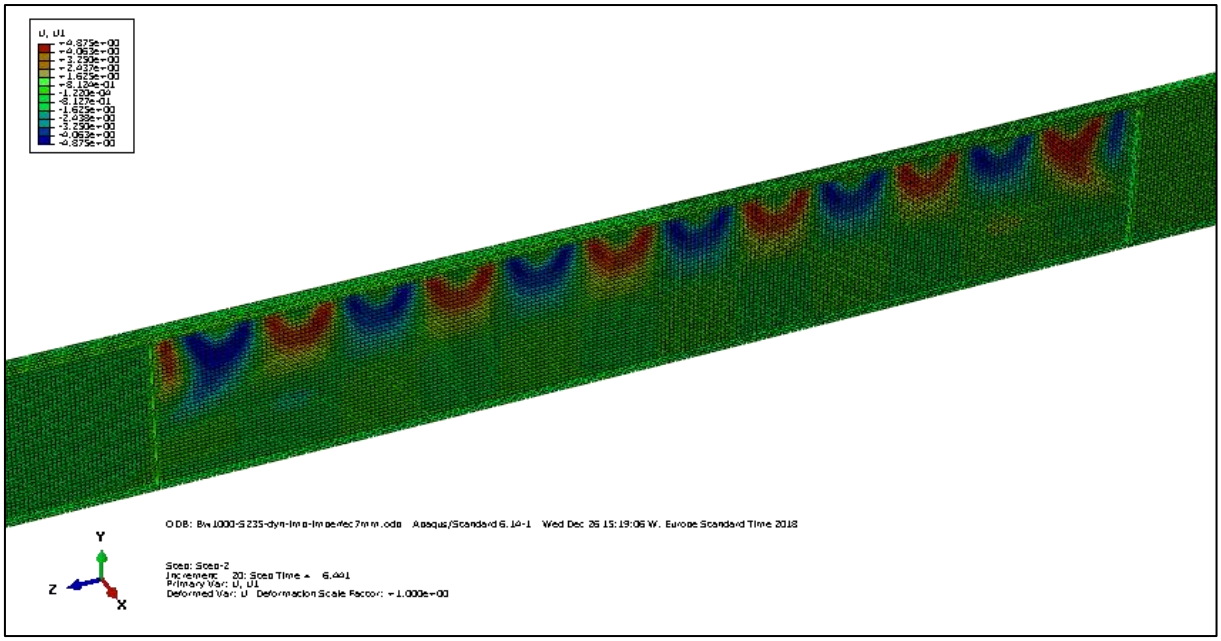

FIGURE 29: OUT-OF-PLANE DISPLACEMENT IN DE MID-SECTION BEFORE YIELDING IS REACHED (BLUE DOT)

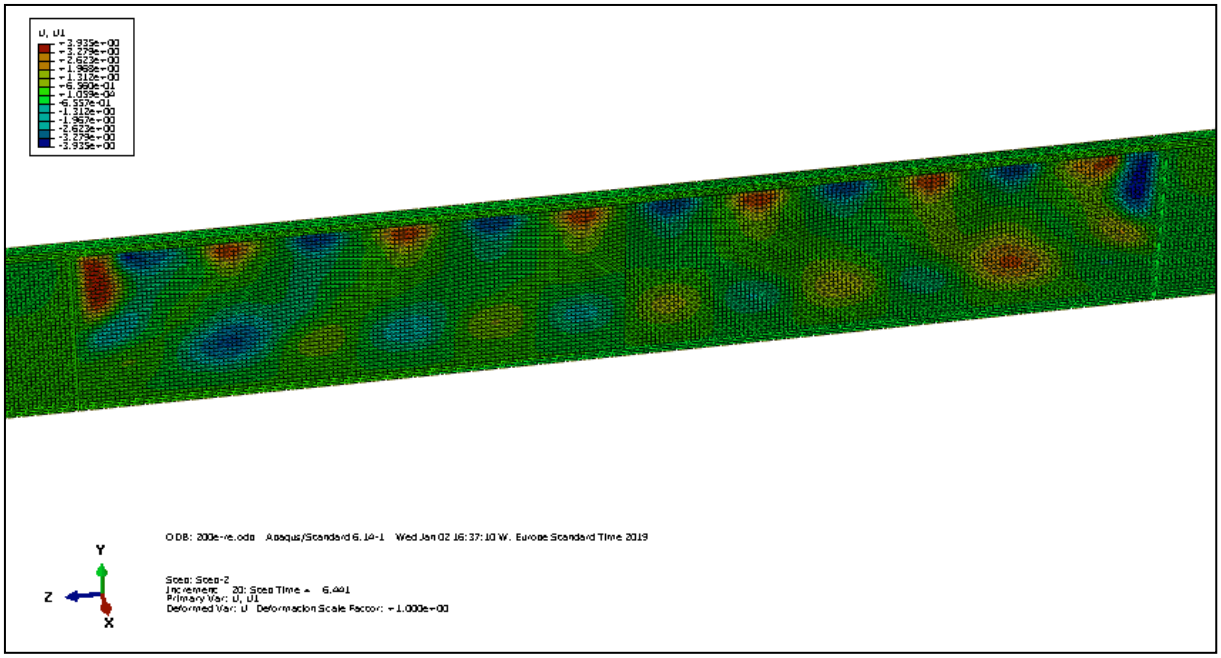

FIGURE 30: OUT-OF-PLANE DISPLACEMENT WHEN THE MODEL HAS A BIGGER INITIAL IMPERFECTION AMPLITUDE

Behavior when loaded to the maximum bending moment capacity

On Figure 31 and Figure 32 the plate girder is shown when experiencing the highest vertical reaction force, which results in the highest bending moment capacity. The first of the 2 pictures show the Von Mises stress in the girder. It can be seen that the top girder experiences the highest load, which is 235N/mm^2, so the flange is yielding before collapse. The stress-distribution left and right are identical, but it can also be seen that some stress trajectories are traveling from the top to the bottom flange. On Figure 32 the displacement in the y-direction is given, which looks like a standard deformation-pattern for a girder in bending, but looking at Figure 33, the out-of-plane displacement has increased close to the transverse stiffeners.

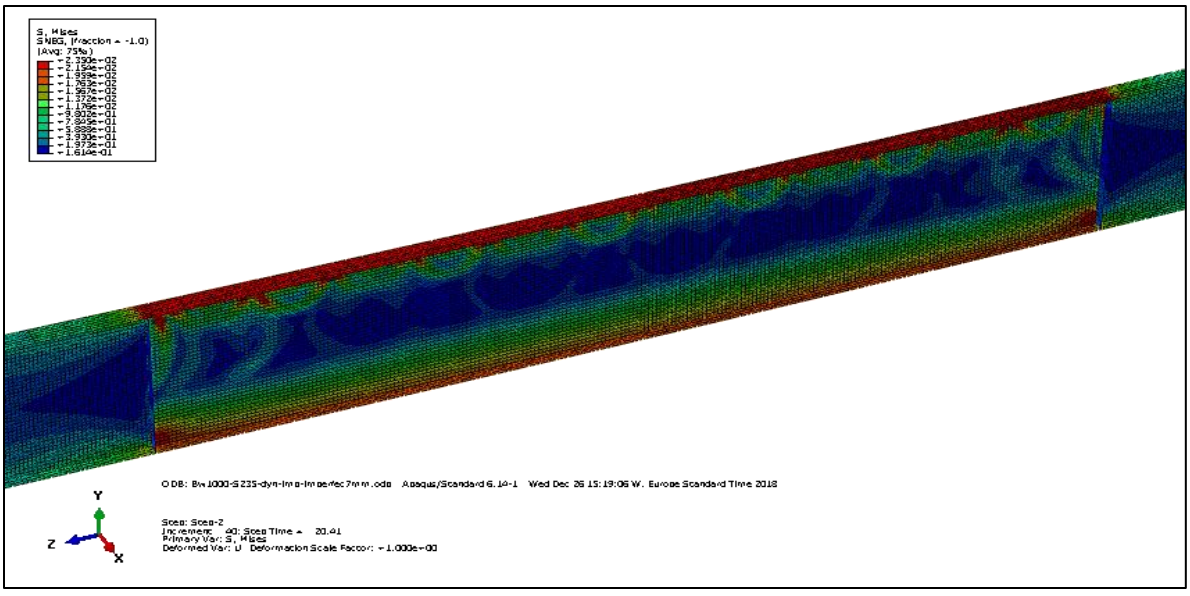

FIGURE 31: VON MISES STRESS AT MAXIMUM BENDING MOMENT RESISTANCE

In comparison to the models with no imperfection and with 0,5% imperfection we see that the stress in the girder behaves the same, with yielding flanges and starting stress trajectories between the flanges. The out-of-plane deflection, which was different at the first investigated point for the bigger imperfection, now changes to an identical shape, shown in Figure 34.

The shape of the out-of-plane deformation is still different, but the biggest deflections are present just below the top flange, which is also happening at the girders without and the 7mm initial imperfection girder.

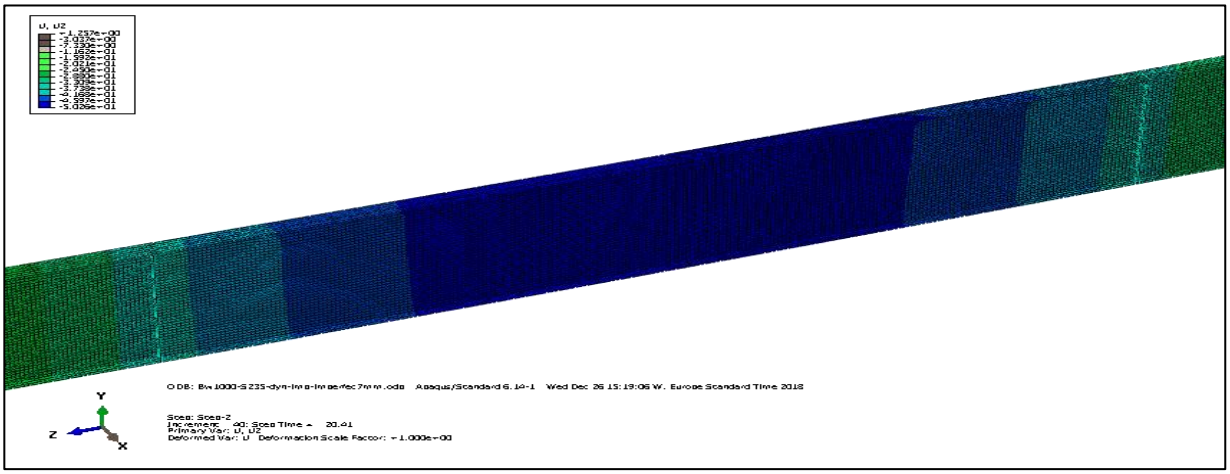

FIGURE 32: THE VERTICAL DISPLACEMENT IS CONTINUES IN THE MIDDLE SECTION AT MAXIMUM MOMENT RESISTANCE (GREEN)

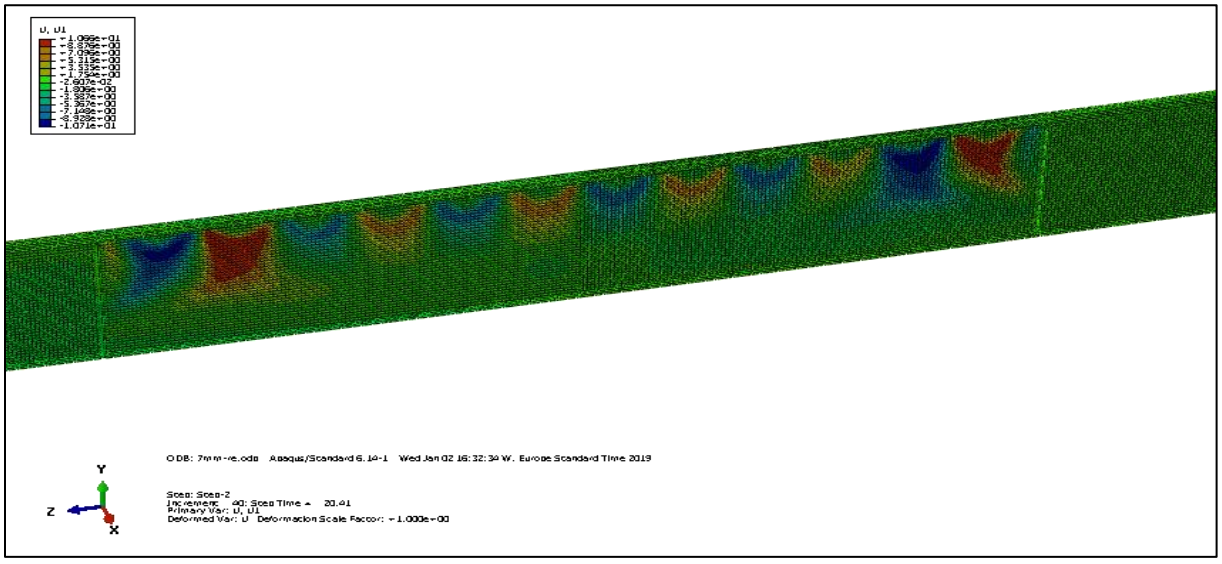

FIGURE 33: OUT-OF-PLANE DISPLACEMENT AT MAXIMUM BENDING MOMENT (GREEN)

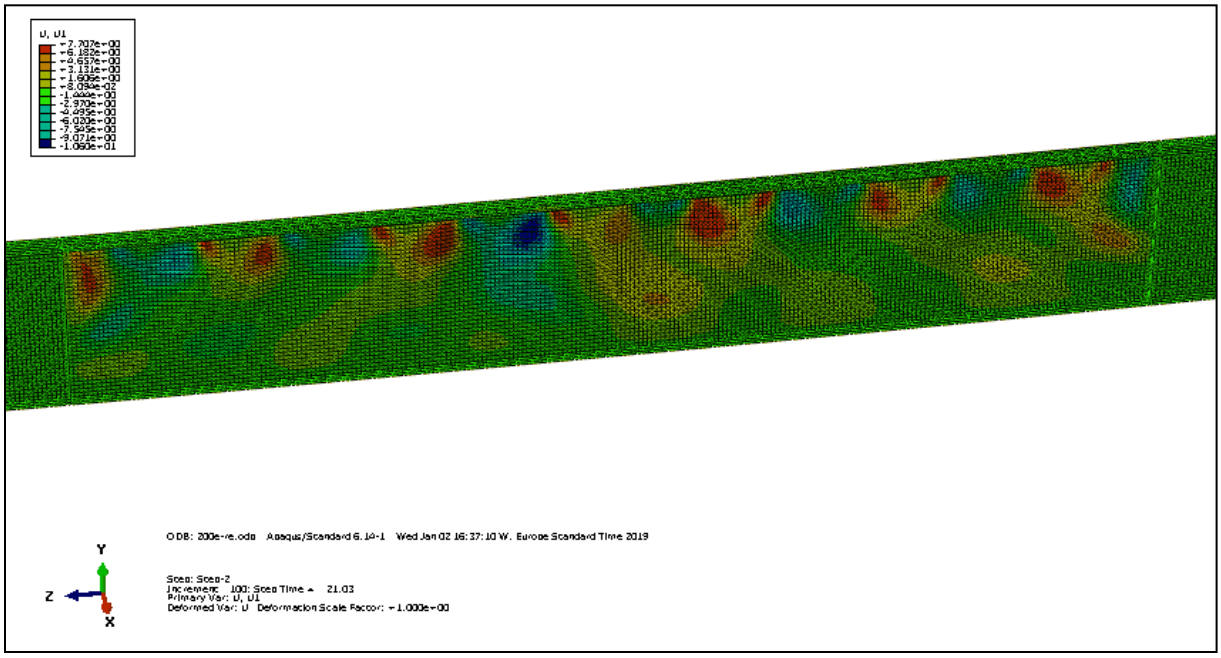

FIGURE 34: OUT-OF-PLANE DEFORMATION FOR MODELS WITH LARGER INITIAL IMPERFECTIONS, AT MAXIMUM MOMENT CAPACITY (GREEN)

Collapse behavior

With increasing deformation, there is a moment where failure sets in and the bearing capacity of the girder dramatically decreases. Before this happens, the bearable force is reduced very slightly, but the deformations, in y- and x-direction increase rapidly. Also, the stress-trajectories grow towards the bottom flange, which is shown on Figure 35. The failure sets in when the top-flange starts to twist, which

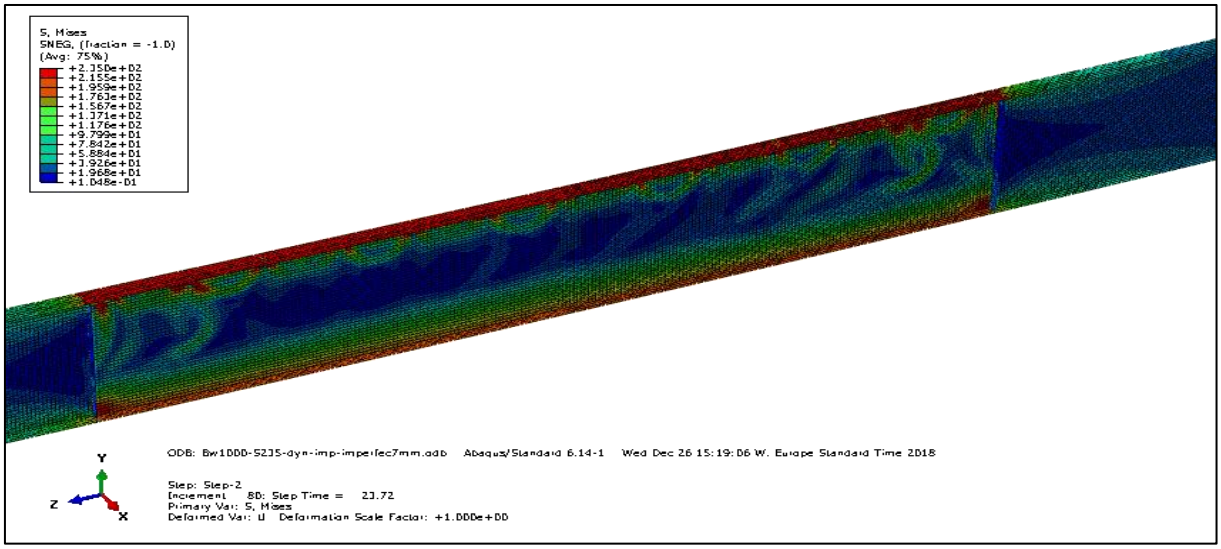

FIGURE 35: VON MISES STRESS JUST BEFORE FAILURE (BLACK)

happens in the 7mm imperfection, as well as the no imperfection-model, close to the right force-application point and is shown on Figure 36.

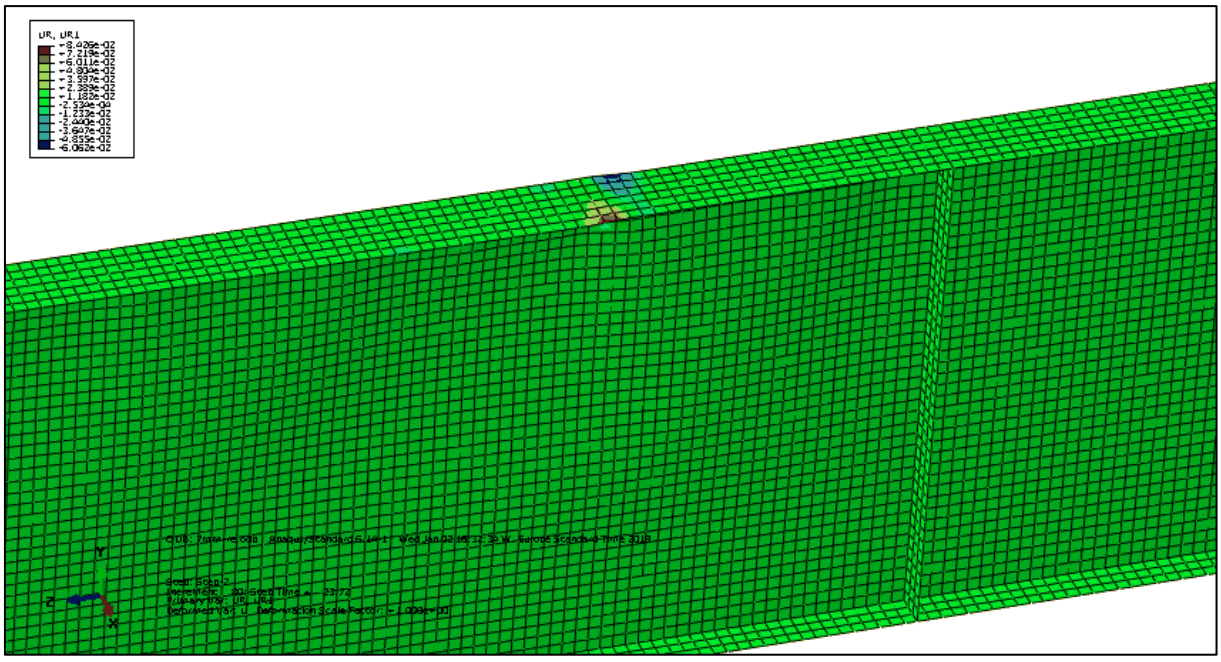

FIGURE 36: ROTATION AROUND THE X-AXIS, ZOOMED IN ON THE TOP-RIGHT PART OF THE MID-SECTION

With further increasing applied deflection, the girder will fail and lose the capacity to transmit the stresses occurring due to bending of the girder. In the figure below, Figure 37, the stresses just after the flange first twisted and the capacity reduced, show an increase in stress in the right side of the web. The trajectories traveled all the way down to the bottom flange and on Figure 39 it is noticeable that the top

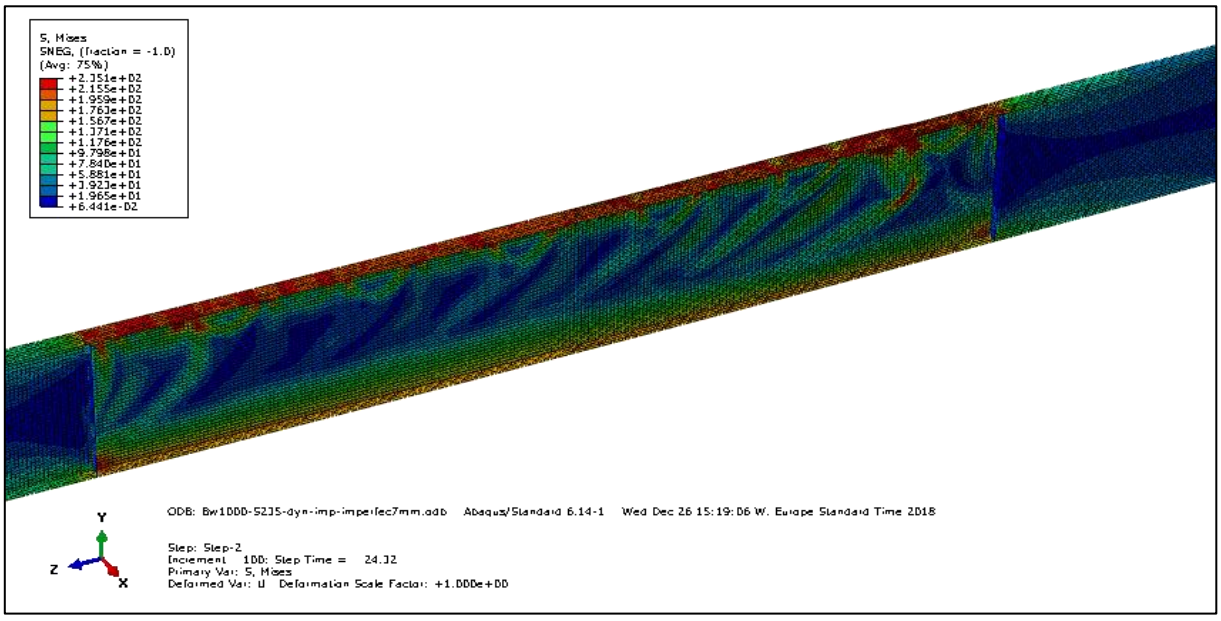

FIGURE 37: VON MISES STRESS JUST AFTER COLLAPSE (RED)

flange rotates around the connection with the web, leading to negative deflection of the side of the flange facing towards the front.

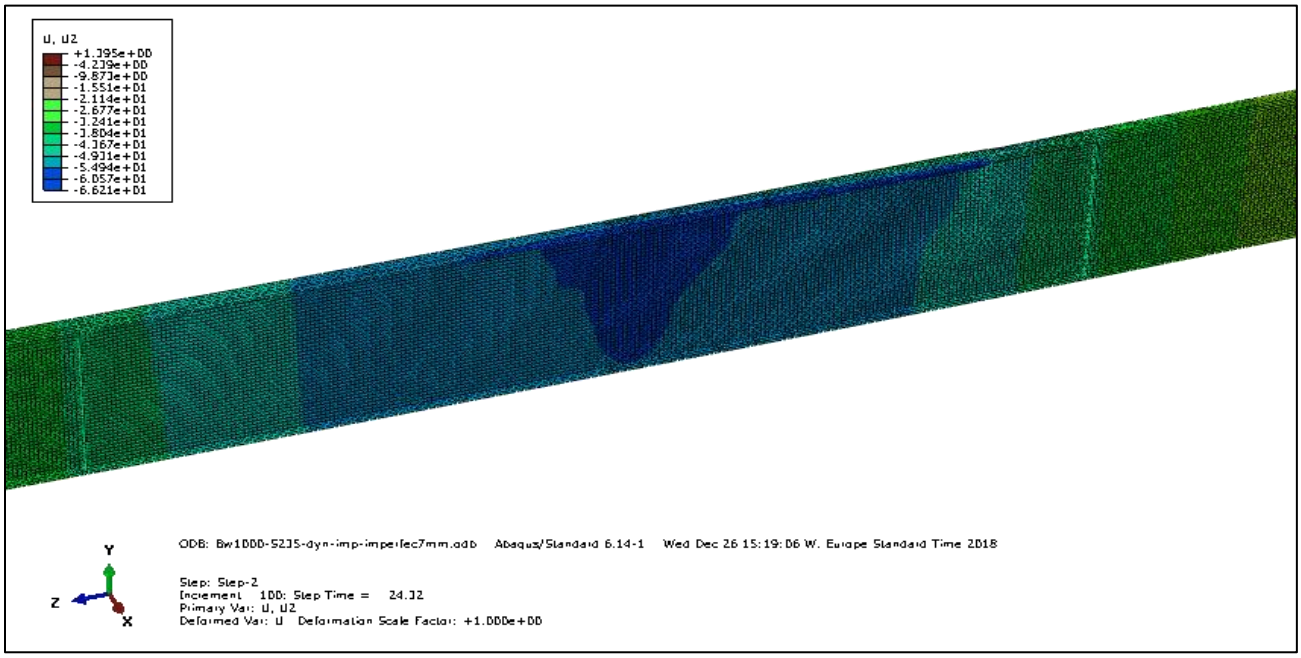

FIGURE 38: VERTICAL DISPLACEMENT IN THE MIDDLE SECTION OF THE GIRDER, JUST AFTER COLLAPSE (RED)

After this step, when increasing the applied displacement, a plastic hinge in the top flange develops, leading to the relaxation of stresses in the flanges and severely increasing the deflection in the middle of the girder, as well as the applies deflection. This can be seen on Figure 39 and Figure 40. A mechanism

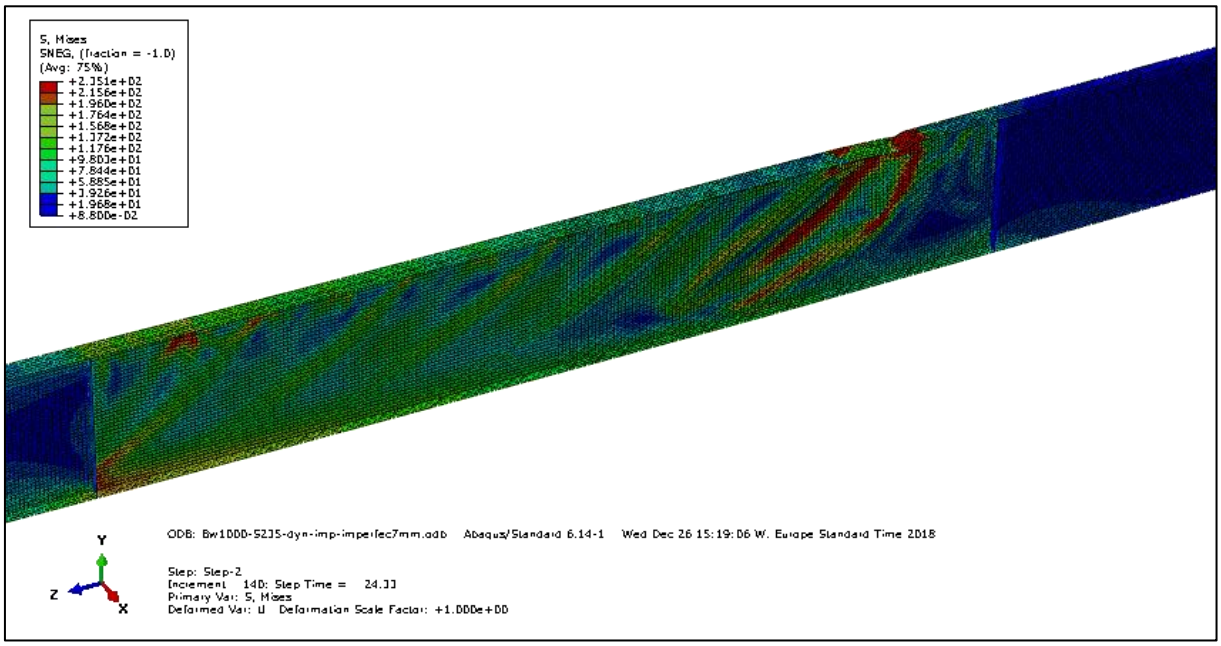

FIGURE 39: VON MISES STRESS WITH INCREASING APPLIED DISPLACEMENT (YELLOW)

forms due to two plastic hinges in the top flange close to each other. A smooth curve in the top flange traveling to the middle of the girder can be noticed as well as large buckles in the web of the girder.

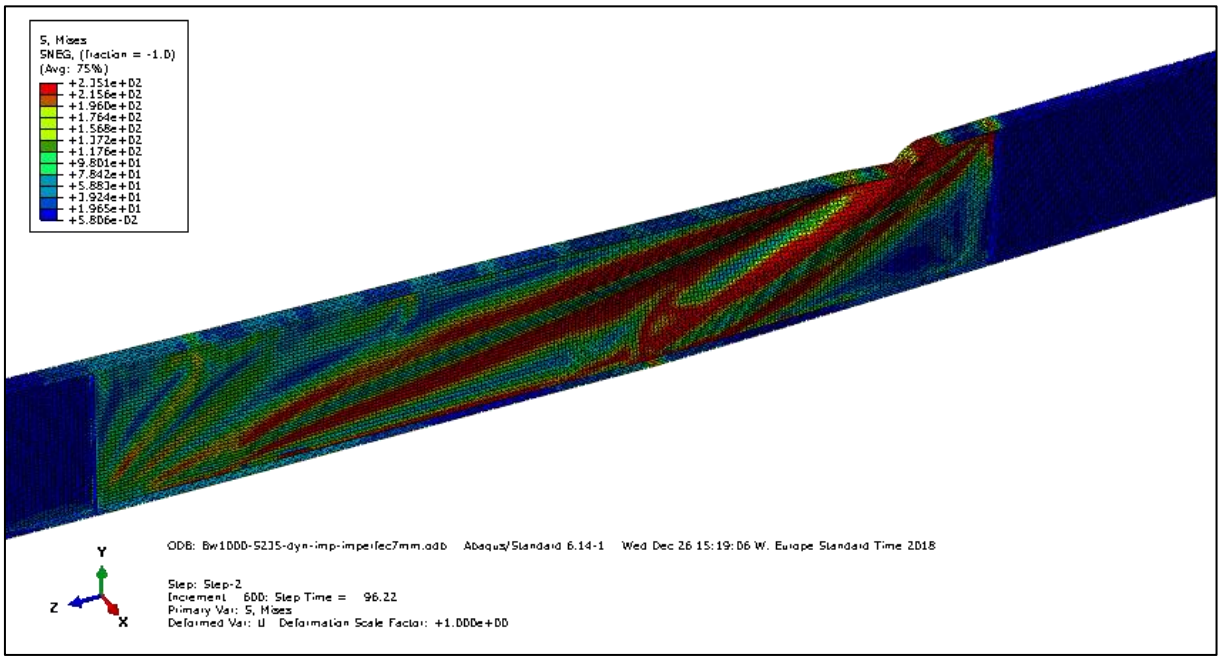

FIGURE 40: VON MISES STRESS IN THE GIRDER WHEN THE APPLIES DISPLACEMENT IS 110MM (NOT IN THE GRAPH)

Compared to the other analysis, the dynamic implicit results all look like they experience similar failing behavior, when looking at the 3 models with the smallest imperfections. The model without any imperfections behaves exactly the same, the model with 0.5% imperfection has the same failing mechanism but this happens in the middle of the mid-section instead of at the side of the middle-section.

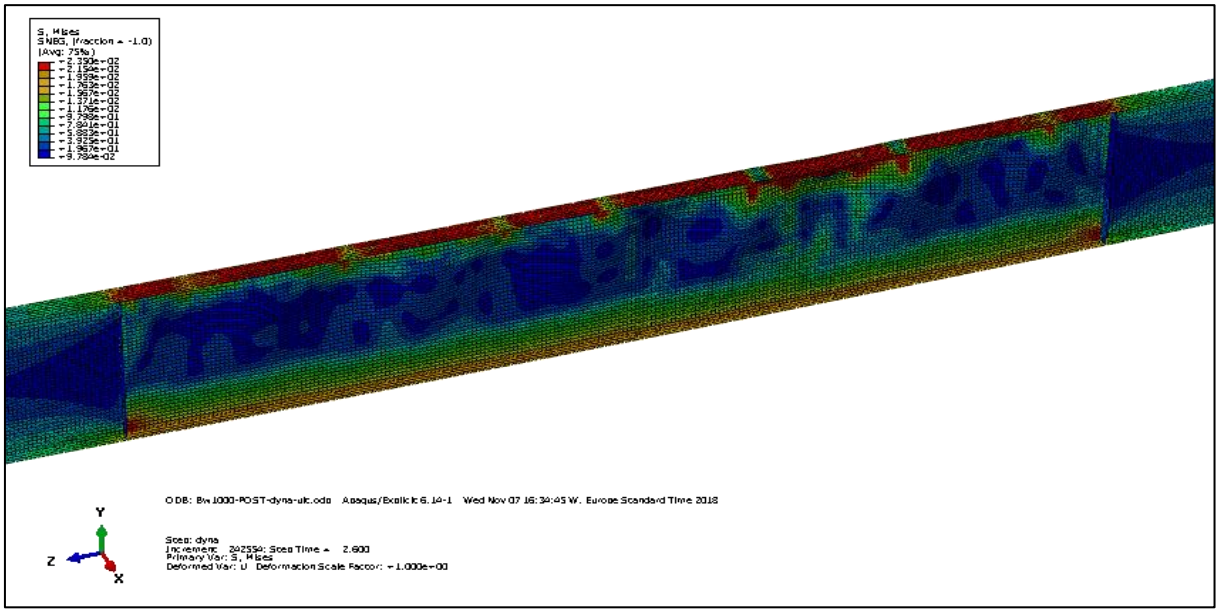

FIGURE 41: JUST BEFORE FAILURE OCCURS AT RIKS AND EXPLICIT DYNAMIC ANALYSIS

When looking at the model using explicit dynamics and the RIKS method, we find different failure methods. When the capacity reaches the limit, no stress-trajectories develop from the top to the bottom flange, but stress concentrations just below the top flange appear.

This phenomenon this can be seen in Figure 41, which is taken form the model for 1000 web slenderness with explicit dynamics as analytical model. It is clearly visible that the stress doesn't travel through the top flange only, but it uses the top part of the web as well. On the right side of the middle, some stress trajectories are forming, which leads to failure, presented on Figure 42.

The shape in which the plate girder fails is described by 3 plastic hinges in the top girder. The girder in Figure 41 does already show the 2 most affected areas left of the middle, where blue dots are shown. The failure occurs when between these 2 plastic hinges an extra hinge is formed. After this happens the girder losses all its capacity to transmit forces.

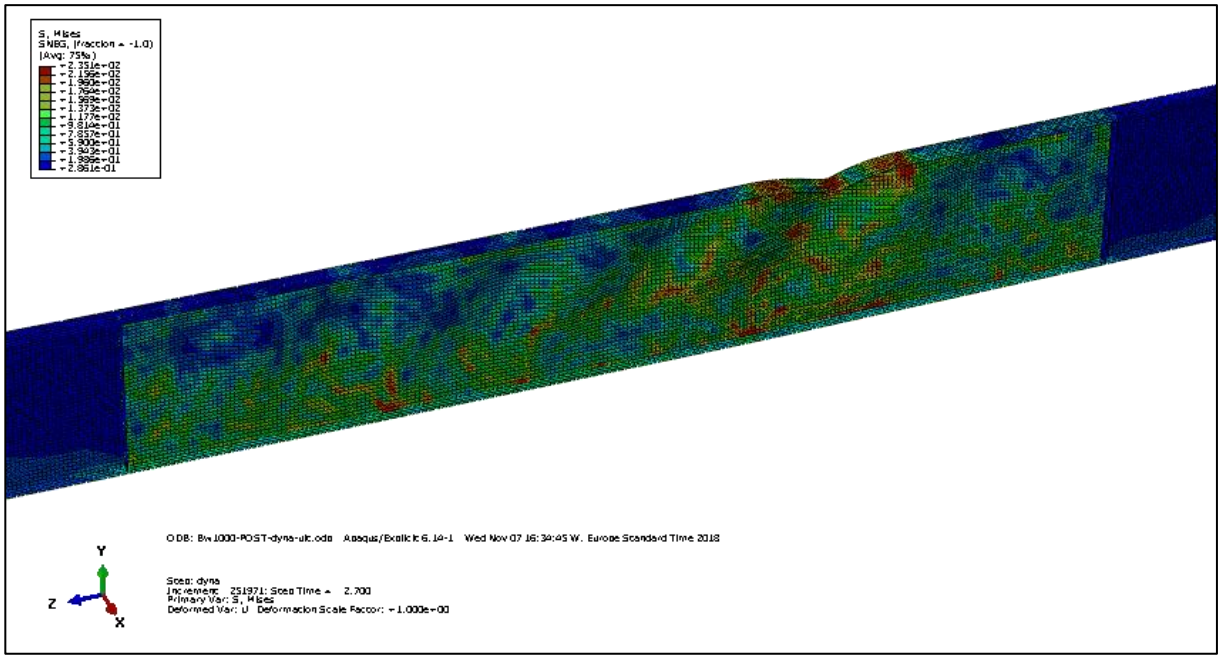

FIGURE 42: FAILURE OF THE PLATE GIRDER USING EXPLICIT DYNAMICS

Comparison with experimental test results

When we analyze the failure mechanism of the girders fabricated and tasted by Abspoel we can address if the reaction of the model is likely to be the mechanism which would occur in an experimentally tested plate girder. For this paragraph, 3 pictures from Abspoel [2] have been given. The web slenderness's of these girders is 400, 600 and 800.

The girder with a slenderness of 400, seen in Figure 43, shows failure through a mechanism similar to that given in Figure 42, found using explicit dynamics, showing only a small effected area in the girder with 3 kinks in the top flange.

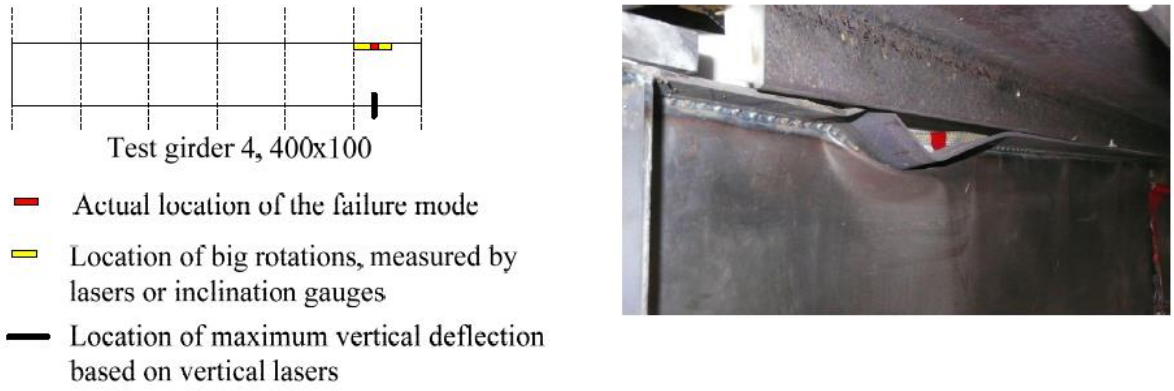

FIGURE 43: GIRDER NUMBER 4 TESTED BY ABSPOEL, WITH A WEB-SLENDERNESS OF 400

The other 2 girders, with slenderness of 600 and 800, are similar to the mechanism given in Figure 40, found using implicit dynamics. Both girders show a 2 hinge-mechanism with a significant part of the girder being affected, although in Figure 44, the mechanism works the other way with the smooth curved top flange traveling to the transverse stiffener. Also, both flanges are rotated after failure, which was also seen on Figure 38 and increased after failure.

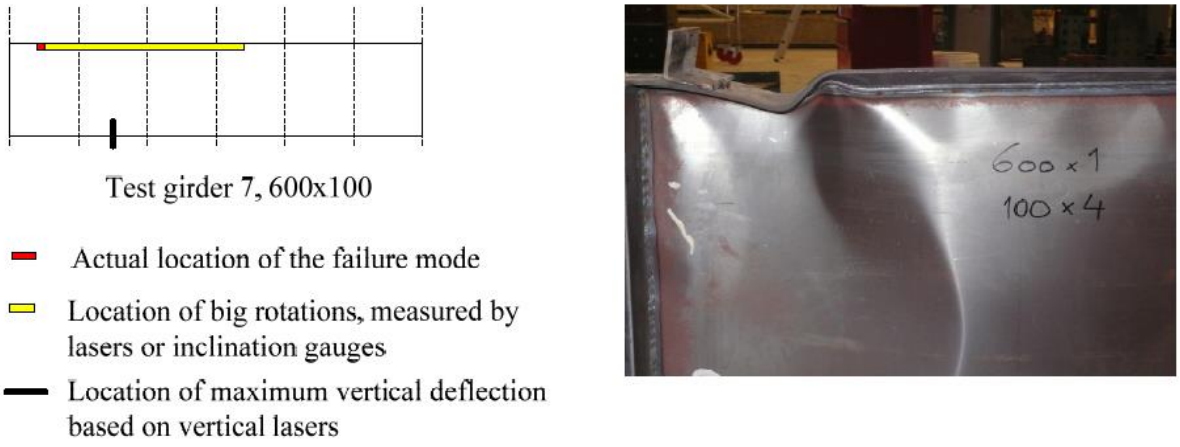

FIGURE 44: GIRDER NUMBER 7, TESTED BY ABSPOEL WITH A WEB-SLENDERNESS OF 600

Looking at the other girders tested by Abspoel it can be concluded that at least 7 out of 10 girders behave like the FEM-model using the implicit dynamic analysis, girder number 4 is the only one failing similar to Figure 42 and 2 girders are difficult to address, which both have a slenderness of 400.

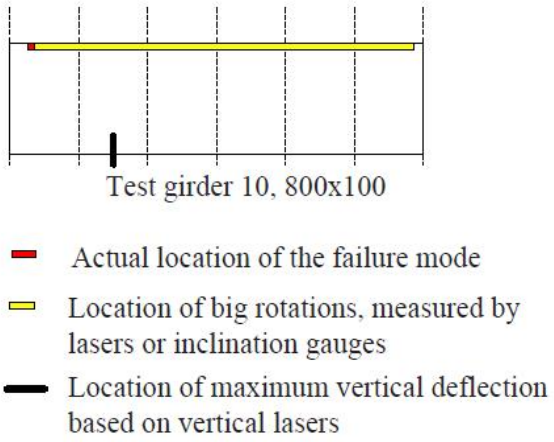

FIGURE 45: GIRDER NUMBER 10, TESTED BY ABSPOEL, WITH A WEB-SLENDERNESS OF 800

Since the modeled girder is given a web-slenderness of 1000, it is more logical to look at the results from the 600 and 800 web-slender girders tested, which all fail with the same mechanism, like the one shown on Figure 40.

3.5.2.e. Conclusion

Looking at the previous paragraph it can be concluded that the models describes the behavior of the plate girder in different ways. The RIKS-analysis seems to work fine to find a maximum bending moment capacity and up to failure the results are very similar to the implicit and explicit dynamic methods. The RIKS analysis, after failure is not capable of presenting a viable post-failure solution for the plate girder. Therefor the RIKS-analysis will not be used in the parametric study.

The difference in the 2 dynamic analysis methods is found in the failure mechanisms. Looking at the experimentally tested girders it can be concluded that the implicit dynamic method shows a more likely way of failing with a girder with a web-slenderness of 1000. Because Cimpoi used the explicit method it was chosen to first use this analysis in the parametric study, but later on the chosen analysis changed to implicit. This process has been described in the parametric study chapter.

To be able to find a realistic maximum bending moment capacity, the imperfections initially applied to the girder should not be too big. Looking at Table 9, the 0,5% imperfection-model was still very accurate, in comparison to the values found by Abspoel. When using the implicit dynamic analysis method, it is also possible to use no initial imperfection and find realistic, but slightly higher values for the bending moment resistance.

The models all have trouble in comparison to the stiffness of the model by Abspoel, given in Figure 26, although the differences in maximum capacity is very similar and only differs from Abspoel's value by 0.7%. To be able to find a maximum bending moment capacity this is of less importance and therefor the implicit model is found to be useful in describing bending behavior of steel slender plate girders.

3.6. 2nd validation on the S235 girder with β_w 700

3.6.1. Introduction

Because the previous chapter already described several comparisons between modelling choices this paragraph will not display every model made, but rather zoom in on not yet described parts comparing the models with a web slenderness of 700 using S235 steel. The total result of the validation is shown with different implicit models, 1 RIKS model and an explicit model, comparing the results to the results found by Abspoel and Cimpoi. Also, the mesh size is checked to address the accuracy of the model as well as an implicit analysis check.

3.6.2. Comparison to Abspoel

The first check is to compare the Force-displacement results of the analysis with the results found by Abspoel and Cimpoi. This comparison for several implicit dynamic analysis can be found on Figure 46. The results show a very similar stiffness and maximum bending moment capacity, which is also presented in Table 10. All results between the new models and those found by Abspoel and Cimpoi are within a range of 1%.

model	*Imperfection amplitude (mm)*	*F (N)*	*M (kNm)*
Fd-Bw700-S235-4%	283,9	578	323
Fd-Bw700-S235-2%	141,9	580	324
Fd-Bw700-S235-1%	70,9	582	325
Fd-Bw700-S235-0,5%	35,4	581	324
Fd-Bw700-S235-0%	0,000	583	326
Fd-Bw700-S235-6mm	5,9	582	325
Cimpoi	5,9	579	323
Abspoel		582	325

TABLE 10: REACTION FORCES AND ULTIMATE BENDING MOMENT FOR 6 IMPLICIT MODELS WITH DIFFERENT IMPERFECTIONS, FOR BW700 S235

Looking at the force-displacement diagram, the models with 0 % – 1 % (0 to 70 mm) initial imperfection show the best comparison with the red line, which is the result of Abspoel. The results the 2 and 4% models show less ductility and fail earlier after the maximum bending moment resistance is found.

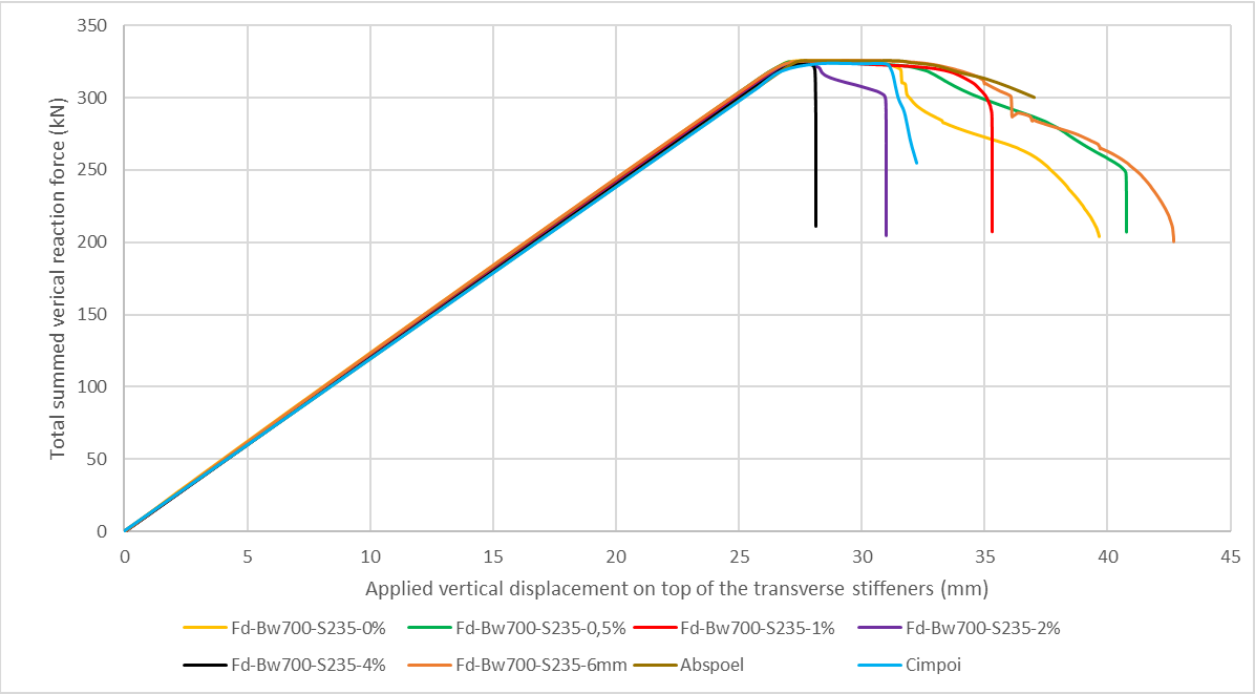

FIGURE 46: DYNAMIC IMPLICIT ANALYSIS FOR BW700 S235, COMPARED TO ABSPOEL AND CIMPOI

When comparing the results given in Figure 46, to those found in a similar comparison for the girders with a web slenderness of 1000, found on Figure 24 and Figure 26, it can be seen that the effect on initial imperfection is less with this lower web-slenderness. For the slenderness of 1000, a significant reduction in ductility was found when using 1% initial imperfection or more, also the bending moment capacity reduces noticeably. With the 700 slenderness-models the moment capacity did not reduce and a decrease in ductility was clearly visible when 2% imperfection was used.

3.6.3. Check of mesh size and analysis comparison

In finite element modelling, in general a result will be more accurate when a finer mesh and therefore more integration points are present in the model. Because the software calculates results for differential equations for all the integration points in the elements. There are several types of elements with a certain amount of integration points per element, but when the element type is not changed the mesh size controls the amount of integration point.

An infinitely small mesh would result in a very accurate result, but also in a very long calculation. Therefor it is needed to optimize the mesh size to be able to get accurate results as well as an acceptable calculation time. To address these 2 identical models are made, with only the mesh size as changing parameter. In this case the models were RIKS-analysis, with results given in Figure 47.

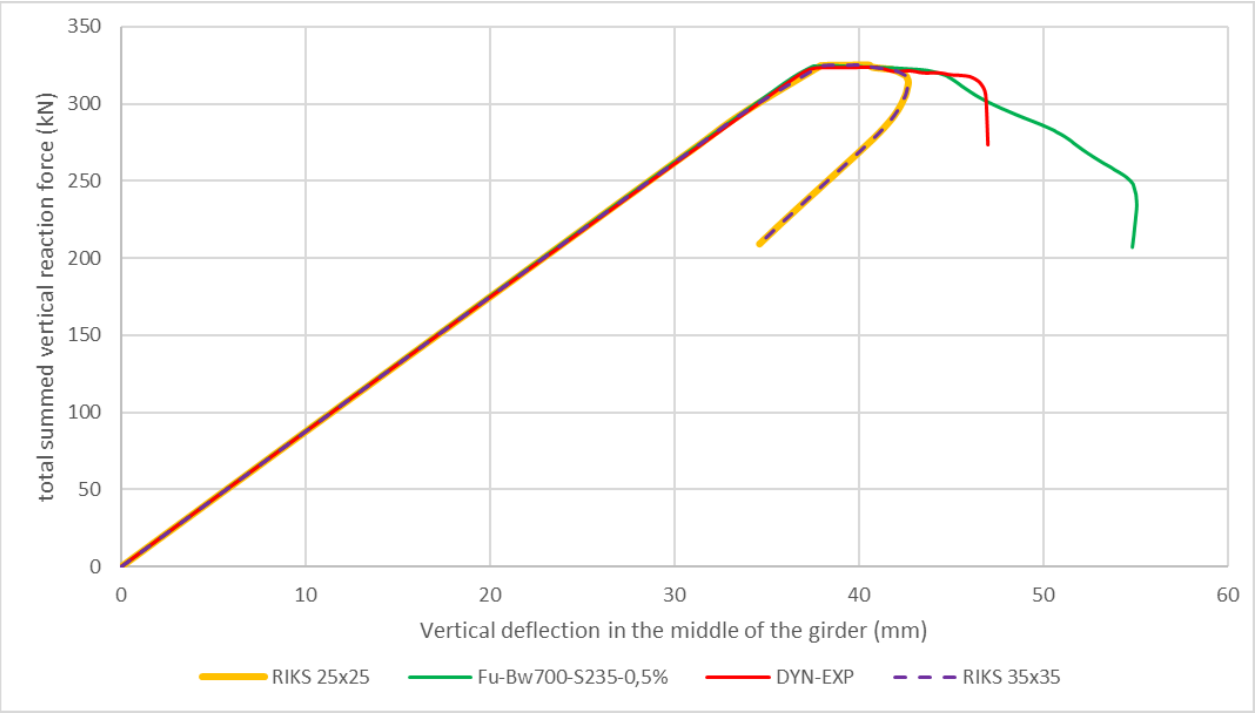

FIGURE 47: 2 RIKS-ANALYSIS WITH DIFFERENT MESH SIZES COMPARED TO 2 DYNAMIC ANALYSIS

It can be seen that the results are identical, or at least on this scale very likely to differ very little from each other. The increased number of elements does not lead to extra accuracy and therefor 35x35mm mesh is chosen as the mesh to model all girders in the parametric study.

In Figure 47 the comparison of the Explicit Dynamic, Implicit dynamic and RIKS method are also presented, with all models having the same initial imperfection of 35 mm. The results of the maximum moment are very similar, with the stiffness and maximum bending moment resistance being almost the same. The post-failure reaction of the models is different, which was also seen in the Bw1000 comparison.

3.6.4. Difference in implicit analysis method parameters

As has been discribed in the previous paragraph of this chapter, the implicit method shows the best results in comparison to the works of Abspoels experimental en parametric study. The Implicit method, but the implicit method is not as easy to control as for example the Explicit and RIKS-analysis, which are largely automated.

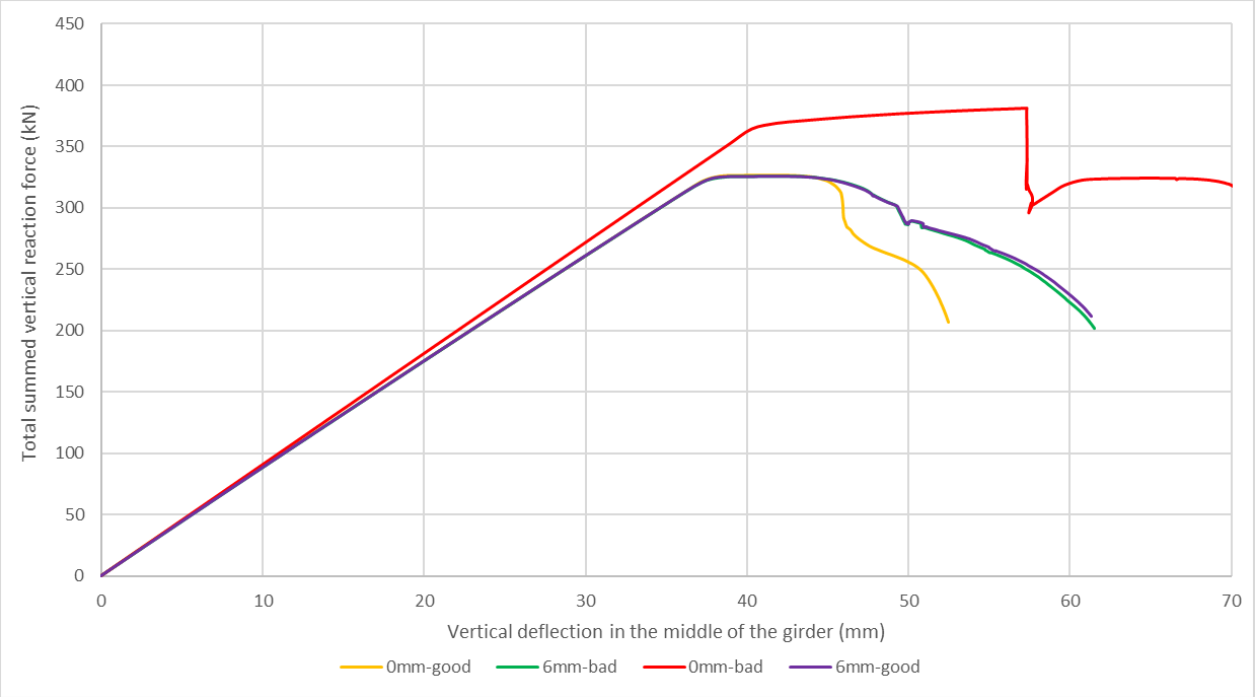

FIGURE 48: IMPLICIT ANALYSIS WITH DIFFERENT STEP SIZES, SHOWING THE IMPORTANCE OF CHOOSING A CORRECT STEP SIZE

To be able to find a valid solution several implicit analyses are modeled and executed to address the impact of the maximum step size used on the result and calculation time and data storage. 3 types of models were constructed all using a quasi-static approach with an applied displacement of 1 mm per second.

1. **Perfect-model:** step-size maximum of 0.025 seconds for 110 seconds total
2. **Good-model:** Step size maximum of 0.025 seconds for 10 seconds, followed by step size maximum of 0.75 seconds for 100 seconds
3. **Bad-model:** step-size maximum of 0.75 seconds for 110 seconds.

The “perfect-model” was the first model, but using the good-model an exact copy of the results was found, but in shorter time and with output-files being approximately 500 megabytes instead of 10 Gigabytes. Therefor the rest of the paragraph only the good and bad model are commented on.

In the figure below, Figure 48, the graph shows 4 lines. 3 lines are almost the same, which can be described as the same behavior shown in Figure 29. The out-of-plane displacement in a girder web does not differ if the initial displacement of the model is small, compared to a model without initial displacement. This is because the girder buckles due to the forced displacement, thereby reducing internal energy and mimicking the shape of the girder where an initial displacement was introduced, seen in Figure 49.

The “bad-model” without initial imperfection doesn’t experience this step and therefor experiences stiffer behavior and a larger maximum applied force, which can be seen in Figure 50. The behavior of the girder with increasing applied displacement is also different.

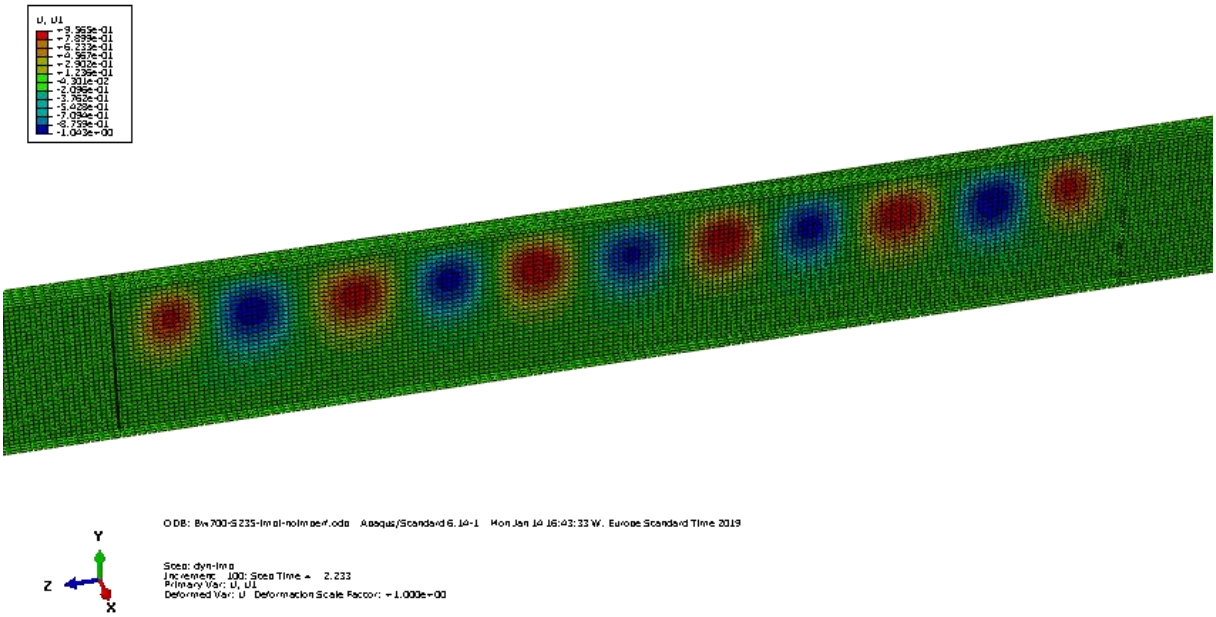

FIGURE 49: GOOD-MODEL WITHOUT IMPERFECTION, EXPERIENCES OUT-OF-PLANE DISPLACEMENT IN THE WEB AT 2 MM APPLIED DISPLACEMENT

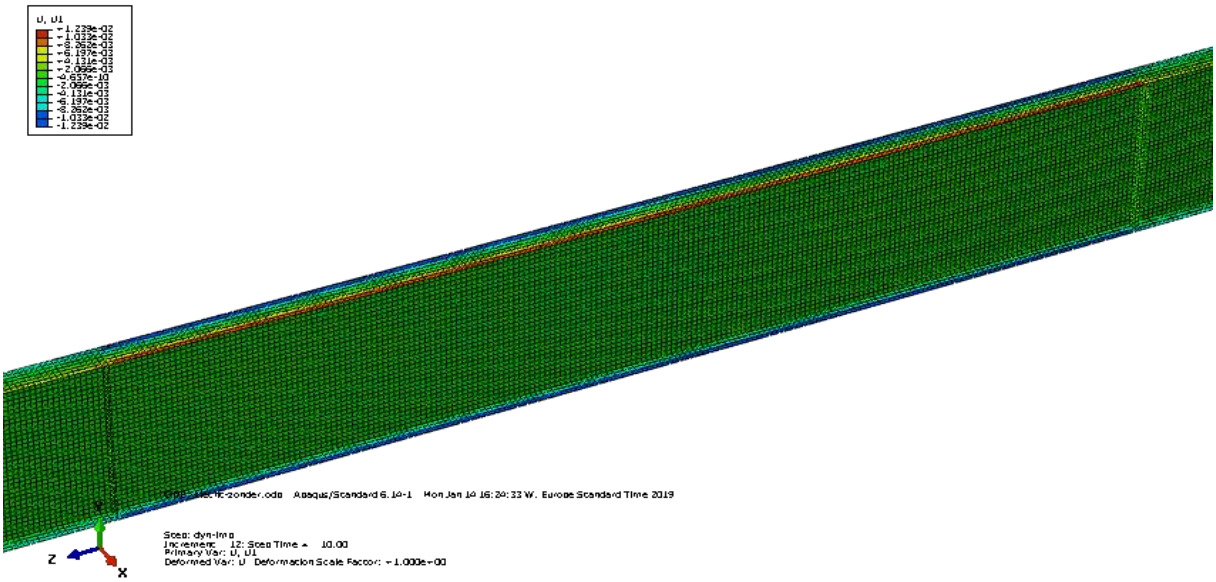

FIGURE 50: BAD-MODEL WITHOUT IMPERFECTION, EXPERIENCES NO OUT-OF-PLANE DISPLACEMENT IN THE WEB AFTER 10MM APPLIED DISPLACEMENT

Compared to the non-uniform stress displacement for the girders which experienced out-of-plane displacement. On the left picture of Figure 51, the non-uniform stress distribution at 29,5 mm-imposed displacement is found with the “good-model”, compared to the right picture, which shows the stress distribution at 40 mm-imposed displacement at the “bad-model”. This stress-distribution is completely uniform, which is very unusual with these slender girders.

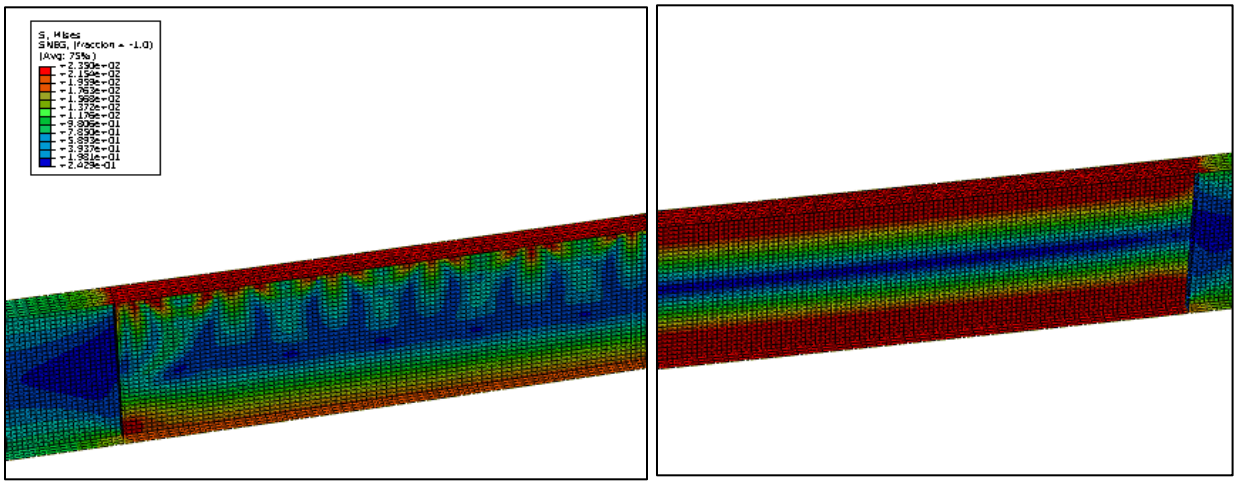

FIGURE 51: STRESS DISTRIBUTION FOR (L) GOOD AND (R) BAD MODEL WITHOUT INITIAL IMPERFECTION AT MAXIMUM MOMENT RESISTANCE

3.6.5. Conclusion

Looking at the previous paragraph and comparing this to the results of the validation of the models with a web slenderness of 1000, the implicit model is the most logical model to use in the parametric study to analyze the moment capacity of slender steel plate girder on bending only. Because Cimpoi used the explicit method, it was nonetheless chosen to use the explicit method as parametric study model.

The implicit analysis is subjectable to errors, which can be seen in Figure 48, so the maximum step must be controlled and the out-of-plane displacement shall have to be monitored to address if the plate girder web develops buckles prior to failure and a non-uniform stress distribution can be observed similar to the left picture of Figure 51. The explicit model is more self-regulating and therefor easier to program.

For the parametric study the imperfection of all the models should be limited to be able to find good results for the maximum bending moment, although the impact on the models with 700 web slenderness was less than the impact on the 1000 web slender models. For both model-collections counts that no imperfection or an initial imperfection with an amplitude of up to 1% of the width of the girder middle-section would lead to good results.

4. Parametric study on bending moment capacity

4.1. Introduction

4.1.1. S690 tests to compare and verify the results found by Cimpoi

The research carried out by Abspoel was continued by Cimpoi, which have been described in paragraph 2.3.4. During the research of Abspoel FEM analysis on plate girders in a 4-point bending test where made with steel grades S235 and S460. These results were used to make an estimation for the maximum bending moment resistance for girders made out of S355 and S690 steels.

Abspoel concluded that the maximum bending resistance was not dependent on the total area of the cross section, but is governed by the steel grade. For S235 this value was found to be 1450 and for S460 the value was 850. Extrapolating these results Abspoel assumed the maximum web slenderness for S690 to be 509.

During the research of Cimpoi the web slenderness for S460 was confirmed to be 850 when the parametric study was conducted on plate girders with 12000 mm^2 cross sectional area. The web slenderness of S690 girders with 6000 and 12000 mm^2 where found to be 800 and 450, thereby challenging Abspoel's conclusions.

Because the results were found to be no-conforming with the results of Abspoel, it is useful to check these results and there for the first part of the parametric study will be to remodel the plate girders, tested by Cimpoi, using S690 steel and assessing the results using Abaqus as FEM-software. Both the total areas, 6000 and 12000 mm^2, will be tested.

4.1.2. Expanding research with higher strength steel

Because the assumption of Abspoel was a linear increasing extrapolation showing a decreasing maximum web slenderness with increasing steel grade. It's not a realistic prediction for every steel grade, because a very high steel grade would need a lot of strain to be able to achieve yielding, because the elastic modulus will stay the same. It's more realistic that a plateau in the trend line would occur.

Therefor more results need to be found for maximum bending moment resistance and its web slenderness using higher strength steels, using in this case S890 steel.

4.2. Modelling and analysis of the girders

4.2.1. Geometry

The same equations were used as have been used by Abspoel to construct this parametric study. These equations are given in paragraph 3.2.2 and were also used in the validation stage.

4.2.2. Applied Imperfection

The software package Abaqus, which has been used in this thesis had the functionality to address the eigenmodes of the structure in combination with an applied force. This process is a linear perturbation analysis called buckle. This analysis is used to find the first 10 eigenmodes of the, to be analyzed, geometries with a unit-displacement on top of the transverse stiffeners. The output of this analysis is a

deformed shape, with the deflection having a value between -1 and 1 and the load needed for this buckling shape to form.

The shape of the first 2 modes always looks like the one showed on Figure 52. Mode 2 is found showing the same 6-sinus-shaped buckle on the top of the web, but with the buckles in opposite direction. The amplitude of all the buckles is almost identical, but the ones closest to the applied force are somewhat bigger.

In the top picture it is not noticeable that the flange also has a deformed shape in mode 1. This is shown on the bottom picture, only showing the top flange, in which the deflection is magnified 10 times in comparison to the top picture.

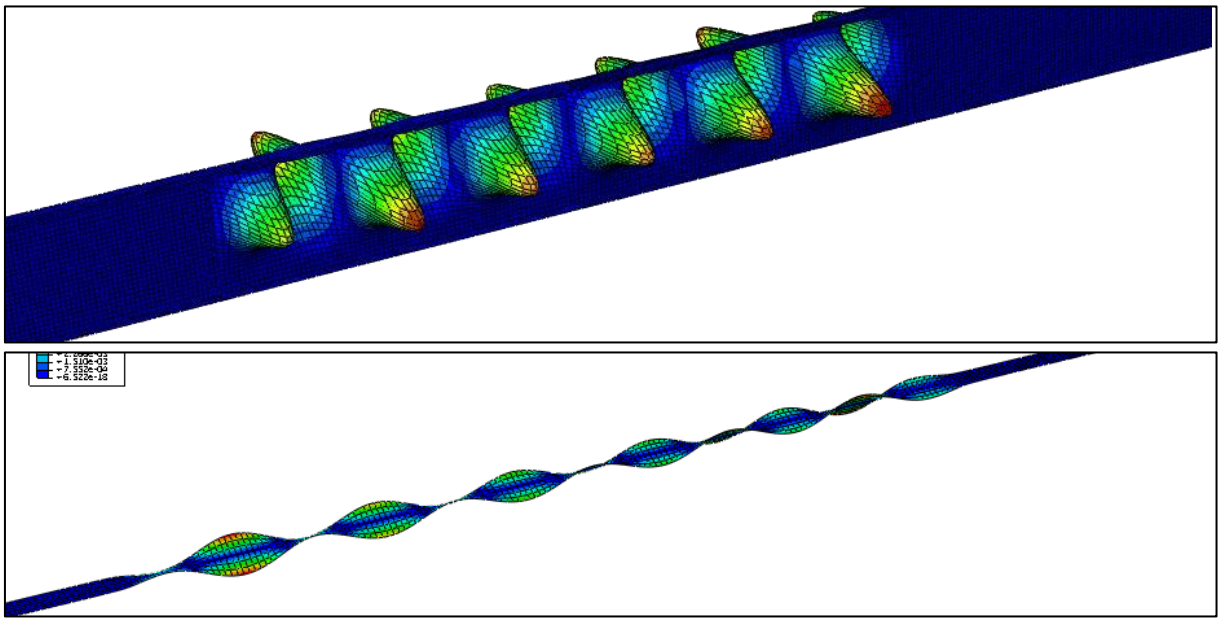

FIGURE 52: EIGEN MODE 1 FOR A GIRDER WITH A WEB OF 6 TIMES THE HEIGHT (T) FLANGE IMPERFECTION X10 (B)

All geometries were analyzed using the buckle analysis and the shape was used as the shape for an initial imperfection applied on the plate girders. To do this the deformed shape was multiplied by a certain amplitude and using a KEYWORD-command in Abaqus applied to the geometry before the load was applied.

4.2.3. Analysis

For the parametric study there have been 2 types of analysis used. Firstly, the explicit non-linear dynamic analysis and secondly the implicit dynamic non-linear analysis. Both analyses were used to mimic a static analysis, using the quasi-static method setting for both analyses.

4.2.4. Material Properties

4.2.4.a. Stress-strain relationship

Just like in paragraph 3.3.1 the stress strain relationship is found using the equations for true stress-true strain, using the elastic modulus for steel as 210 GPa. The relationship for both S690 and S890 are given, as well as the values for S460 which are used in paragraph 4.6.4 only.

We find the relationship between the stresses and strains in the 3 tables of table 11

nominal		true	
stress	strain	stress	strain
460	0,00219	461,0076	0,002188
460,0007	0,0025	461,1507	0,002497
460,0017	0,003	461,3817	0,002996
460,0028	0,0035	461,6128	0,003494
460,0038	0,004	461,8438	0,003992
460,0049	0,0045	462,0749	0,00449
460,0059	0,005	462,3059	0,004988
460,007	0,0055	462,537	0,005485
460,008	0,006	462,768	0,005982
460,0091	0,0065	462,9991	0,006479
460,0101	0,007	463,2302	0,006976
460,0112	0,0075	463,4612	0,007472
460,0122	0,008	463,6923	0,007968
460,0133	0,0085	463,9234	0,008464
460,0143	0,009	464,1544	0,00896
460,0154	0,0095	464,3855	0,009455
460,0164	0,01	464,6166	0,00995
460,0175	0,0105	464,8476	0,010445
460,0185	0,011	465,0787	0,01094

nominal		true	
stress	strain	stress	strain
690	0,003286	692,2671	0,00328
690,0005	0,0035	692,4155	0,003494
690,0015	0,004	692,7615	0,003992
690,0026	0,0045	693,1076	0,00449
690,0036	0,005	693,4536	0,004988
690,0047	0,0055	693,7997	0,005485
690,0057	0,006	694,1457	0,005982
690,0068	0,0065	694,4918	0,006479
690,0078	0,007	694,8379	0,006976
690,0089	0,0075	695,1839	0,007472
690,0099	0,008	695,53	0,007968
690,011	0,0085	695,876	0,008464
690,012	0,009	696,2221	0,00896
690,0131	0,0095	696,5682	0,009455
690,0141	0,01	696,9142	0,00995
690,0152	0,0105	697,2603	0,010445
690,0162	0,011	697,6064	0,01094
690,0173	0,0115	697,9524	0,011434
690,0183	0,012	698,2985	0,011929

nominal		true	
stress	strain	stress	strain
890	0,004238	893,7719	0
890,0006	0,0045	894,0056	0,000261
890,0016	0,005	894,4516	0,000758
890,0027	0,0055	894,8977	0,001256
890,0037	0,006	895,3437	0,001753
890,0048	0,0065	895,7898	0,00225
890,0058	0,007	896,2358	0,002746
890,0069	0,0075	896,6819	0,003243
890,0079	0,008	897,128	0,003739
890,009	0,0085	897,574	0,004235
890,01	0,009	898,0201	0,004731
890,0111	0,0095	898,4662	0,005226
890,0121	0,01	898,9122	0,005721
890,0132	0,0105	899,3583	0,006216
890,0142	0,011	899,8044	0,006711
890,0153	0,0115	900,2504	0,007205
890,0163	0,012	900,6965	0,007699
890,0174	0,0125	901,1426	0,008193
890,0184	0,013	901,5886	0,008687

TABLE 11: STRESS-STRAIN RELATIONSHIP FOR S460 (L), S690 (MID) AND THE STRESS STRAIN RELATIONSHIP FOR S890 (R)

4.3. Parametric studies on bending moment capacity for steel plate girders using S690 steel

4.3.1. 1st Parametric study on S690 steel plate girders with 6000mm^2 total area using explicit dynamics

4.3.1.a. Introduction

The first parametric study conducted was the study of the steel slender plate girder with a total steel-area of 6000 mm^2, using S690 steel. This was to check the results found by Cimpoi and therefor the same modeling and analysis was used. This parametric study was similar to the validation, to check if the results of the model would be the same and validate the found results.

The Explicit Dynamic, quasi-static analysis was used to model plate girders with different web-slenderness keeping the flanges the same throughout all of the models. The first models were tested in a range between a web slenderness of 300 and 800, with an initial interval of 100. After the results of these first 6 models have been analyzed intermediate models will be created to find the ultimate web slenderness which gives the highest bending moment resistance, with a maximum interval of 50.

4.3.1.b. Force displacement behavior

The behavior of the girders with applied deformation on top of the transverse stiffeners has been plotted to show the reaction and stiffness of the girders, this can be found on Figure 53. It can be seen that when the web slenderness is kept below a certain value, the graph is fluent and some redundancy can be observed, shown by the flattening of the curve leading to a plateau in which the top flange of the plate girder is yielding. This limiting slenderness is in close vicinity of a web slenderness of 600.

When the slenderness is increased, a loop is formed in the force-displacement diagram and the total vertical reaction force also reduces quite fast, as well as a lack of rotational capacity and therefor sudden failure. The shape of the graph seems strange, but can be explained by the nature of the graph. The graphs show the relation between the force and the vertical deflection of the girder in the middle of the bottom flange. It is possible that this point is not the lowest point, or that this point does not deflect proportionally to the applied force. This is shown in Figure 54, for a girder with a slenderness of 450 using S890 steel, this is because the model-results of the explicit dynamic tests for S690 steel have been damaged and could not be retrieved. The red line, representing the applied displacement in relation with the reaction force, shows a logical shape, while the other line shows the similar loop as found in Figure 53. This figure shows the results with the loop are also valid, although they could have been presented clearer.

The stiffness of all the girders is linear until a certain point in which the flanges yield, or sudden failure occurs. The girders with a higher web slenderness seem to have a lower stiffness, which would not be logical. This can be explained by the fact that the lever arm of the girders is different from each other and increasing with increasing web slenderness, in fact it is 3 times the height of the girder.

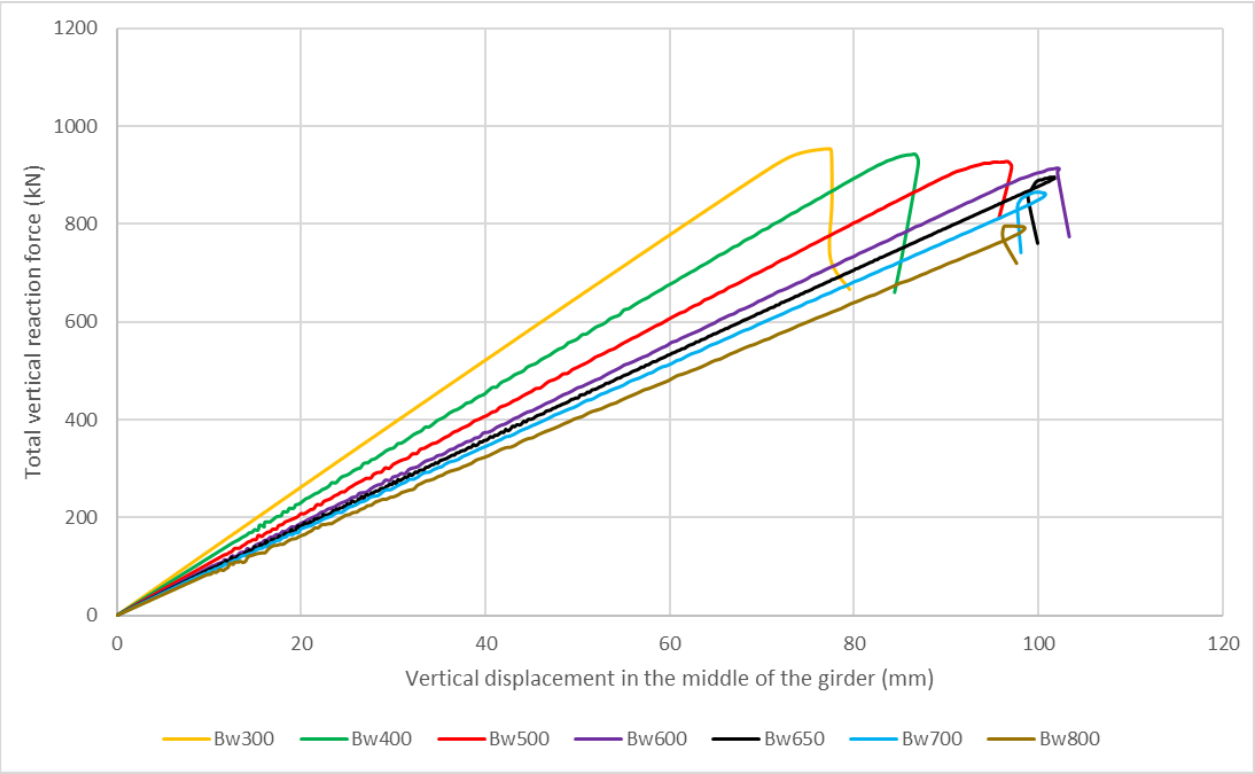

FIGURE 53: RANGE OF LOAD-DISPLACEMENT DIAGRAMS FOR S690 STEEL GIRDERS WITH 6000 MM^2, USING EXPLICIT DYNAMICS

Using the lever arms to calculate the resulting bending moment resistance of the girders the optimal web slenderness can be found. These results are given in Table 12. This table shows a maximized bending moment resistance with a web slenderness 700, but would probably be somewhat lower if the interval of tested slenderness would have been increased. The increase in capacity is seen to climb fast until a slenderness of 600, after this it is only increased very slightly and reduces after 700.

Web slenderness	*Length end-section (mm)*	*F (kN)*	*M (kNm)*
300	2323,8	953,7	1108,1
400	2683,8	942,2	1264,4
500	3000,0	927,6	1391,4
600	3286,3	914,7	1502,9
650	3420,5	896,3	1532,8
700	3549,7	865,4	1535,8
800	3794,7	795,9	1510,0

TABLE 12: MAXIMUM FORCE AND MOMENTS FOR S690 WITH 6000 MM^2 USING EXPLICIT DYNAMICS

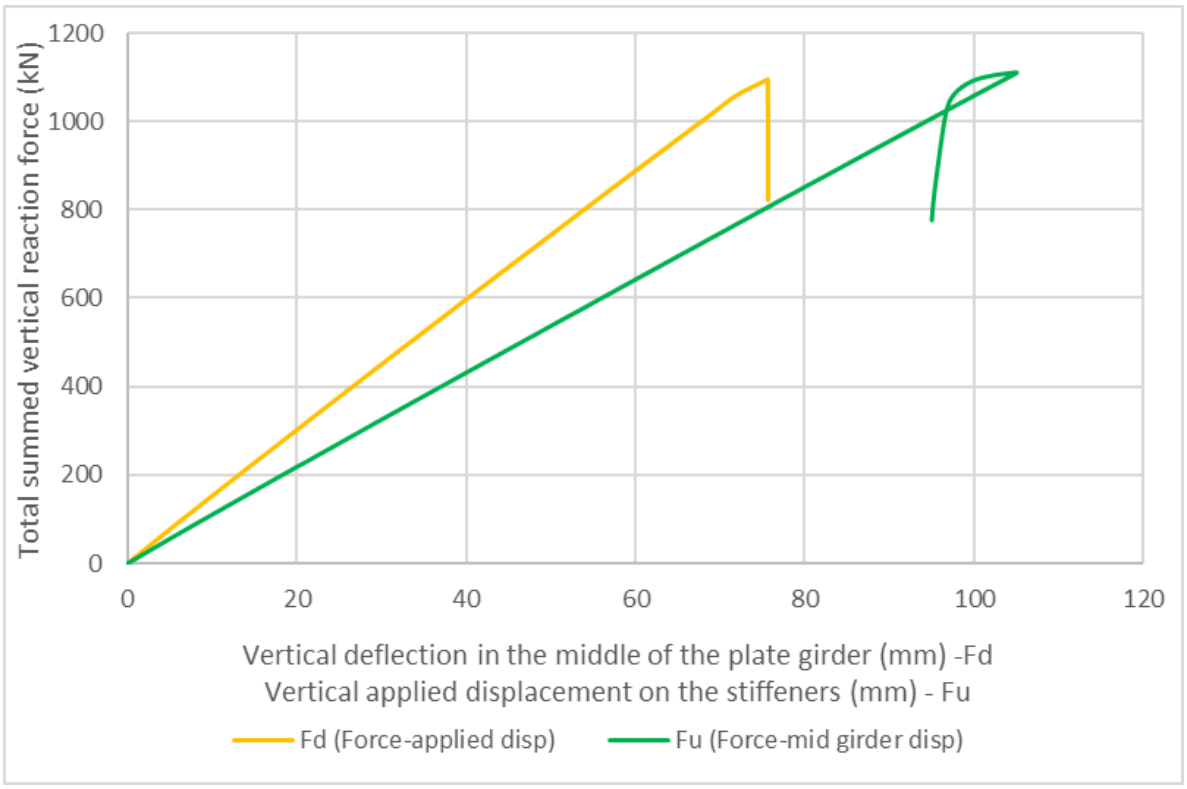

FIGURE 54: DIFFERENCE BETWEEN 2 APPROACHES IN LOAD DISPLACEMENT GRAPHS (BW=450, A=6000MM^2, STEEL S890)

4.3.1.c. Failure mode

The failure of the girders has been presented with the use of 2 examples, two sets of deformed plots from the results of tested girders with a slenderness of 400 and 600 are presented. The shapes of these examples resemble the full range of girders tested, the modes for girders up to 500 where similar to the 400 examples, while the 600 and more slender models followed the same mechanism as the girder with a slenderness of 600.

Figure 55 shows the failure of the 400-web slender girder. At the first picture it can be seen that both top and bottom flange are stressed to a high level and yielding has been recorded in the top flange. After a certain extra rotation, in which some extra capacity is found the top flange starts to twist, close to the left transverse stiffener, leading to the rotation of the top flange. After this occurred the flange buckles vertically at this point and develops excessive out-of-plane deformation in the web.

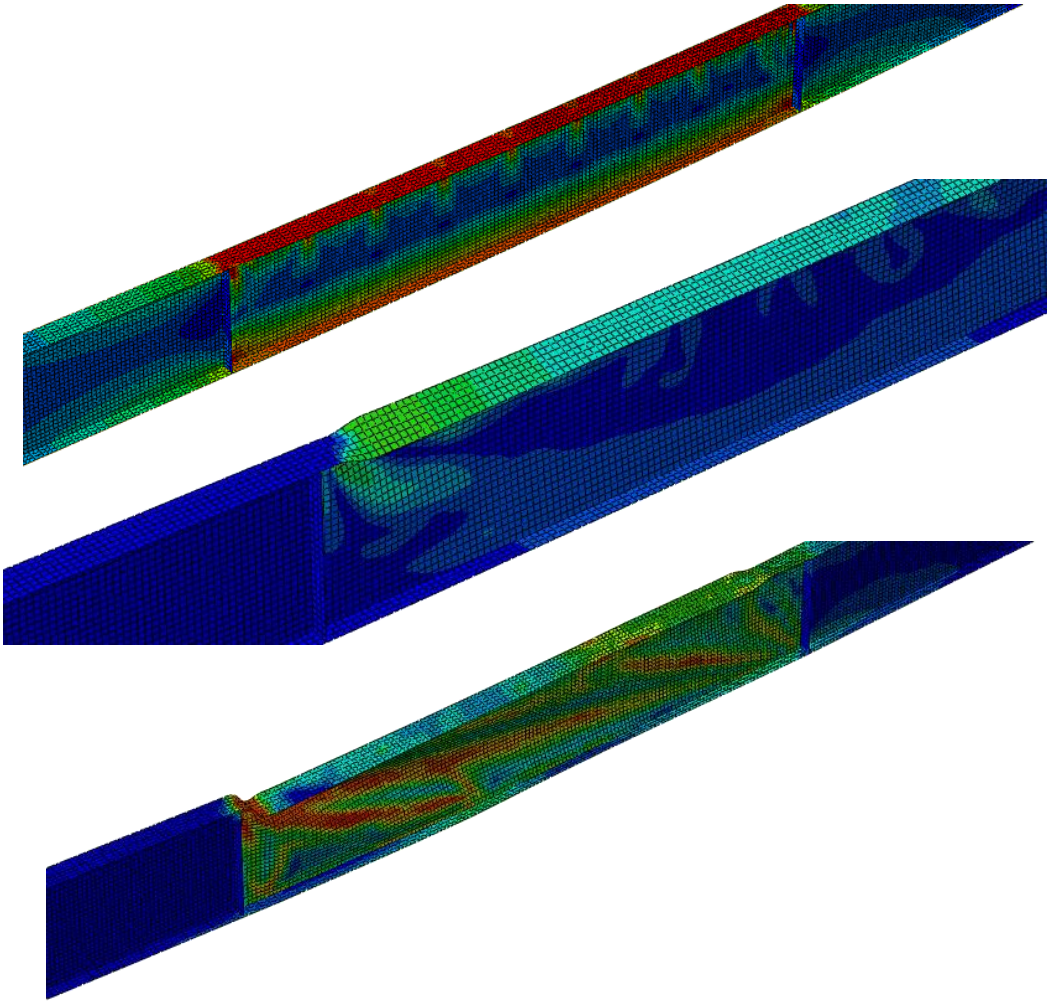

FIGURE 55: FAILURE MODE FOR EXPLICIT DYNAMIC TEST ON S690 GIRDER WITH 6000 MM2 AND A WEB SLENDERNESS OF 400

Figure 56 shows the behavior of the girder with a slenderness of 600. Until yielding of the top flange is recorded, the girder reacts linear to the applied deformation. When the applied deformation is increased slightly, sudden flange-collapse occurs. The top flange gets pushed into the web and the web buckles out-of-plane very far.

When more deformation is applied, the flange and web-buckles increase in size, but the bottom flange stays in the same position, leading to the loop in the diagram.

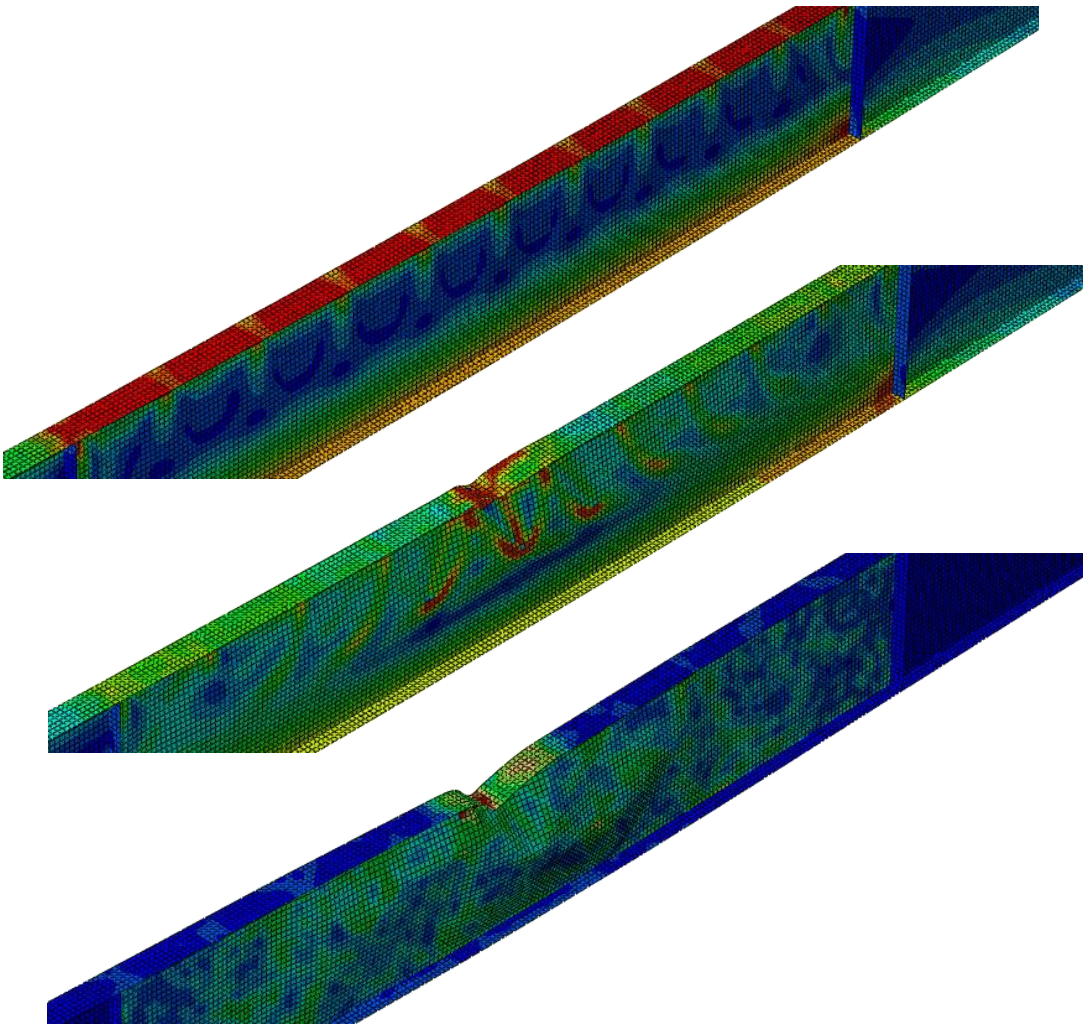

FIGURE 56: FAILURE MODE FOR EXPLICIT DYNAMIC TEST ON S690 GIRDER WITH 6000 MM2 AND A WEB SLENDERNESS OF 600

4.3.1.d. Maximum web slenderness and ultimate bending moment resistance

The found maximum web slenderness using the explicit dynamic analysis is somewhere between 650 and 700. For the used models the limiting moment capacity is found using a web slenderness of 700. The found maximal capacity is 1535 kNm.

The results have been presented in Figure 57, with the addition of the results which have been found by Cimpoi. It can be noticed that the models with slenderness of 400, 500 and 600 give very similar results, but the maximum bending moment resistance for Cimpoi was found in a girder with a web slenderness of 800, showing 1700 kNm as the maximum capacity. A logical explanation could not be found for this difference, only the initial imperfection was different in these models. Cimpoi used 1/200 of the height, while this parametric study was conducted using no initial imperfection.

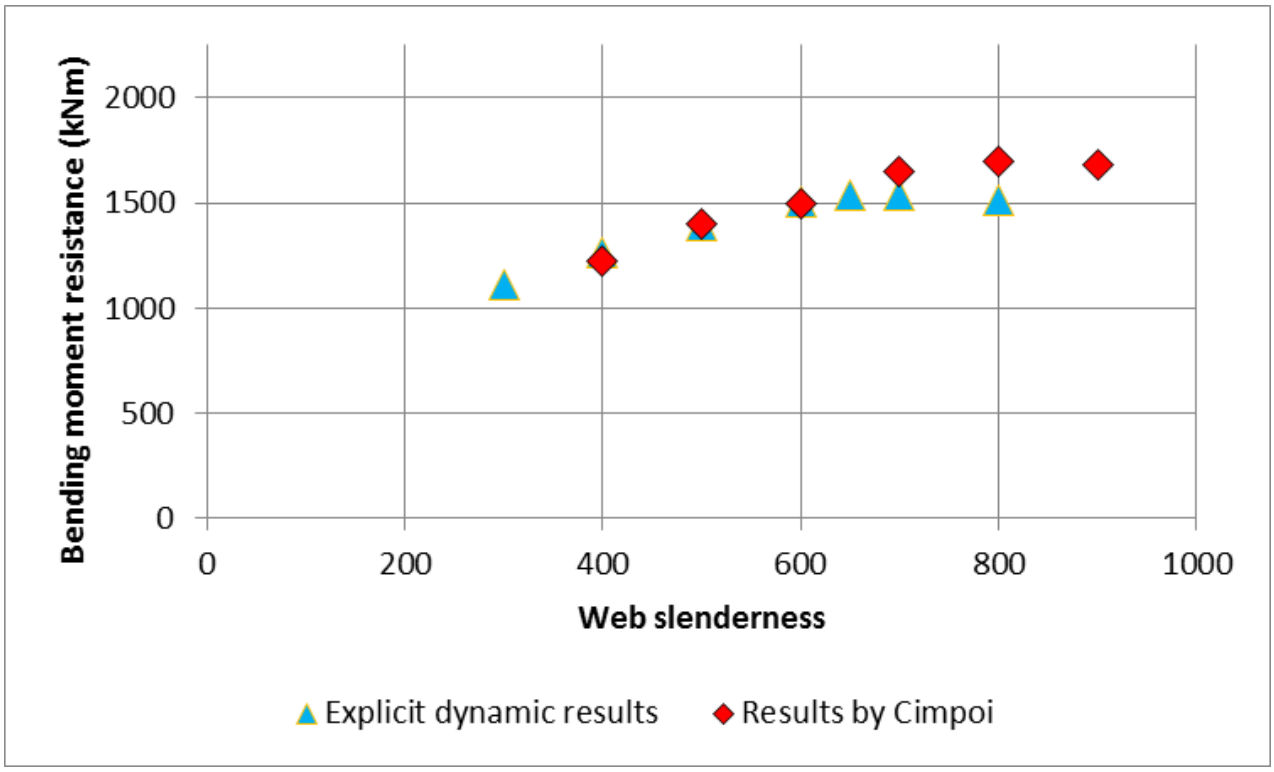

FIGURE 57: MAXIMUM MOMENT CAPACITY FOR S690 GIRDER WITH 6000 MM^2 AREA, USING EXPLICIT DYNAMICS

4.3.2. Explicit dynamic parametric study on S690 steel plate girders with 12000mm^2 total area

4.3.2.a. Introduction

The models for this parametric study were created using the equations from the validation chapter, in a range from a slenderness of 300, 400 and from 500 to 800 with increments of 50. The results will be given in the form of force-displacement diagrams and moment capacities resulting from the maximum summed vertical reaction force.

4.3.2.b. Force-displacement behavior

The reaction forces are summed and their relation with the vertical displacement in the middle of the girder has been plotted on Figure 58. The 2 graphs for the least slender girders show a similar path as was shown in the plot of the girders with 6000 mm^2 area, although it seems the rotational capacity is somewhat less.

The other graphs show a remarkable path. First a linear elastic part is observed, which is followed by a peak upwards. The peaks seem to get bigger when the web slenderness increases and with the models for 600 and 700 the peak looks to go straight up, insinuating that the middle part of the bottom flange stays on the same level, but the applied force increases significantly. This seems strange and is very unlikely to be real behavior.

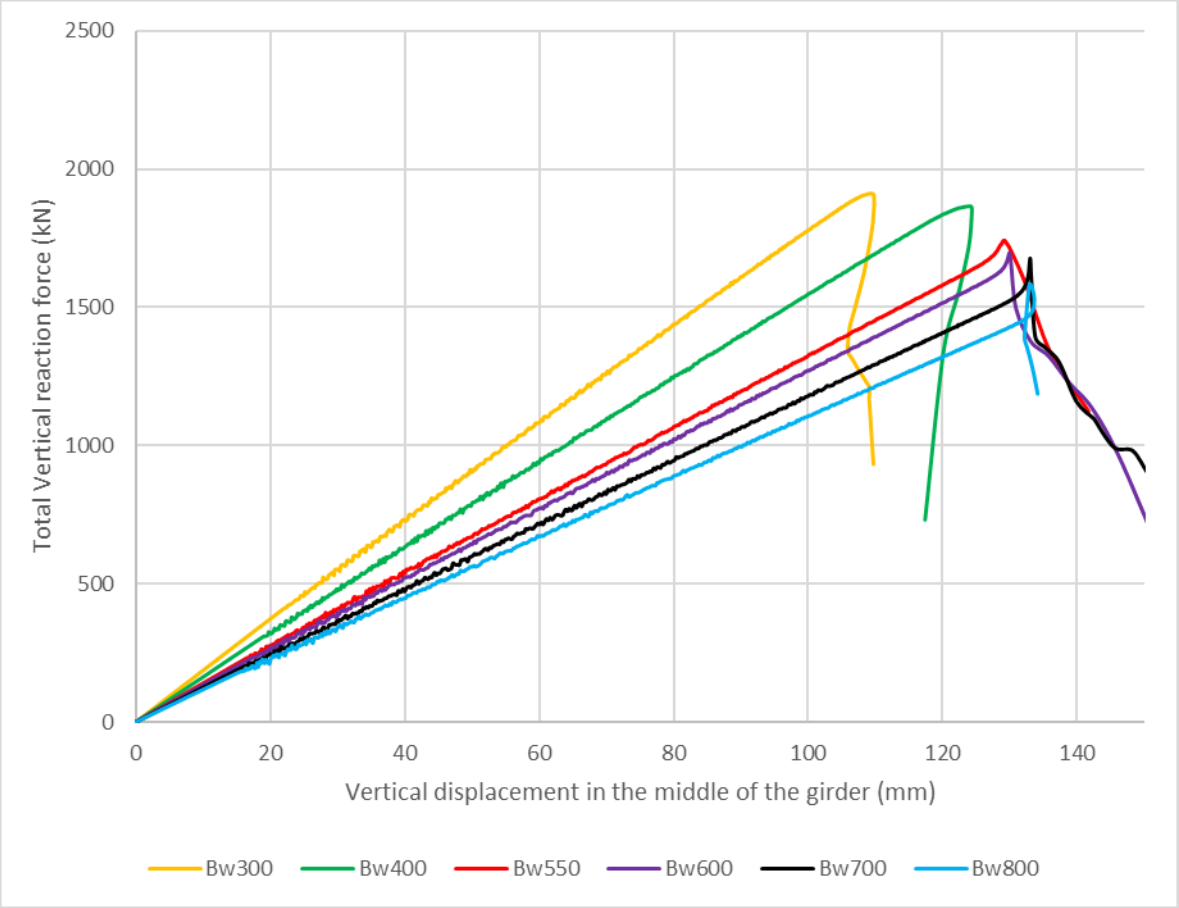

FIGURE 58: RANGE OF LOAD-DISPLACEMENT DIAGRAMS FOR S690 STEEL GIRDERS WITH 12000 MM^2, TESTED WITH EXPLICIT DYNAMICS

4.3.2.c. Failure mode

The models have a transition point in which the failure mode changes. This point is at a web slenderness of approximately 550. For this model the force displacement diagram starts to change shape.

Before this point we find the top flange to rotate after the top flange yields, leading into the flange buckling into the web, shown on Figure 55. After the transition point the failure mode is different and much more local, also showing vertical buckling of the flange, but the rotation prior to this failure is not recorded. The failure mode is very similar to the one depictured on Figure 56.

4.3.2.d. Maximum web slenderness and Ultimate bending moment resistance

Using the maximized reaction forces the bending moment capacity can be calculated, using the applied end-section lengths as lever arm. The results are given in Table 13. It can be seen graphically in Figure 59. The bending moment resistance found by Cimpoi is also added to this picture and does not achieve the values found in this parametric study. The result for the model with a 300 slender web looks similar, but the rest of the results differ significantly from the results found in this parametric study.

Web slenderness	*Length end-section (mm)*	*F (kN)*	*M (kNm)*
300	3286,3	1912,5	3142,5
400	3794,7	1866,2	3540,8
500	4242,6	1787,5	3791,8
550	4449,7	1742,0	3875,8
600	4647,6	1697,4	3944,4
650	4837,4	1680,7	4065,0
700	5020,0	1676,7	4208,5
750	5196,2	1599,0	4154,4
800	5366,6	1583,8	4249,7

TABLE 13: MAXIMUM FORCE AND MOMENTS FOR S690 WITH 12000 MM^2 USING EXPLICIT DYNAMICS

The limit found by Cimpoi was achieved using a girder with a web slenderness of 450 and was valued at 3750 kNm, were in this parametric study the limiting web slenderness was found to be 800 or above and maximized at 4249.7 kNm. The strange value for the capacity of 750, which happened to be lower than that of 700 and 800, could not be explained logically, but as can be seen in Figure 58, the behavior of the model with the 800 web slender girder was very different from the other girders close to this slenderness and is not likely to be valid.

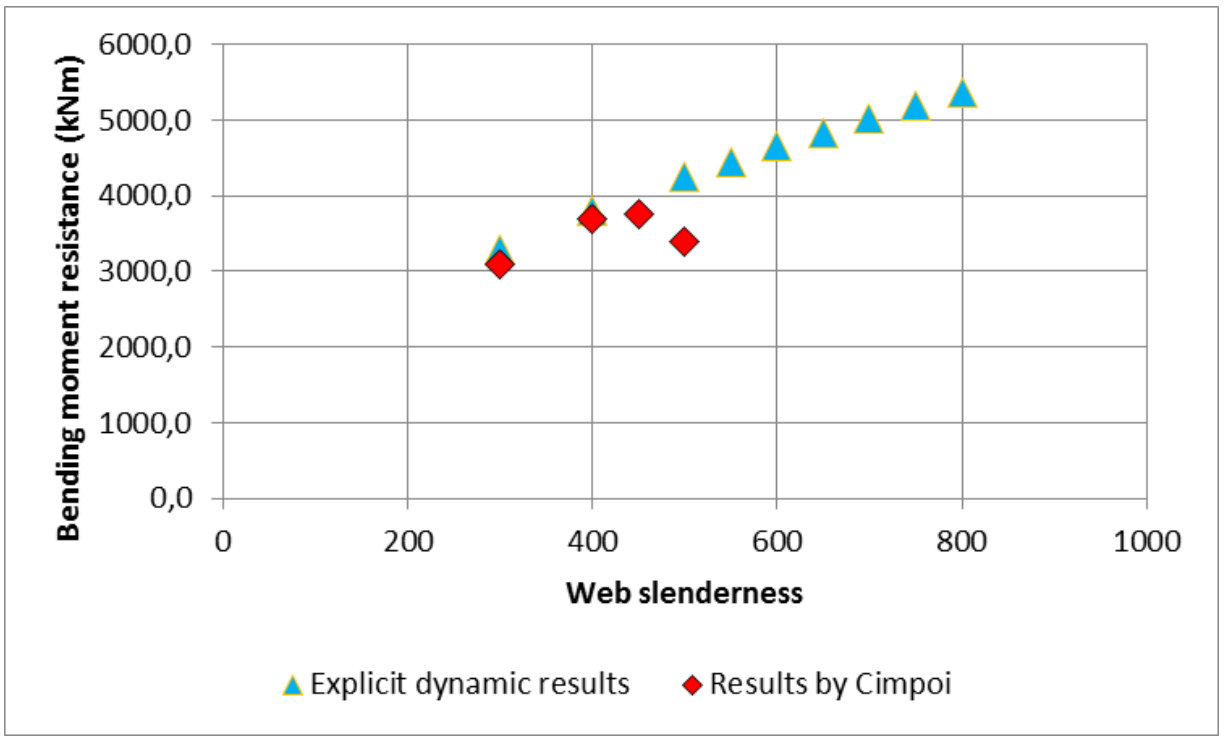

FIGURE 59: MAXIMUM MOMENT CAPACITY FOR A S690 GIRDER WITH 12000 MM^2 AREA USING EXPLICIT DYNAMICS

4.3.3. Conclusions with respect to the explicit dynamic results for S690 steel plate girders

Looking at both the results of the explicit dynamic parametric studies, the behavior shows force displacement behavior is very strange for the models with a total area of 12000mm^2. The results found by Cimpoi, for these same models could not be matched. Because the results also do not match with the predictions done by Abspoel, it is chosen to look for an alternative analysis to see if the results can be validated. The analysis using implicit dynamics is used to do this.

4.3.4. 2st Parametric study on S690 steel plate girders with 6000mm^2 total area using implicit dynamics

4.3.4.a. Introduction

After consulting some experts and remodeling to check mistakes and hiccups the models did not show any strange things and were reused, with a different analysis. The quasi-static implicit dynamic analysis was used now, as have been described in the validation chapter. The geometry and the rest of the model were kept the same, only the application of the loading had to change because of the implicit dynamic quasi static analysis prefers a linear increasing load, instead of a slow starting, but rapidly increasing loading in the explicit dynamic quasi static analysis.

4.3.4.b. Force displacement behavior

The force-displacement relationship for several models, build with S690 steel and a total cross-sectional area of 6000 mm^2, has been given on Figure 60. It can be noticed that the curves of the less slender webbed girders, up to a web slenderness of 500, have a linearly increasing first part, leading to a maximum reaction force, after which the plate girder fails rapidly. On the 300-web slender model, there is a little plateau, showing yielding of the top flange not leading to immediate failure, but having a small amount of extra rotational capacity.

The girders with a slenderness of more than 550 show a different path, after their linear elastic behavior, which is similar to the graph on Figure 54, showing this is not an unreal curve. With increasing slenderness, the high slender girders show a decreasing maximized deflection and reaction force.

The curve for the model with a web slenderness of 525 is a transition between the 2 other shapes of the force-displacement curves, in which the curve almost completely flattens out as the maximum force is applied. This behavior is similar to the looping of the curve found in Figure 54 and can be described by non-uniform deflection over the length of the girder.

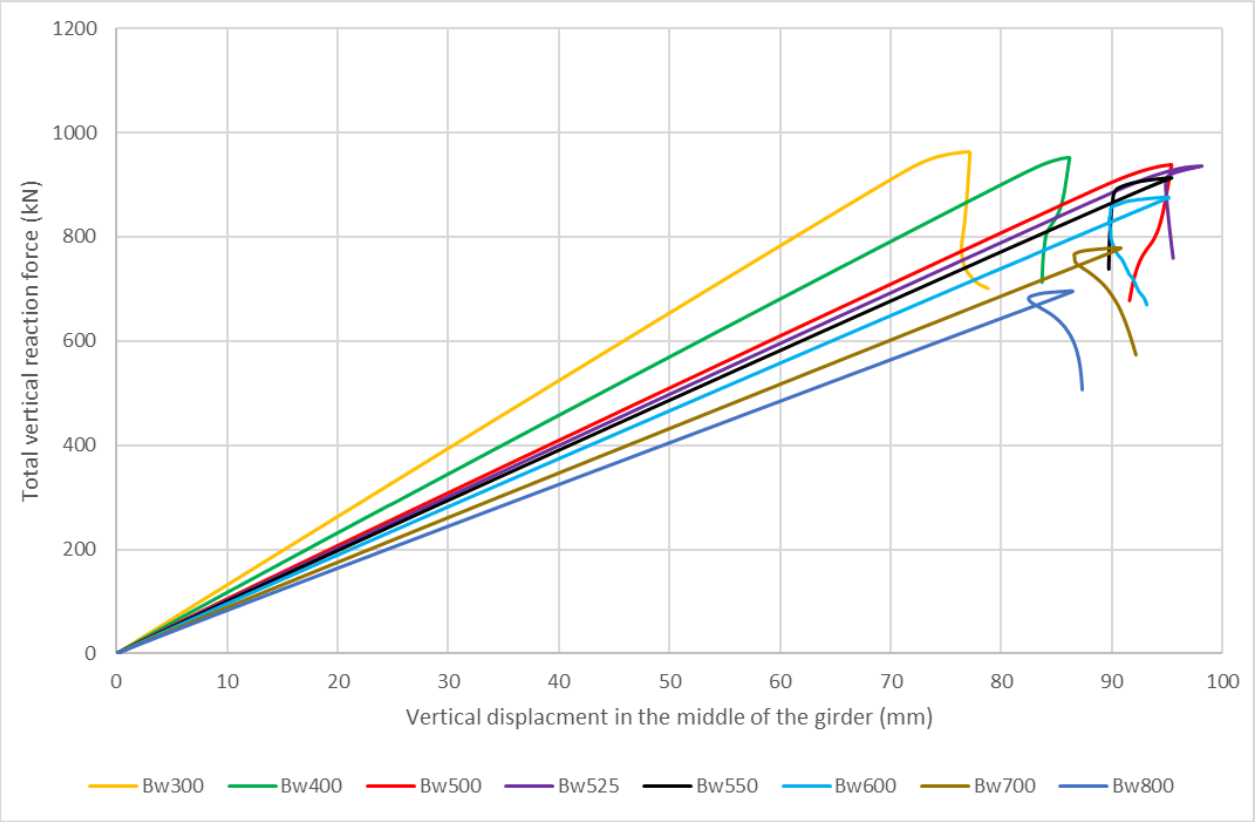

FIGURE 60: RANGE OF LOAD-DISPLACEMENT DIAGRAMS FOR S690 STEEL GIRDERS WITH 6000 MM^2, TESTED WITH IMPLICIT DYNAMICS

4.3.4.c. Failure mode

The fore-displacement diagram of the modelled plate girders is only one site of the result. It is of interest to see how the girders fail and what stresses are achieved in the cross-sections. Looking at Figure 60, it seems like 2 different bending behaviors can be found in these girders. The first is up until a web slenderness of 500, the other after 525.

Behavior of the 400-web slender plate girder in S690 steel.

The results of the four point bending test on the plate girder with a web slenderness of 400 can be found in Figure 61, which shows the stress distribution in the girder. The picture show 3 stages of its behavior in bending. First the displacement on top of the transvers stiffeners is increased, leading to a linear elastic reaction. The top picture shows the girder at maximum bending moment, in which the top flange is yielding and the bottom flange almost yields. The stresses in the web are non-uniform, in the top of the web, shown by the various colors in the web.

After the applied displacement in increased a little more, the top flange fails by a small rotation of it, also shown on Figure 62. The stress distribution changes dramatically, showing diagonal stress trajectories

over the web and the flanges are much less stressed. Increasing the load more, results in the flange being pushed into the web (bottom picture of Figure 61)

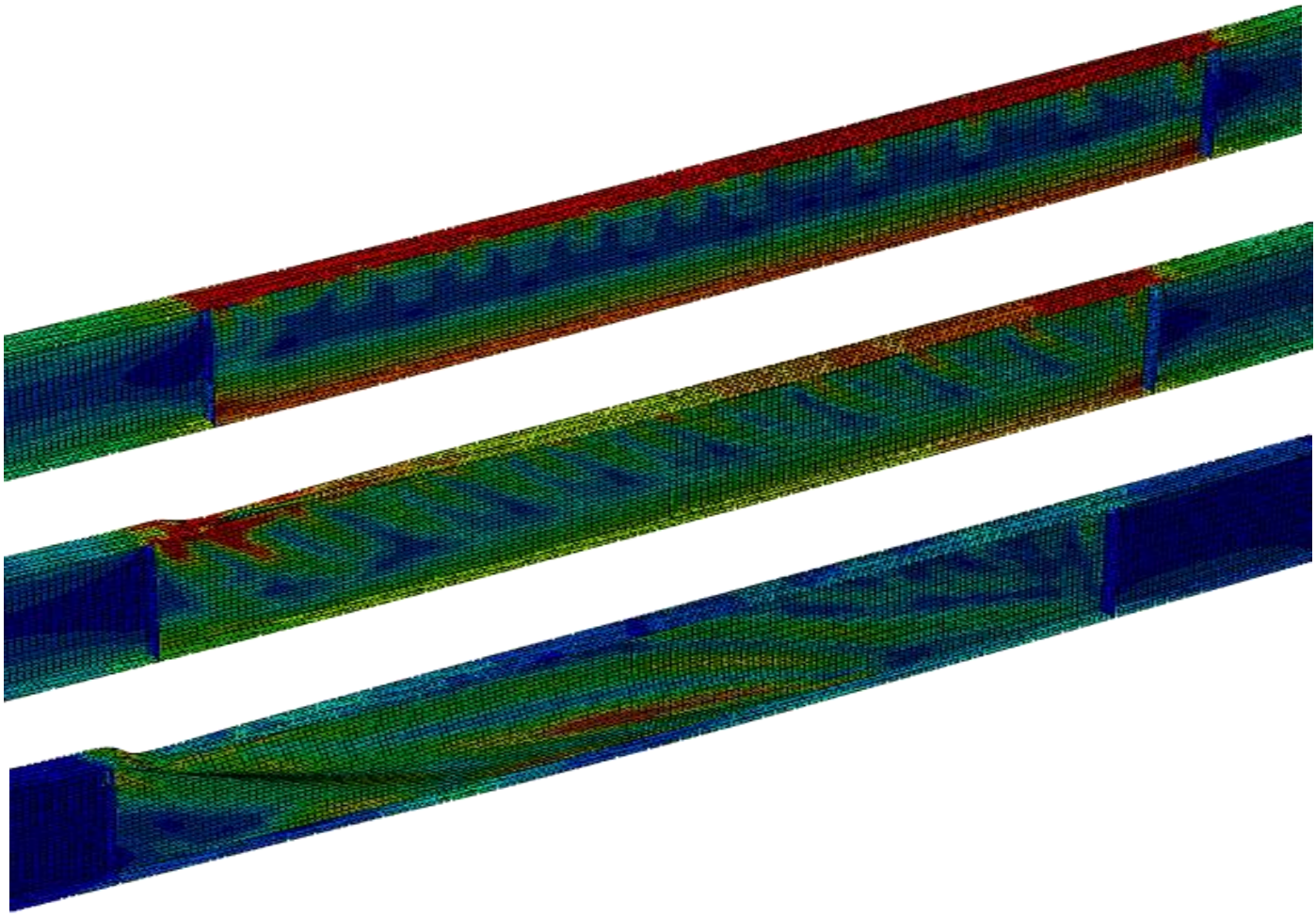

FIGURE 61: 3 STAGES OF REACTION OF THE PLATE GIRDER, WITH A WEB SLENDERNESS OF 400 IN BENDING.

This behavior is also noticed in the girders with a web slenderness of 300 and 500 and 525, although this is also somewhat of a mix between this failure mode and the mode found in more slender girders, shown next.

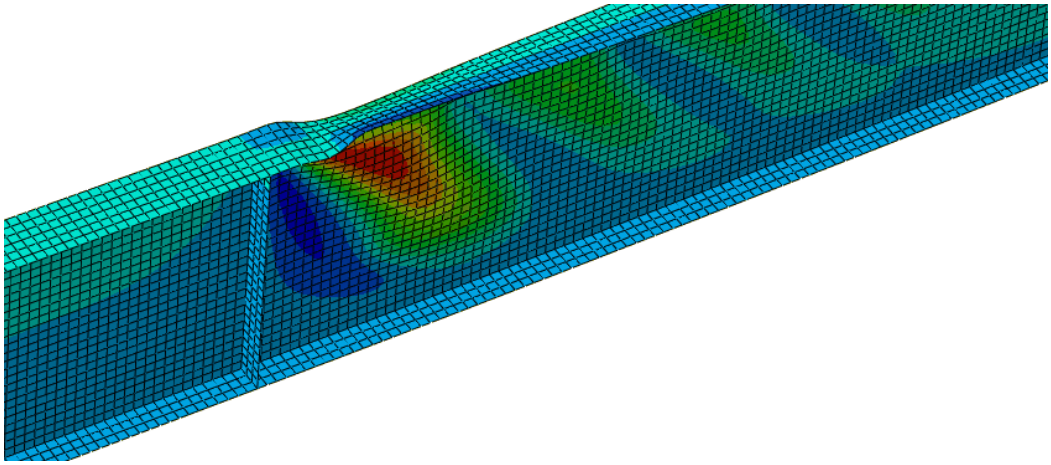

FIGURE 62: ZOOMED PART OF THE 400-WEB SLENDER GIRDER, SHOWING FLANGE ROTATION, JUST AFTER YIELDING

Behavior of the 700-web slender plate girder in S690 steel.

The behavior of the girder with a web slenderness of 700 can be found on Figure 64. It shows the girder without a large imposed deformation already has a significant non-uniform stress distribution. The top flange shows spots of lower stress, below this the web is extra stressed.

With increasing deformation, the non-uniformity is much better to see in the middle picture, also showing a band of the web being much more stressed than the rest of the web. This is the plot of the girder with the maximal force on it. The top flange is not yielding in this stage, but starts to rotate around the web-flange connection.

If the deformation is increased after this, the flange rotates more and the web bulges out. This is better shown in Figure 63. Since the top flange is horizontally supported in the web-flange connection, this part stays in the same line as the end-panels.

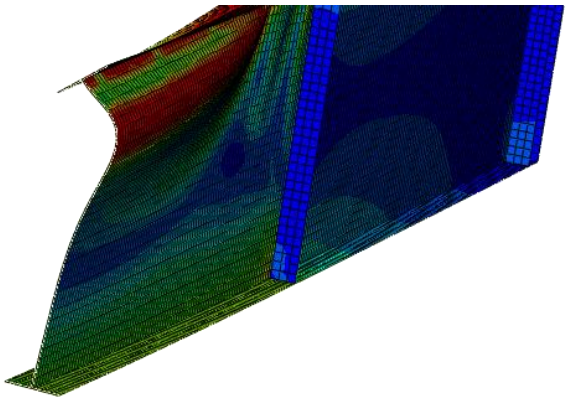

FIGURE 63: ROTATION OF THE TOP FLANGE AND BULGING OUT OF THE WEB

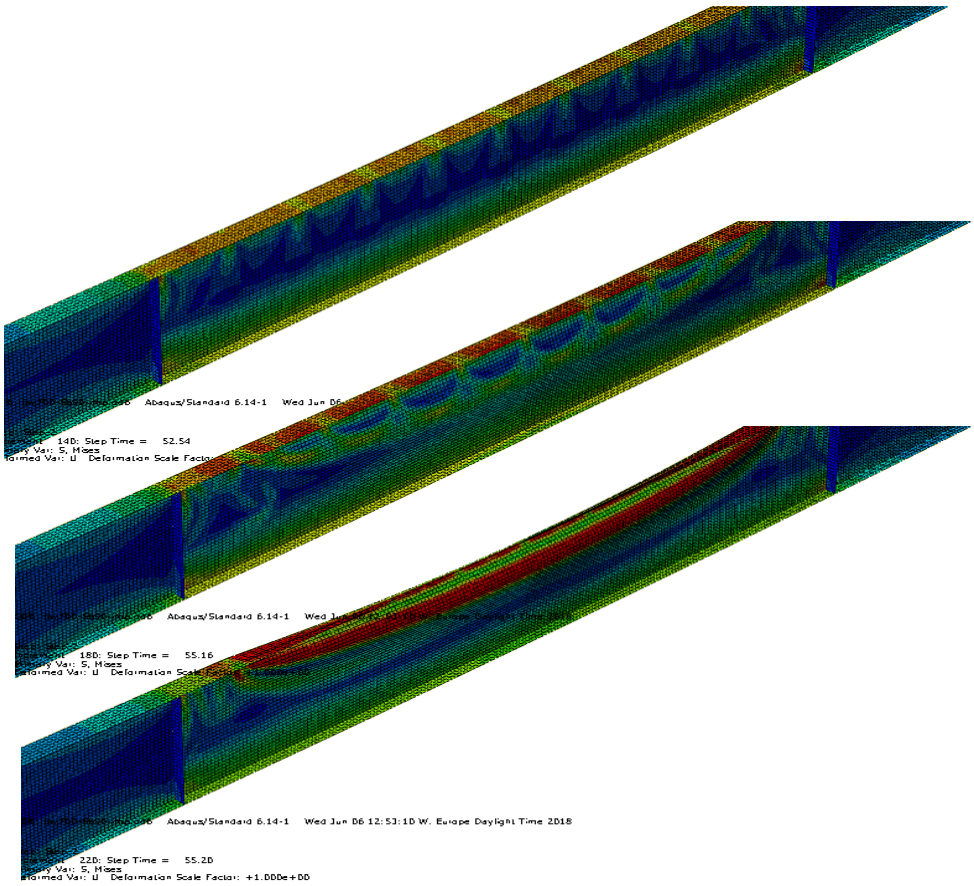

FIGURE 64: 3 STAGES OF REACTION OF THE PLATE GIRDER, WITH A WEB SLENDERNESS OF 700 IN BENDING.

The failure shown in the pictures above, has been given for 700-web-slender girder in S890, but was also seen in the models this web slenderness of 550, 600 and 700.

4.3.4.d. Maximum bending moment capacity

Due to the choice of keeping the geometry of the girders in proportion to the height of the girder, the maximum summed reaction forces do not show a direct relationship with the bending moment. The lever-arm of the force is always 3 times the height of the girder and there for a more slender, higher girder with a lower force could be subjected to a higher bending moment.

For all models analyzed with S690 steel and an area of 6000 mm^2, the summed vertical reaction forces, lever arms and the resulting bending moments are given in Table 14. The table shows a maximum bending moment capacity of almost 1440 kNm at a web slenderness of 525, 550 and 600. The capacity first increases rapidly with increasing slenderness, up to 525, than stays somewhat constant and finally reduces after a web slenderness of 600, which can also be seen on Figure 65. This also shows the difference between the explicit and implicit models. The explicit and implicit dynamic models show, up until a slenderness of 500 to be almost the same, but after this the implicit model result in lower bending moment capacity. It is also interesting to see that the maximum is found at web slenderness of 525, because the prediction of Abspoel for this slenderness was 509.

Web slenderness	Length end-section (mm)	F (kN)	M (kNm)
300	2323,8	963,2	1119
400	2683,8	952,2	1277
500	3000,0	938,6	1407
525	3074,1	936,1	1438
550	3146,4	913,4	1436
600	3286,3	876,4	1439
700	3549,7	779,0	1382
800	3794,7	695,9	1320

TABLE 14: MAXIMUM FORCE AND MOMENTS FOR S690 WITH 6000 MM^2 USING IMPLICIT DYNAMICS

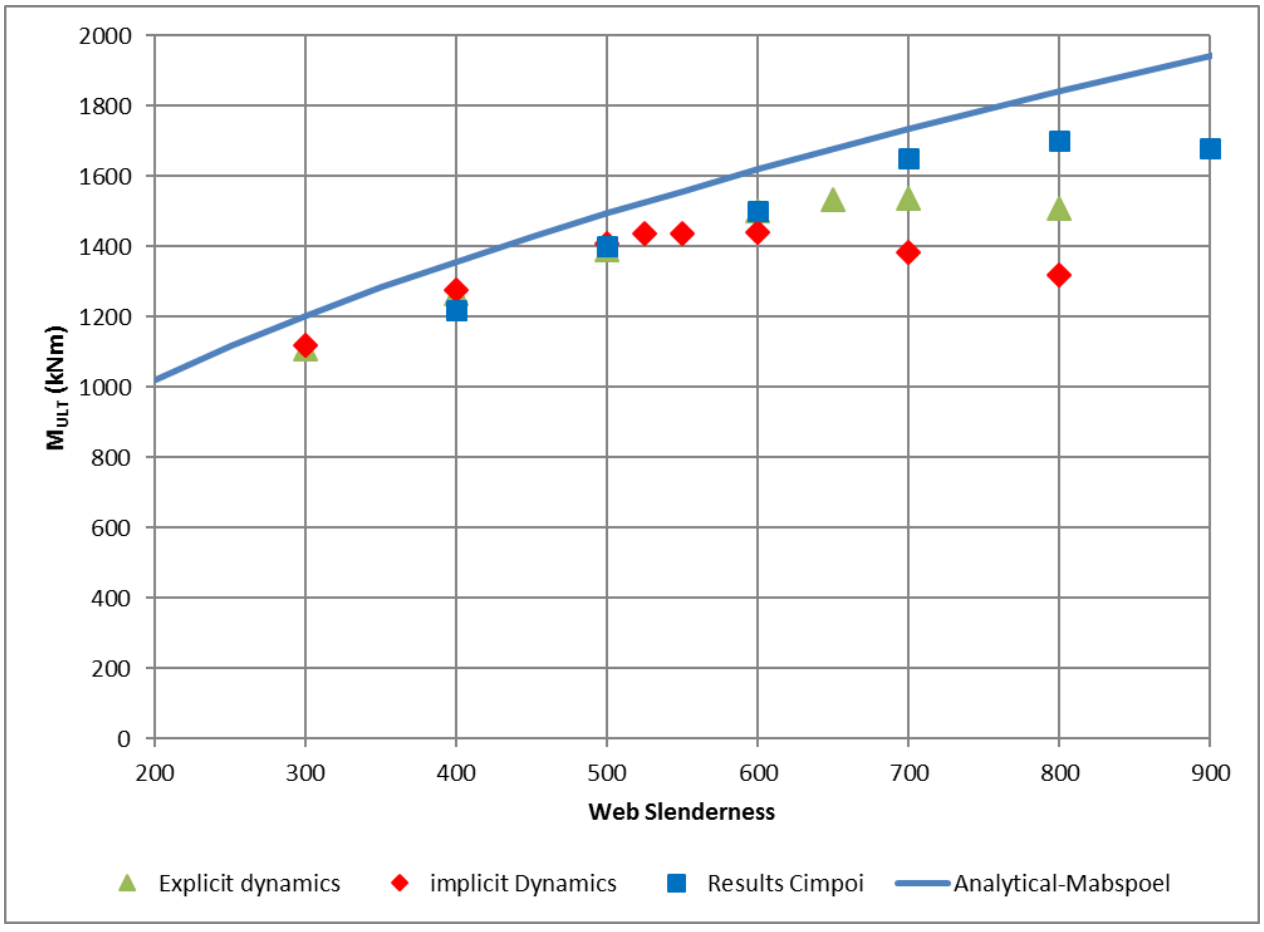

FIGURE 65: MAXIMUM BENDING MOMENT CAPACITY FOR S690 GIRDER WITH 6000 MM^2 AREA

4.3.5. 2nd parametric study on S690 steel plate girders with 12000mm² total area using implicit dynamics

4.3.5.a. Introduction

The results of the first parametric study on plate girders made from S690 steel with an area of 12000mm² were found to be highly unlikely. The results, given in Figure 58, for very slender girders showed a strange peak in loading after yielding was achieved, there for a new parametric study, using implicit dynamics instead of explicit dynamic is conducted.

4.3.5.b. Force displacement behavior

The relationship between the summed vertical reaction force and the displacement in the middle of the girders bottom flange is given in Figure 66. Compared to the results found in Figure 60, for the girders with 6000 mm² cross-sectional area, it can be seen that the shapes of the curves for girders with the same web slenderness are of the same shape.

The girders with a 400, 450 and 500 web slenderness show the same shape curves as have been seen for 300, 400 and 500 in the previous parametric study. The transition, which was found in the previous paragraph, is also present on Figure 66, at a slenderness of 525. The girders with a higher slenderness follow the same path as well, showing a loop at failure.

A significant difference between the 2 figures is the amount of force being generated by the girder to carry the applied vertical deflection on the transverse stiffeners. In this case it maximizes at 1900 kN, where in the 6000 mm² girders the maximized force was 960 kN.

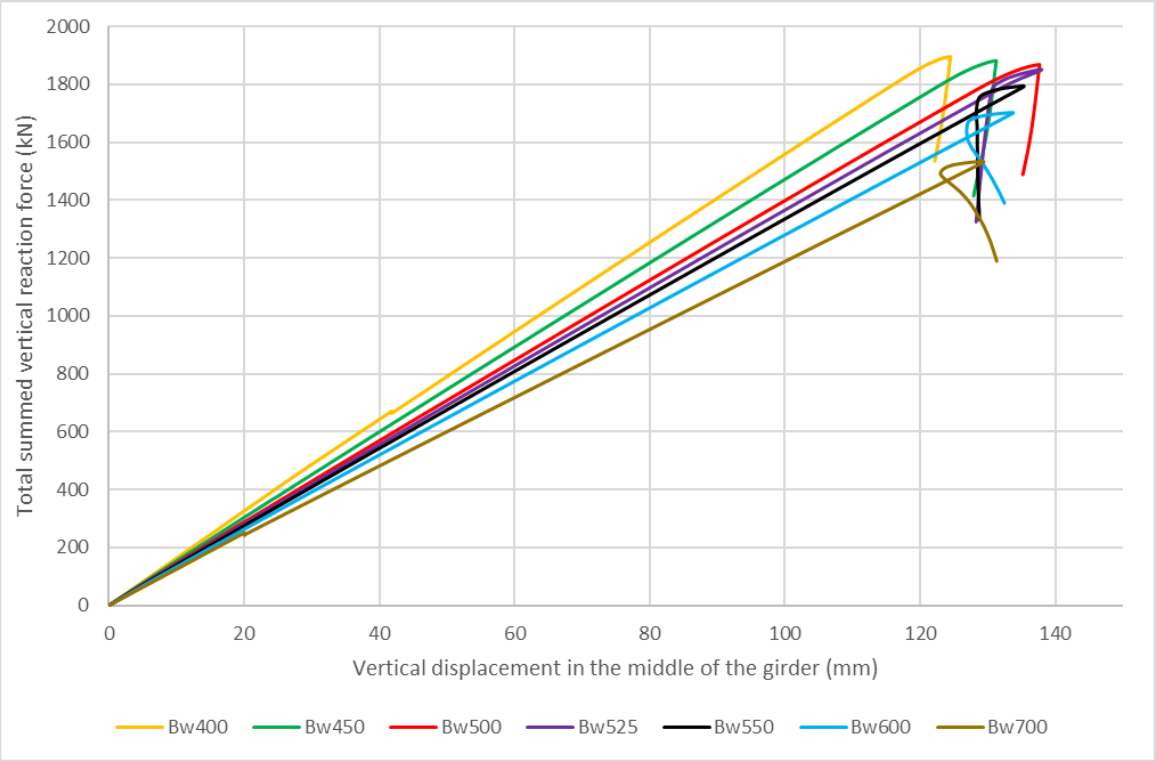

FIGURE 66: RANGE OF LOAD-DISPLACEMENT DIAGRAMS FOR S690 STEEL GIRDERS WITH 12000 MM², TESTED WITH IMPLICIT DYNAMICS

4.3.5.c. Failure mode

The failure mode and behavior of the girders has been studied as well, this will be described shortly. The failure mode are, like the shapes of the deflection curves, almost equal to the modes found in the 6000 mm^2 S690 girders.

The girders up until a web slenderness of 525 fail after the top flange has achieved the yielding stress, followed by a rotation in the flange, leading to the top flange vertically buckling into the web. The girders follow the same path as was shown on Figure 61. For girders with a higher web slenderness the pictures found in Figure 64, show the failure mode of all these girders. Before the top flange is able to yield, the top flange rotates over the full length of the middle section of the girders.

4.3.5.d. Maximum bending moment capacity

Looking at Table 15, the results are given, combined with the length of the end-panels to find the maximum bending moment capacity of the tested girders, which is also presented in Figure 67. The maximum bending moment resistance is found at a web slenderness of 525, being 4023 kNm.

Web slenderness	*Length end-section (mm)*	*F (kN)*	*M (kNm)*
400	3794,7	1896,5	3598,396
450	4024,9	1882,4	3788,196
500	4242,6	1868,9	3964,473
525	4347,4	1850,9	4023,238
550	4449,7	1794,9	3993,319
600	4647,6	1702,8	3956,935
700	5020,0	1534,3	3851,067

TABLE 15: MAXIMUM FORCE AND MOMENTS FOR S690 WITH 12000 MM^2 USING IMPLICIT DYNAMICS

Just like the slenderness limiting the bending moment at the girders of 6000 mm^2, the maximum web slenderness is 525. Abspoel [2]concluded that the web slenderness was a constant for a steel grade. This result validates this claim, which was not the case in the explicit-dynamic study, done by Cimpoi [3]and in this work

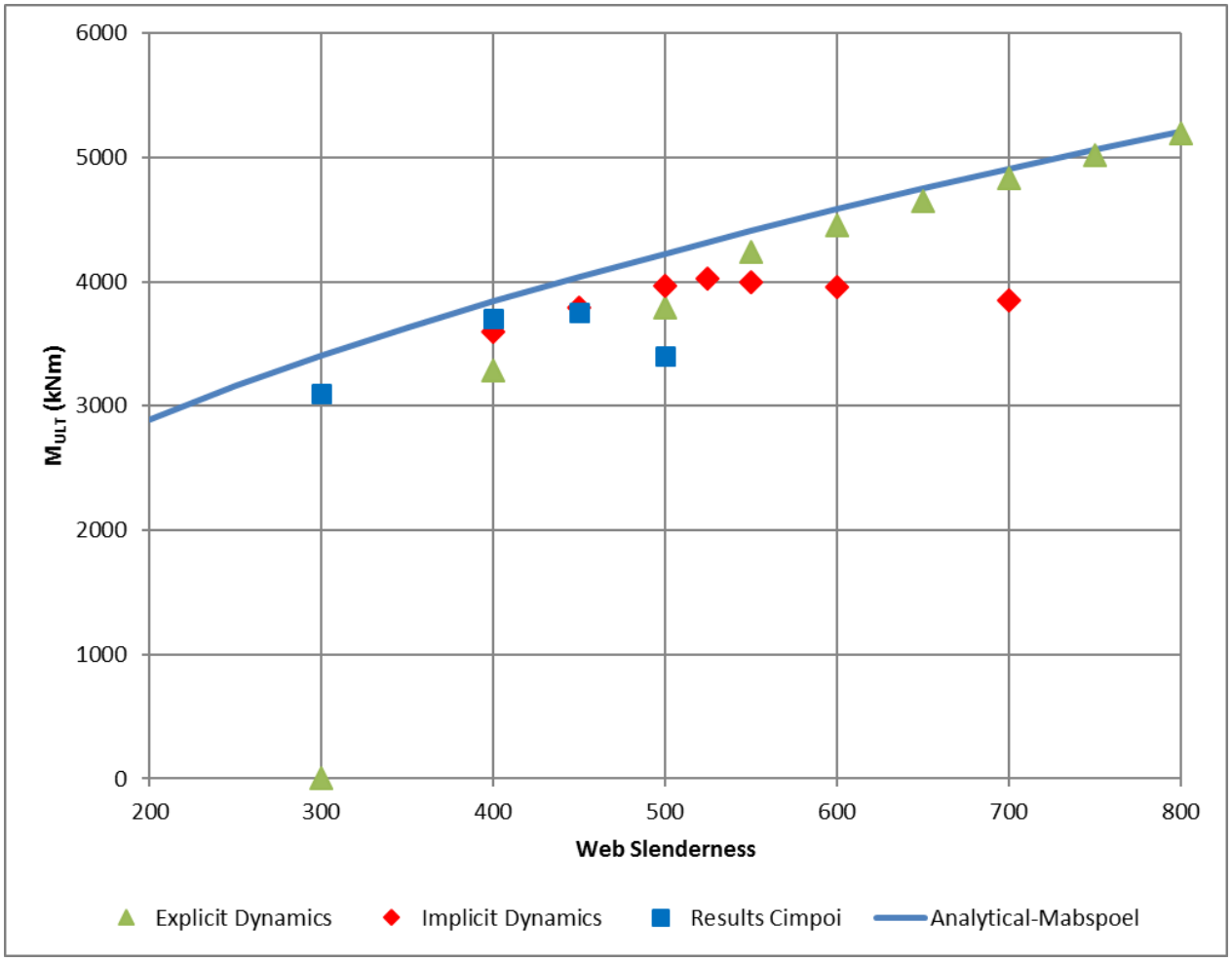

FIGURE 67: MAXIMUM BENDING MOMENT CAPACITY FOR S690 GIRDER WITH 12000 MM^2 AREA

4.4. Parametric study on bending moment capacity for steel plate girders using S890 steel

4.4.1. Introduction

The parametric study to find the bending moment capacity for S890 slender steel plate girders has been done on the same models, which also have been used for the investigation on the bending moment resistance for S690 steel, with a change in the material properties. The true stress - true strain properties of the steel have been given in paragraph 4.2.4. In this parametric study the Explicit Dynamic method has first been used, after this the implicit method has been used. Because the results of the implicit method have been categorized as more likely to describe the real behavior, only the implicit results are described in detail in this paragraph, while the explicit results are given without context.

4.4.2. Implicit Dynamic Parametric study on S890 steel plate girders with 6000mm^2 total area

4.4.2.a. Introduction

The main results in testing the girders with 6000 mm^2 are found using no initial imperfection in the web plate. During the investigation on the results the main focus was to check if the web did buckle under the applied deformation and as a result of this, the stress distribution was found to be non-uniform. All models have been checked and only for 1 model minor adjustments in the step size were needed to get this result because the model initially the girder-web failed to produce a buckle prior to failure.

The impact of the initial imperfection has been checked on certain models to address the behavior on the bending moment resistance for the range of web-slenderness. Also, the influence of the shape of the flange has been analyzed to verify its impact.

4.4.2.b. Load displacement curves

To show the results of the range of tested girders with a total area of 6000 mm^2 with S890 steel can be seen in Figure 68. It can be seen that the stiffness of the girder is lower with increasing web slenderness, this is the result of the increasing girder length. It can also be seen that after a certain slenderness the girders start to behave in a different way, with the transition being somewhere between a web slenderness of 400 and 425 for this type of girder.

The graph of the model with a web slenderness of 300 seems to have some sort of plateau, with a very small amount of deformation capacity before failure occurs, the other girders do not show any form of ductility.

It can be observed that the 3 graphs with the lowest web slenderness (300, 400 and 425) do not differ a lot from each other when it comes to their maximum summed reaction force, where higher slenderness lead to a larger decrease in maximal reaction forces. These values can be found in Table 16. This table also shows the length of the end-section, which is the lever arm for the force and can be used to find the corresponding moment, given in the 4th column and in Figure 69.

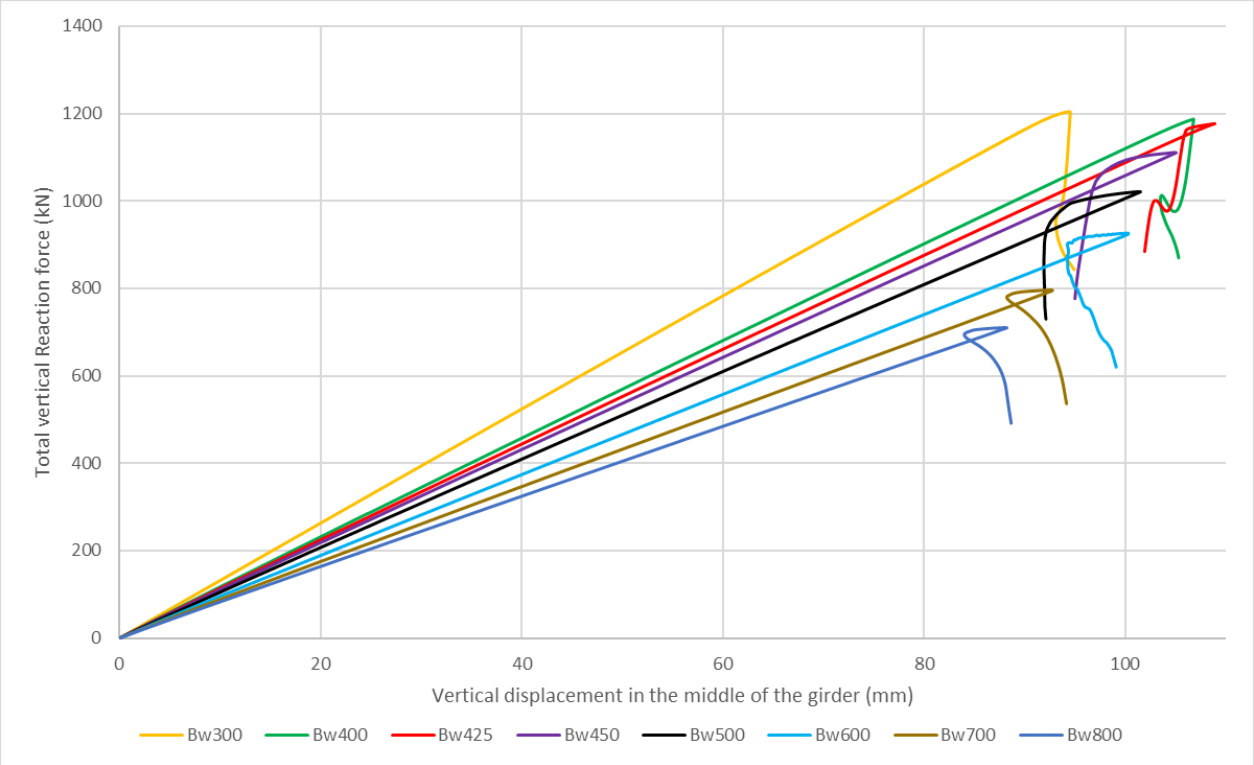

FIGURE 68: RANGE OF LOAD-DISPLACEMENT DIAGRAMS FOR S890 STEEL GIRDERS WITH 6000 MM^2

Web slenderness	*Length end-section (mm)*	*F (kN)*	*M (kNm)*
300	2323,7	1204,2	1399,1
400	2683,8	1187,0	1592,9
425	2765,8	1176,9	1627,6
450	2846,0	1110,8	1580,7
500	3000,0	1021,3	1532,0
600	3286,3	926,2	1521,9
700	3549,6	796,3	1413,3
800	3794,7	710,4	1347,9

TABLE 16: MAXIMUM FORCE AND MOMENTS FOR S890 WITH 6000 MM^2

Looking in Table 16, it can be observed that the maximum moment capacity for girders with a 6000 mm^2 total area made from S890 steel is found in the model with a girder having a web slenderness of 425, which was also the slenderness where the behavior changed. In Figure 69 the results for the explicit dynamic analysis, in which 500 is the governing slenderness and the analytical method found by Abspoel are also given.

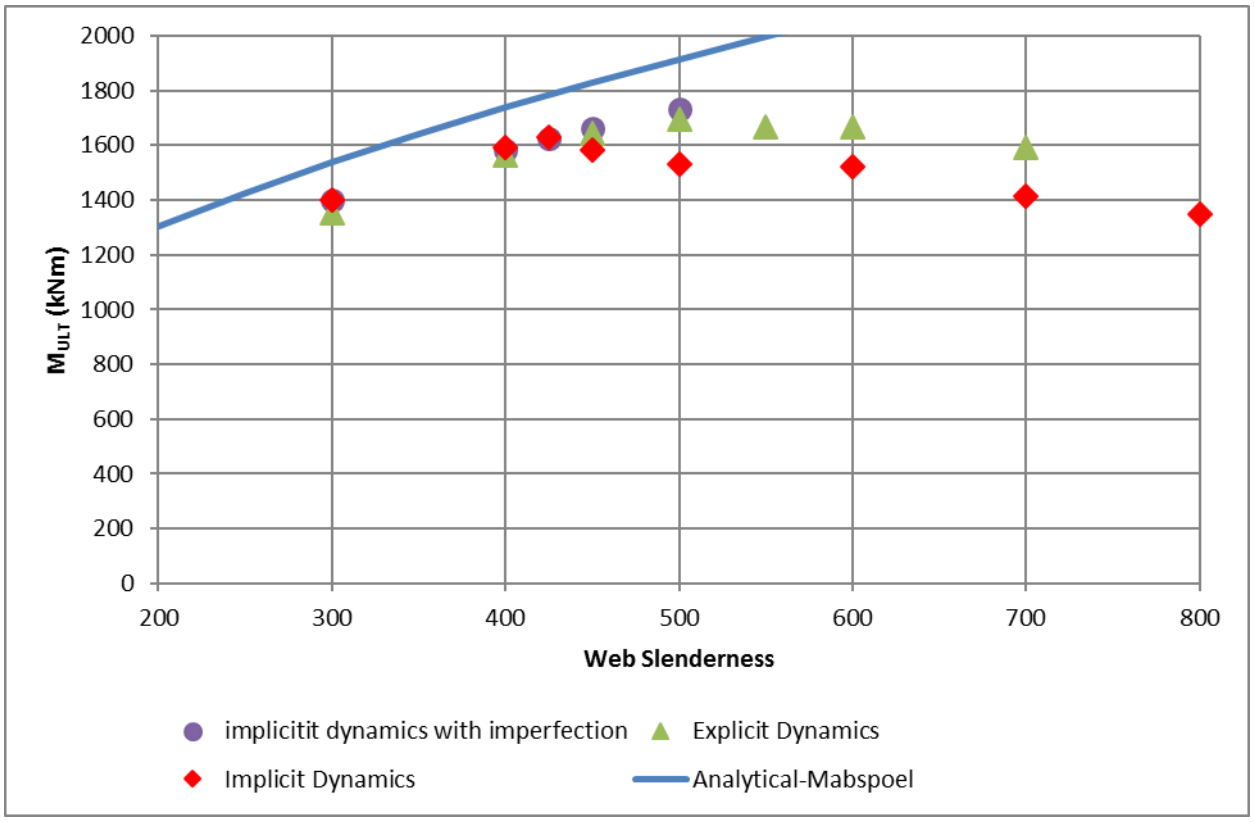

FIGURE 69: MAXIMUM MOMENT CAPACITY FOR S890 GIRDER WITH 6000 MM^2 AREA

4.4.2.a. Failure mode

As have been shown in the previous paragraph, the girders fail roughly in 2 different ways, when the models are not provided with initial imperfections. When there is an initial imperfection modeled into the girders the girders fail, on any web slenderness, very similar. The modes can be observed on the previous pages. Leading to failure the steps will be described using plots of the deformation of the girders made with a web slenderness of 400 and 500.

Web slenderness of 400

Figure 70 shows the deformation in 4 steps. Starting with the top picture showing the buckles which occur with only a small applied deformation, also described to be necessary for good results in the validation chapter.

The second picture shows the top flange yielding, before final failure occurs in picture 3 of the 4. The top flange on the right side of the middle-section twists around the transverse direction and leads to vertical buckling of the top flange into the web of the girder. With increasing applied deformation, the carrying capacity reduces to almost nothing and the deformations grow excessive.

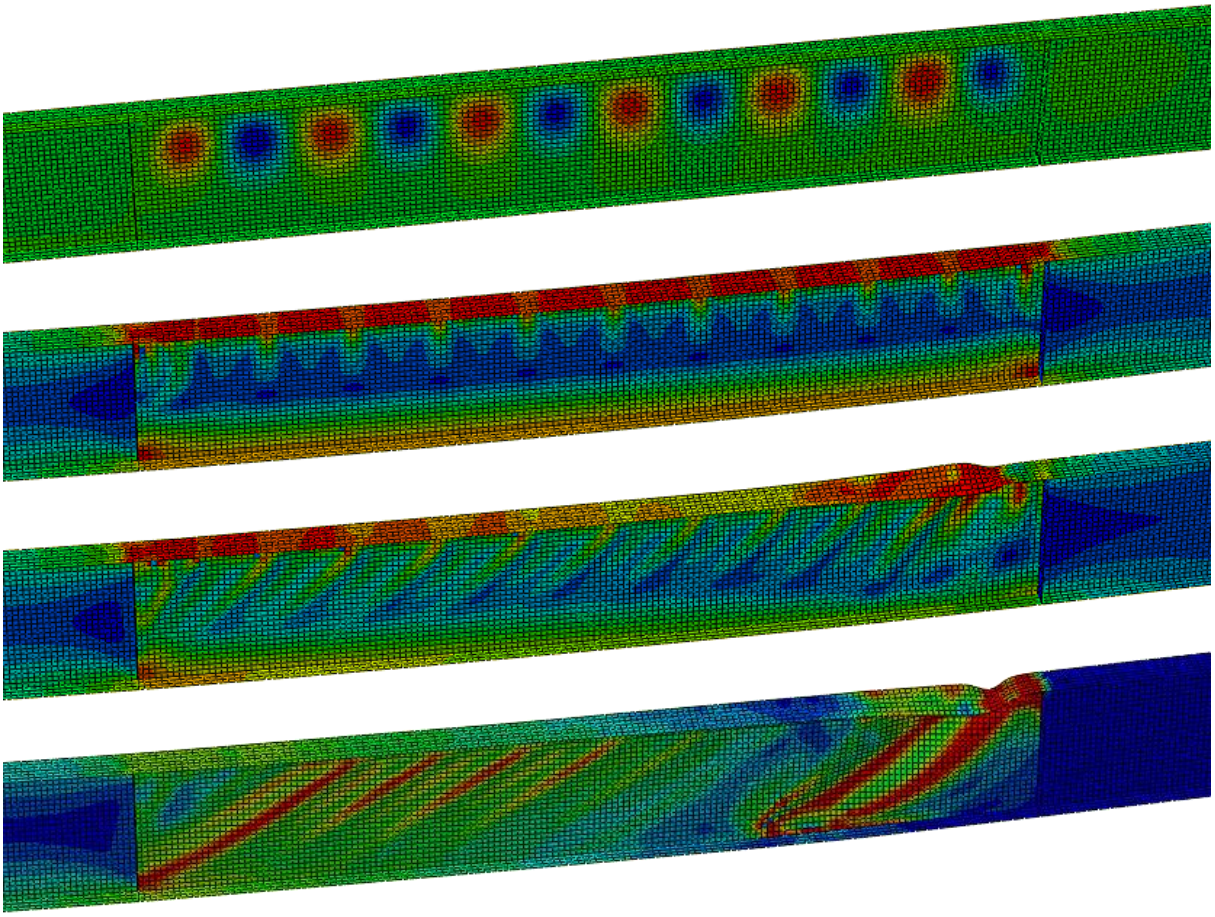

FIGURE 70: DEFORMATION AND STRESS OF A 6000MM^2 GIRDER WITH A WEB SLENDERNESS OF 400 IN S890 STEEL

Web slenderness of 500

The behavior of the girders with higher a slenderness than 425 behave in a different way, which is illustrated on Figure 71 for a slenderness of 500. The first picture shows the out-of-plane deflection after the first buckling of the web has occurred and is similar to the first picture on the 400-model. After this stress distributions are given.

The second figure from the top shows the maximum stress in the top flange, just prior to failure. In this case the stresses are between 710 N/mm^2 in the orange areas and maximize at about 820 N/mm^2, while the yield limit for S890 is 890 N/mm^2 and therefor yielding was not achieved before failure, which is shown on the 3rd picture.

The top flange rotates around the web-flange connection, while the web buckles toward the viewer, out of the plane. Increasing the deformation applied results in a folded web, which is not able to resist the bending forces applied.

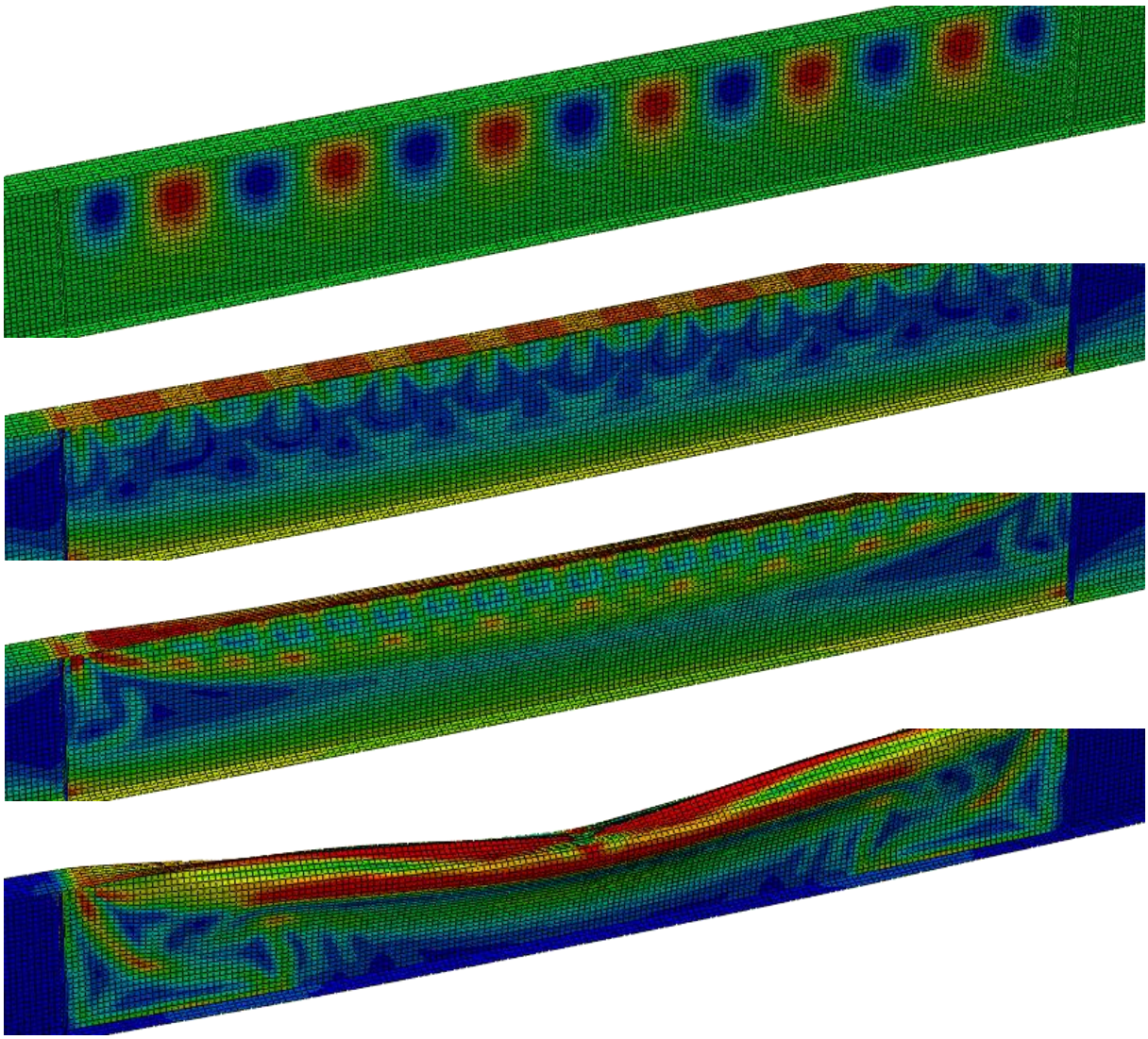

FIGURE 71: DEFORMATION AND STRESS OF A 6000MM^2 GIRDER WITH A WEB SLENDERNESS OF 500 IN S890 STEEL

Looking at other models, the behavior is very similar with one of both described behavior in resisting the bending forces applied. In the range of web slenderness tested it can be observed that the models for 300, 400 and 425 behave like the 400 model. Showing a twisting top-flange leading to a buckled top flange pushing into the web.

For the 500, 600 and 700 model, the behavior is the same as for the 500-model described, but the 450-web slender model shows a sort of combination between the two models. Because of this specific behavior it has been presented in plots as well, this can be found in Figure 72.

The first picture presented is the state just before collapse, in which the top flange partially yields. The, in this view, backside of the top-flange shows stresses of above 890 N/mm^2, while the front part only goes up to about 820 N/mm^2. In the second picture the reason for this is shown, the top-flange rotating around the longitudinal axis in the direction of the frontal part of the top flange. In this state, the

backside of the top-flange still achieves stresses of over 890 N/mm^2 but the front side is much less stressed. The 500 model also showed the top flange rotation, in Figure 71.

After increasing the deformation only very slightly, picture 3 is found, showing the top flange also twisting, which was also observed in the model with a web slenderness of 400. When the applied deformation after this occurred is increased even further it can be seen that the girder predominantly uses the top of the web to transfer some forces. The shape of the deformations can be described as vertical flange buckling into the web, with excessive top-flange rotation. The rotations found in the second picture is still visible in the last picture, now with the addition of the buckled flange.

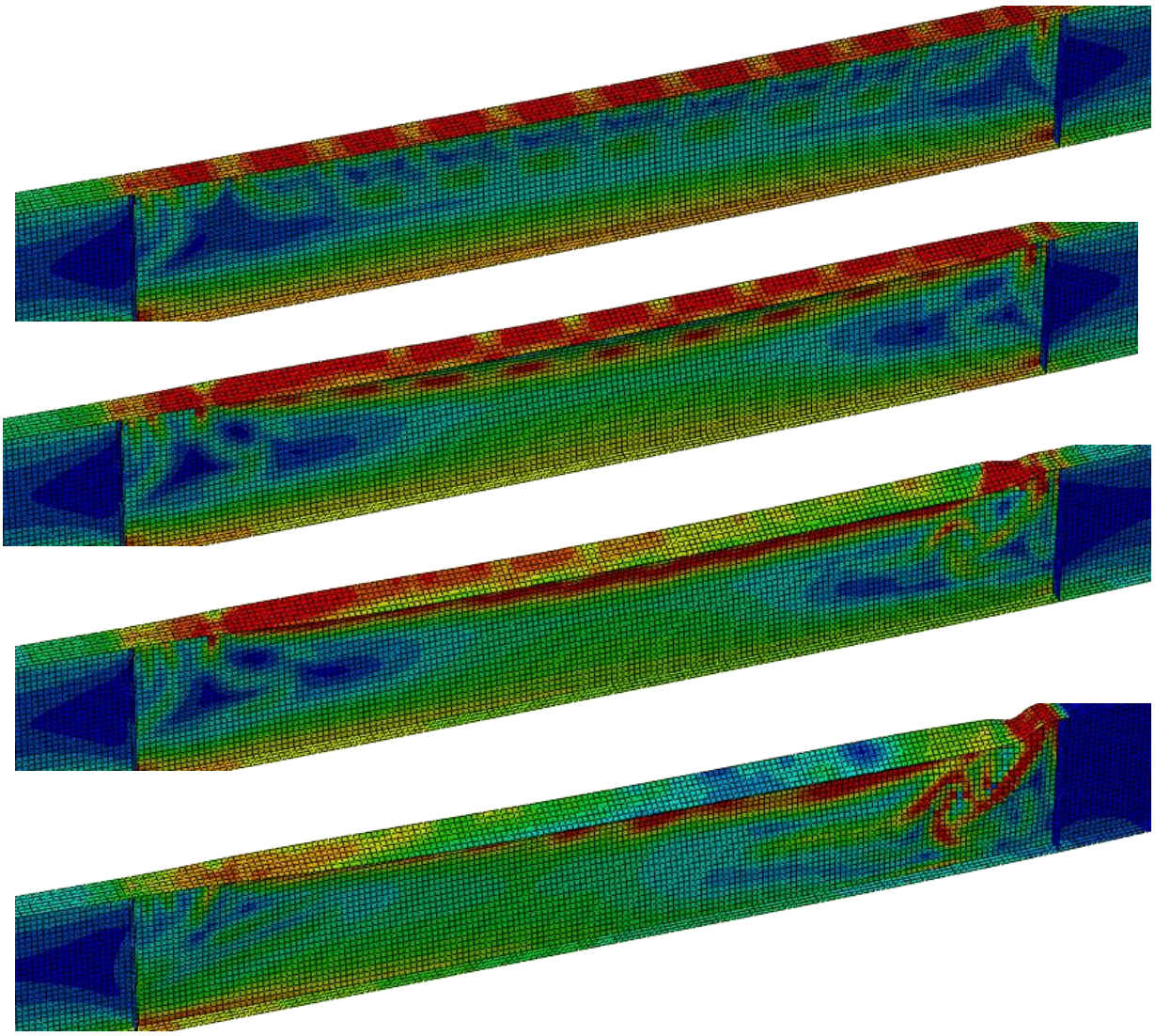

FIGURE 72: DEFORMATION AND STRESS OF A 6000MM^2 GIRDER WITH A WEB SLENDERNESS OF 450 IN S890 STEEL

4.4.2.b. Imperfection influence

The initial imperfection has been introduced in 3 models with different web slenderness, 400, 450 and 700, with the use of S890 steel. Figure 73 shows the difference in force displacement for these models: For the 400 and 450 two different amplitudes were used, 1/200 of the height of the girder (imp, dots) and 1/200 of the length of the middle section (imp2, stripes). For the 700-model only the imperfection related to the height was introduced.

It can be observed that introducing an initial imperfection does not influence the stiffness of the plate girders to a noticeable amount, but certainly increase the maximum reaction force of the girders. In the region and at lower values of the maximum web slenderness, the influence is not very large. Looking at the 700-web slender model with an imperfection of only 5,9mm increases the bending capacity drastically. Looking at the model it was found that the maximum top-flange stress in the model without imperfection was approximately 605 N/mm^2, but for the model with the initial imperfection stresses between 885 and 890 N/mm^2 were measured, resulting in a very high bending moment resistance close to the flange moment capacity.

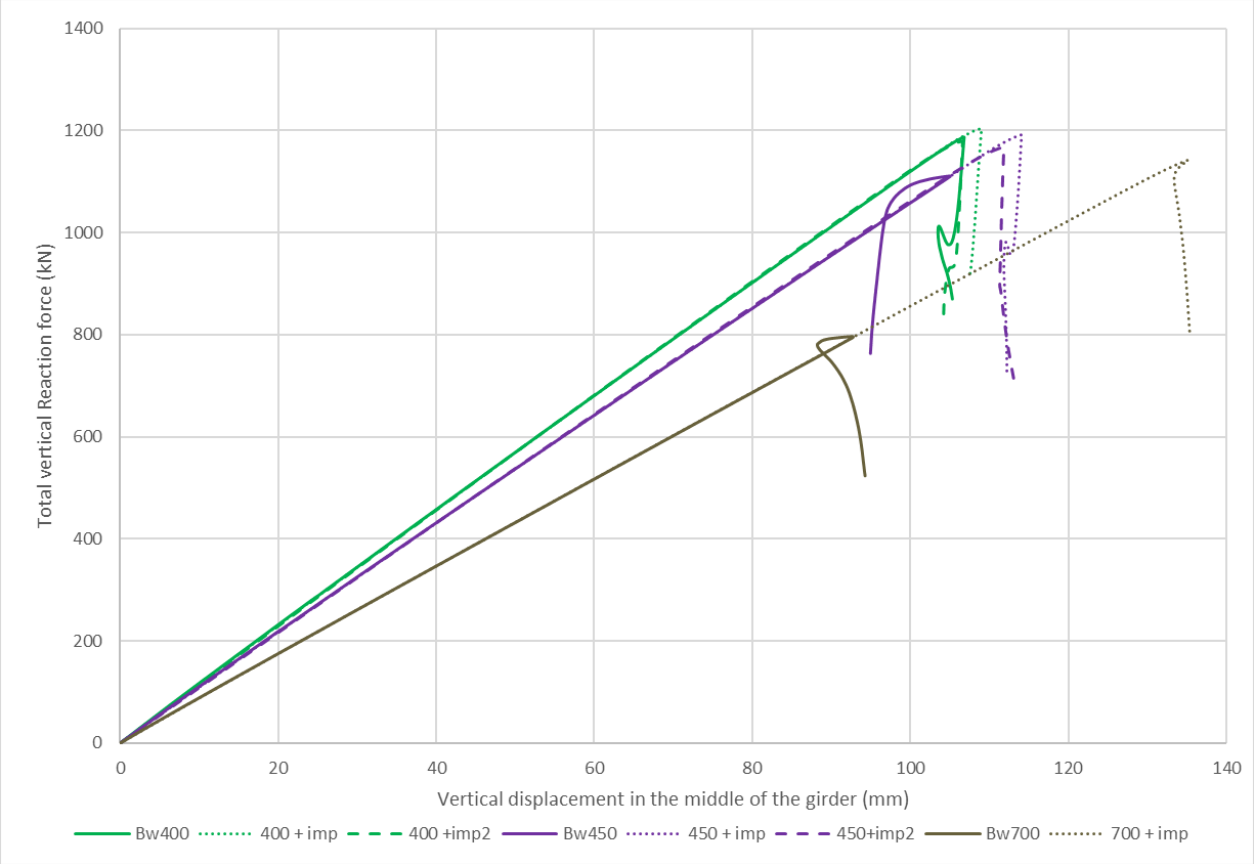

FIGURE 73: DIFFERENCE IN FORCE DISPLACEMENT DIAGRAMS WITH AND WITHOUT IMPERFECTION FOR 6000MM S890 MODELS

The resulting capacity can be found in Table 17. The increase in moment capacity for the 400-model is only 23 kNm, for 450 is it already significantly large increasing it with 115 kNm, but the increase in the

700 model is very large, more than 600 kNm. This also results in a much higher maximum bending moment than was found for Bw425 in Table 16, 1627 versus 2026 kNm.

Web Slenderness and imperfection	*Length end-section (mm)*	*F (kN)*	*M (kNm)*
400	*2683,8*	*1187,1*	*1593,0*
400 + imp	*2683,8*	1203,6	1615,1
400 +imp2	*2683,8*	1179,3	1582,5
450	*2846,1*	1110,8	1580,8
450 + imp	*2846,1*	1191,5	1695,6
450+imp2	*2846,1*	1167,4	1661,3
700	*3549,7*	796,4	1413,4
700 + imp	*3549,7*	1141,9	2026,7

TABLE 17: MAXIMUM REACTION FORCE AND MOMENT WITH(OUT) IMPERFECTION FOR 6000MM2 S890

The influence on the maximum bending moment resistance can be observed in Figure 69. Where both the explicit and implicit results without imperfections show a limit, the results for the models with imperfection show an increasing value for the resistance. The models were made up until a web slenderness of 700. After this value it is expected to increase even further.

Looking at the mode of failure, it can be concluded that this changes also in comparison to the mode of failure without imperfection, but only for values of the web slenderness above the maximum slenderness found by the models without imperfection.

For the failure in the model describing a plate girder with a web slenderness of 400 the modes can be found in Figure 74, which shows a similar deformation pattern, consisting of the top flange developing 2 plastic hinges close to the right intermediate stiffener.

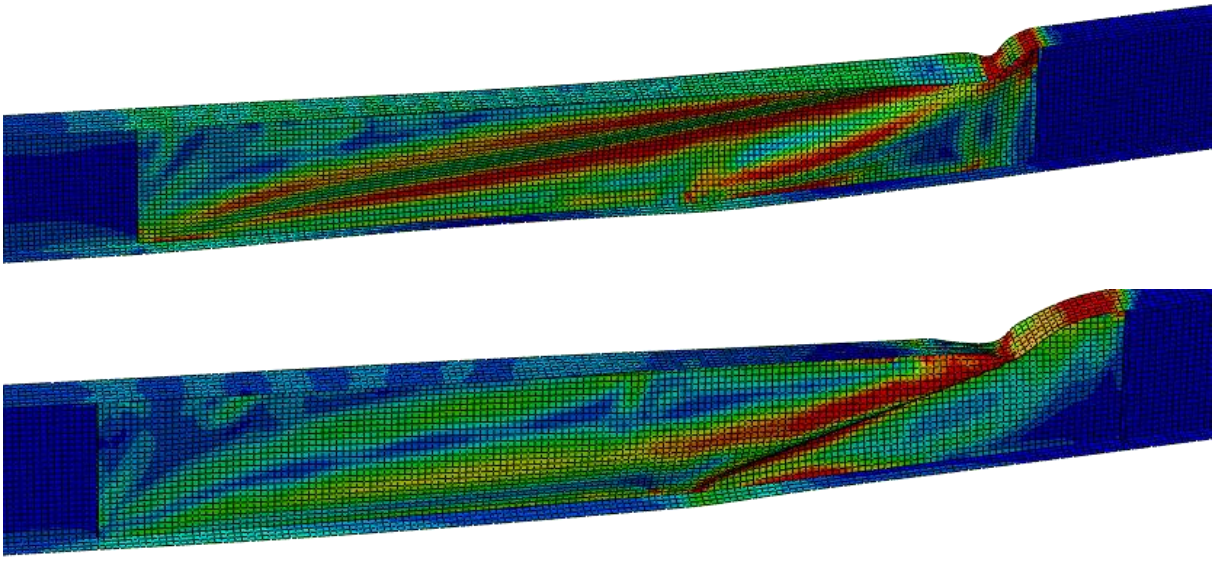

FIGURE 74: FAILURE FOR A MODEL OF WEB SLENDERNESS OF 400 WITH (TOP) AND WITHOUT (BOTTOM) IMPERFECTION

For a web slenderness of 450, which is just past the limiting slenderness, the deformation is shown in Figure 75. The modeled girders show a big difference. The failure occurs in the model with the initial imperfection by a mechanism similar to that seen in the models for 400 web slenderness. The top flange stays horizontal for most of the length. The model without imperfection on the other hand shows failure in which the top flange gets pushed into web of the girder over a significant length, while rotating around the longitudinal axis. The mode is not very different but it is noticeable.

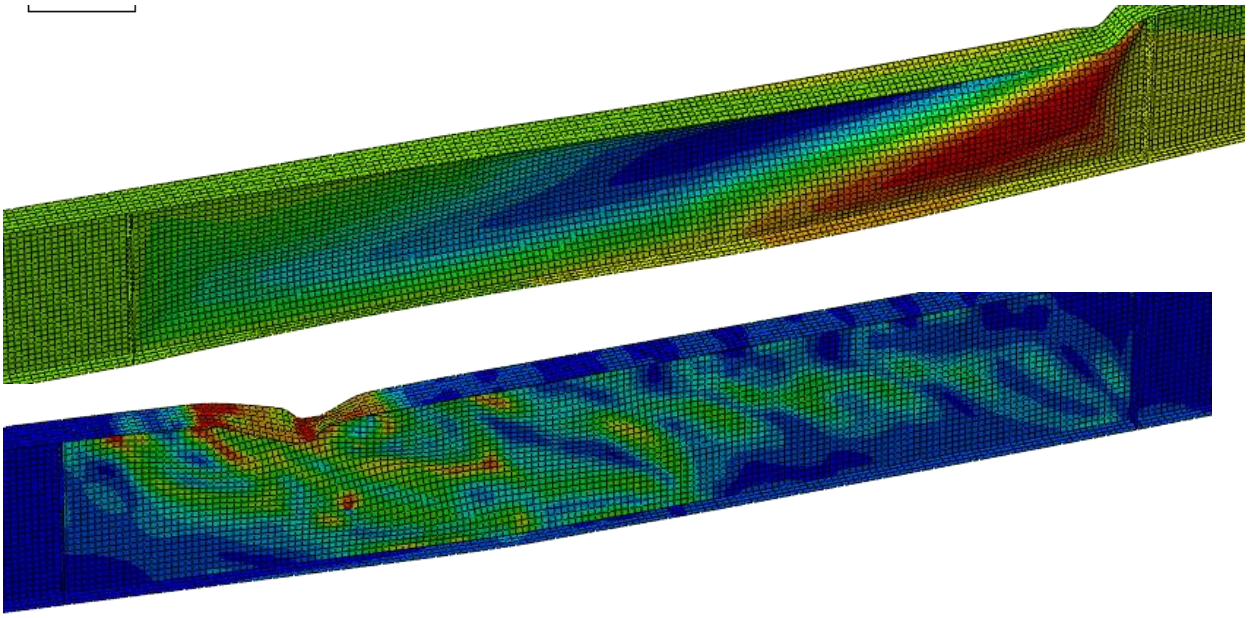

FIGURE 75: FAILURE FOR A MODEL OF WEB SLENDERNESS OF 450 WITH (TOP) AND WITHOUT (BOTTOM) IMPERFECTION

Looking at the results for the 500 and 700 web slender girders, which are presented in Figure 77 and Figure 76, a big difference can be seen. The models without imperfection shows mechanism in which the top flange can't be supported by the web anymore, over the full length of the girder. The flange is getting pushed into the web, which buckles outwards very far. In the bottom-pictures, showing the initially imperfect girders, a failure mode with vertical flange buckling can be seen again, like in the 400 models. In this model the flange did have enough support from the web to be able to yield, as have been described earlier in this paragraph for the 700 model.

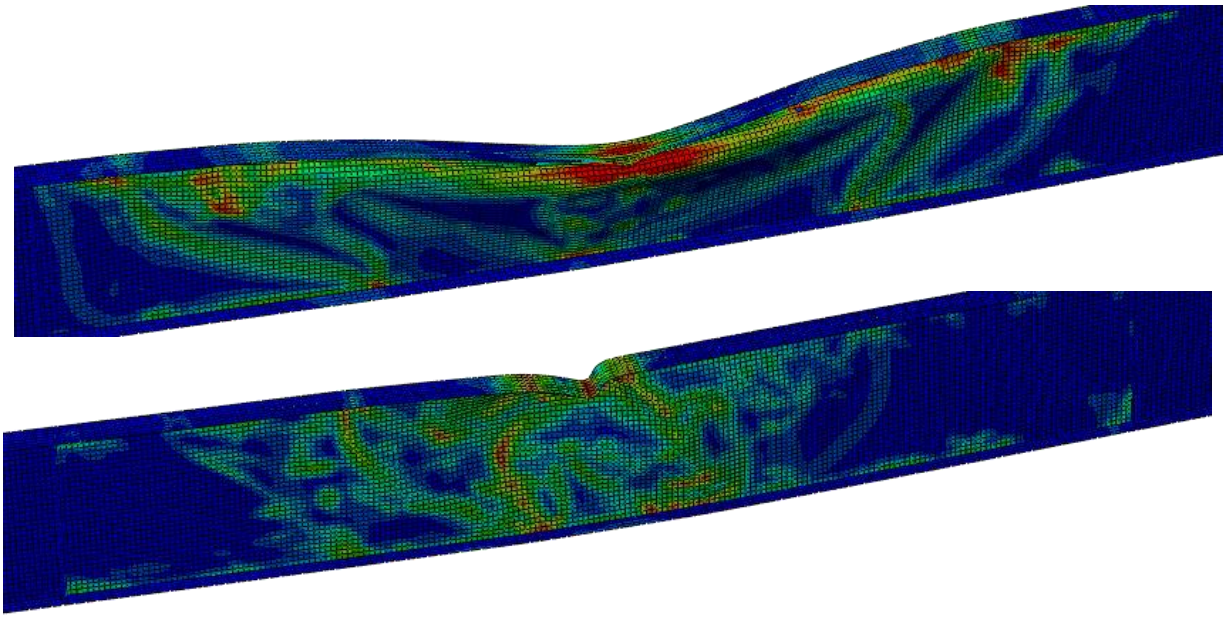

FIGURE 76: FAILURE FOR A MODEL OF WEB SLENDERNESS OF 700 WITH (TOP) AND WITHOUT (BOTTOM) IMPERFECTION

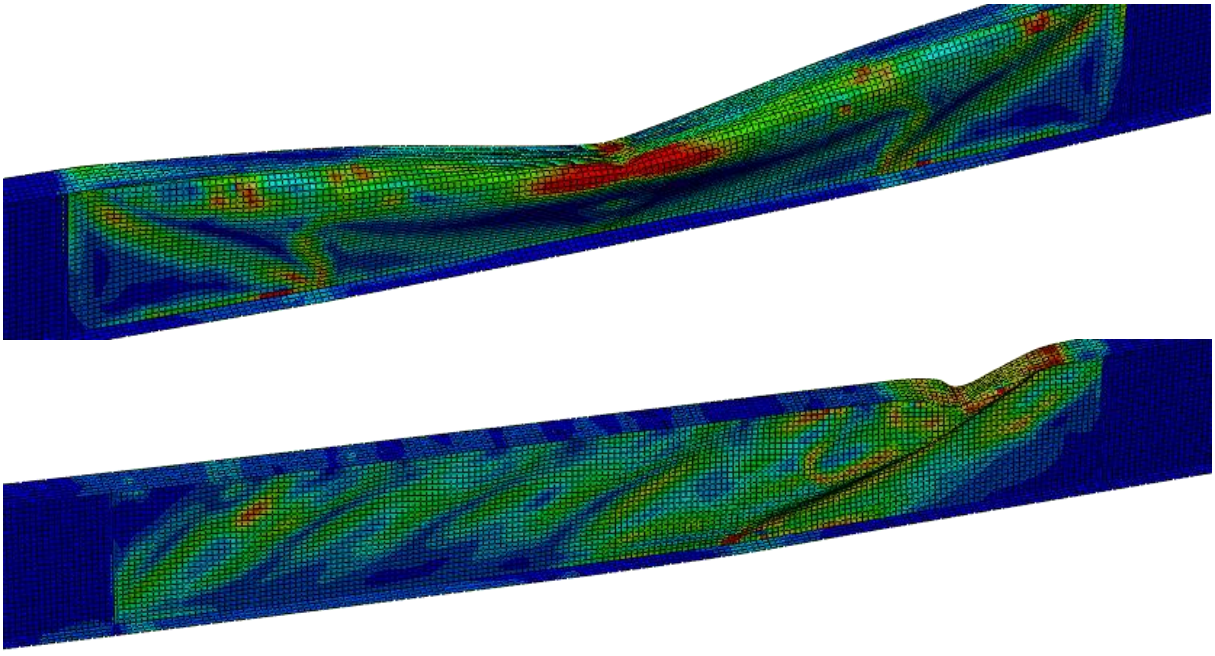

FIGURE 77: FAILURE FOR A MODEL OF WEB SLENDERNESS OF 500 WITH (TOP) AND WITHOUT (BOTTOM) IMPERFECTION

4.4.2.c. Maximum web slenderness and ultimate bending moment resistance

The maximum web slenderness of the girders made from S890 steel with a total steel area of 6000 mm^2 and an aspect ratio of 1 between the flange and the web area, the results show that the maximum bending capacity. This can be seen in Figure 69. The results show 2 maxima and a non-maximizing set of results for implicit results with a small initial deformation.

In the previous paragraph it was found that using imperfections on a model with an implicit analysis, the bearing capacity of the girder will become much larger for models which have a web-slenderness beyond the maximum web slenderness, which was found to be 425, without an initial imperfection. This resulting in a maximum bending moment resistance of 2026kNm with a slenderness of 700. The maximum bending moment resistance at a web slenderness of 425 was found to be 1628 kNm and is considered to be the most likely to be the true value of the failure load.

Looking at the results for the explicit method, without using imperfections, it can be concluded that these models also show a maximum, but this time it is found to be at a slenderness of 500, with a maximum bending moment resistance of 1696 kNm.

4.4.3. Parametric study on S890 steel plate girders with 12000mm^2 total area

4.4.3.a. Maximum Bending moment resistance and web slenderness

The Load displacement curves, found by modelling the 12000 mm2 girders with different slenderness using the implicit dynamic analysis are shown on Figure 78. The figure looks remarkably similar to the graphs found for S890 girders with 6000 mm^2 area. It can be seen that, with increasing web slenderness, the stiffness of the girders decreases. Also, the behavior of the 300, 400 and 425 web slender-girders can be coupled while the 450, 500 and 550 model do result in a different shaped force-displacement diagram, which all three look similar as well.

Looking at the resulting moment capacity, which is given in Table 18, it can be seen that the maximum bending moment resistance for these girders is found in a girder with a web slenderness of 425 and is found to be 4551 kNm.

Web slenderness	*Length end-section (mm)*	*F (kN)*	*M (kNm)*
300	3286	2417	3972
400	3795	2338	4437
425	3912	2327	4551
450	4025	2225	4477
500	4243	2045	4339
525	4347	1961	4264
550	4450	1914	4259

TABLE 18: MAXIMUM FORCE AND MOMENTS FOR S890 WITH 6000 MM2

4.4.3.b. Failure mode

The failure mode shows differences before and after the web slenderness with the highest moment capacity. Before the peek in the ultimate bending moment resistance graph, shown on Figure 87, the plate girders fail in a different way. In the force displacement diagram a difference in noticeable as well. Where until a web slenderness of 425 the diagram is continues until sudden failure, the higher slenderness' show a loop backwards, see Figure 78.

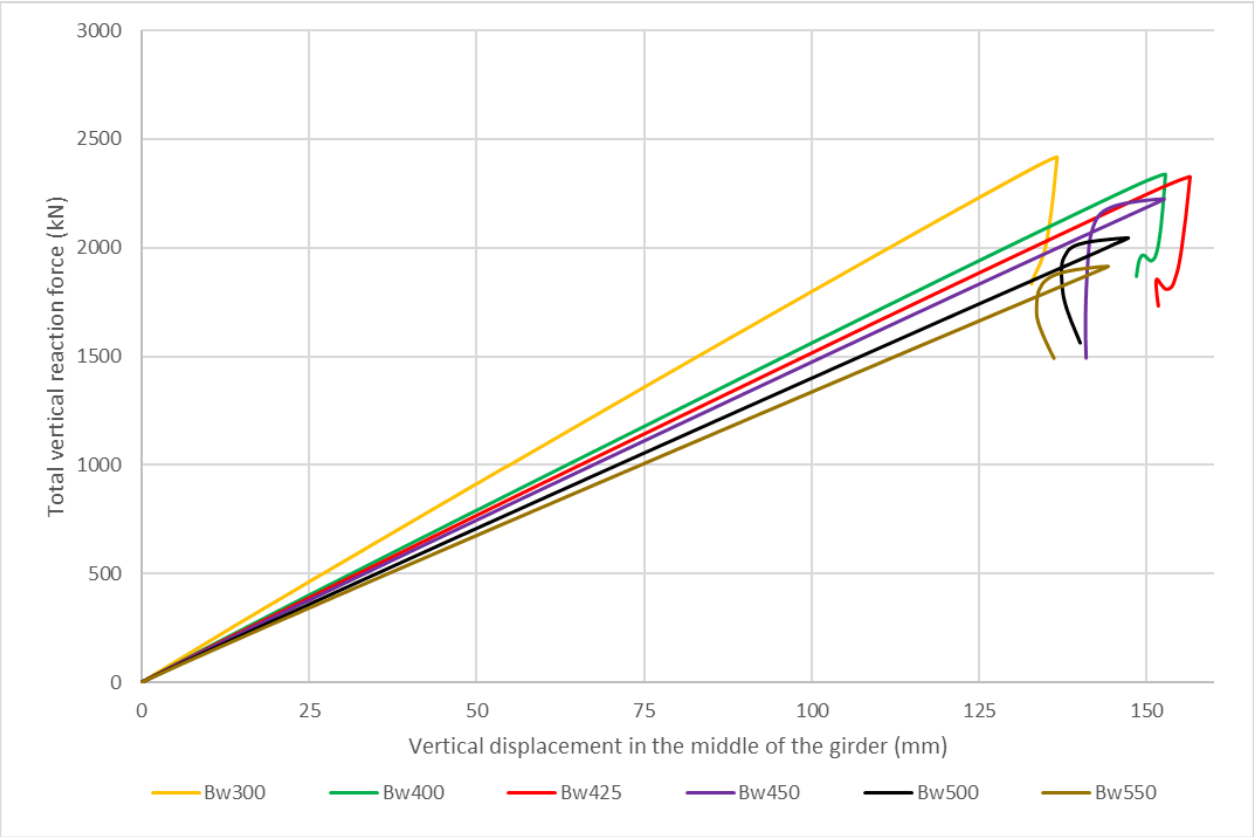

FIGURE 78: RANGE OF LOAD-DISPLACEMENT DIAGRAMS FOR S890 STEEL GIRDERS WITH 12000 MM2

In the pictures below the difference is shown and described for the 3 tests resulting in the highest bending moment resistance, with a web slenderness of 400, 425 and 450.

Web slenderness of 400

On Figure 79 the stress distribution is shown just before failure occurred. The stress in the top flange is in red, showing approximately 900 N/mm^2, which means the top flange stress has led to the yielding of the material. With increasing deformation, the plate girder suddenly fails on one side of the mid-span, reducing all stresses in the girder due to the fact that a displacement driven method is used. The behavior of the girder is shown on Figure 80, showing the top flange rotating around the z-axes, on the left side the rotation is positive, on the right side the rotation is negative. When the displacement is increased after this, the flange gets pushed into the web, which has been described by Basler as vertical flange induced buckling.

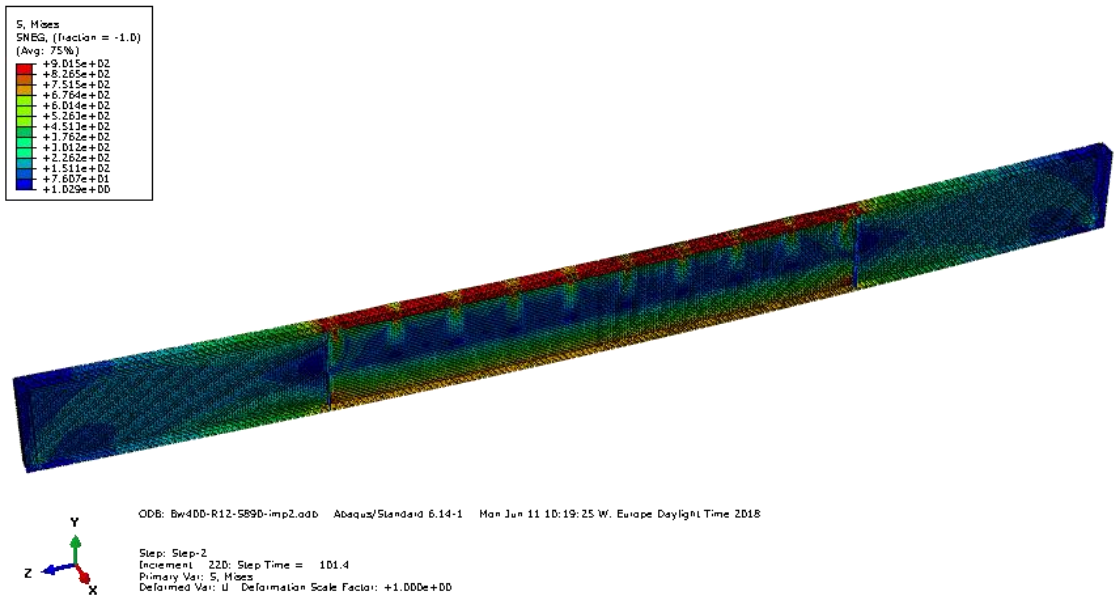

FIGURE 79: BW400 S890- 12000MM2 PRE-FAILURE, YIELDING FLANGES, DISCONTINUES STRESS PATTERN

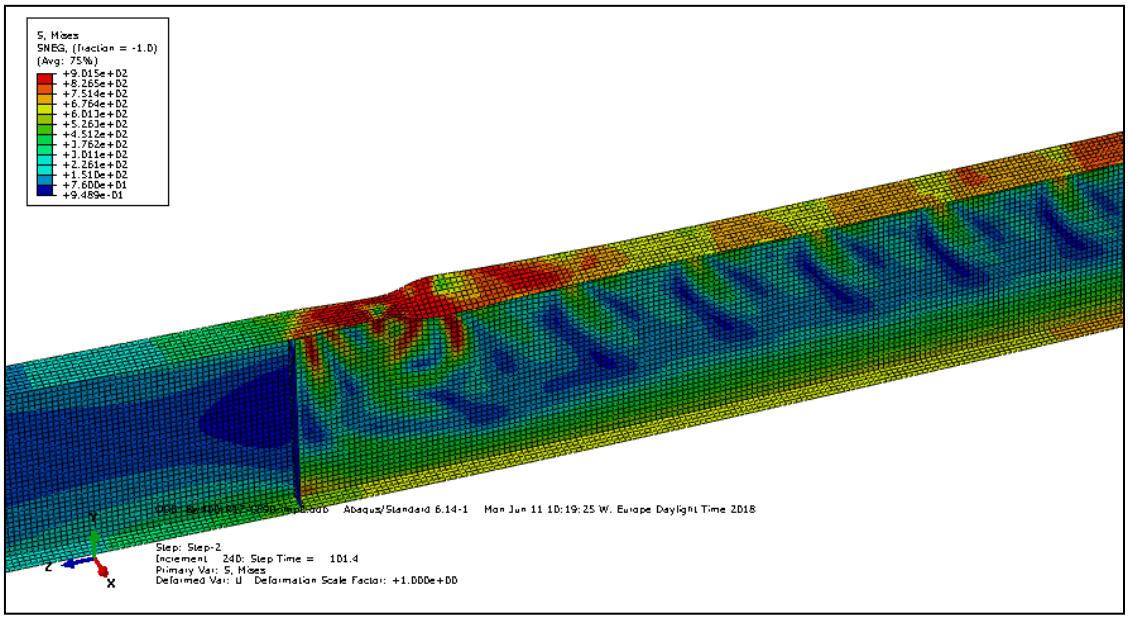

FIGURE 80: BW400 S890- 12000MM2 FAILURE, ROTATING FLANGE

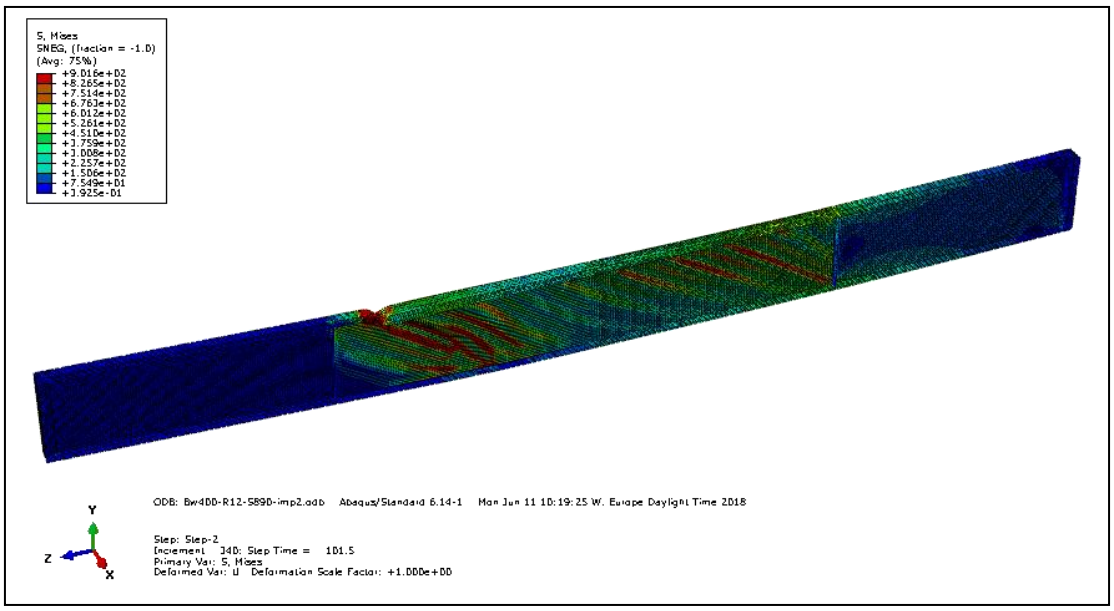

FIGURE 81: BW400 S890-12000MM2 POST-FAILURE, FLANGE INDUCED BUCKLING

Web slenderness of 425

The behavior of the plate girder with a slenderness of the web of 425 behaves in the same manner as that of the 400-plate girder, shown on Figure 82 and Figure 83

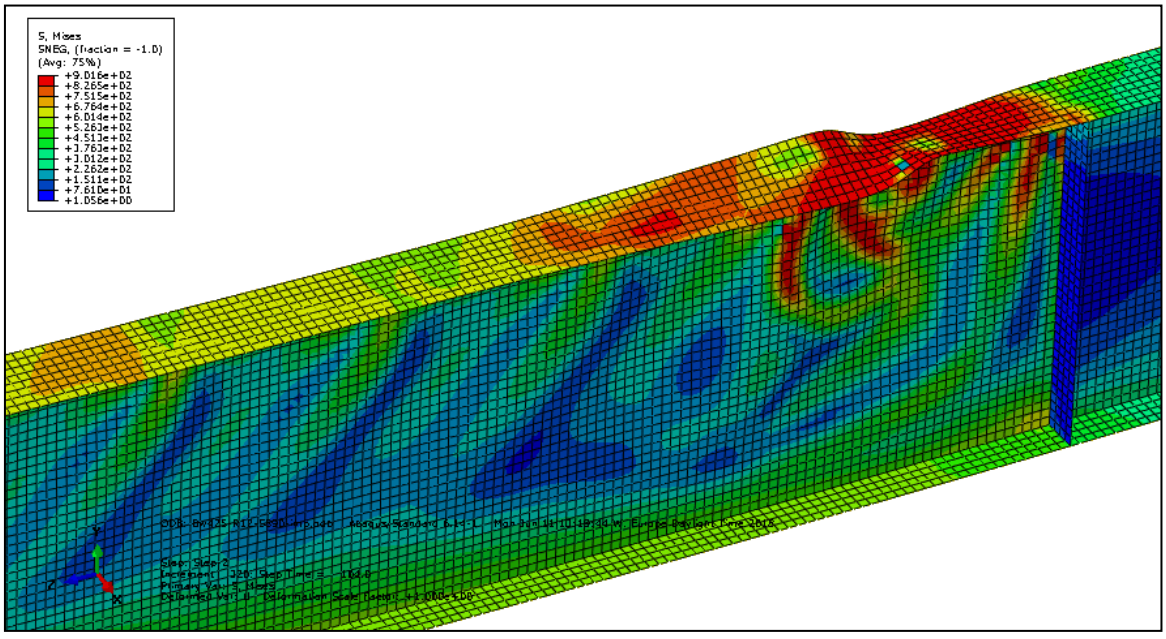

FIGURE 82: BW425 S890- 12000MM2 FAILURE, ROTATING FLANGE

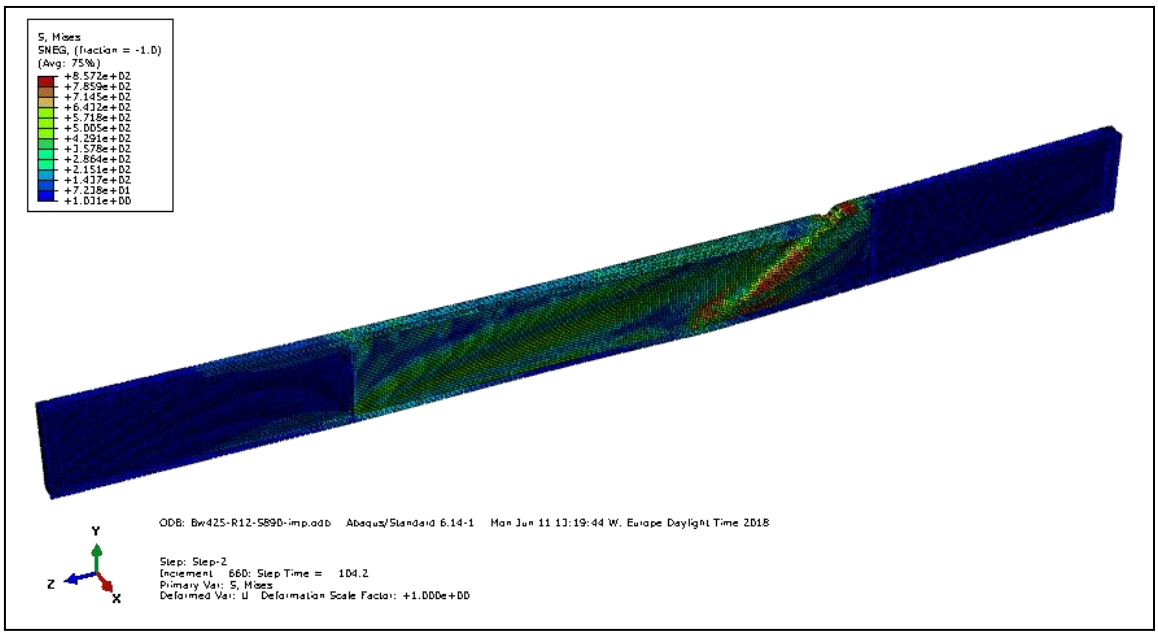

FIGURE 83: BW425 S890-12000MM2 POST-FAILURE, FLANGE INDUCED BUCKLING

Web slenderness of 450

The behavior of the plate girder with a web slenderness of 450 is different from that of the above-mentioned girders. It can be seen in Figure 84, that the pre-failure behavior is similar, but showing a little less stress in the top flange before failure. Than failure occurs on 2 sides at the same time, rotation a significant part of the top flange between to plastic hinges. Increasing the displacement increases the severity of this rotation, which leads to the flange folding onto the web, which can be seen on Figure 86.

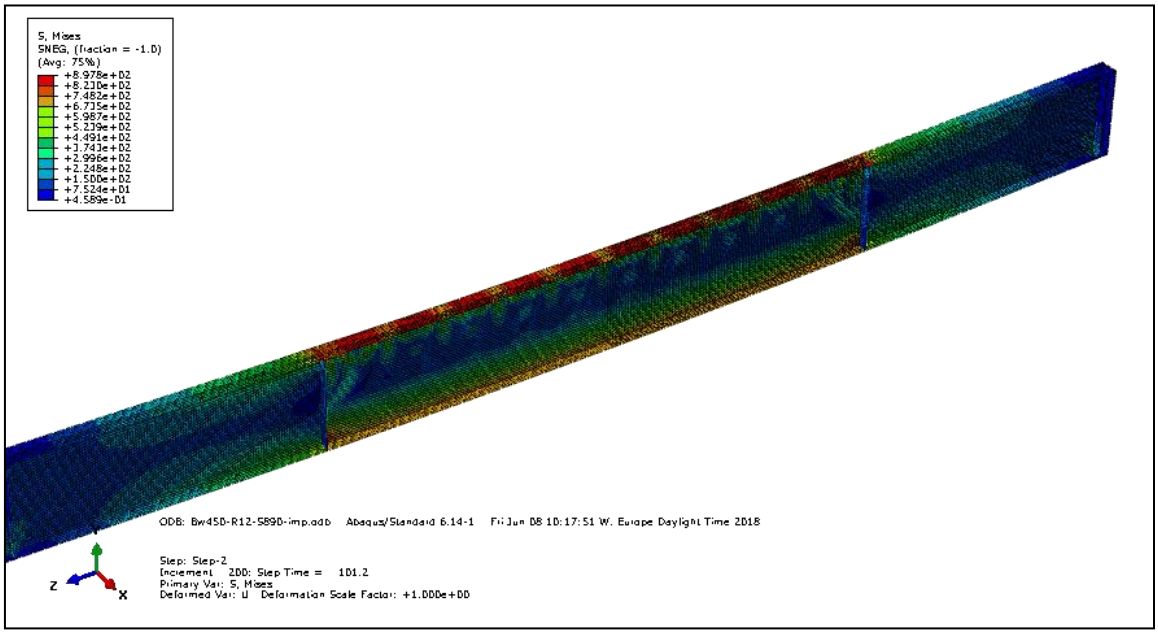

FIGURE 84: BW450 S890- 12000MM2 PRE-FAILURE, YIELDING FLANGES, DISCONTINUES STRESS PATERN

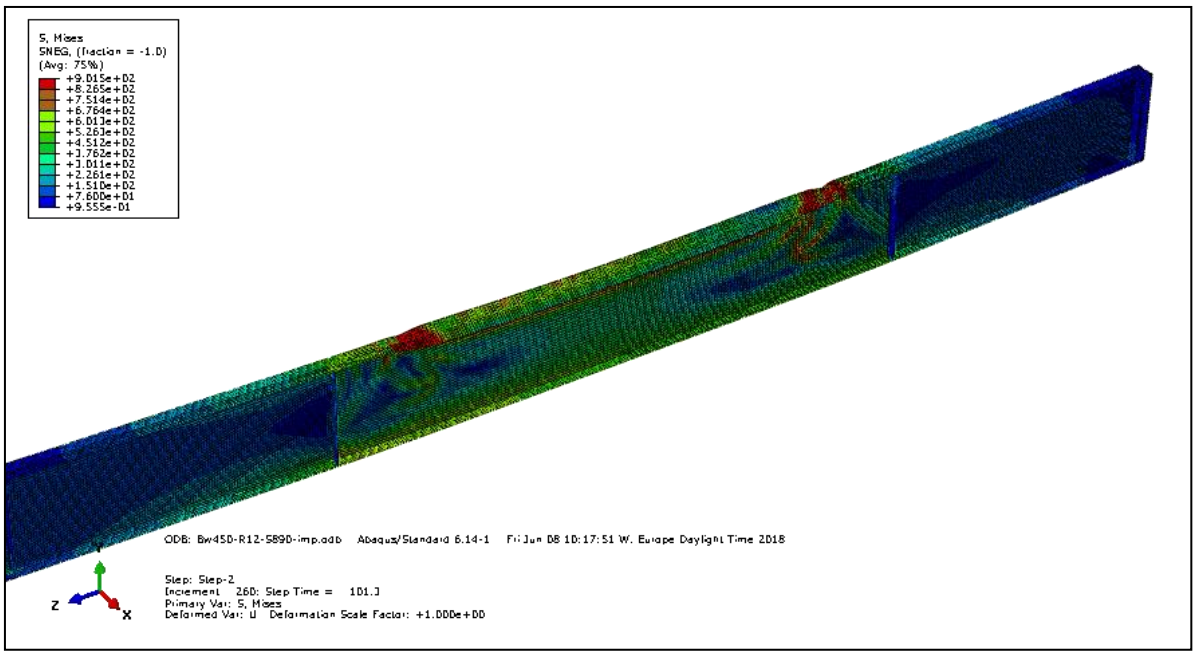

FIGURE 85: BW450 S890- 12000MM2 FAILURE, ROTATING FLANGE ON TWO SIDES

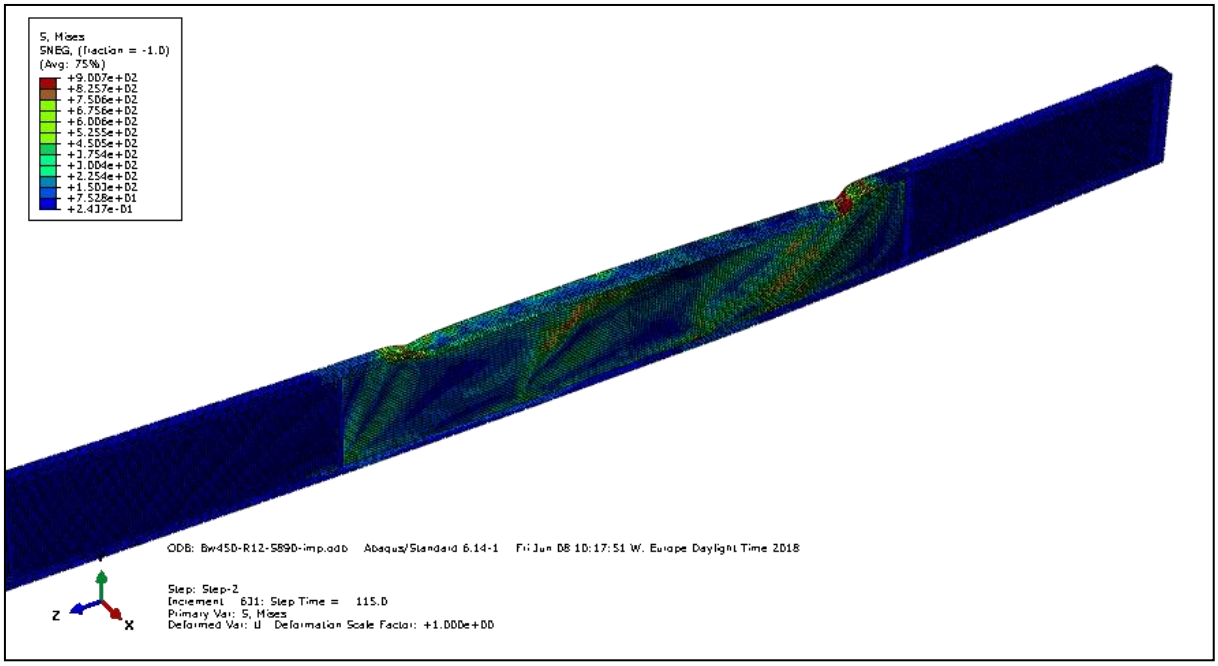

FIGURE 86: BW450 S890- 12000MM2 POST-FAILURE, TWISTED TOP FLANGE OVER A SIGNIFICANT LENGTH

The maximum bending moment resistance for plate girders modeled in the shape shown in Figure 18 can also be found using the graph shown in

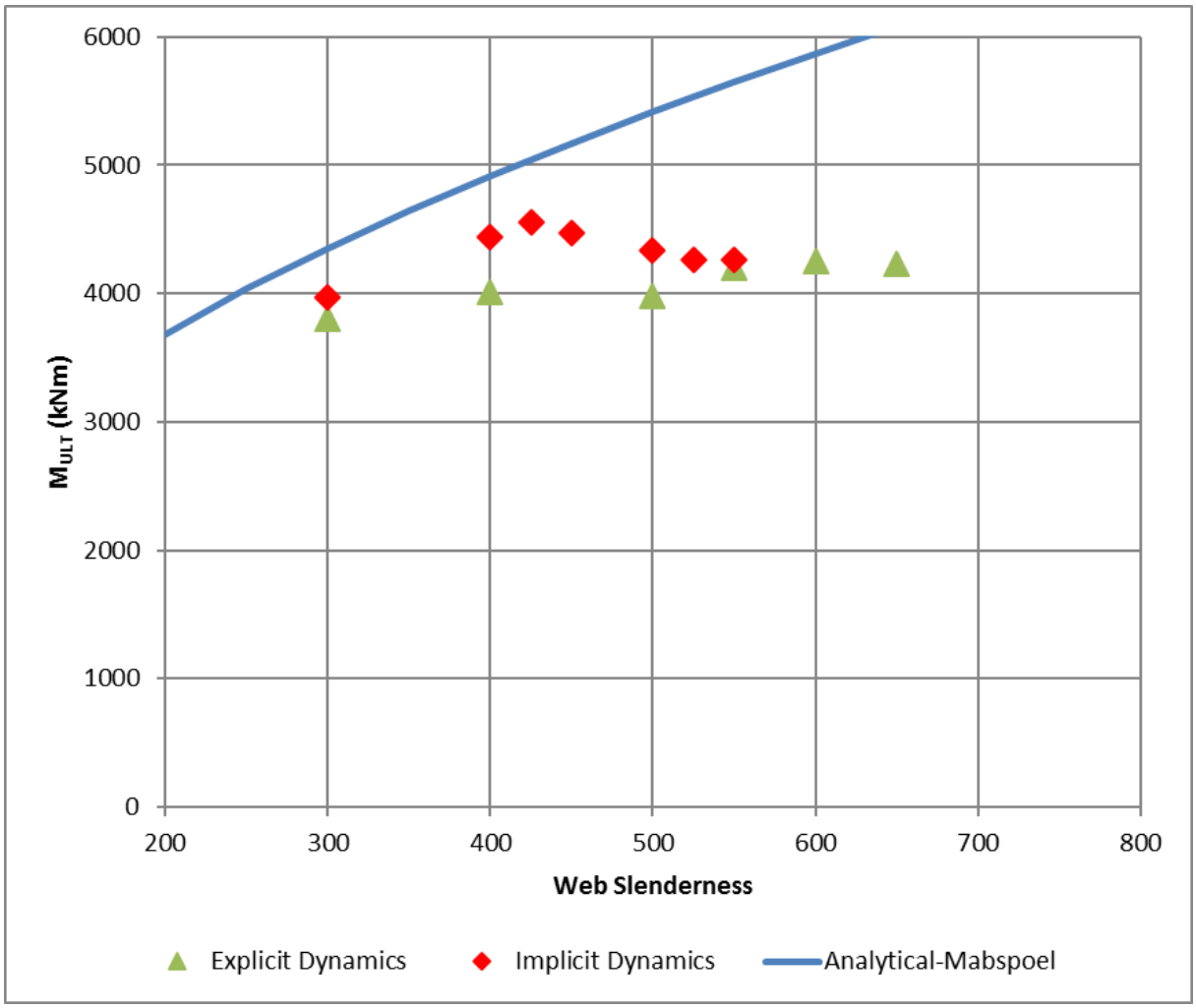

Figure 87, which also gives results for the implicit dynamic models without initial imperfection. The given results are found using a perfect geometry due to the fact that the results of the girders with S890 and 6000 mm^2 and S690 with 12000 mm^2 in previous paragraphs, showed this analysis was found to result in a lower ultimate resistance value. This has been checked for this range and found to be also a valid hypothesis.

It can be observed that the explicit method doesn't seem to produce a clear maximum and the use of implicit dynamics gives a noticeable maximum. This maximum value for the ultimate bending moment resistance is found using a web slenderness of 425 and is found to be 4550 kNm for the implicit method. The explicit maximum was found with a web slenderness of 600 and was 4250 kNm.

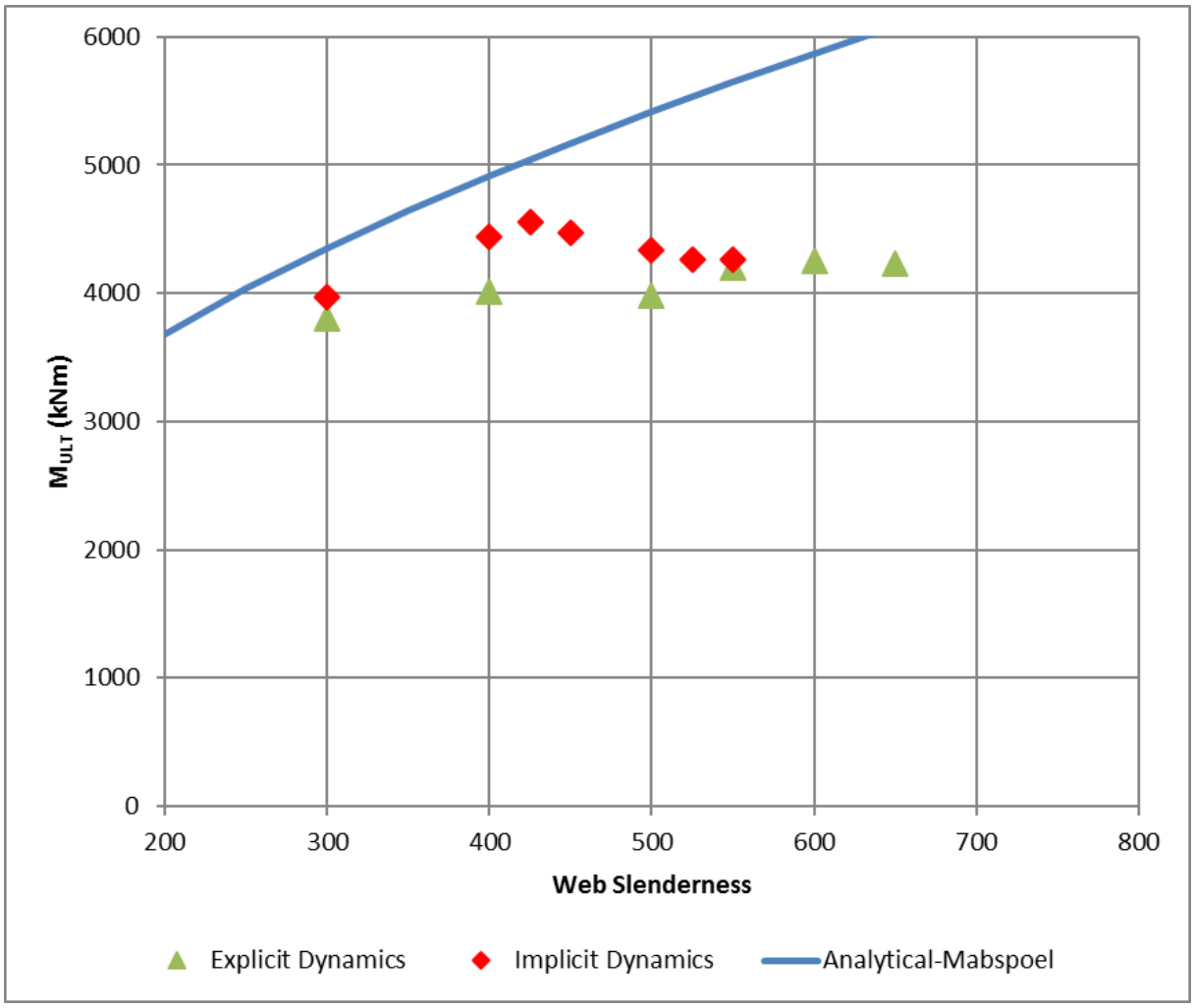

FIGURE 87: MAXIMUM ULTIMATE MOMENT CAPACITY FOR S890 12000MM2

4.4.3.c. General observations

As can be seen in the previous paragraphs, the maximum bending moment resistance for S890 steel for 6000 mm^2 and 12000mm^2 is found in both cases in the models with a web slenderness of 425. Just like the S690, which was both found with a web slenderness of 525.

The impact of small amounts of imperfections, modeled as initial imperfection has been shown to be large, certainly with girders with very slender webs. In the next paragraph the results will be implemented in the graphs found by Abspoel and discussed.

4.5. Analysis of the parametric study results

4.5.1. Introduction

After the 6 parametric studies were conducted, the results of these studies are analyzed in comparison to the results found in earlier research. The results found with models using S690 steel will be discussed with respect to the prediction of Abspoel and the results of Cimpoi. The new results will also be added to the graphs first described by Abspoel and discussed. After the parametric studies are discussed extra remarks and made on the results.

4.5.2. Discussion about the results by Cimpoi

First of all, the results of the work by Cimpoi are discussed with respect to the work done. The results found by Cimpoi, were found using explicit dynamic calculations, which in the validation phase showed to less accurate models to describe the behavior of the steel plate girders in finding the most logic failure mode. Also, the models do not show strict change in failure behavior. The use of initial imperfections has also been shown to distort the results, looking at paragraph 4.4.2.b and paragraph 4.6.5. The initial buckled shape increased the resistance of the top-flange to the rotating failure mode, leading to increased bending moment capacity at high web slenderness.

Also, the results found in the work of Abspoel, as well as the done work show a clear maximum and a web slenderness in which both the 6000 mm^2 and the 12000mm^2 models failed at the highest bending moment capacity. Cimpoi found a very significant difference in the maximum bending moment capacity.

The highest bending moment found by Cimpoi was found to be limited by the yielding of the top flange, which was also the case in the implicit models for this work, but no notion was given to the rotational failure of the top flange. It can be concluded that using the implicit dynamic results found in this work are more likely to describe the real behavior, although it cannot be confirmed by addressing reference to experimental tests, which would be an important improvement in validating the found results.

In the rest of this chapter the implicit dynamic results will be assumed to model the real behavior of the steel plate girders.

4.5.3. Modes of failure

The parametric studies have shown that the girders do fail in 2 different ways, which also govern the maximum web slenderness leading to the highest bending moment resistance. The two failure modes were shown in Figure 77, which is also shown below on Figure 88. The failure mode for girders with a limited web slenderness is shown on the bottom picture, showing the top, compressive flange being pushed into the web. This happened after the top flange reached the yield-limit of the steel and a small local rotation was seen, like on Figure 80.

The mode on the top picture is the failure mode found on girders with a slenderness higher than the limiting slenderness, which was found to be 525 for S690 steel and 425 for S890 steel. The flange rotates around the connection between flange and web, in which it is horizontally supported. This rotation was shown to happen across the full length of the top flange between the transverse stiffeners where the load was applied and always before yielding of the top flange did occur.

The exceptions to the above were found when an initial imperfection in the shape of the first eigenmode was applied to a plate girder above the limiting slenderness, also when this was of very small

proportions. The failure mode changed from the rotation to the vertical flange buckling mode. The initial imperfection also leads to an increased bending moment capacity, because the top flange could be stressed until yielding.

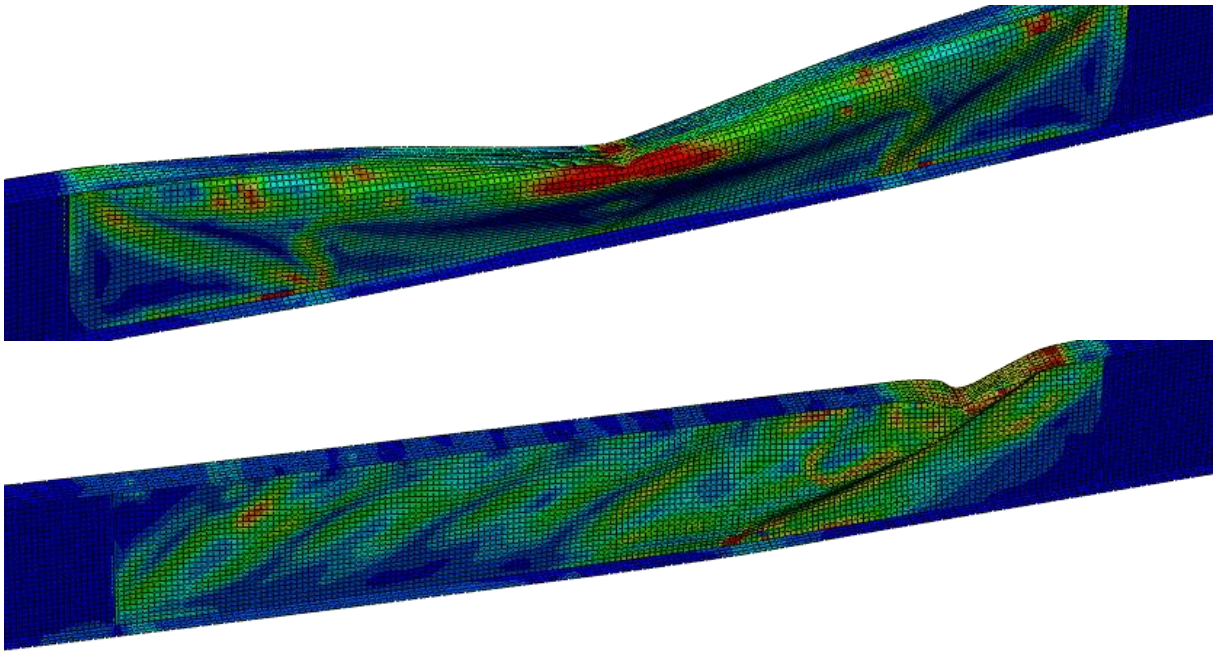

FIGURE 88: 2 DIFFERENT FAILURE MODES FOUND IN STEEL SLENDER PLATE GIRDERS: FULL FLANGE ROTATION (TOP) AND VERTICAL FLANGE BUCKLING INTO THE WEB (BOTTOM)

Both the modes of failure showed very sudden collapse with the use of S690 and S890 steel. The force displacement diagrams show only at the least slender girders in which S690 was used a small plateau before the curve drops suddenly and very fast.

4.5.4. Maximum web slenderness and bending moment capacity

The graph for maximum bending moment resistance made by Abspoel, showing the relationship between the maximum bending moment capacity and the web slenderness has been given in Figure 89 for 6000 mm^2 area and on Figure 90 the 12000 mm^2 is given. The results of Cimpoi and the previously described implicit dynamic parametric study have been added to be able to address if the results are in line with the approximations given by Abspoel. Abspoel predicted the graph to travel linear for a certain time and reach a plateau which limits the use of higher strength steels, as well as the steel grades having the same maximum effective web slenderness. At first glance the linearity seems to be present in the results, until the S890 results come and the line peaks up. In both the graphs we see that all steel grades have the same maximum web slenderness for their maximum bending moment resistance models. The results of Cimpoi in these graphs are again looking very far from logical and do not show the same web slenderness for S690.

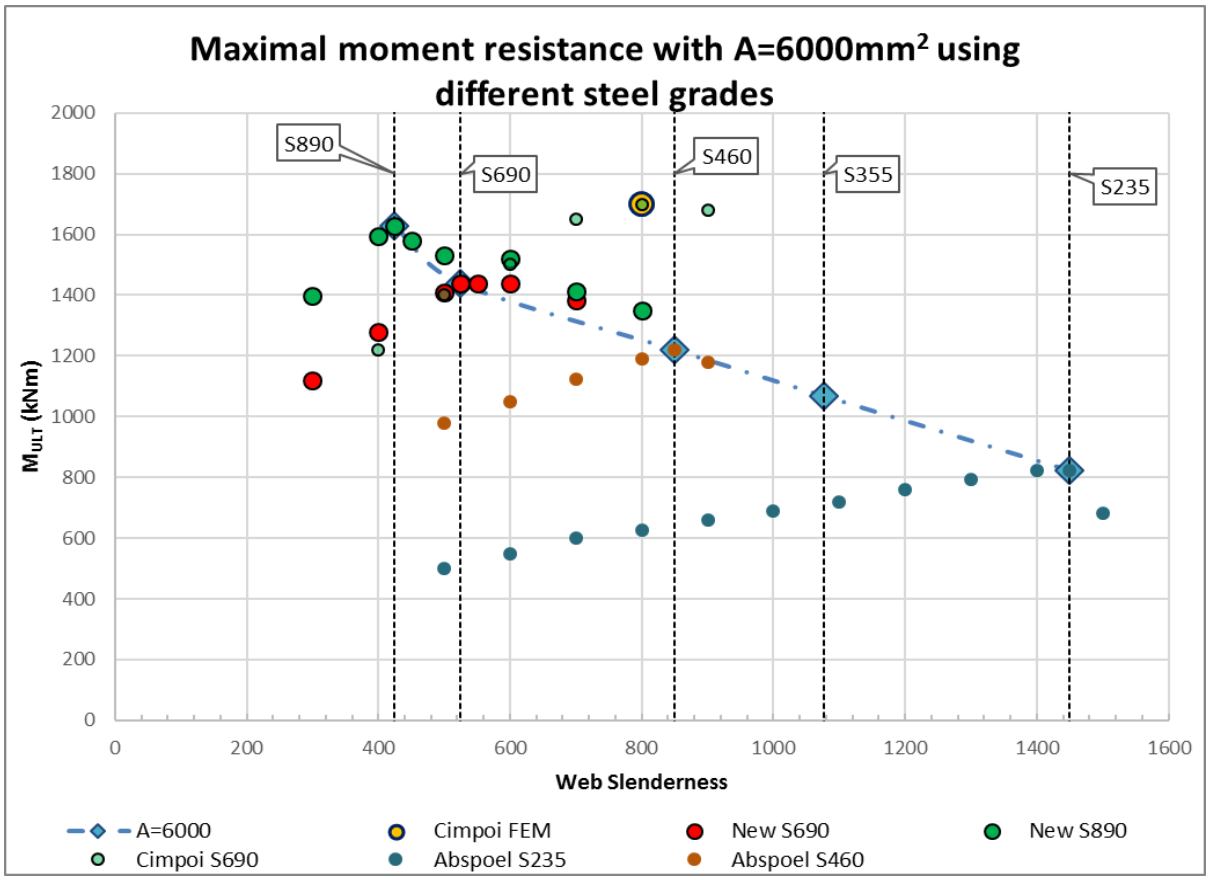

FIGURE 89: RESULTS FROM 3 RESEARCHES GIVING BENDING MOMENT RESISTANCE FOR DIFFERENT STEEL GRADES AND WEB SLENDERNESS' WITH A TOTAL AREA OF 6000 MM²

Looking at the table below, table 19, the results are shown for, in which also the comparison can be made between the S690 results found by Cimpoi, this research and the extrapolation done by Abspoel. It shows the results in this research found by explicit dynamic analysis are very close to the predicted values by Abspoel. The limiting web slenderness are much higher than the limitation proposed by Basler, found in paragraph 2.3.1.a.

	A=6000		*A=12000*	
Fy-"model"	Bw	Mu	Bw	Mu
S235-Abspoel	1450	822,4	1450	2357,4
S355-Interpolation	1076	1068,5	1076	3025,9
S460-Abspoel	850	1220,3	850	3495,4
S690-Extrapolation	509	1445,7	509	4095,4
S690-Cimpoi	800	1700	450	3700
S690-New	525	1438,8	525	4023,2
S890-New	425	1627,7	425	4550,9

TABLE 19: MAXIMUM BENDING MOMENT CAPACITY AND WEB SLENDERNESS' FOUND IN DIFFERENT RESEARCHES

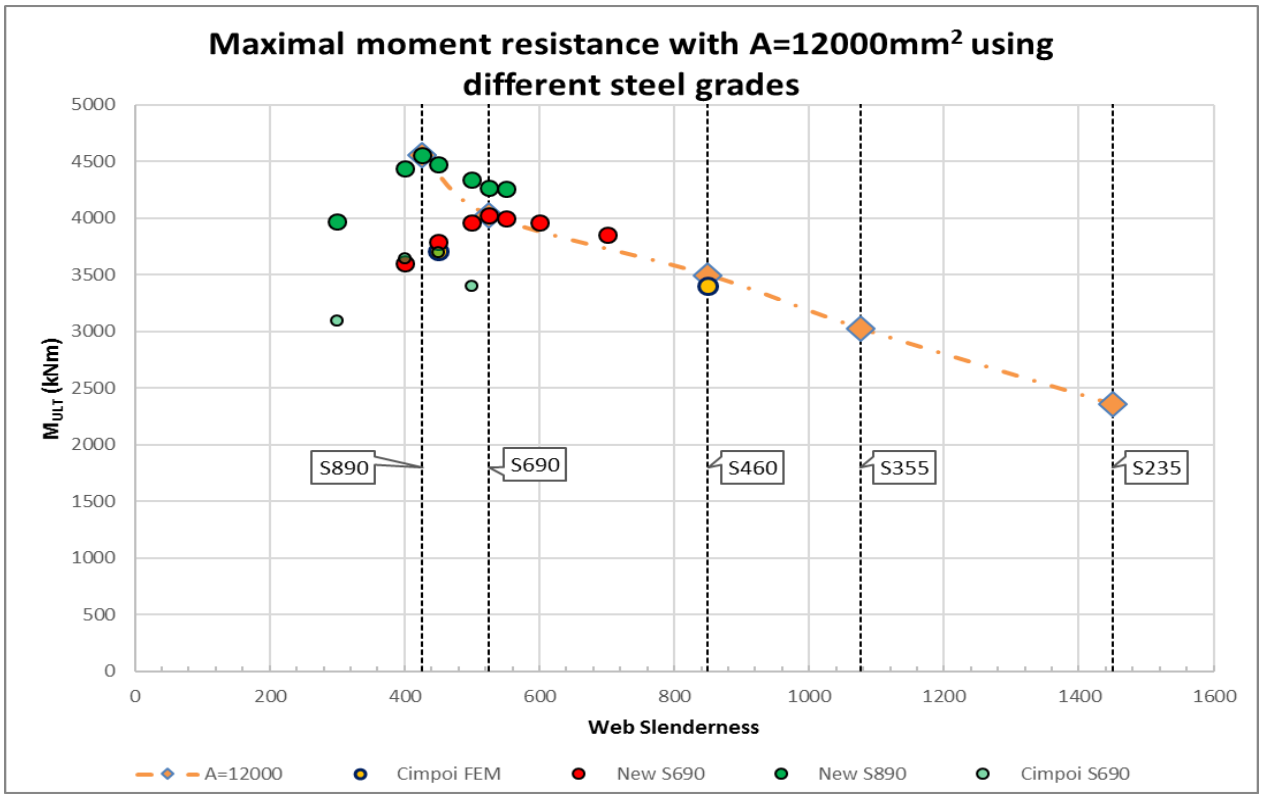

FIGURE 90: RESULTS FROM 3 RESEARCHES GIVING BENDING MOMENT RESISTANCE FOR DIFFERENT STEEL GRADES AND WEB SLENDERNESS' WITH A TOTAL AREA OF 12000 MM²

4.5.4.a. Maximum moments in relation with girder heights

Because the graphs showing the results in the previous paragraph show a non-linear relation between the slenderness of the girder and the bending moment capacity. When the results are presented differently, another picture is found. Since the web-slenderness is a parameter with an indirect link to the moment, it is more logical to use a parameter directly linked to this. In Figure 91 and Figure 92 the graph is showing the flange moments for 5 steel grades, with the blue dots being the found maximum bending moment resistance for the plate girders.

The linear estimated line between the result-dots fits very well onto the results and looking at Table 20, which shows the values of the maxima. It can be seen that multiplying the maximum bending moments with the eta, which belongs to the steel grade, we find that the last column of both results is almost the same value for all steel grades.

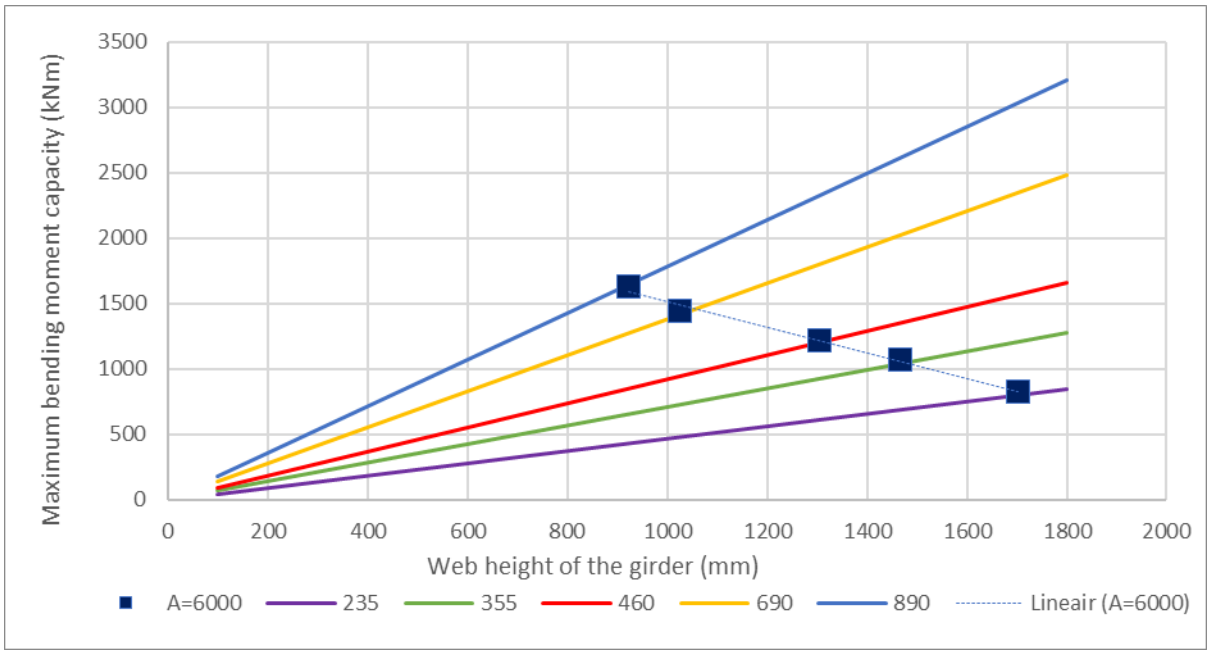

FIGURE 91: MAXIMUM BENDING MOMENT CAPACITY AND FLANGE-MOMENTS FOR 5 STEEL GRADES USING 6000 MM^2 STEEL AND AN RATIO BETWEEN FLANGE AND WEB OF 1.

		A=6000			A=12000		
steel grade	eta	Bw-max	Mult	Mult*eta	Bw-max	Mult	Mult*eta
S235	1	1450	822,4	822,4	1450	2357,4	2357,4
S355	0,813617	1076	1068,5	869,3	1076	3025,9	2461,9
S460	0,714751	850	1220,3	872,2	850	3495,4	2498,3
S690	0,583592	525	1438,7	839,6	525	4023,2	2347,9
S890	0,513853	425	1627,6	836,3	425	4550,9	2338,5

TABLE 20: MAXIMUM RESULTS FOR 6000 AND 12000 MM^2 MULTIPLIED BY ETA

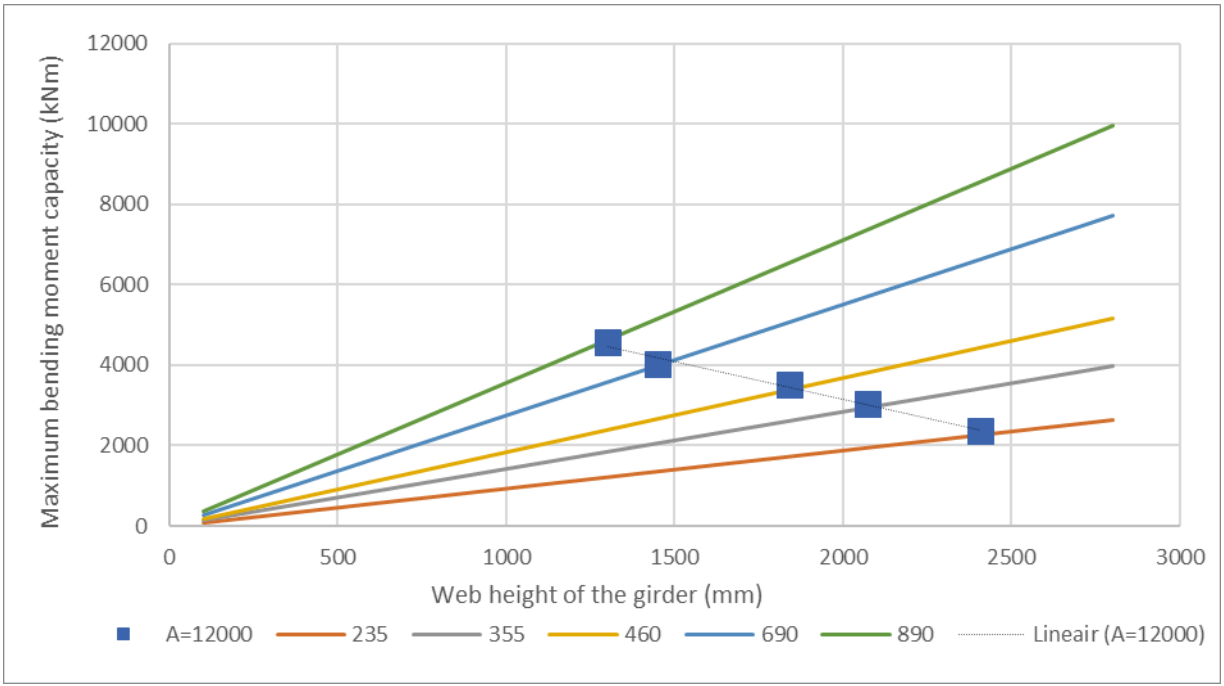

FIGURE 92: MAXIMUM BENDING MOMENT CAPACITY AND FLANGE-MOMENTS FOR 5 STEEL GRADES USING 12000 MM^2 STEEL AND AN RATIO BETWEEN FLANGE AND WEB OF 1.

Looking at the table again it can be noticed that the height of the limiting girders also is related to the steel grade, using eta. We have seen that the ultimate bending moment is almost equal to the plastic flange moment.

		A=6000			A=12000		
steel grade	eta	Bw-max	hw	Hw/eta	Bw-max	hw	Hw/eta
S235	1	1450	1702,93	1702,93	1450	2408,32	2408,32
S355	0,813617	1076	1466,97	1803,02	1076	2074,61	2549,86
S460	0,714751	850	1303,84	1824,18	850	1843,91	2579,79
S690	0,583592	525	1024,69	1755,84	525	1449,14	2483,13
S890	0,513853	425	921,95	1794,19	425	1303,84	2537,38

TABLE 21: RELATIONSHIP BETWEEN THE MAXIMUM WEB HEIGHT AND THE STEEL GRADE

If we look only to the girders with the set geometry, we could make an approximate equation to find the ultimate bending moment capacity of any steel grade, when the geometry set.

$$\beta_{w.235} = 1450 \tag{4.1}$$

$$h_{w.S235} = \sqrt{\frac{A_{fl}}{A_{tot}}} * \sqrt{\beta_{w.235}} * \sqrt{A_{tot}} \tag{4.2}$$

$$h_{w.f_y} = h_{w.S235} * \varepsilon, \quad \varepsilon = \sqrt{\frac{235}{f_y}} \tag{4.3}$$

$$M_{u.f_y} = h_{w.f_y} * A_{fl} * f_y \tag{4.4}$$

When we use the equations above the table for the ultimate web slenderness and ultimate bending moment capacity are given in. The results of the maximized bending moment are compared to the results from Table 21 and are shown in Table 22 the 4th columns of the 2 parts. It can be seen that the capacity is never overestimated, but for the S460 steel the results are not very accurate. The S355 results do not match very good as well, but the results given is an interpolation by Abspoel, which has not been verified by tests.

		A=6000				A=12000			
steel grade	eta	Bw-calc	hw	Mu	% MFEM	Bw-calc	hw	Mu	% MFEM
S235	1	1450,0	1702,9	805,1	98%	1450,0	2408,3	2273,2	96%
S355	0,813617	959,9	1385,5	990,8	(93%)	959,9	1959,4	2796,6	(92%)
S460	0,714751	740,8	1217,2	1129,0	93%	740,8	1721,3	3185,7	91%
S690	0,583592	493,8	993,8	1385,3	96%	493,8	1405,5	3906,7	97%
S890	0,513853	382,9	875,1	1575,4	97%	382,9	1237,5	4441,2	98%

TABLE 22: CALCULATED BENDING MOMENT CAPACITY AND LIMITING WEB SLENDERNESS FOR 4 STEEL GRADES, USING EQUATION (4.1) TO (4.4)

4.5.5. Numerical capacity compared to calculated capacity

When using non-slender beams in general, the plastic moment capacity governs the bending moment capacity. With slender girders, classified in section class 4 the effectiveness of the girder can be less than 100%, resulting in a bending moment capacity below the elastic moment capacity.

To check the numerical results with respect to several calculated bending capacities, plots are presented below to address the effectiveness of the girders. In these plots the plastic capacity, the elastic capacity, the plastic capacity for only the flanges, the bending moment capacity by Abspoel, using equation (2.31) and the effective bending moment capacity, found by using equation (2.32) to (2.36).

The 4 plots, Figure 93 to Figure 96 on the next pages, show that the capacity of the girders is close to the flange moment and the capacity found by Abspoel. For the S690 results the numerically found capacity is somewhat higher than the flange moment, while the S890 steel plate girders show a little less capacity compared to the flange moment capacity. It can be seen that the plastic capacity is much higher, as well as the elastic capacity of the full cross section.

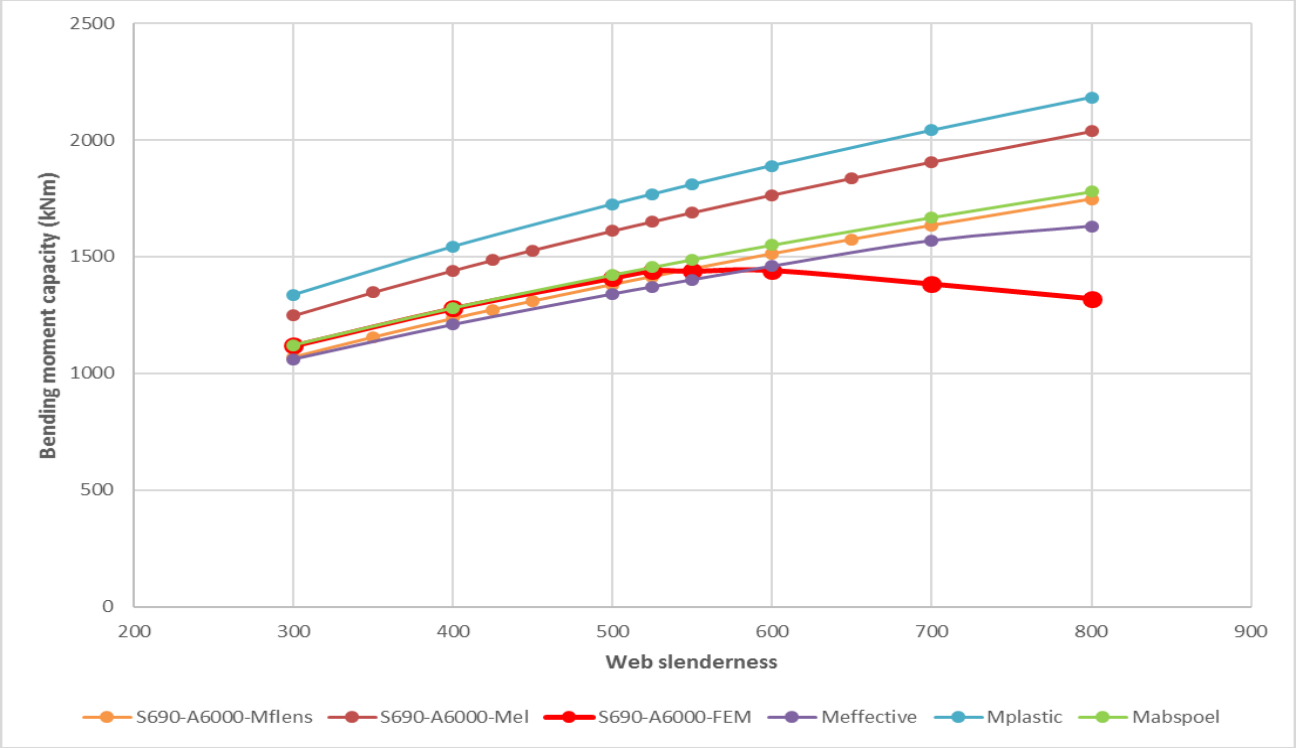

FIGURE 93: RESULTS FROM THE NUMERICAL MODELS DONE ON S690 STEEL, WITH 6000 MM^2 AREA, COMPARED TO ANALYTICAL MODELS FOR BENDING MOMENT CAPACITY

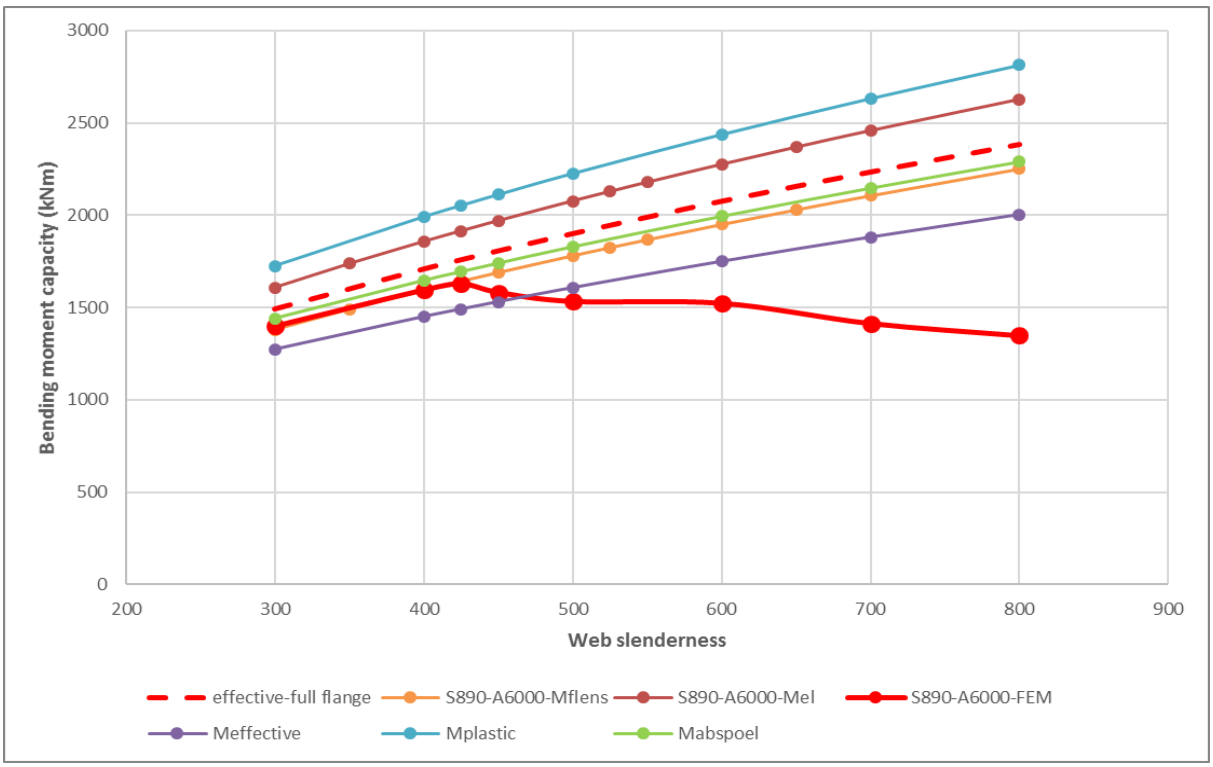

FIGURE 94: RESULTS FROM THE NUMERICAL MODELS DONE ON S890 STEEL, WITH 6000 MM^2 AREA, COMPARED TO ANALYTICAL MODELS FOR BENDING MOMENT CAPACITY

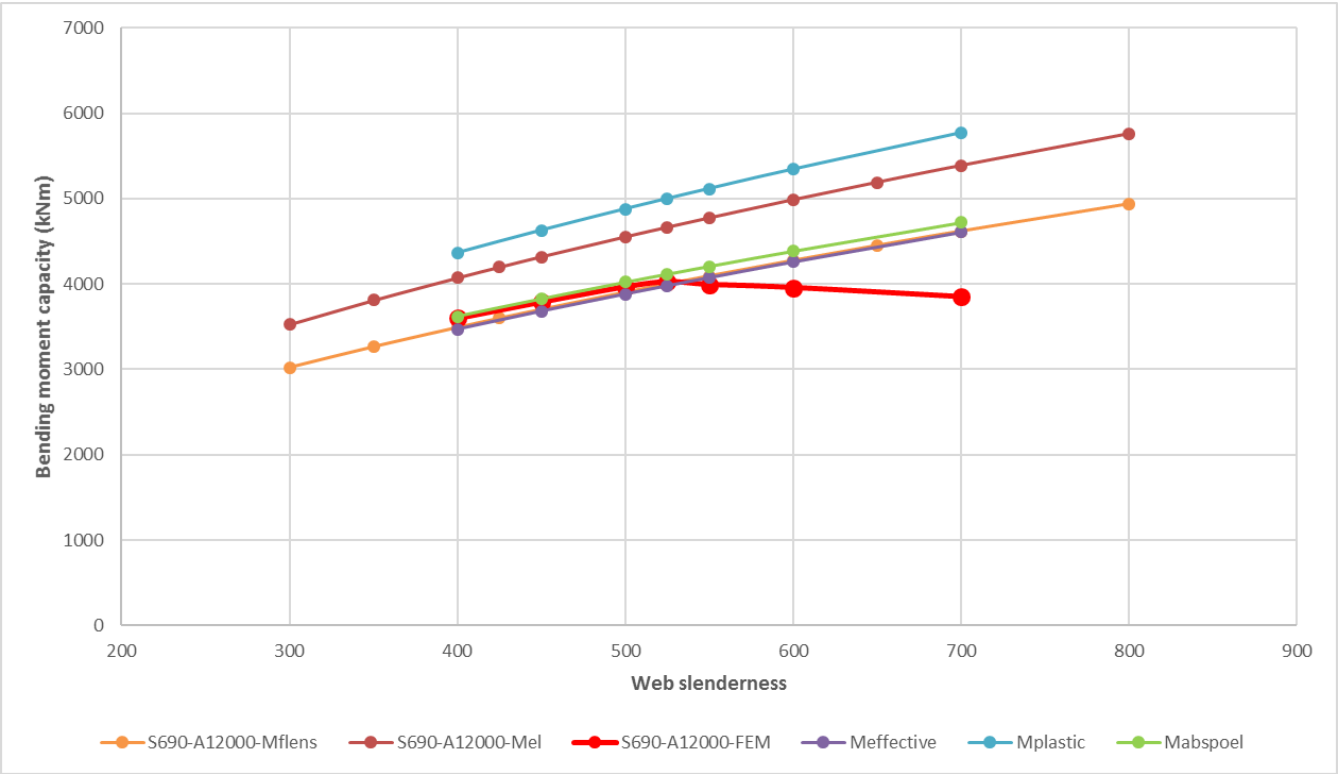

FIGURE 95: RESULTS FROM THE NUMERICAL MODELS DONE ON S690 STEEL, WITH 12000 MM^2 AREA, COMPARED TO ANALYTICAL MODELS FOR BENDING MOMENT CAPACITY

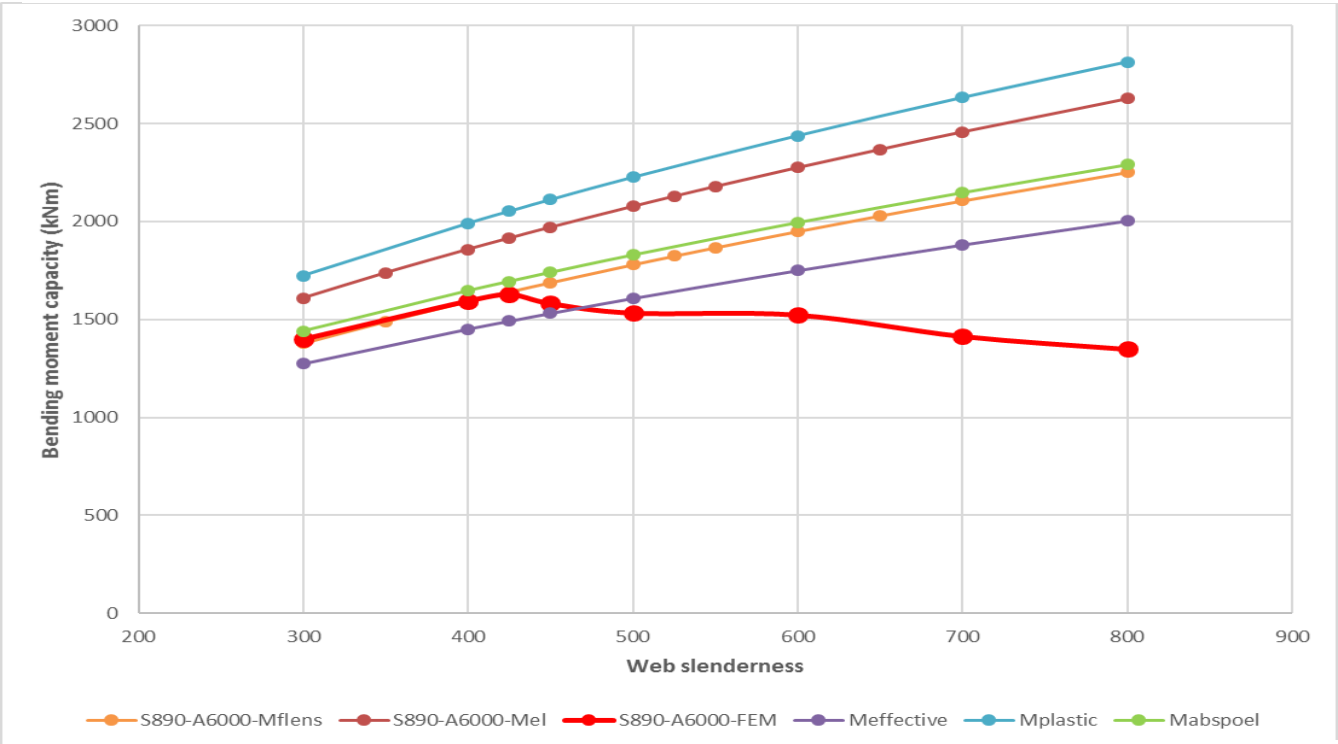

FIGURE 96: RESULTS FROM THE NUMERICAL MODELS DONE ON S890 STEEL, WITH 12000 MM^2 AREA, COMPARED TO ANALYTICAL MODELS FOR BENDING MOMENT CAPACITY

We can see that the plastic flange moments show a good comparison to the results, prior to the maximum, but the full plastic capacity is much higher. The effective moment capacity, calculated using the equations from the eurocode, are much lower. This is because the capacity of the top flange can not be fully used, because it is to slender. The effective bending moment capacity, with the full top flange being effective is only calculated for the girders with S890 and 6000 mm^2 area, found on Figure 94.

Looking at Figure 97, the results for all numerical tests on girders with a total area of 6000 mm^2 are presented against the elastic and flange moments. All results prior to the maximum web slenderness are between the 2 calculated capacities. The S235 results are further above the plastic flange moment capacity, with values of about 105% of the flange moment. This reduces for S460 to about 103%, S690 about 100% and S890 results being just below it at about 99% at the limiting web slenderness.

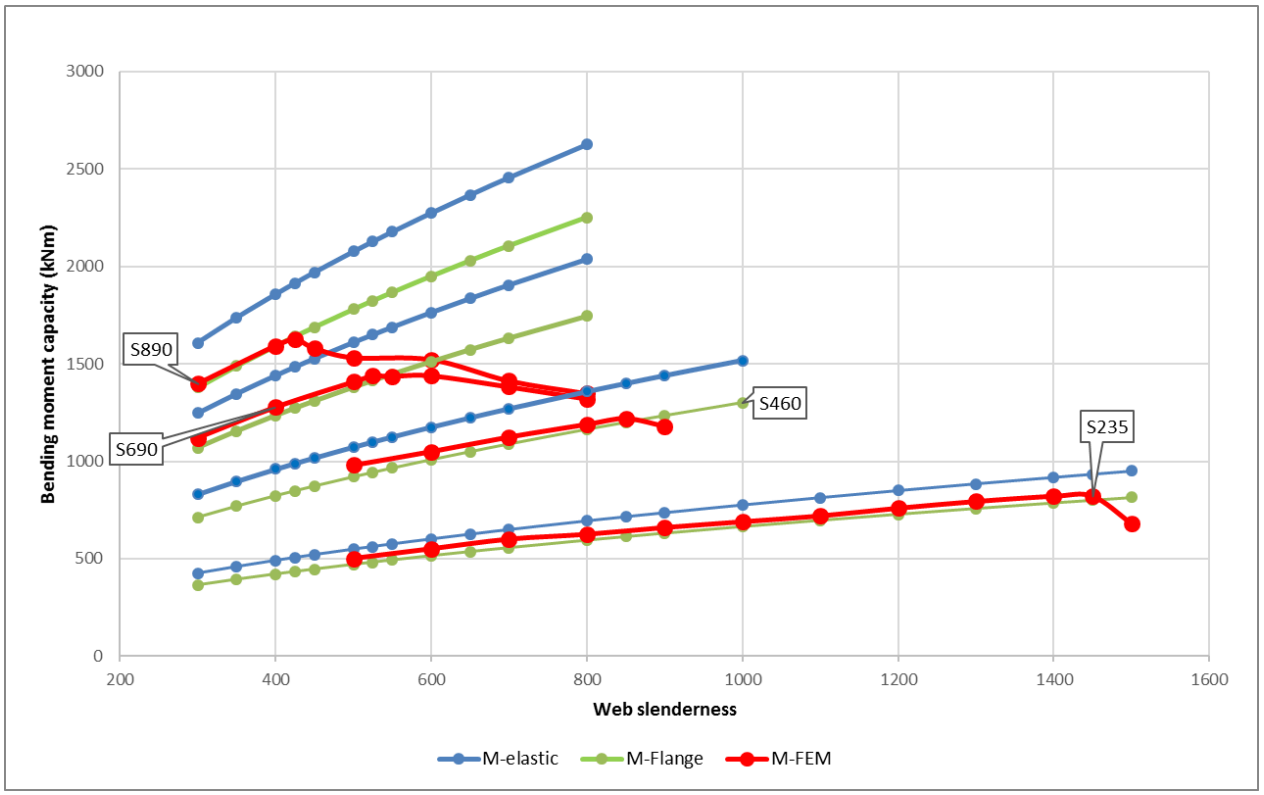

FIGURE 97: PLASTIC AND FLANGE MOMENTS COMPARED FOR 4 STEEL GRADES WITH PLATE GIRDERS HAVING 6000 MM^2 AREA.

When we look at the capacities compared to the flange platic moments and combine them in one graph, we find Figure 98 as the result. It is noticeable that, before the maximum bending moment for a steel grade is achieved, the moment found in the numerical model, is close to the plastic capacity of only the flanges. The results are very simmilar over the full range of tests and show a sudden decrease in capacity at the limiting web slenderness, dropping the percentage to a level well below 100%.

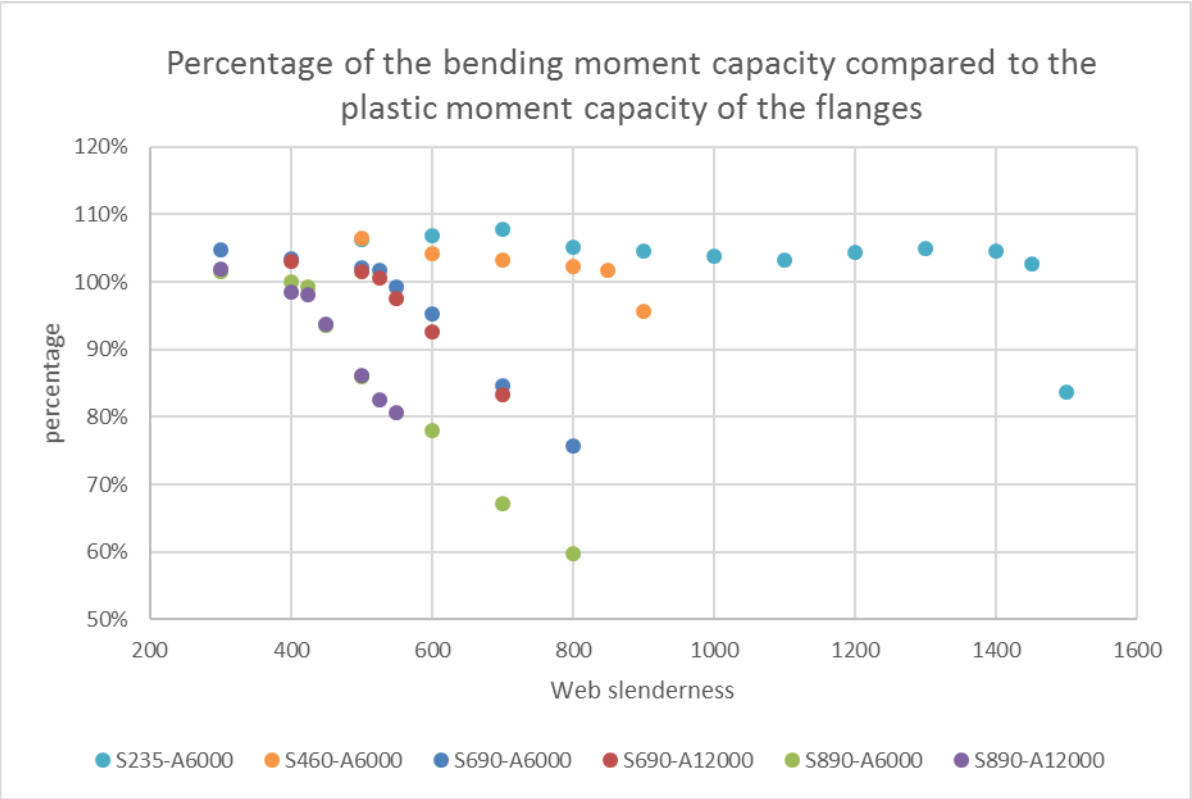

FIGURE 98: NUMERICAL BENDING MOMENT CAPACITY COMPARED TO THE CALCULATED PLASTIC FLANGE MOMENT CAPACITY

4.6. Extra investigations on S890 steel girders

4.6.1. Introduction

In the previous paragraphs 6 different parametric studies were conducted on slender steel plate girders, using S690 and S890 steel. The results of the parametric studies using the implicit dynamic analysis show promising results and a repeated behavior. For the results to be more significant some extra investigations have been committed. In this paragraph the impact of some modeling choices has been analyzed using small-scale parametric studies.

- The strain in the models has been looked into to check if the used engineering material properties are usable in these models.
- The influence of the shape of the flange is investigated.
- An investigation on the impact of a hybrid composition in the plate girders has been tested on 4 types of girders.
- Extra numerical simulations have been conducted into the way the initial imperfection has been modeled and if the choice to use the results without initial imperfections is a correct assumption.
- The influence of the length of the plate girder on the bending moment capacity is look into, because the modeled geometry, described in paragraph 3.2.1 has dependent parameters.

4.6.2. Strain in the top flange

Because an engineering model for the stress-strain relationship has been chosen to represent the behavior of the steels in use, a check has to be made to address the impact of this modelling. The engineering model does not describe the real behavior in which strain hardening and after a while loss of capacity is see, but makes use of a simplified, ever increasing formulation of the relationship between stress and strain.

If the results before failure show high amounts of strain it is needed to verify if the results are still viable and will represent the real behavior. The strain which is found in several FEM-results on the before described steel plate girders, can be found in Table 18. It can be seen that the strain in the top flange of the girder, which is the highest stressed part of the girder throughout the test, is never higher than 0.60%. In general, this is an easily achievable and also an acceptable value for all types of construction steel.

TESTED SLENDERNESS	STEEL GRADE	A (MM2)	MAXIMAL STRAIN (LOCAL)	STRAIN PERCENTAGE	MAXIMAL PLASTIC STRAIN IN TOP FLANGE (LOCAL)	CALCULATED ELASTIC STRAIN
BW300	S690	6000	-0,0046400	-0,46%	-0,00143	-0,0032100
BW425	S890	6000	-0,0053390	-0,53%	0	-0,0053390
BW700	S890	6000	-0,0041820	-0,42%	0	-0,0041820
BW300	S690	12000	-0,0046100	-0,46%	-1,20E-03	-0,0034100
BW300	S890	6000	-0,0059577	-0,60%	-0,001935	-0,0040227

TABLE 23: STRAIN CHECK IN SEVERAL NUMERICAL MODEL RESULTS AT MAXIMUM BENDING CAPACITY

Because the results all show low strains over all the models, it can be concluded that the results will not be affected significantly by changing the stress-strain diagram after the yield stress is achieved. The girders all fail with only a small amount of plastic strain, in most cases there isn't any plastic strain before failure.

4.6.3. Flange geometry impact

The geometry of the flange has been chosen to have a fully functional flange, in section class 2. The choice was made using S235 steel, in which the maximum slenderness should be 20. The geometry was chosen to have this value, so the width of a flange with 2000 m ^{2} area was 200 mm and the thickness 10mm.

The criteria of the section classes change with different steel grades and must be multiplied by $\boldsymbol{\varepsilon}$, which is $\boldsymbol{\varepsilon} = \sqrt{\frac{235}{f_y}}$, therefor changing 20 to 10.72 and leading to a geometry of 146.5 x 13.6 mm. The impact of this changed flange have been investigated, with and without imperfection and is shown in . Again, the results with imperfection are larger than those without imperfection. It can also be concluded that the bending moment capacity for the new flange is less than the capacity of the wide, less thick original flange.

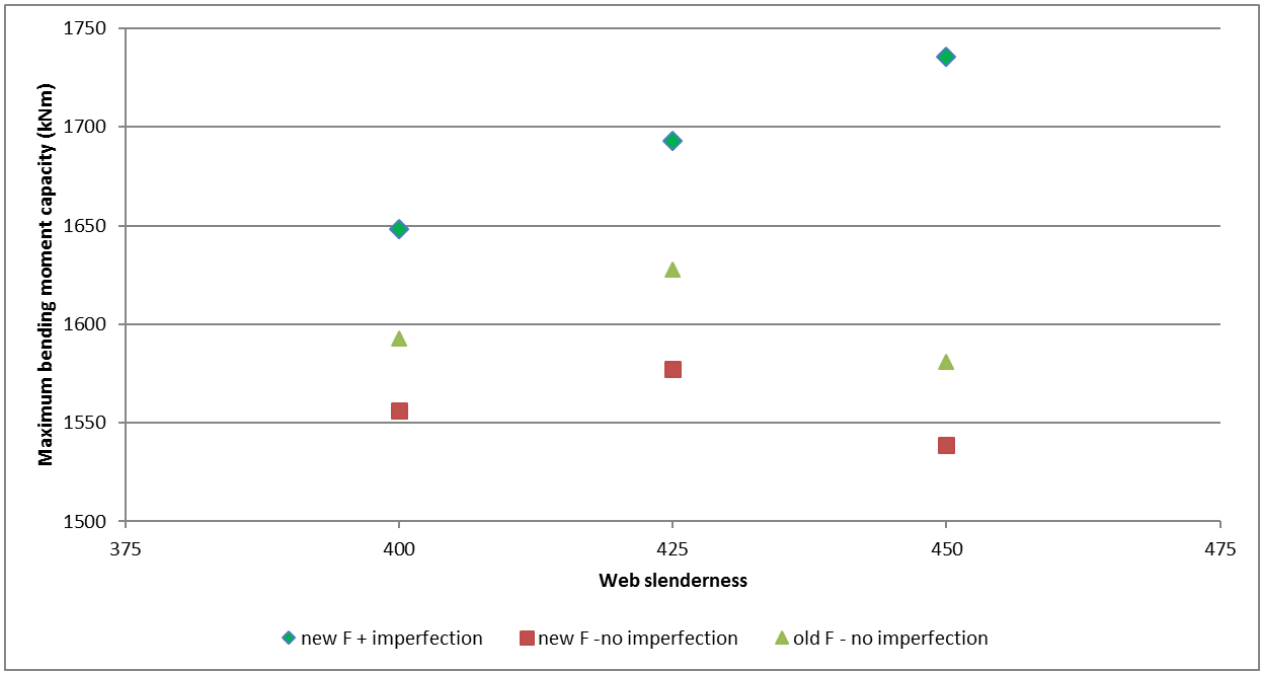

FIGURE 99: IMPACT OF THE FLANGE GEOMETRY TO THE BENDING MOMENT CAPACITY

It can be seen that increasing the bulkiness of the flange, reduces the bending moment capacity by 3%, for girders with a slenderness of 400, 425 and 450. Reducing the width and increasing the thickness, increases the bending resistance along the strong axis, but decreases the bending stiffness around the weak axis. This might be an influencing factor in the bending moment resistance.

4.6.4. Hybrid structures

Using high strength steel can be beneficial in increasing capacity, while the steel consumption is kept low. The increase in yield strength for the used steels can therefore be an interesting idea, but the high strength steels are more expensive to produce. It is there for useful to look at optimizing the cross section, by using less high strength steels in parts of the structure which are less stressed.

The previous results show the top flanges are stressed the most, followed by the bottom flanges and the web is the least stressed. The first hybrid girder which will be tested is a S890 steel girder with a web made from S460 steel, after this a girder with a top flange of S890, a web of S460 and a bottom flange of S690 will be tested. For all test a total cross-sectional area of 6000 mm^2 is used.

4.6.4.a. Model adaption

The girders used for this analysis have been modelled for the S890-6000 mm^2 parametric study, and only the used material in the middle-section of the girder had to be changed to S460 steel. The models for web slenderness of 400, 425, 450 and 500 were used in this analysis. The models were named Hybrid 1 for the S460 web and S890 flanges. For the other Hybrid cross section, which is called Hybrid 2, also the material used in the bottom flanges had to be changed into S690 steel. Both compositions are shown in Figure 100. For both hybrid-model the analysis was chosen to be the implicit dynamic analysis, using quasi-static parameters.

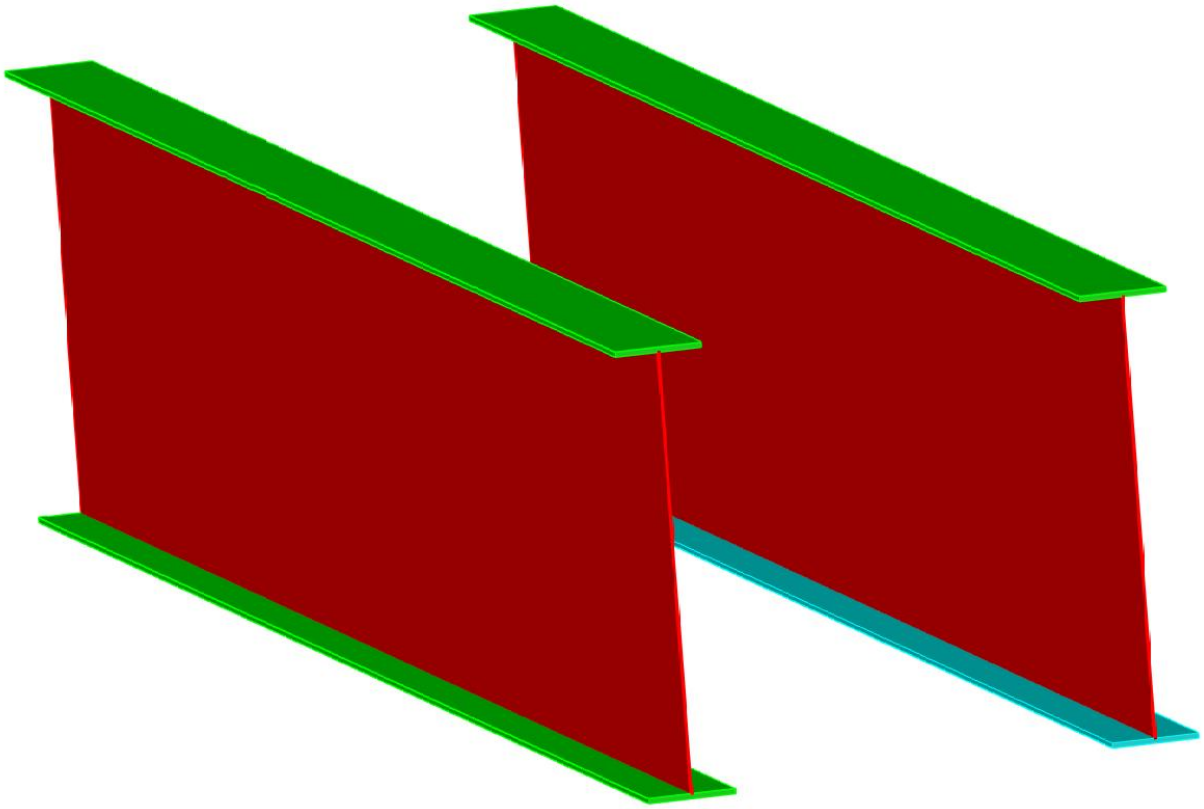

FIGURE 100: HYBRID 1 (L) AND HYBRID 2 (R) COMPOSITION, GREEN = S890, RED = S460, BLUE = S690.

4.6.4.b. Results for the hybrid sections

The results generated by the analysis can be found in Table 24 and on Figure 101. It can be seen that using S460 steel in the web reduces the moment capacity in all 4 analyzed geometries. When the bottom flange is also reduced to S690, the capacity of the girders further reduces.

Looking into the failure modes, it can be seen that the failure for all girders is still the same, compared to the non-hybrid girder. The girders with a slenderness of 400 and 425 fail after the top flange yields and then buckles, the 450 and 500 girders fail with a rotation of the top flange along the longitudinal axis.

It can also be seen that the hybrid girders with a web slenderness of 500 do not differ in bending moment capacity. This is because, before the bottom flange would get to its yield limit, the top flange fails. The stress in the bottom flange, found in both the hybrid 1 and the hybrid 2 configuration, was below 690 N/mm^2 and therefor the results show no difference in capacity.

Web Slenderness	*Non-hybrid Capacity (kNm)*	*Hybrid 1 Capacity (kNm)*	*Hybrid 2 Capacity (kNm)*
400	1593,0	1533,0	1502,1
425	1627,7	1579,4	1526,8
450	1580,8	1559,0	1540,7
500	1532,1	1460,6	1457,8

TABLE 24: BENDING MOMENT CAPACITY FOR 3 TYPES OF HYBRID SECTIONS

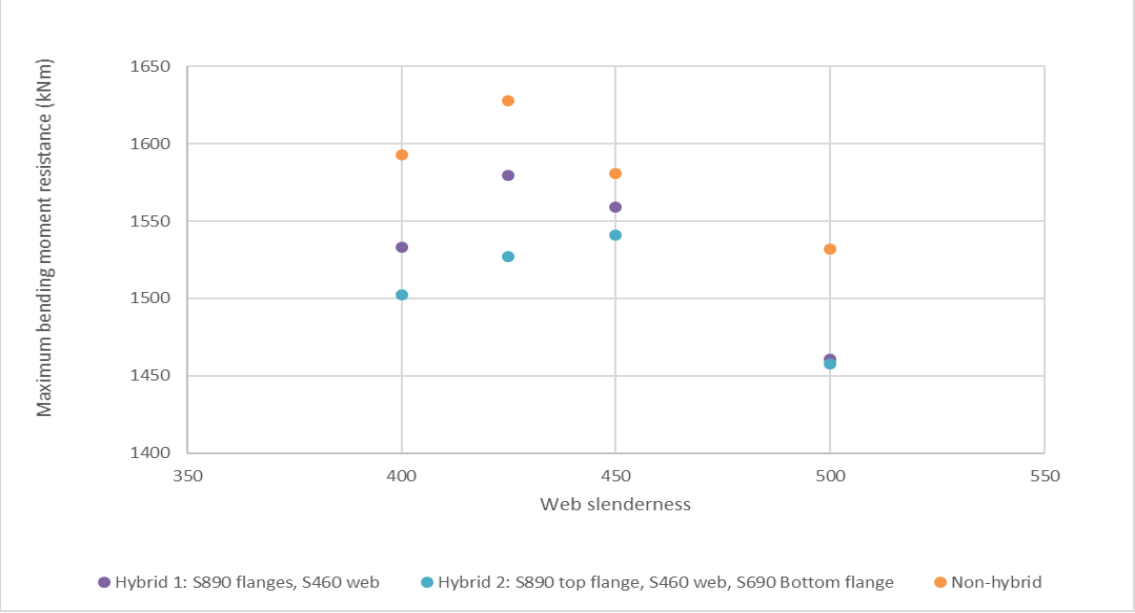

FIGURE 101: ULTIMATE BENDING MOMENT CAPACITY FOR 3 HYBRID SECTION

What cannot be seen in the bending moment capacity is how the girder behaves. Looking at the force displacement diagrams, on Figure 102 and Figure 103, of the 3 analysis done on girders with a web slenderness of 400 and 425 it can be seen that the stiffness of the girders is somewhat different. The

girders with a S460 web show a little reduced stiffness in the second part of the increasing part of the plot. In this part the web was partially yielding.

At failure the non-hybrid girder, as well as the girder with Hybrid 1 configuration show little to no ductility, while in the Hybrid 2 plot, a clear plateau can be seen. This occurs due to the fact that the bottom flange in this analysis is yielding, before the top flange yields. From a safety point of view this is a preferable situation in comparison to the sudden failure found in the parametric studies conducted.

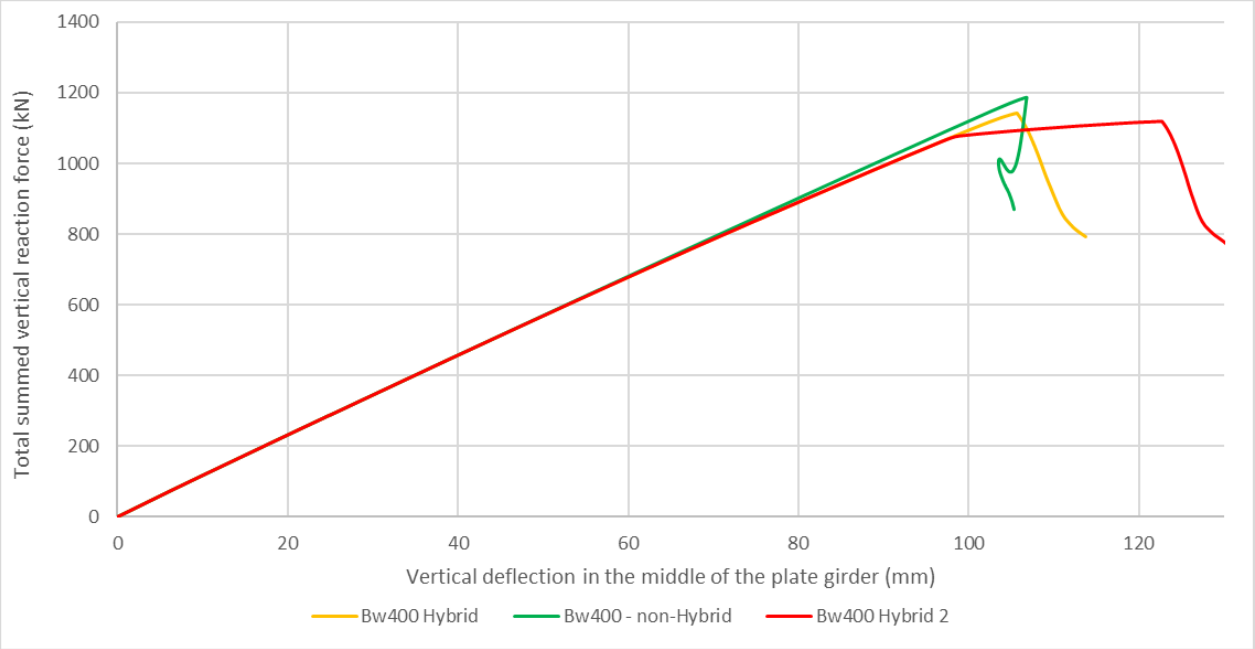

FIGURE 102: FORCE DISPLACEMENT DIAGRAM FOR 3 HYBRID BW400 GIRDERS WITH 6000MM2 TOTAL AREA

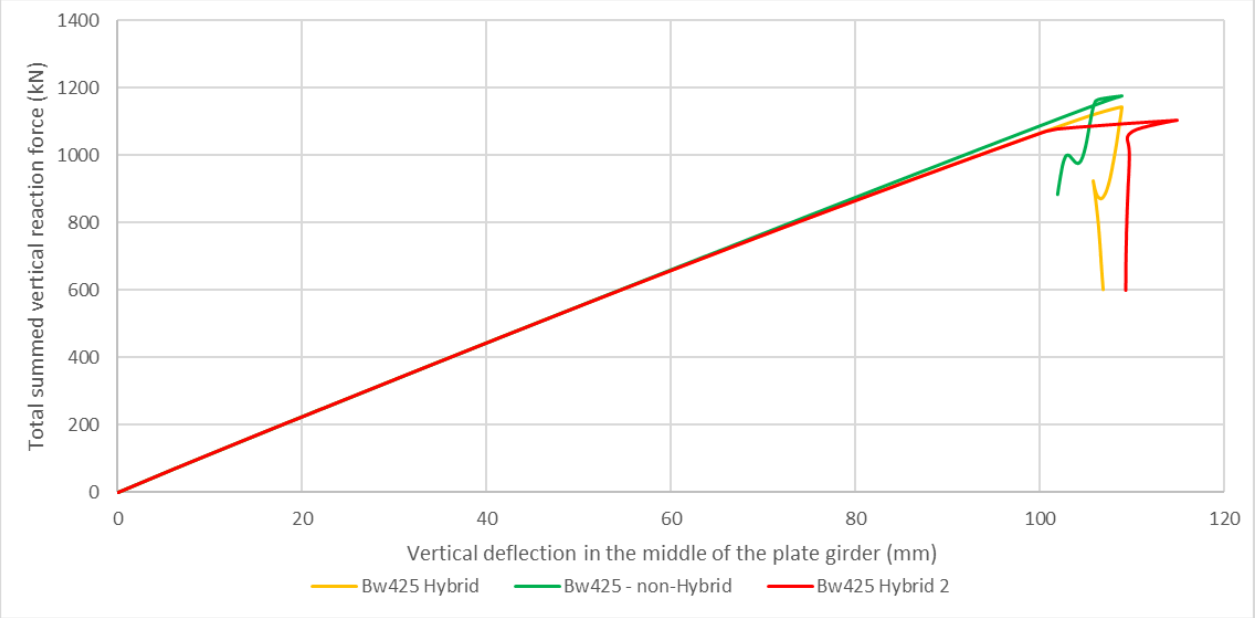

FIGURE 103: FORCE DISPLACEMENT DIAGRAM FOR 3 HYBRID BW425 GIRDERS WITH 6000MM^2 TOTAL AREA

4.6.5. Check on Imperfection modelling

4.6.5.a. Introduction

In the previous paragraphs the results of several analysis were given, in which it was shown that the imperfection applied initially had a large influence on the maximum bending capacity of the girder, when the web slenderness is higher than the slenderness in which the behavior changes. Using an imperfection showed an increase of bearing capacity after the slenderness limit which leads to a different failure mechanism. For S690 this limit was 625 and for S890 the limit was 425, which was also the slenderness with the highest bending moment capacity.

The results also showed the failure mode always involved the top flange of the girder failing, in the pre-limiting slenderness' this was after yielding, showing a rotation of the flange which let into a vertical buckle into the web. For a slenderness higher than the limiting value, this was a rotation of the top flange around the longitudinal axis.

Because of this seen phenomenon, the impact of the type of imperfection was chosen to be analyzed as well. In the previous paragraphs, if an imperfection was used, the shape was given by the first eigenmode, given in Figure 52. In this initial deflection-shape, the flange deflection was very limited, therefor it was chosen to use only the deflection of the flange and to amplify this to a certain angle of flange-rotation. This was performed for the first mode as well as the third eigenmode and also the impact of using only the web-part of the first eigenmode was analyzed. The flange-shapes are given on Figure 104 and Figure 105. The first mode is a 6-sin shape, the third mode a single-sin shape.

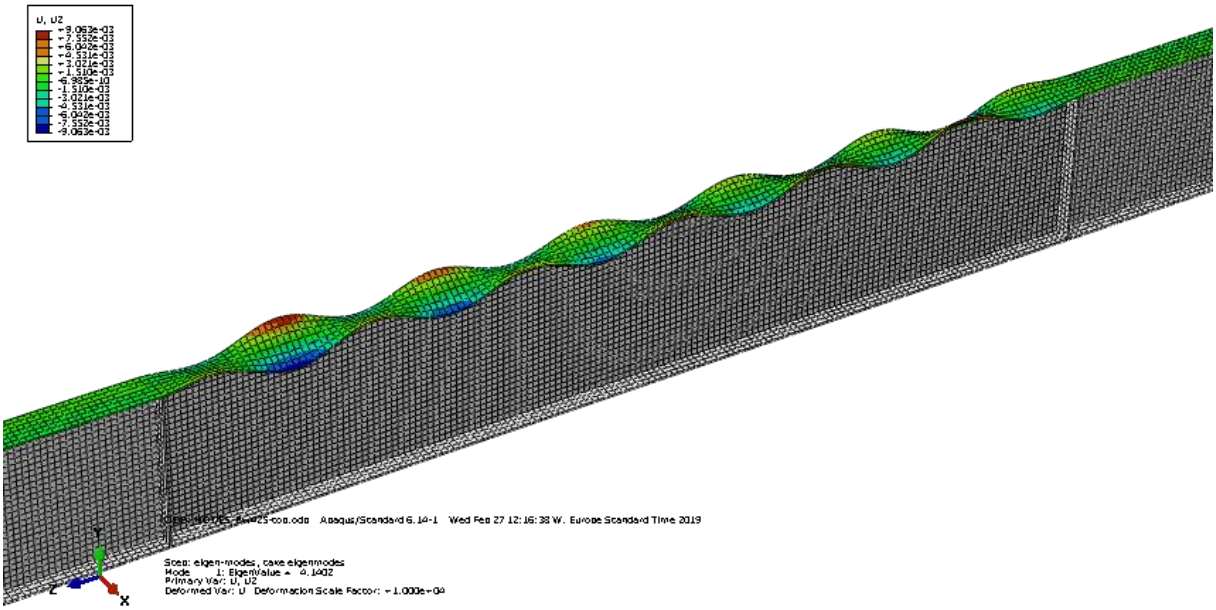

FIGURE 104: THE INITIAL IMPERFECTION FLANGE SHAPE OF THE FIRST EIGENMODE (LARGER THAN USED IN THE ANALYSIS)

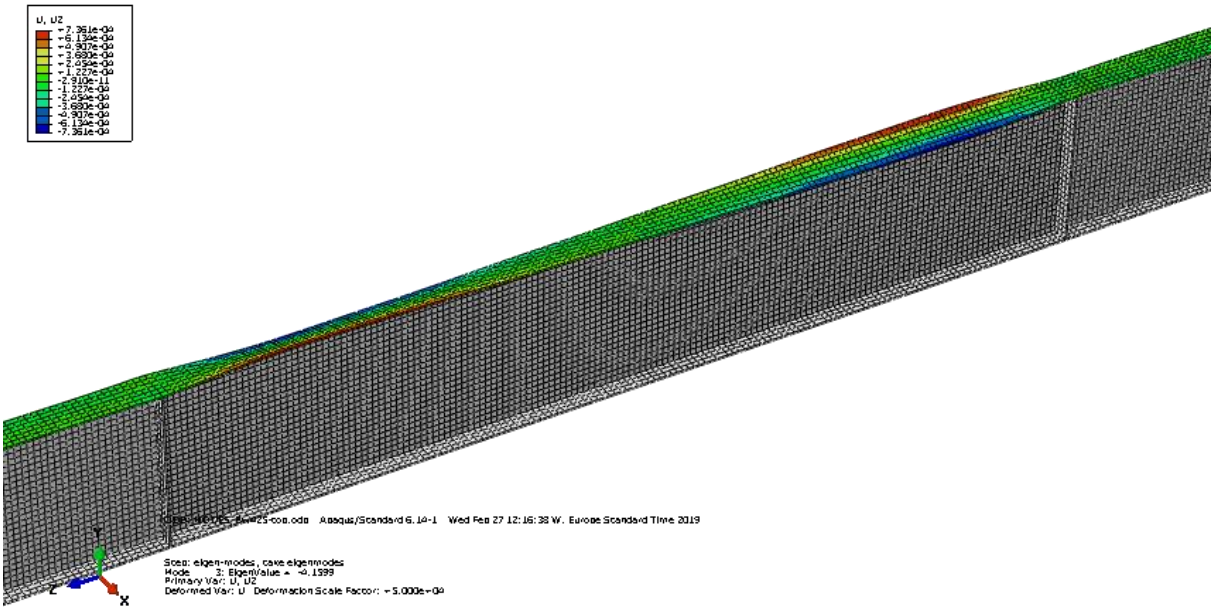

FIGURE 105: THE INITIAL IMPERFECTION FLANGE SHAPE OF THE THIRD EIGENMODE (LARGER THAN USED IN THE ANALYSIS)

The amplitude of the imperfection used in the previous paragraphs was based on the Eurocode in which 1/200 of the length or height of a panel is prescribed. Since the panels are very large, but the thickness is very small, it is not very realistic that these imperfections would in reality be found in a construction like this. Because the sin-shape is only visible in the top of the web, a better value would be 1/200 of half of the height, or to use the thickness of the steel-sheet used for the web. This is also analyzed and its results shall be described below.

In this paragraph 3 different girders are used to look into the effect of the imperfection shape, namely the S890 girders with web slenderness: 300, 425 and 700, to get insight on the effect on girders before-the-limit, on the limit and after the limiting value.

4.6.5.b. Results for web slenderness 425

The first results to be discussed are the results found using a web slenderness of 425, using S890 steel in all the sections of the girder. This slenderness was chosen to analyze because it yielded the highest maximum bending moment capacity in the parametric study on girders without initial imperfections.

For this test, the initial imperfection was chosen as a maximum angle in which the flange rotates around the longitudinal axis. This angle is given as a vertical deflection divided by the width of half the flange. The flange in this case was 200 mm wide, so an angle of $1/50^{th}$ results in 2 mm of deflection in the flange tips. The Eurocode advises to use $1/50^{th}$ as the rotation angle, but in this case more angles are analyzed. There resulting force-displacement diagram is given in Figure 106.

The difference between the analyses can be observed in the maximal summed reaction force, which is smaller for the girders with larger initial imperfections. For the girders with an imperfection amplitude of $1/200^{th}$ and $1/400^{th}$ the resulting curve is very much comparable to the result for the girder without imperfections.

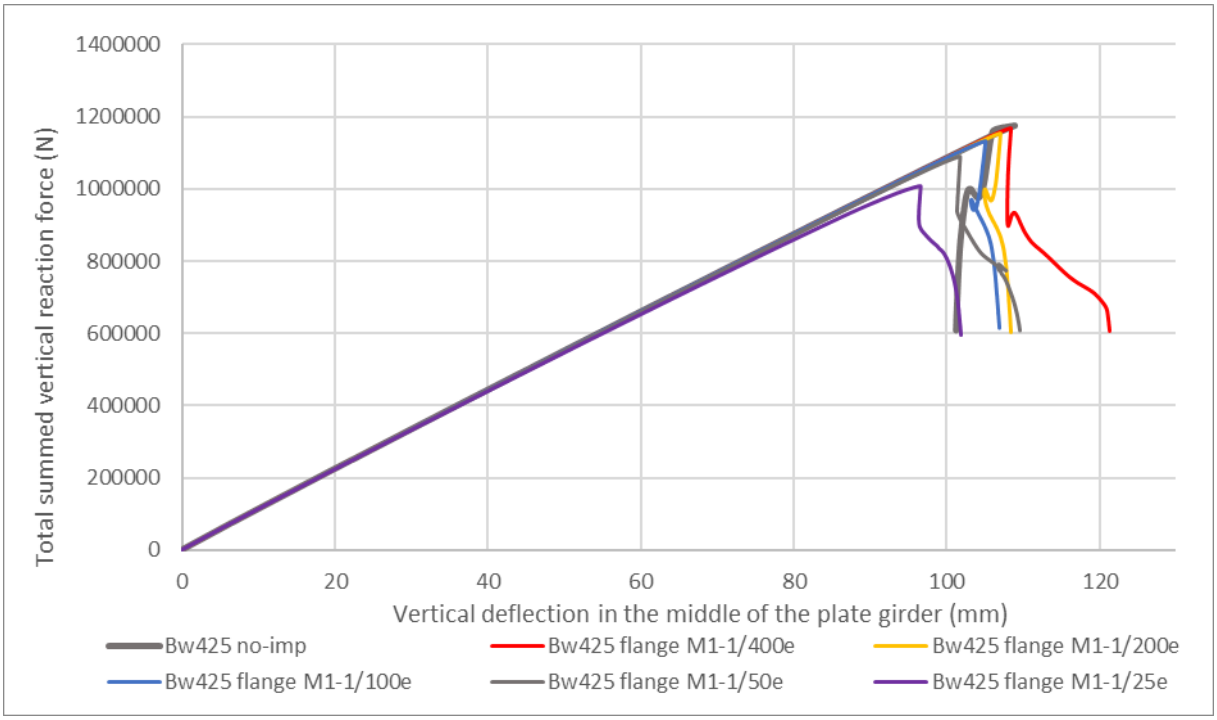

FIGURE 106: RESULTS OF SEVERAL ANALYSIS WITH AN INITIAL FLANGE IMPERFECTION SHAPE OF THE FIRST EIGENMODE

When the results of the other analysis are also shown it can be seen that an imperfection of the total first eigenmode, with an amplitude of the thickness of the web is identical to the result generated by the girder which had only the web-part of the imperfection of the first eigenmode. It can also be noticed that the impact of the amplitude of the initial flange imperfection for mode 1 and mode 3 is different. $1/50^{th}$ in mode 1 results in a larger decrease in comparison to the same amplitude using mode 3.

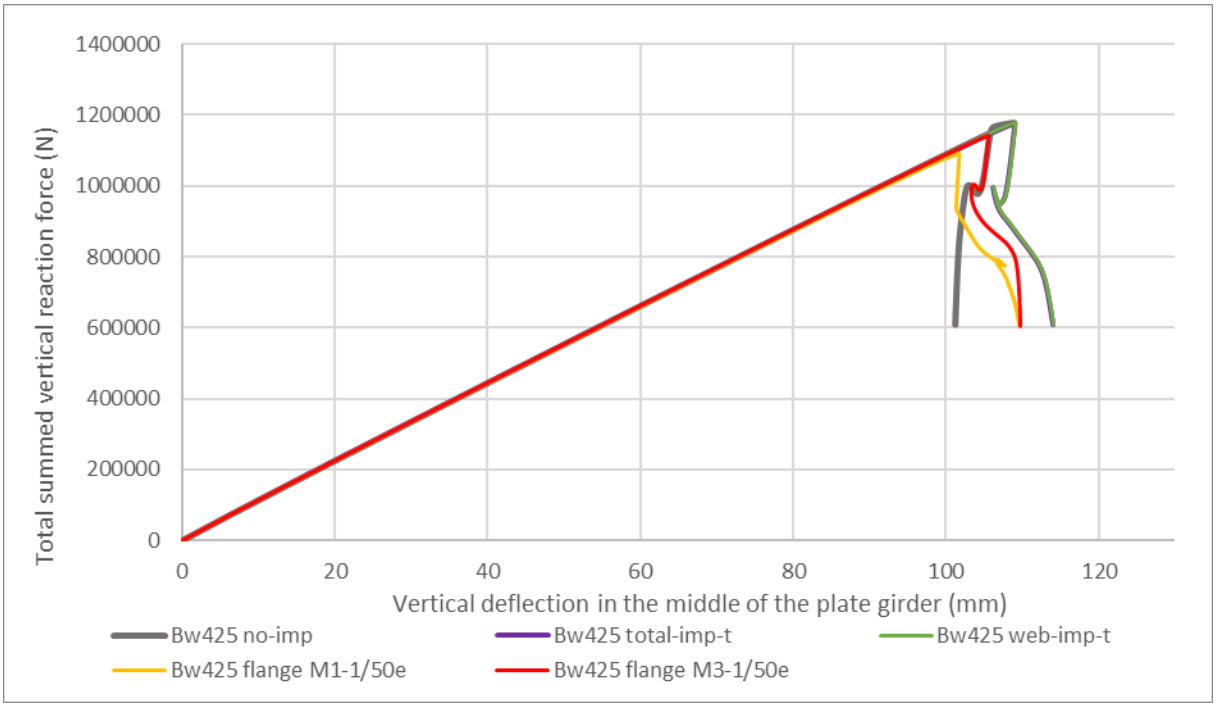

FIGURE 107: RESULTS OF SEVERAL ANALYSIS WITH DIFFERENT INITIAL IMPERFECTIONS

When the results are given in tabular for the results are easier to interpret, this can be found in Table 25. It has been divided in 3 parts, the first part showing the web and total mode 1 imperfection. The second part resembles the flange first mode results and the third part gives the results for mode 3 flange imperfections.

	Maximum moment	*Imperfection amplitude (mm)*	*Fraction of no-imperfection capacity (%)*
Bw425 no-imp	1627,6	0	100,00%
Bw425 web-imp-t	1626,2	2,17	99,91%
Bw425 total-imp-t	1626,2	2,17	99,91%
Bw425 no-imp	1627,7	0	100,00%
Bw425 flange M1-1/400e	1615,9	0,25	99,28%
Bw425 flange M1-1/200e	1597,0	0,5	98,12%
Bw425 flange M1-1/100e	1564,4	1	96,11%
Bw425 flange M1-1/50e	1506,6	2	92,56%
Bw425 flange M1-1/25e	1396,0	4	85,77%
Bw425 no-imp	1627,7	0	100,00%
Bw425 flange M3-1/100e	1624,5	1	99,81%
Bw425 flange M3-1/50e	1576,3	2	96,85%
Bw425 flange M3-1/25e	1530,9	4	94,05%

TABLE 25: RESULTS OF THE INITIAL IMPERFECTION ANALYSIS ON BW425 GIRDERS.

The results are also given graphically in Figure 72. Note that the graph had a y-axis which doesn't go all the way down to 0 kNm. The graph shows that the effect of the imperfection amplitude is more severe for the first mode, in comparison to the third mode. When the imperfection is 1 mm, the results of the third mode initial imperfection is almost identical to the mode without imperfections, while the first mode still has 4% less bearing capacity.

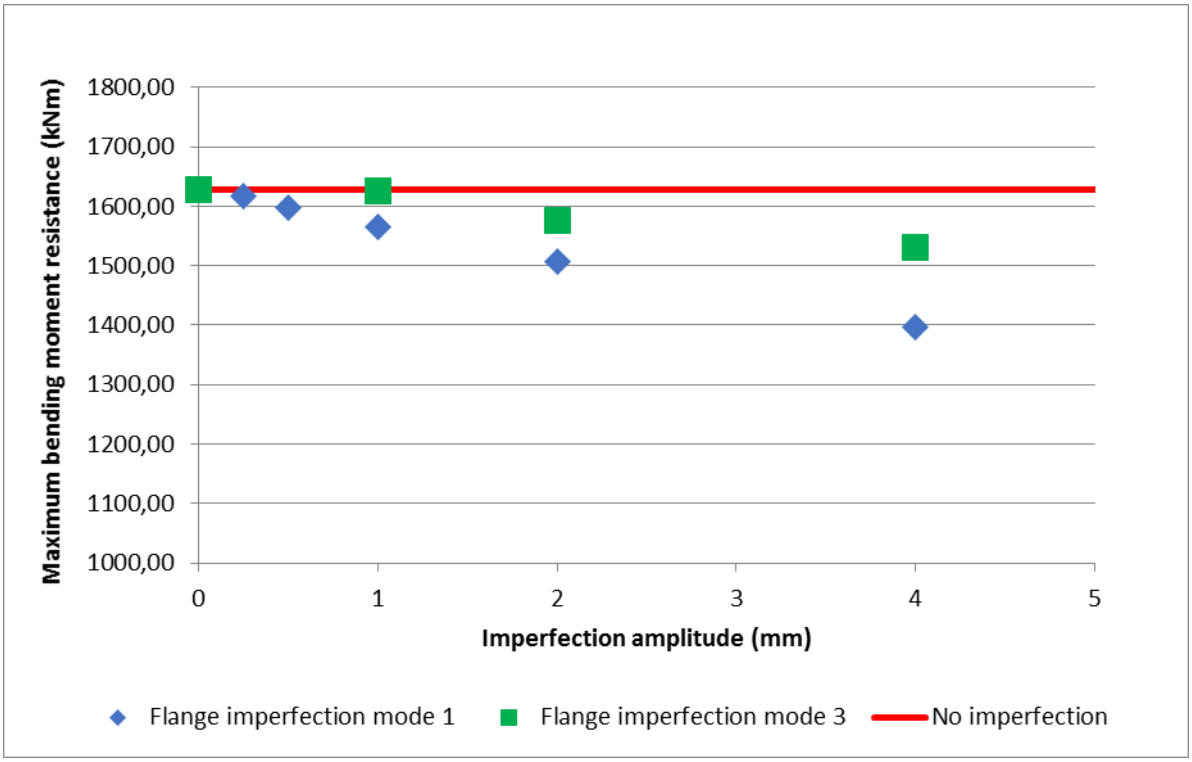

FIGURE 108: MAXIMUM BENDING MOMENT CAPACITY WITH DIFFERENT FLANGE IMPERFECTIONS

Looking at the failure mode of the tested geometries, the initial imperfection doesn't influence the mode of failure for the girders with a web slenderness of 425. The flange first yields, or in the case of the larger imperfections almost yields due to the fact that the stress doesn't run fully through the tops of the imperfect shape, this leads into a rotation of the flange, which after this buckles vertically. This can be seen on Figure 109, showing the non-uniform stress distribution in green in the flange on the top picture, were the red shows yielding steel. The deformation and failure mode are identical to the non-initially deformed girders, for example shown on Figure 82.

Looking at the results, the impact of the flange imperfection is noticed. It disturbs the uniform stress distribution of the top flange, leading into a lower capacity to bear bending moments. The reduction in capacity is however is not very large in the range of amplitudes which are likely to be encountered. The top flange is a strip of 200x10 mm. The first mode has 6 sin-shaped buckles over a length of 5531 mm, so the tops of 2 buckles are 5531/12 = 460 mm apart from each other. A prescribed rotation over the full length in Eurocode is $1/50^{th}$. A realistic rotation for this first mode shape is probably about 10% of this, so the results of $1/200^{th}$ and $1/400^{th}$ are more logical to use. These results only had a reduction of 1.9 and 0.7%. In this case the results for no imperfection are there for a good approximation for the real result, but this can't be generalized without checking other slenderness.

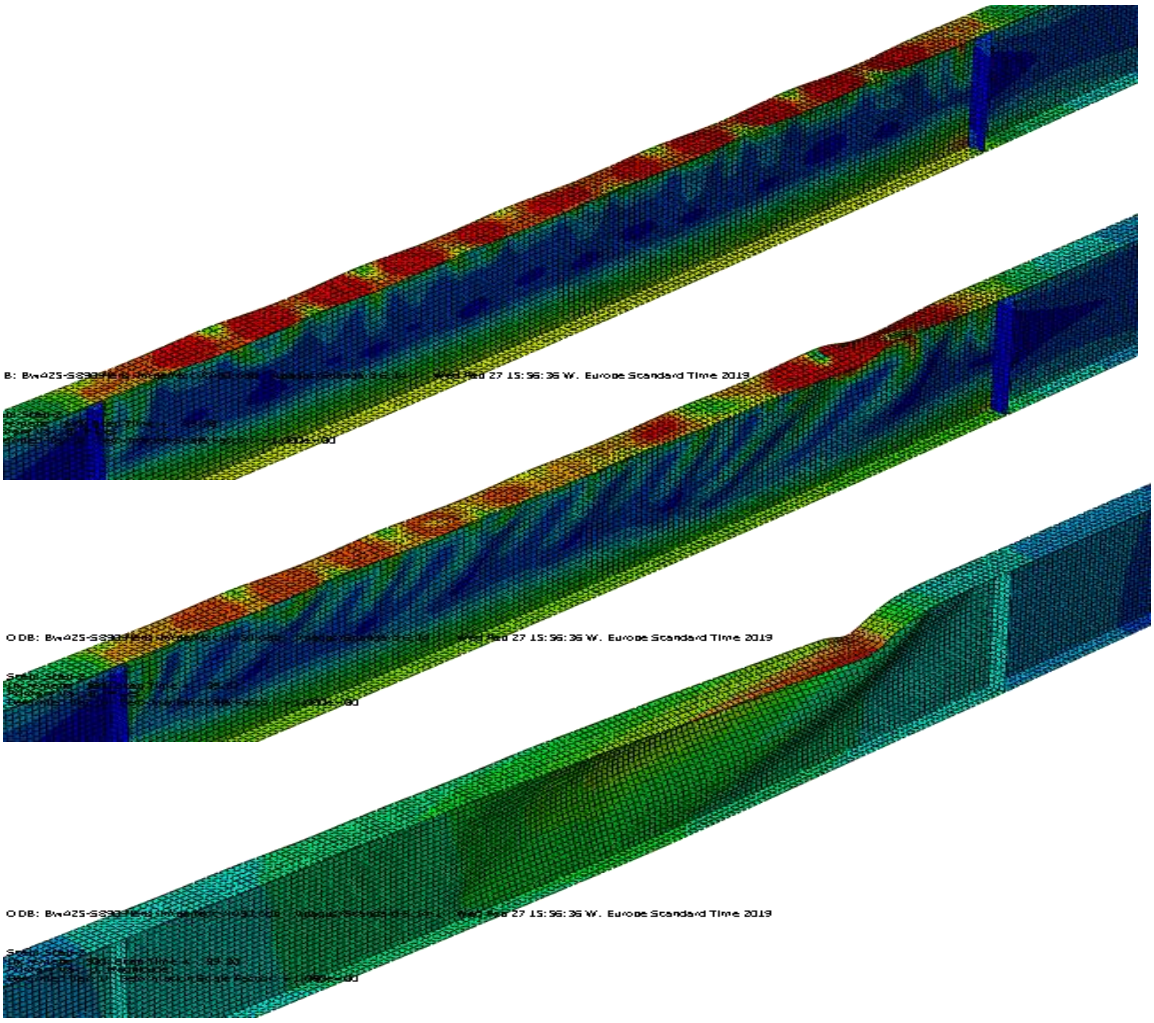

FIGURE 109: STRESS DISTRIBUTION AND FAILURE MODE OF A PLATE GIRDER WITH S890 STEEL AND FLANGE IMPERFECTION OF MODE 1

4.6.5.c. Results for web slenderness 300 and 700

The impact of imperfections should also be addressed in other geometries to be able to generalize the statement of imperfection impact. This is why the geometries of the plate girders with a web slenderness of 300 and 700 are also addressed. Because the difference of the full first mode in comparison to only the web-part was near to none, only the full first mode, with an amplitude of the web thickness will be addressed as well as only realistic values of the flange-part. In previous chapters the girder with a slenderness higher than the limiting value, failed by rotation of the full flange, therefor an extra flange-mode is used, this is mode 4, which describes a half sin shape over the length of the middle section.

Both the results for a slenderness of 300 and 700 are given in Table 26. It can be seen that for the girder with a slenderness of 300, the imperfections do not change the bearing capacity very much. The results are similar to the results in paragraph 4.4.2.b, showing a little increase in capacity for girders less slender girders compared to the limiting slenderness.

The top 2 results of the girders with a web slenderness of 700 also show similarities with the results found in 4.4.2.b, where the result of the imperfect girder of this paragraph is also shown, as the result of

model “Bw700 total-imp-1/200e” with an amplitude of a 200th part of the height of the girder. It can be seen that the smaller amplitude of the full first mode shape leads to a somewhat smaller, but still large increase of bearing capacity. The failure mode is the same as the one found in the previous paragraph, only the flange is not fully yielding this time before failure.

Looking at the flange-imperfection models, we see a small increase in the models were mode 1 and mode 3 were used as the shape of the flange imperfection. These models show only an increase of 1.4 and 2.7%, which leads to believe that the results for the non-initially imperfect model are valid and can be used for the full range of tested girders.

The forth eigenmode, which resembles the fail-shape of the girder, does not lead to a lower capacity, but increases the capacity significantly.

	Maximum moment	*Imperfection amplitude*	*fraction of no-imperfection*
Bw300 no-imp	1399,1	0	100,00%
Bw300 total-imp-t	1429,7	2,582	102,18%
Bw300 flange M1-1/200e	1392,8	0,5	99,55%
Bw700 no-imp	1413,3	0	100,00%
Bw700 total-imp-1/200e	2026,6	5,916	143,39%
Bw700 total-imp-t	1940,6	1,69	137,30%
Bw700 flange M1-1/200e	1433,2	0,5	101,40%
Bw700 flange M3-1/50e	1451,8	2	102,72%
Bw700 flange M4-1/50e	1882,0	2	133,16%

TABLE 26: RESULTS OF THE INITIAL IMPERFECTION ANALYSIS ON BW300 AND BW700 GIRDERS.

Looking at the failure mechanisms, the results can be categorized in 2 shapes, which were already found in paragraph looking into the effect of the imperfection previously. The mechanisms in which the bearing capacity increased significantly, show a failure mode comparable to the bottom picture of Figure 76, with the flange buckling vertically into the web. The no-increasing models show a failure mechanism looking like the top picture of Figure 76, showing a bulged-out web and a rotated flange over the full length of the middle section.

4.6.6. Influence of the length of the middle section

Using the equations to model the geometries of the girders, leads to models which have different lengths of end and mid-sections. To be able to address the bearing capacity of plate girders in general, the influence of the length of the beam has to be taken into account. Because the end-panels are in all geometries over dimensioned and the girder always fails in the middle-section, the influence of the middle-section length will only be looked into.

Figure 110 shows the geometry of the tested girders. The end panels are kept the same as in the original models, the length is 3 times the height. The middle panel was 6 times the height in the original tested geometry, but will in this test be the changing variable.

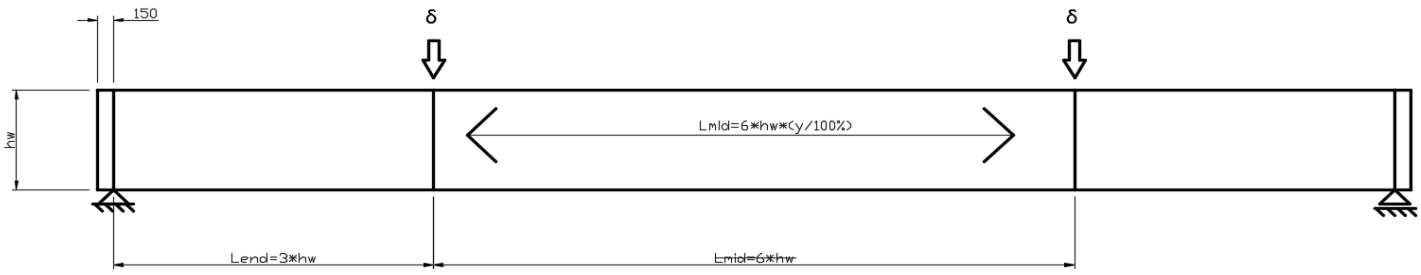

FIGURE 110: GEOMETRY OF THE TESTED PLATE GIRDERS

4.6.6.a. Models with varying middle-section lengths

To be able to address the influence several models were constructed to find if the length of the middle-section made the plate girders behave differently form the girders found in the different parametric studies. For this analysis again the girders with S890 steel and a total cross-sectional area of 6000 mm^2 were used as the base. All models use no initial imperfection in these analyses.

As was done with the imperfection analysis in the previous paragraph the web slenderness of the analyzed girders was 300, 425 and 700, to try and give a view over the full width of the analyzed spectrum of geometries.

In paragraph 4.4.2 we found the bending moment capacity of the girders increasing, with increasing web slenderness until the web slenderness reached 425. In the force displacement diagram the shape of the resulting curve changed from a straight, linear-elastic line, with a sudden drop due to failure before the 425-web slenderness was achieved, to a straight line, followed by a loop and then failure. The results of the analysis are given in Figure 111, Figure 112, Figure 113 and Table 27.

Girders with a web slenderness of 300

It can be seen on Figure 111 that the influence of the length in the girders made with a slenderness of 300 does not result in lower bearing capacity, because the distance between the part where the displacement is applied and the support is kept the same. The force-displacement curves are different. The stiffness of the longer girders is lower, because the middle-section is longer. The applied moment, the moment of inertia and the material properties stay the same, therefor the deflection is larger in the middle. It can be seen that the top of all 3 girders is nearly on the same height, which leads to the same maximum bending moment.

This bending moment is around 1400 kNm for the three models, which is nearly identical to the plastic moment capacity if only the flanges would be taken into account. The mode of failure for all the girders is the same for all 3 girders and comparable to the failure mode found in paragraph 4.4.2 on Figure 70.

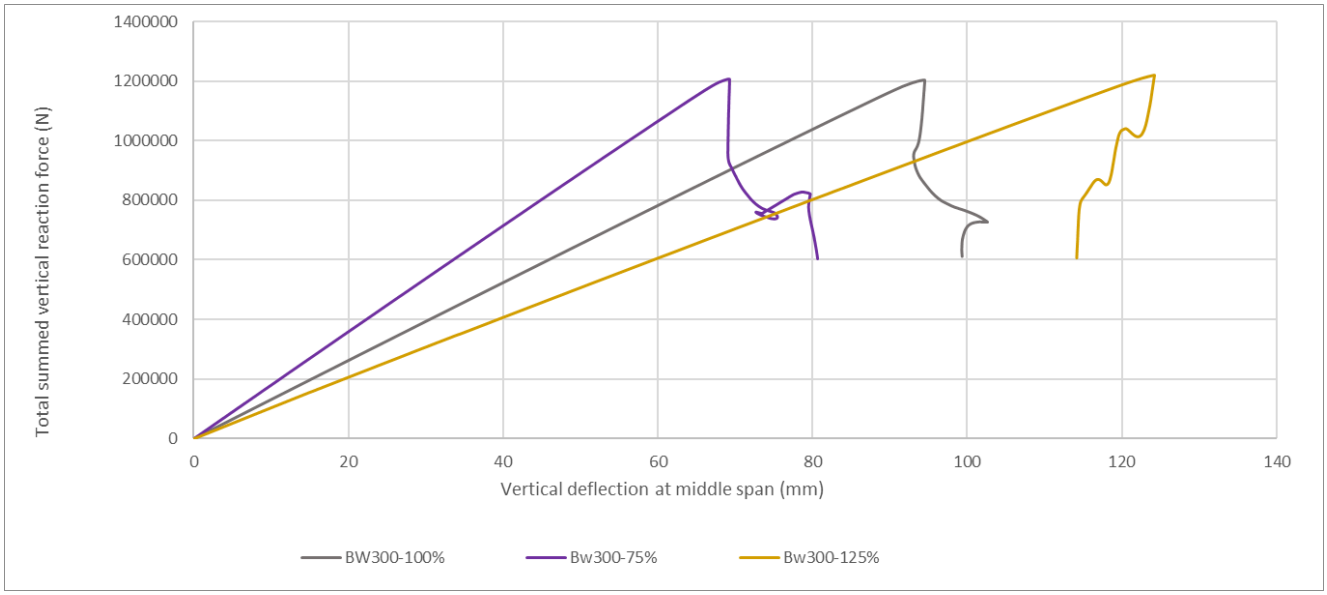

FIGURE 111: LOAD DISPLACEMENT DIAGRAM FOR 3 BW300 MODELS

Girders with a web slenderness of 425

Figure 112 shows the results of the models with a slenderness of 425 for the web, in which the original curve is the green line, showing the little loop mentioned before. This graph shows significant changes for the different length of the middle section. With a shorter panel, the bearing capacity does not increase significantly, but increasing the length by 25%, gives a decrease of bending moment capacity of 10%. This model, when looking at the failure mode, shows also different behavior to the original model.

In the original model yielding of the flange was seen, which could also be seen in the shorter model. But the model with an extra 25% length didn't achieve yielding, but failed prior to it. The failure mode was found to be similar to the one given on Figure 71.

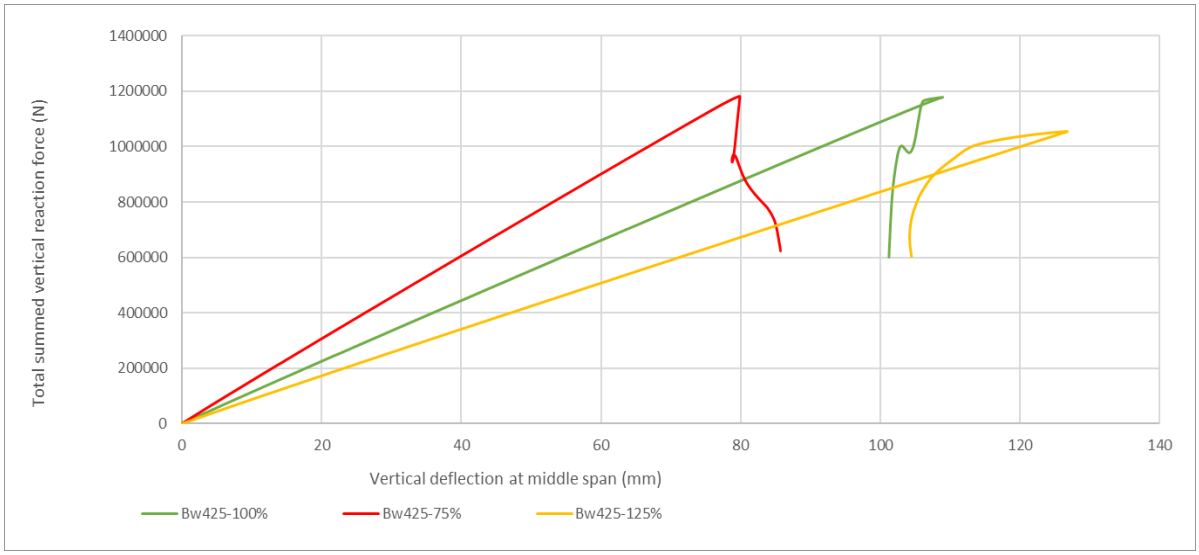

FIGURE 112: LOAD DISPLACEMENT DIAGRAM FOR 3 BW425 MODELS

Girders with a web slenderness of 700

The results given in Figure 113 show the results for 3 girders with a web slenderness of 700 and show 2 different shapes. The 100% and 75% girder show a loop, the 50% girder show a similar path as all the girders with a 300-web slenderness. In this case the top flange was also yielding and, looking at the table, shows this girder almost reaching the capacity of the plastic flange moment, increasing the outcome of the FEM-analysis compared to the longer, original beam by 42%.

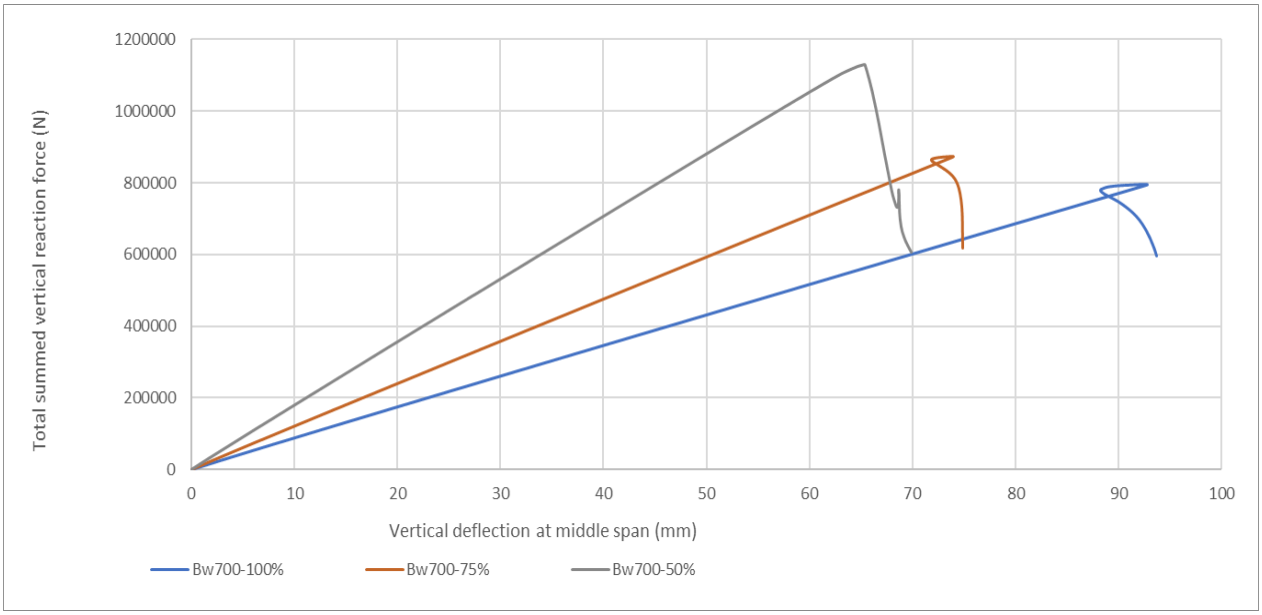

FIGURE 113: LOAD DISPLACEMENT DIAGRAM FOR 3 BW700 MODELS

Slenderness	*Length (%)*	*Length (mm)*	*Moment (kNm)*	*Percentage of M-original (%)*	*Percentage of M-flange (%)*
300	*M-flange*		*1378,8*	*99%*	*100%*
300	*100*	4647,6	1399,2	100%	101%
300	*75*	3485,7	1401,3	100%	102%
300	*125*	5809,5	1417,7	101%	103%
425	*M-flange*		1641,1	101%	100%
425	*100*	5531,7	1627,7	100%	99%
425	*75*	4148,8	1633,3	100%	100%
425	*125*	6914,7	1460,7	90%	89%
700	*M-flange*		2106,1	149%	100%
700	*100*	7099,3	1413,4	100%	67%
700	*75*	5324,5	1552,7	110%	74%
700	*50*	3549,6	2004,9	142%	95%

TABLE 27: RESULTS OF THE MIDDLE-SECTION LENGTH ANALYSIS ON BW300, BW425 AND BW700 GIRDERS.

4.7. Analysis of the extra investigations

4.7.1. Hybrid structures

Looking at the force displacement diagrams of all the tests done in the first parametric studies, we find that the girders made from S690 and S890 steel don't behave ductile when failure sets in. We see the curves rapidly decreasing after the maximum summed reaction force is achieved. Looking at the curves of the S690 plate girders in the parametric study, we see some flattening in the curves with a web slenderness of 300, but with higher slenderness, this isn't the case anymore, the curves of all the S890 girders show sudden failure.

For safety reasons this is not ideal behavior, because the construction doesn't show the limits of its capacity are nearly met. When a little extra load is added sudden failure sets in and it will be too late to evacuate. Ductility would in this case be an extra buffer to show the construction is nearly at its capacity. To be able to get ductility, the limiting slenderness can be lowered, probably leading to a plateau in the force displacement behavior, but also dramatically decreasing the bending moment capacity.

In 4.6.4 we found that using a hybrid composition in the girders could lead to less sudden failure. This happened in the girders composed of a S890 top flange, a S690 bottom flange and a S460 web. Increasing the applied bending moment resulted in yielding of the bottom flanges, before the top flange had reached its elastic limit. When this happens, the deflection increases largely, but failure doesn't set in immediately. Using this specific hybrid composition reduced the bending moment capacity by only 3-6%, compared to the fully S890 composition.

4.7.2. Imperfection modeling

The results found in paragraph 4.6.5 show that the influence of the modeling of the initial imperfection influences the results found when looking at the maximum bending moment capacity. The capacity of the plate girder with a web slenderness of 425 is reduced when the flange imperfection is applied. This result is also found when introducing a flange imperfection to a 300 web slender girder. Looking at the magnitude of this reduction in Figure 108, it can be seen that only with a relatively large imperfection the influence is significant. Eurocode gives a value for the amplitude which should be used, which is 1/50 of the length of the deformation. Since the 1st mode has 6 buckles, the shape has 12 half sin lengths over the middle section. Therefor the amplitude used should be 1/12 of 1/50 = 1/600 of the length of the middle section. For mode 3 this is 1/100, because a single sin shape has 2 lengths. The reduction for these values of amplitude are less than 1%. Because of this outcome, the results of the parametric study are shown to be of a good approximation for the real behavior of steel plate girders, certainly for girder with a less slender web compared to the maximum web slenderness found in the parametric studies.

The paragraph also shows that the introduction of an initial imperfection in a girder, independent of the shape of this imperfection, with a web slenderness of 700 increases the capacity rapidly, which was also found during the parametric studies for girders with a high slender web. Therefor it can be concluded that, for the girders with a more slender web compared to girder with the highest bending capacity, a perfect geometry, without any initial imperfections, gives a good approximation for its bending moment resistance.

4.7.3. Length of the middle section

4.7.3.a. Introduction

The results found in paragraph 4.6.6 show a dependency between the length of the middle section of the plate girder and there bending moment capacity, as well as the length having an influence on the mode of failure. The table shows the capacity of the original tested girders (100% length) and the different other girders. It can be seen that limiting the length of the middle section in a girder with a web slenderness of 700 results in a much higher bending capacity. Making the middle section longer in a 425 web slender girder can result in a lower capacity, but making it shorter is does not change the capacity.

The given results found by addressing the length of the middle-section of the girder show that the results found in the parametric studies do not necessarily show the ultimate bending moment capacity for all long, unstiffened slender plate girders, but only for a specific range of geometries. The results in the table above show, when a different mid-section length was used, a girder with a web slenderness of 700 could have a larger bending moment capacity than the earlier found maximum of a girder with a web slenderness of 425.

4.7.3.b. Comparison to the set geometry

Looking at paragraph 4.5, which addressed the geometries tested in the parametric studies, it looks like a general maximum web slenderness can be pointed for all steel grades. These tests however haven't addressed the length of the middle section of the plate girders, in which a constant moment is present.

When the results of paragraph 4.6.6 are addressed we see that a plate girder with a steel grade of S890 can also transfer a much larger bending moment, when the middle section of the plate girder is shorter. Also, it can be seen that the bending moment capacity for a plate girder with the found the maximum web slenderness of 425, is much lower when the middle section is longer.

The impact of the middle section length is only addressed for 3 web slenderness' with the use of S890, but the results show a dependency of the bearing capacity related to the length of the middle section. When the middle section gets longer, at some point the failure mode changes from the vertical flange buckling mode, to a failure mode in which the top flange rotates over the full length of the middle section, before the top flange material achieves the yielding stress.

We found that the maximum bending moment capacity for a plate girder in S690 and S890 is reached, when the top flange yields. When this happens, vertical flange buckling occurs and sudden failure occurs. In these cases the flange force can be calculated using (4.5).

$$F_{fl} = A_{fl} * f_y \tag{4.5}$$

For all the tested girders with a constant total area this maximum flange force is the same. Because it looks like the flange behavior leads to failure, we'll try to describe the behavior using the relative slenderness of the flange. The flange is supported by the web in the y-direction, therefor it is more logical to address the transvers stiffness of the flange. This can be calculated using equation (4.6)

$$I_{trans} = \frac{1}{12} * {b_f}^3 * t_f \tag{4.6}$$

The relative slenderness, can be calculated using equation (4.7) and will be calculated using the critical stress found by using the equation proposed by Basler for torsional buckling. This has been given in equation (4.8), using the r, which is the radius of gyration, from (4.9).

$$\lambda_{rel} = \sqrt{\frac{f_y}{\sigma_{cr}}} \tag{4.7}$$

$$\sigma_{cr} = \frac{\pi^2 * E}{\left(\frac{l_{buc}}{r}\right)^2} \tag{4.8}$$

$$r = \sqrt{\frac{I_{trans}}{A_{fl}}} = \sqrt{\frac{1/12 * {b_f}^3 * t_f}{b_f * t_f}} = \sqrt{1/12 * {b_f}^2} = \frac{b_f * \sqrt{3}}{6} \tag{4.9}$$

Because the radius of gyration is a constant, when the flange dimensions don't change, we find that the critical stress is only dependent on the length of the flange. When we assume the connection between the flange, web and transverse stiffener is a fixed connection in the transverse direction, we can use half of the flange length to describe the buckling length, we find that the buckling length is described using equation (4.10), because in the used geometry the length of the middle section was always 6 times the height of the girder.

$$l_{buc} = \frac{1}{2} * l_{mid} = 3 * h_w \tag{4.10}$$

If we introduce the found maximal web slenderness' from the parametric studies by Abspoel and the parametric studies done on S690 and S890 steel we find the following values for the critical stress and relative slenderness, given in Table 28 and Table 29. The tables show the critical stress being almost equal to the yield stress of the girders, therefor the relative slenderness for all girders is close to 1.

A=6000 --> R = 57,73MM					
STEEL GRADE	β_w	h_w	L_{buc}	σ_{cr}	λ_{rel}
S235	1450	1702,94	5108,82	264,70	0,94
S355	1076	1466,97	4400,91	356,71	1,00
S460	850	1303,84	3911,52	451,55	1,01
S690	525	1024,70	3074,09	731,08	0,97
S890	425	921,95	2765,86	903,10	0,99

TABLE 28: RESULTS OF THE FOUND MAXIMUM WEB SLENDERNESS USED IN THE GIVEN EQUATIONS FOR A = 6000MM^2

A=12000 --> R = 81,65MM					
STEEL GRADE	B_w	h_w	L_{buc}	σ_{cr}	λ_{rel}
S235	1450	2408,32	7224,96	264,70	0,94
S355	1076	2074,61	6223,83	356,70	1,00
S460	850	1843,91	5531,73	451,54	1,01
S690	525	1449,14	4347,41	731,07	0,97
S890	425	1303,84	3911,52	903,08	0,99

TABLE 29: RESULTS OF THE FOUND MAXIMUM WEB SLENDERNESS USED IN THE GIVEN EQUATIONS FOR A = 12000MM²

4.7.3.c. Influence of the flange geometry

When we look at the results from paragraph 4.6.3, we find that the moment capacity of the girders with a different flange geometry lost some of their capacity in comparison to the girders with the flanges with a slenderness of 20. Looking at the equations it can be seen that a flange of 200x10 mm has a larger transverse bending stiffness than a flange with an area of 146.5x13.6 mm. The transvers stiffness of the original 6000 mm^2 flange is $6.67*10^6$ mm^4, the stocky flange has a stiffness of $3.54*10^6$ mm^4, reducing it by 47% and therefore limiting the r from 57.73 to 42.06.

Above mentioned equations and the results of the tests with a different flange geometry show a dependency of flange dimensions and yield strength of the steel to the maximum length of the flange in compression. Using the equations, a maximum length to achieve yielding in the top flange, using a specific flange in a specific steel grade could be found. This equation is given in equation (4.11)

$$\lambda_{rel} = 1, \quad \sigma_{cr} = f_y, \; f_y = \frac{\pi^2 * E}{\left(\frac{l}{r}\right)^2}, \; l_{\max} = \sqrt{\frac{\pi^2 * E * r^2}{f_y}}, \; \text{with } r = \sqrt{\frac{I_{trans}}{A_{fl}}} \qquad (4.11)$$

When we look at the results from the analyses in paragraph 4.6.6, we should add some remarks. Looking at table 27, we see the length of the mid-sections of the girders with a web slenderness 300 being 3485 mm, 4647 mm and 5809 mm. The steel grade is S890, which would lead to a maximum flange length of 5572 mm. The table shows that the longest girder still has no reduction in the bending moment capacity, which in terms shows the flange yields before failure. This girder has a relative slenderness of 0.96, which could also be just enough to resist flange rotational failure.

Looking at the girders with a web slenderness of 700, having a mid-section length of 7099mm, 5324mm and 3549mm, we see that only the shortest girder comes close to the flange moment (95%), having a relative slenderness of 1.570. The 75% length girder, with a mid-section length of 5324mm, has a relative slenderness of 1.046, but has a bending moment capacity, which is not close to the plastic moment capacity of only the flanges, with 74% of this capacity. For the 425-web slender girder, we see that the capacity is maximized when the mid-section is smaller or equal to the original length of 5531mm. The capacity reduces to 90% when the mid-section is 6914mm long.

Since the range of the study on mid-section length was only very small, we can only conclude that there is an influence on the bending capacity of the girder by the web. The girders with a web slenderness of 300 had a web which is 2,58 mm thick and 776 mm high, the 425 girders has a size of 2,17x922mm and

the 700 girders 1,69 x 1183mm. With the analysis done, we cannot conclude if the slenderness, the thickness or the height has the largest influence. We can change the equation for the critical stress to address this unknown influence see equation (4.12) in which c_1, c_2, c_3 and c_4 are unknown describing the influence of the height and the thickness of the web.

$$\sigma_{cr}(h_w, t_w) = \frac{\pi^2 * E}{\left(\frac{l}{r}\right)^2} * \left(\frac{(h_w * c_1)^{c_2}}{(t_w * c_3)^{c_4}} \right) \tag{4.12}$$

4.8. Conclusions

4.8.1. Introduction

In this paragraph the results of all the numerical modelled analysis are combined and discussed. The paragraphs in which the results of the parametric studies (paragraph 4.5) and the paragraph discussing the extra investigations (paragraph 4.7) will be the input for these conclusions.

4.8.2. Failure mechanism

In the previous chapter, looking at only the implicit dynamic analysis results there has been 2 failure modes found, which describe the behavior of the slender steel plate girders tested in pure bending.

4.8.2.a. Limiting factors

The first failure mode was found in girders having a web slenderness which is equal or less than the girder in which the maximum bending moment capacity was found, when looking at the set geometry used in the parametric studies. For S690 the limiting slenderness of 525 was found and for S890 the limiting slenderness is 425. Looking at paragraph 4.7 it can be concluded that girders with the top flange having a relative slenderness smaller than 1 will fail in the first failure mode, which is described as top flange yielding.

More slender girders, compared to the limiting girders or with a higher relative flange slenderness, experience another failure mode, in which the top flange rotates around the longitudinal axis. The exception to this claim is when an initial imperfection is used in the girders with higher slenderness' or a lower relative slenderness. The numerical analysis showed these girders also experience top flange yielding prior to failure.

4.8.2.b. Failure mode description

The behavior for the girders experiencing the top flange yielding mode, can be described as failure after the yield stress is achieved in the compressed top flange. After yielding a top flange rotation was noticed, leading into the top flange vertically collapsing into the web of the girder. This behavior is described in more detail in paragraph 4.4.2.a and on Figure 70.

In more slender girders the other, top flange rotational, failure mode was found. These very slender girders fail prior to yielding. The top flange experiences instability and rotates around its longitudinal axis, after this the web bulges out and the bearing capacity is lost. This behavior is visualized on Figure 71.

4.8.3. Maximum bending moment capacity

The goal of this work is to optimize the placement of the material in the cross section. As limitation the ratio between the area of the flange and the area of the web was kept 1.0, which was also used in the work of Abspoel and Cimpoi.

The parametric study supplied data to form a conclusion about the maximum bending moment capacity for S690 and S890 steel using a total area of 6000 and 12000 mm^2.

4.8.3.a. Bending moment capacity using the set geometry

Looking at Figure 91 and Figure 92 we see that the maximum bending moment resistance for plate girders in bending increase when the yield stress of the used steel in increased. When the geometry found in Figure 18 is used we find that the maximum bending moments for the tested steel grades are given in Table 20, which also shows the efficiency of the steel. This shows how much capacity is generated per square millimeters of steel. It can be concluded that the maximum capacity is increased with an increasing yield strength. It can also be shown that this increase is similar to the following equation: $\% \approx \frac{1}{\varepsilon} = 1/\sqrt{\frac{f_{y.S235}}{f_y}} = \sqrt{\frac{f_y}{f_{y.S235}}}$, which shows a square rooted increase. The table also shows the increase in steel yield strength, which is linear compared to the increase in bearing capacity

	A=6000 mm^2						A=12000 mm^2			
Fy	Bw	Mu	Nm/mm^2	%	1/eta	Fy/235	Bw	Mu	Nm/mm^2	%
S235	1450	822,4	137,07	100%	1,00	1,00	1450	2357,4	196,45	100%
S355	1076	1068,5	178,08	130%	1,23	1,51	1076	3025,9	252,16	128%
S460	850	1220,3	203,38	148%	1,40	1,96	850	3495,4	291,28	148%
S690	525	1438,8	239,80	175%	1,71	2,94	525	4023,2	335,27	171%
S890	425	1627,7	271,28	198%	1,95	3,79	425	4550,9	379,24	193%

TABLE 30: EFFICIENCY OF THE STEEL IN THE SET GEOMETRY FOR 5 STEEL GRADES

4.8.3.b. Influence of the length of the middle section

Paragraph 4.7 shows the influence of the length of the middle section. The analytical models show a decrease in bending moment capacity, when the relative slenderness of the flange gets larger than 1. We can conclude that table 30 is therefor only valid for a length of the middle sections smaller or equal to the length which were tested during the parametric study. For longer spans the capacity of the flange is less than the yield stress, therefor reducing the maximum bending moment resistance.

On the other hand, a more slender plate girder, with a smaller span could have a higher bending moment resistance than the maxima given in the table, if its relative flange slenderness is kept below 1.

4.8.3.c. Influence of the web and flange dimensions

The influence of the flange dimensions are present in the relative slenderness of the flange. Reducing the transvers stiffness of the flange, will reduce relative slenderness and could result in a reduced maximum bending moment resistance if the critical flange length is exceeded. The influence of the web thickness could not be quantified from the results of the analysis, although the results found in table 27 show there is a significant influence.

Using equations (4.7) to (4.10) with a constant flange geometry it is possible to calculate the critical buckling stress of the flange for every buckling length, this is shown for the used flange geometries in Figure 114. This graph is an assumption, which does not contain the influence of the web thickness. The bullets in the figure show the numerical model results for the maximum bending moment resistance using there yield stress as y-coordinate. The graph shows a very good similarity between the calculated dotted line and the numerical results. The span between the points of force application is double the critical buckling length.

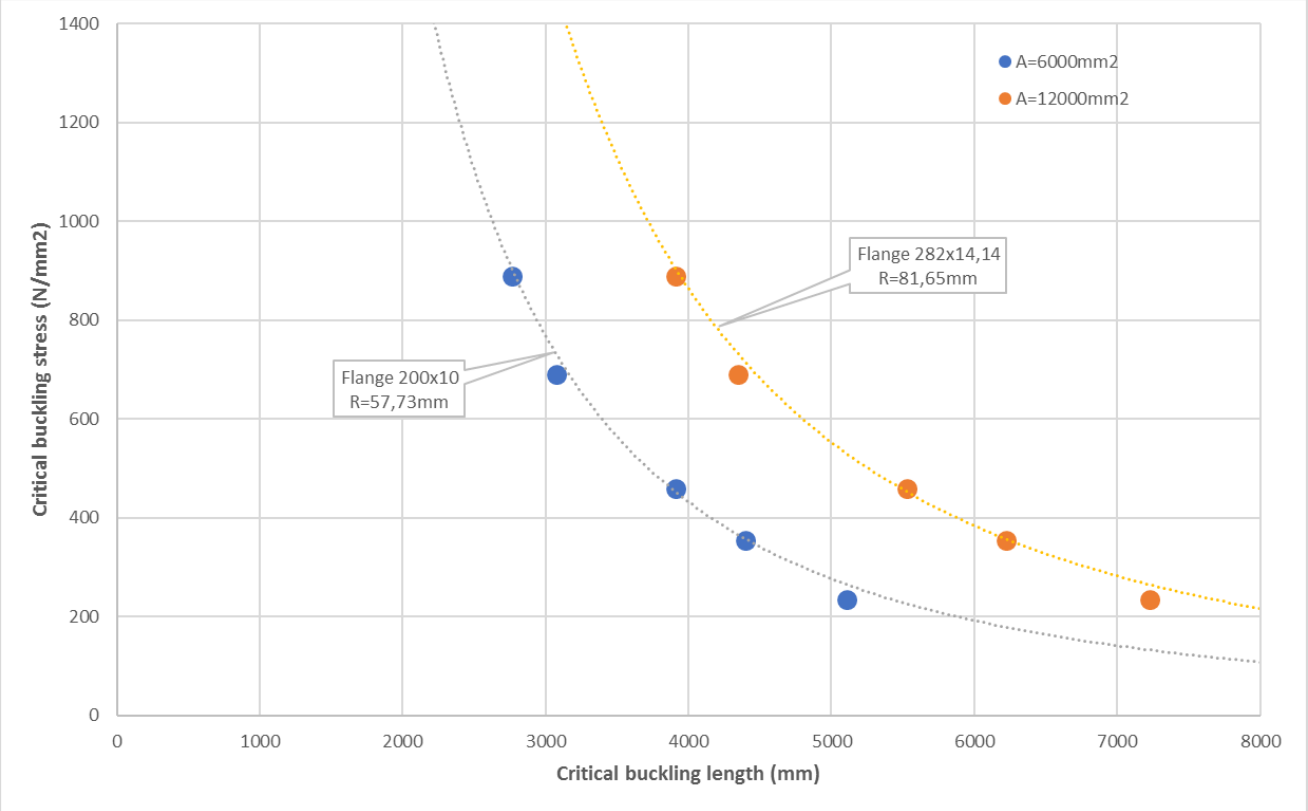

FIGURE 114: ASSUMED BUCKLING LENGTH FOR ANY CRITICAL BUCKLING STRESS, WHEN THE FLANGE GEOMETRY OF THE PARAMETRIC STUDY IS USED

The graph does not say anything about the moment capacity, because the distance between the flanges is the most important parameter in the bending moment capacity. It cannot be said that all the points in the graph are achievable, because the web slenderness was seen to have a significant influence.

4.8.3.d. Using a hybrid composition in plate girders

Decreasing the steel grade in less important parts of the cross section results in a lower bending moment capacity, it is there for not interesting to use lower grade steel when only the maximum bending moment capacity is concerned. The results of the parametric study showed sudden failure, in which almost no warning of the material could be seen. The use of a hybrid composition has the potential to be promising with respect to this ductility question, leading to a potentially safer solution. The small scale test, described in paragraph 4.6.4, showed more ductility when using S460 in the web and S690 steel in the bottom flange.

4.8.4. Comparison to hot rolled sections

The discussion about the benefits of using steel plate girders to reduce the consumption of steel in comparison to using hot rolled steel sections, has been started in the introduction of this work. In this paragraph the comparison is made using the maximum bending moments found during the parametric studies. The comparison will be done using the girders made from a total cross sectional area of 6000 and 12000 mm^2, which will be compared to IPE girders, with the same steel grade and for comparison to more common steel grades S235 and S355.

The modelled girders were tested on a 4-point bending setup, in which the tested area only experienced bending. The comparison will be conducted only on bending moment capacity. It is shown in the two tables of below in table 30 and Table 32. The capacity of the 6000 mm^2 girders can be compared the best to an IPE 500 girder with the same steel grade, which has 48200 mm^2 total area and consumes 7 times more steel per unit length. If the S890 girder with a slenderness of 425 is compared to a S235 steel IPE-girder, the standard IPE girders are not able to achieve this capacity, but a HEB 650 girder can. This section has an area of 210600 mm^2, which is 35 times more than 6000.

The efficiency of the material in girders, in bearing the applied bending moment is also given. The table shows the placing of the steel in the hot rolled sections is much less optimized in comparison to the plate girders. For the S890 plate girder the comparison is visualized on Figure 115, showing the plate girder is much more slender and higher compared to the hot rolled sections.

	βw 525	**IPE 500**	**βw 425**	**IPE 450**	**IPE 500**	**HEB 650**	
Grade	S690	S690	S890	S890	S890	S235	
A_{tot}	6000	48200	6000	33740	48200	210600	mm^2
W_{pl}		2194		1702	2194	7320	cm^3
M_{ult}	**1438,8**	1513	**1627**	1515	1953	1720	kNm
Efficiency	**240**	31	**271**	45	41	8	Nm/mm^2

TABLE 31: BENDING MOMENT CAPACITY FOUND IN THE PARAMETRIC STUDY FOR GIRDERS WITH 6000 MM^2 TOTAL AREA COMPARED TO HOT ROLLED SECTIONS

In the bottom table the larger girders are compared. It can be seen that the IPE600 section does not achieve the bending moment found in a S690 plate girder with a web slenderness of 525, but a HEB550 does, this beam has 11 times more area compared to the plate girder. This type is also comparable to the S890 plate girder with a slenderness of 425. Finding a comparable S355 girder needs a HEB900 girder, which is a steel area of 42 times more. The S890 girders with a 12000 mm^2 total area are again shown on Figure 115.

	βw 525	**IPE 600**	**HEB 550**	**βw 425**	**HEB 550**	**HEB900**	
Grade	S690	S890	S690	S890	S890	S355	
A_{tot}	12000	92080	136700	12000	136700	494100	mm^2
W_{pl}		3512	5591		5591	12580	cm^3
M_{ult}	**4023,2**	3126	3858	**4551**	4976	4466	kNm
Efficiency	**335**	34	28	**379**	36	9	Nm/mm^2

TABLE 32: BENDING MOMENT CAPACITY FOUND IN THE PARAMETRIC STUDY FOR GIRDERS WITH 12000 MM^2 TOTAL AREA COMPARED TO HOT ROLLED SECTIONS

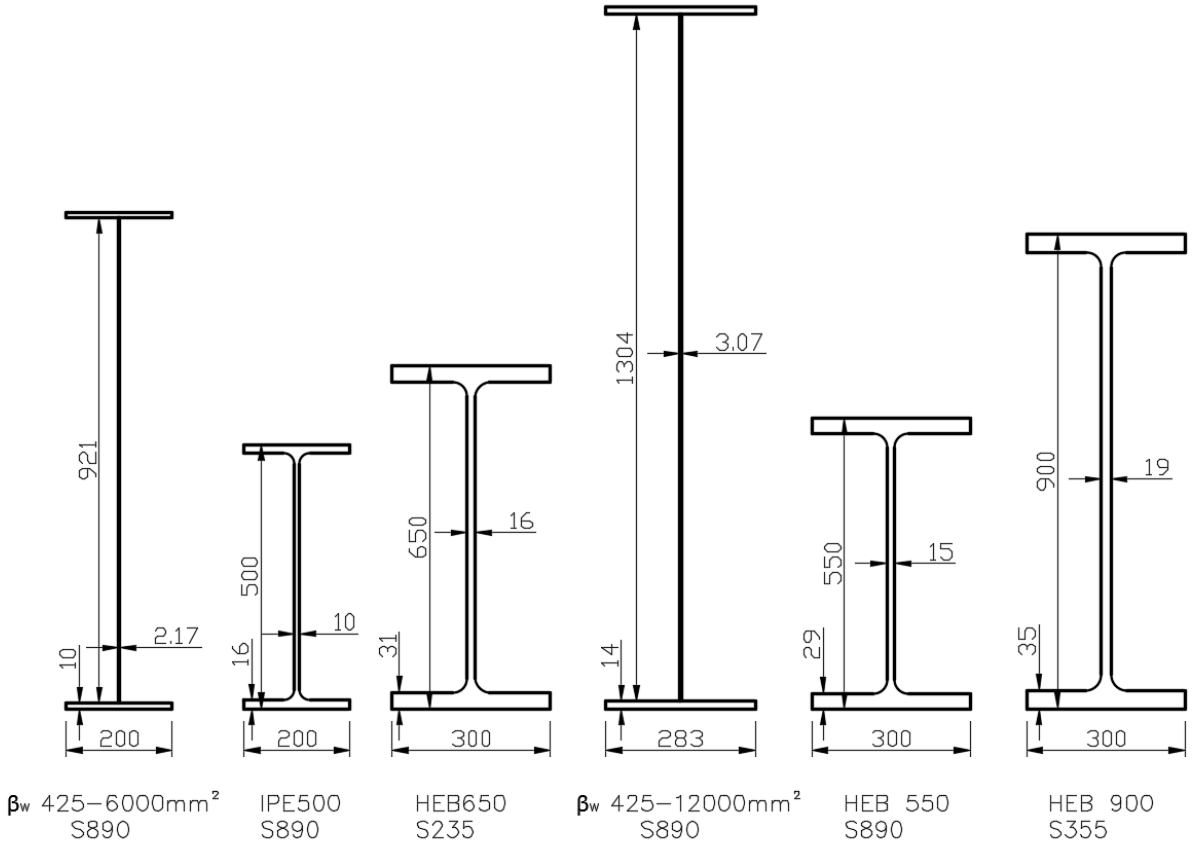

FIGURE 115: COMPARISON BETWEEN HOT ROLLED SECTIONS AND THE S890 PLATE GIRDERS WITH THE HIGHEST BENDING MOMENT CAPACITY.

These tables show the potential of using very slender plate girders, showing a reduction of more than 80% of the used steel in a situation in which a constant bending moment is present. In a more common application, in which a shear force is also present, the plate girders will likely need a less slender web or extra transverse stiffeners.

5. Conclusions and recommendations

5.1. Conclusions

The following conclusions are drawn in this research:

1. The results found by Cimpoi using explicit dynamics to find the maximum bending moment capacity of S690 steel plate girders are found to be unlikely. Using implicit dynamic analysis without initial imperfection shows more likely results, which gives similar and predictable results with changing parameters.
2. Using S690 and S890 steel in unstiffened plate girders subjected to pure bending is shown to be useful. Increasing the yield strength shows a significant increase in the optimized bending moment capacity when the total steel area is kept constant.
3. The maximum bending moment capacity for plate girders in S690 and S890 is found in girders where the compressed flange is fully yielding prior to failure. In these girders the failure is not governed by flange induced buckling. The influential parameters to achieve top flange yielding are shown to be the relative slenderness of the top flange and the slenderness of the web.
4. When the relative slenderness of the top flange is too high, the girder fails due to instability of the top flange.
5. The failure mechanisms of the tested S690 and S890 plate girders happened very sudden and almost without ductile behavior. Using a hybrid plate composition could lead to safer design possibilities without losing much bending moment capacity, due to a more ductile failure mechanism in which other parts than the top flange of the girder yield prior to failure.

5.2. Recommendations

To be able to say more about optimization of steel plate girders in bending, research is needed to describe the influence of the length of the girder in which the bending moment is constant. In particular the influence and behavior of the dimensions of the web and flange, related to the instable rotational failure mode.

- Research the influence of the length of the top flange with different web dimensions
- Research the geometry of the top flange
- It is also of interest to research if the addition of a single transvers stiffener in the middle of the section subjected to a constant moment, would limit the failure mode found in girders with long middle sections.

Research in hybrid sections can be of interest to add ductility in plate girders with high strength steels in use. Also, in this respect finding a balance in the ratio between the cross-sectional area of the top and bottom flange, to prevent the plate girders from failing before the bottom flange reaches yield stress, resulting in more ductility.

The end-panels in this and previous works have been over-dimensioned in the numerical studies. To be able to use the information found in the researches, it is needed to optimize these end-panels as well. It would be useful to research the amount of steel needed to bear the stresses resulting from the found maximum bending moments of the middle section. Also, the influence of less thick end-panels on the bending moment capacity of the middle section should then be studied. Optimization could be studied by subjecting (a combination) of the following parameters to numerical tests:

- Decreasing the web thickness of the end-panels, without losing bending moment capacity in the middle section
- Tapering the end-panels, hereby reducing the amount of steel of the end-panel.

6. References

[1] R. Abspoel, “Plate girders under bending,” 2016 [Online]. Available: Item Resolution URL http://resolver.tudelft.nl/uuid:55929dca-f18b-4e26-a4ac-a0310422d154

[2] R. Abspoel, “Optimisation of plate girders,” TU Delft, Delft, 2015.

[3] L. Cimpoi, “Optimization of plate girders in bending using high strength steel,” Master Thesis, Technische Universiteit Delft, Delft, 2015.

[4] Hasan Q.A., Wan Badaruzzaman W.H., Al-Zand A.W., and Mutalib A.A., “The state of the art of steel and steel concrete composite straight plate girder bridges,” *Thin-Walled Struct.*, vol. 119, pp. 988–1020, 2017.

[5] K. Basler and B. Thurlimann, *report 251-19 Strength of Plate girders in Bending*. Bethlehem, Pennsylvania, 1961.

[6] K. Basler, *report 251-20 strength of plate girders in shear*. Bethlehem, Pennsylvania, 1961.

[7] T. Höglund, “Shear buckling resistance of steel and aluminium plate girders,” *Thin-Walled Struct.*, vol. 29, no. 1–4, pp. 13–30, 1997.

[8] T. HÖGLUND, “Simply Supported Long Thin Plate I-Girders without Web Stiffeners Subjected to Distributed Transverse Load.” 1971.

[9] A. W. DAVIES, D. S. C. GRIFFITH, and T. HOGLUND, “SHEAR STRENGTH OF STEEL PLATE GIRDERS.,” *Proc. Inst. Civ. Eng. - Struct. Build.*, vol. 134, no. 2, pp. 147–157, 1999.

[10] J. D. Glassman and M. E. Moreyra Garlock, “A compression model for ultimate postbuckling shear strength,” *Thin-Walled Struct.*, vol. 102, pp. 258–272, 2016.

[11] J. W. B. Stark, *Optimaal dimensioneren van plaatliggers*. Eindhoven : Vakgroep Konstruktief Ontwerpen, Faculteit Bouwkunde, Technische Universiteit Eindhoven, 1995.

[12] S. P. Timoshenko and J. M. Gere, *Theory Of Elastic Stability*, 2e ed. McGraw-Hill Book Company, 1963.

[13] T. Kárman, von, E. E. Sechler, and Donnell, “Strength of thin plates in compression,” *ASME Transit.*, vol. 54, 1932.

[14] G. Winter, “Post-buckling strength of plates in steel design,” *IABSE*, vol. final report, no. 1952.

[15] K. Basler, *report 251-12 Plate girders under combined bending and shear, theoretic considerations and experimental results*. Bethlehem, Pennsylvania, 1961.

[16] Unterweger H. and Kettler M., “Momententragfähigkeit schlanker Biegeträger - Einfl uss des fl anschinduzierten Stegblechbeulens,” *Stahlbau*, vol. 83, no. 1, pp. 26–34, 2014.

[17] M. Veljkovic and B. Johansson, “Design of hybrid steel girders,” *J. Constr. Steel Res.*, vol. 60, no. 3, pp. 535–547, 2004.

[18] “EN 1993-1-5: Eurocode 3: Design of steel structures – Part 1-5: Plated Structural elements.” 2012.

[19] “EN 1993-1-1:Eurocode 3: Design of steel structures - Part 1-1: General rules and rules for buildings.” .